MINERALOGIA

formerly Mineralogia Polonica

Original paper

Thermal alterations of organic matter in coal wastes from Upper Silesia, Poland

Magdalena MISZ-KENNAN

Faculty of Earth Science, University of Silesia, ul. Będzińska 60, 41-200 Sosnowiec, Poland
e-mail: magdalena.misz@us.edu.pl
* Corresponding author

Abstract Self-heating and self-combustion are currently taking place in some coal waste dumps in the Upper Silesian Coal Basin, Poland, e.g. the dumps at Rymer Cones, Starzykowiec, and the Marcel Coal Mine, all in the Rybnik area. These dumps are of similar age and self-heating and combustion have been occurring in all three for many years. The tools of organic petrography (maceral composition, rank, etc.), gas chromatography-mass spectrometry, and proximate and ultimate analysis are used to investigate the wastes.

Organic matter occurs in quantities up to 85 vol.%, typically a few to several vol.%, in the wastes. All three maceral groups (vitrinite, liptinite, and inertinite) are present as unaltered and variously-altered constituents associated with newly-formed petrographic components (bitumen expulsions, pyrolytic carbon). The predominant maceral group is vitrinite with alterations reflected in the presence of irregular cracks, oxidation rims and, rarely, devolatilisation pores. In altered wastes, paler grey-vitrinite and/or coke dominates. The lack of plasticity, the presence of paler-coloured particles, isotropic massive coke, dispersed coked organic matter, and expulsions of bitumens all indicate that heating was slow and extended over a long time. Macerals belonging to other groups are present in unaltered form or with colours paler than the colours of the parent macerals.

Based on the relative contents of organic compounds, the most important groups of these identified in the wastes are *n*-alkanes, acyclic isoprenoids, hopanes, polycyclic aromatic hydrocarbons (PAHs) and their derivatives, phenol and its derivatives. These compounds occur in all wastes except those most highly altered where they were probably destroyed by high temperatures. These compounds were generated mainly from liptinite-group macerals. Driven by evaporation and leaching, they migrated within and out of the dump. Their presence in some wastes in which microscopically visible organic matter is lacking suggests that they originated elsewhere and subsequently migrated through the dump piles. During their migration, the compounds fractionated, were adsorbed on minerals and/or interacted.

The absence of alkenes, and of other unsaturated organic compounds, may reflect primary diagenetic processes that occurred in coals and coal shales during burial and/or organic matter type. Their absence may also be a consequence of heating that lasted many years, hydropyrolysis, and/or the participation of minerals in the reactions occurring within the dumps. The wastes contain compounds typical of organic matter of unaltered kerogen III type and the products of pyrolytic processes, and mixtures of both. In some wastes, organic compounds are completely absent having been destroyed by severe heating.

The distributions of *n*-alkanes in many samples are typical of pyrolysates. In some wastes, narrow *n*-alkane distributions reflect their generation over small temperature ranges. In others, wider distributions point to greater temperature ranges. Other wastes contain *n*-alkane distributions typical of unaltered coal and high pristane content or mixtures of pyrolysates and unaltered waste material. The wastes also contain significant amounts of final $\alpha\beta$ hopanes. Polycyclic aromatic hydrocarbons are represented only by two- to five-ring compounds as is typical of the thermal alteration of hard coal.

Correlations between the degree of organic matter alteration and the relative contents of individual PAHs and hopanes and geochemical indicators of thermal alteration are generally poor. The properties of the organic matter (its composition and rank), temperature fluctuations within the dumps, migration of organic compounds and mineral involvement are probably responsible for this.

The processes taking place in coal waste dumps undergoing self-heating and self-combustion are complicated; they are very difficult to estimate and define. The methods of organic petrology and geochemistry give complementary data allowing the processes to be described. However, each of the dumps investigated represents a separate challenge to be surmounted in any regional attempt to delineate the regional environmental impact of these waste dumps.

Key-words: coal wastes, dumps, macerals, bitumens, biomarkers, self-heating, pyrolysis

Contents

1. Introduction

Coal wastes that originate during coal production are inseparable components of all coal fields in Poland and around the world. They are generated during the preparation of coal seams for exploitation and during the coal separation processes. Coal wastes, mostly composed of mineral matter, also contain several % of organic matter (Skarżyńska 1995a). Most of the wastes are deposited in dumps typically adjacent to their parent mines.

The quantity of wastes generated during coal mining is strongly related to the amount of coal mined. In recent years, the amount of mined coal has decreased slightly and, likewise, the amount of wastes deposited in the dumps. Some of the wastes are used as construction material in hydraulic-, harbour-, highway, and mining engineering; some in the remediation of derelict land, the restoration of open pits, quarry sites and mining subsidence areas; and some in the manufacture of building materials and the recovery of minerals (Skarżyńska 1995b). Some of the wastes are deposited in dumps in which weathering processes lead, in some cases, to self-heating and self-combustion.

Despite much research, the processes of self-heating and self-combustion are not fully understood. It is well known that these processes result in gaseous and particulate pollutants that are emitted to the atmosphere and leached into surface- and ground waters (e.g. Grossman et al. 1994; Stracher, Taylor 2004; Finkelman 2004; Pone et al. 2007; Zhao et al. 2008; Querol et al. 2008; Carras et al. 2009; Hower et al. 2009; O'Keefe et al. 2010; Skręt et al. 2010). It has been estimated that 1 t of coal mine wastes can generate 0.84 kg of SO_2, 0.61 kg of H_2S, 0.03 kg of NO_x, 99.7 kg of CO, and 0.45 kg of smoke (Liu et al. 1998).

Self-heating can be easily recognised on the dumps. In winter, heated places on dump surfaces remain free of snow. Rising steam and other gases are typical features of heated dumps. The fact that coal waste dumps are an environmental hazard can be easily appreciated by the smells in their vicinity and, particularly, the distinctive smell of hydrocarbons generated by the self-heating. For these environmental and health reasons, it is important that the processes that occur in the dumps be defined and that the types of chemical compounds generated during self-heating and self-combustion documented.

Up to relatively recently, the problems of self-heating and self-combustion, and their consequences, e.g. mining safety, deterioration of coal properties and environmental problems, were addressed mostly in relation to coal seams and coal heaps (e.g. Urbański 1983; Brooks et al. 1988; Misra, Singh 1994; Clemens, Matheson 1996; Walker 1999; Jones 2000; Beamish et al. 2001; Kuenzer et al. 2007; Pone et al. 2007; Singh et al. 2007a; Stukalova, Rusinova 2007; Stracher 2007; Wachowicz 2008; Carras et al. 2009; Hower et al. 2009; Quintero et al. 2009; Sahu et al. 2009; Liu, Zhou 2010). Relatively little attention has been given to self-heating in coal waste dumps (Wagner 1980; Liu et al. 1998; Walker 1999; Sawicki 2004). In Poland, this is a consequence of the neglect of coal utilisation in heat and energy production until the end of the last century. Recent years have seen an increase in research on waste dumps worldwide (e.g. Ribeiro et al. 2010) and in Poland (Ćmiel, Misz 2005; Misz et al. 2007; Hanak, Nowak 2008; Parafiniuk, Kruszewski 2009; Misz-Kennan, Fabiańska 2010; Misz-Kennan et al. 2011a, b).

In the context of self-heating, the situation is very different in coal seams compared to coal-waste dumps. The relative amounts of organic matter in coal and coal wastes and the geometric or morphological forms of coal seams and waste heaps are critical differences. The occurrence of coal-seam fires relates to mining methods, ventilation, coal geology, and the relative abundance of methane (Liu, Zhou 2010). Coal-waste fires, in contrast, depend on the manner of waste deposition and access of air into the dump (Urbański 1983; Szafer et al. 1994; Tabor 2002, 2002-2009). Some influencing factors, e.g. the properties of organic matter, are common to both. Some research has begun to focus on the new organic compounds that form as a result of the self-heating of coal wastes (Misz et al. 2007; Misz-Kennan, Fabiańska 2010; Ribeiro et al. 2010; Misz-Kennan et al. 2011b).

The limited knowledge that exists on the transformations of organic matter in coal wastes during self-heating and self-combustion inspired the author to investigate this subject – a subject potentially very important in terms of pollutants generated during these processes that influence the chemistry of soils and are leached to waters. It has been shown that pollutants can migrate within dumps (Misz-Kennan et al. 2011b) and out of them (Pone et al. 2007; Skręt et al. 2010). The question is very complex and a number of factors are influential. In addition, it has to be appreciated that thermally active coal waste dumps change dynamically, i.e. temperatures in any given place can and do fluctuate up and down and as the fire fronts migrate (Tabor 2002-2009; Misz-Kennan, Tabor 2011; Misz-Kennan et al. 2011a). In an attempt to define exactly what takes place, this work focuses on the transformations of organic matter in three coal waste dumps in the Rybnik area, Upper Silesia.

2. Aims of the research

The interrelated aims of the research were:

➢ To determine and explain the petrographic and geochemical changes occurring in organic matter in coal wastes deposited in dumps undergoing self-heating.

➢ To identify organic compounds in wastes that experienced heating and oxidation to varying degrees.

➢ To establish the influence of organic matter type, and of the heating history of the dumps, on the self-heating and self-combustion products.

➢ To define the various reactions that occurred in the wastes as a result of heating and oxidation.

➢ To outline the conditions occurring within the selected dumps and their influence on the organic matter present.

3. Coal wastes and self-heating processes

3.1. Origin and composition of coal wastes

In the Upper Silesian Coal Basin (USCB) in southern Poland, 0.6-0.7 tons of coal wastes are generated for every ton of coal mined. These wastes can be divided into (a) mining wastes and (b) washery wastes. Mining wastes come from preparatory mining works and coal-seam exploitation. In these, individual fragments commonly range up to 500 mm. Washery wastes are generated during coal separation. These may be divided into (a) coarse-grained (10-250 mm) wastes produced from suspension plants, (b) fine-grained (0.5-30 mm) wastes produced from sedimentation processes, and (c) very fine-grained (< 1 mm) slurries (tailings) resulting from flotation processes (Skarżyńska 1995a).

The wastes are composed of mineral matter and, to a lesser extent, organic matter. In petrographic terms, the USCB coal wastes are composed mainly of claystones (40-98%), mudstones (2-40%), coal shales (2-40%), sandstones (< 33%), coal (3-30%, usually 8-10%), and rare conglomerates and carbonates. Typically minestone contains clay minerals (50-70%); quartz (20-30%); and other minerals (10-20%) such as chlorite, pyrite, siderite, ankerite, gypsum, and jarosite, in addition to carbonaceous matter (Skarżyńska 1995a). The content of organic matter in wastes is typically 7-15% but can reach a few tens % (Skarżyńska 1995a; Alonso et al. 2002). This organic matter plays the crucial role in waste self-heating processes.

3.2. Self-heating in coal wastes

Immediately after their deposition in a dump, coal wastes undergo weathering processes that may lead to fires. In terms of their origin, two types of fires are distinguished. Exogenic fires are linked to an external source of heat, e.g. hot slag from combustion, badly protected welding works, etc. (Urbański 1983). Endogenic fires, as discussed here, are related to self-heating processes believed to be caused by low-temperature oxidation of organic matter (Urbański 1983; Itay et al. 1989; Krishnaswamy et al. 1996a, b; Walker 1999; Sensogut, Cinar 2000; Lu et al. 2004; Shi et al. 2005; Singh et

al. 2007a). At the present time, endogenic fires are a feature of several coal-waste dumps in the USCB.

Self-heating occurs only when three influencing factors exist at the same time. These are (a) the presence of components (organic matter, pyrite) that may easily react with air, (b) access for air into the interior of the dump, and (c) conditions that make heat accumulation possible (Urbański 1983; Szafer et al. 1994; Brooks et al. 1988; Tabor 1999, 2002; Barosz 2002, 2003; Kaymakçi, Didari 2002; Pone et al. 2007). At a heated spot on a dump, the difference between the surface temperature of the dump and the atmospheric temperature is > 3°C (e.g. Szafer et al. 1994; Barosz 2002; Tabor 2002). The hot-spot is commonly located *ca* 1.5-2.5 m below the dump surface (Urbański 1983; Walker 1999). In attempting to inhibit or avoid fire, it is impossible to completely eliminate organic matter from the wastes. Air access can be limited by compaction of the wastes using vibrating rollers where dumps are currently being formed or by the insertion of screens of inert material (e.g. fly ash, clay) in existing dumps. However, despite all of these efforts, self-heating occurs in a number of USCB dumps (Misz-Kennan, Fabiańska 2010; Misz-Kennan, Tabor 2011; Misz-Kennan et al. 2011a).

The self-heating process occurs in two stages. During an initial incubation stage, no change in temperature is observed (Walker 1999; Sawicki 2004). Exothermic oxidation processes occurring at this stage are linked to the release of gases such as CO, CO_2, hydrocarbons, and hydrogen (Cygankiewicz 1996; Wang et al. 1999, 2002a, b, 2003; Lu et al. 2004).

During this incubation stage, a number of changes in organic and mineral matter occur at low temperatures. Coal oxidation is considered to be the essential preliminary precursor of self-heating. The oxidation of organic matter includes, in sequence, the chemisorption of oxygen and the formation of intermediate oxygenated complexes, the decomposition of the unstable intermediates and the formation of stable oxygenated complexes, the destruction of the stable oxygenated complexes and the formation of new active sites and, finally, the decomposition of the solid complexes (van Krevelen 1993).

The incubation stage is followed by self-heating during which the temperature rises continuously (Walker 1999; Sawicki 2004). The critical temperature is 60-80°C (Sawicki 2004; Sokol 2005; Pone et al. 2007). Above, a rapid increase in temperature takes place up to self-ignition; this is strongly dependent on coal rank. The temperature of ignition is *ca* 150°C for subbituminous coal, *ca* 200°C for bituminous coal, *ca* 250°C for coke, and *ca* 300°C for anthracite. Temperatures within burning dumps may reach as high as 1300°C (Sawicki 2004; Sokol 2005).

Several internal and external factors influence the self-heating processes (Urbański 1983). Internal factors determine the reactivity of the waste material to atmospheric oxygen at low temperatures, e.g. mineral composition, maceral composition, the presence of chemical compounds that inhibit oxidation reactions, and moisture (Urbański 1983; Rosiek, Urbański 1990; Walker 1999; Kaymakçi, Didari 2002). External factors influence the filtration abilities of dumps and their heat balance (Urbański 1983; Krishnaswamy et al. 1996a, b; Walker 1999; Kaymakçi, Didari 2002).

Organic matter present in coal wastes occurs in a form of macerals belonging to all three maceral groups (vitrinite/huminite, liptinite, and inertinite). Their classification, origin, and properties have been discussed in numerous publications (e.g. ICCP 1998, 2001;

Taylor et al. 1998 and references therein; Sýkorová et al. 2005). The organic matter occurs interlayered with mineral matter, as lenses and laminae of various length and width, and as dispersed organic matter (Misz et al. 2007; Misz-Kennan, Fabiańska 2010; Ribeiro et al. 2010; Misz-Kennan et al. 2011b). Individual macerals show different propensities for self-heating. Vitrinite is the maceral group that self-ignites most easily (Strumiński, Rosiek 1990; Taylor et al. 1998; Machnikowska et al. 2003). Vitrite undergoes oxidation earlier than durite, a difference especially marked during the earliest stages of oxidation (Taylor et al. 1998; Machnikowska et al. 2003). Apart from vitrinite, liptinite macerals are also very reactive and highly prone to spontaneous combustion (Misra, Singh 1994; Mastalerz et al. 2010). However, other research has shown that resinite from this group is not prone to spontaneous combustion (Beamish et al. 2001). Some workers, e.g. Strumiński and Rosiek (1990), suggest that because of its high specific area, fusinite can also be the cause of endogenic fires.

The rank of organic matter in coal and coal wastes influences ignition temperatures (Sawicki 2004). In general, the ability of organic matter to self-heat decreases with increasing rank (Rosiek, Urbański 1990; Walker 1999; Beamish et al. 2001; Mastalerz et al. 2010). However, self-heating of coal wastes generated during anthracite mining has been reported (Ribeiro et al. 2010). Subbituminous coals are considered to be those most prone to self-heating (Beamish et al. 2001; Beamish 2005).

Moisture is always present in the wastes. During self-heating, a considerable quantity of heat energy is used in its evaporation. Moisture facilitates pyrite decomposition and participates in chemical reactions that promote self-heating processes. Influenced by moisture, the activation of coals promotes oxygen absorption and oxidation (Clemens, Matheson 1996). At moisture contents > 6%, coals are more prone to self-heating (Rosiek, Urbański 1990). Though a certain amount of moisture can speed up the process of self-heating, too much acts to inhibit that process (Rosiek, Urbański 1990; Sawicki 2004; Smith, Glasser 2005).

The shape and size of a dump determine its filtration properties and influence the generation and accumulation of heat within it (Urbański 1983). Commonly, self-heating processes occur in high- and/or steep scarps of dumps, particularly so in the case of cone type dumps because of particle fractionation and the enhanced influence of wind on their slopes (Urbański 1983; Krishnaswamy et al. 1996b; Misz-Kennan, Tabor 2011; Misz-Kennan et al. 2011a). The flow of the wind enhances oxidation, leading to a natural, asymmetric, convection within the dump (Krishnaswamy et al. 1996b; Moghtaderi et al. 2000). Temperatures can be much higher on windward slopes than elsewhere (Urbański 1983; Moghtaderi et al. 2000; Misz-Kennan, Tabor 2011).

Particle size and particle surface area are important with regard to oxygen absorption. They influence the availability and consumption of oxygen within the dump (Krishnaswamy et al. 1996b). Some authors consider that larger particles lead to fires more easily than smaller particles do (e.g. Krishnaswamy et al. 1996b). On the other hand, larger particles can be considered to catch fire more slowly due to the reduction in the global reaction rate. However, Misra and Singh (1994) favour the conclusion that small particles favour spontaneous combustion. The influence of particle size is clearly not settled.

Fractionation of particles during the building of cone-type dumps generates conditions conducive to the infiltration of air into dump interiors; the process of self-

heating is thus promoted. Smaller particles tend to accumulate in the upper parts of these dumps and larger particles in lower parts. Coarse-grained (and porous) dumps are prone to self-heating in autumn and winter, and fine-grained dumps in spring and summer (Urbański 1983; Szafer et al. 1994).

Atmospheric conditions also influence the self-heating process. Rainfall, particularly when heavy, tends to damage the structure of the dump, enabling the migration of air into the interior. Seasonal changes in air temperature are also an influence; the ventilation of a dump is twice as effective in winter compared to summer (Urbański 1983).

Hot spots in coal waste dumps usually occur at depths of 1.5-2.5 m. As material is burnt out, the fire zone migrates inwards. In the hot spots, the burnt out places, 'wolf's pits', are hot cavities that can easily subside and collapse under small pressures (Urbański 1983; Szafer et al. 1994).

There are several theories that purport to explain the phenomenon of self-heating and self-combustion. Some authors, e.g. Urbański (1983), Skarżyńska (1995a), Evans et al. (2003), Sawicki (2004) suggest that the self-heating of coal results from the reaction of pyrite in coal with atmospheric oxygen or bacterial- or catalytic non-saturated compounds, functional groups and oxygen complexes. At the present time, it is considered that low-temperature oxidation of organic matter is the essential driver of the self-heating process (Krishnaswamy et al. 1996a, b; Lu et al. 2004; Singh et al. 2007a).

3.3. Maceral changes during self-heating

All macerals present in coal and/or as dispersed organic matter in various rocks respond to heating in various ways. These have been extensively investigated for both natural- and industrial processes.

Organic matter consists of three groups of microscopic components - macerals (huminite/vitrinite, liptinite, and inertnite groups) that are distinguished on the basis of their colour, reflectance, fluorescence, and morphology. They have different origins and respond in different ways to rising temperature (ICCP 1998, 2001; Taylor et al. 1998, and references therein; Sýkorová et al. 2005). However, as Taylor et al. (1998) have shown, their behaviour also depends on whether they occur in association with other macerals (as microlithotypes) and/or with minerals (as carbominerites). The co-occurrence of vitrinite and liptinite leads to the formation of more porous solid residues after combustion, whereas the co-occurrence of vitrinite and semifusinite leads to less porous residues (Taylor et al. 1998, and references therein; Suárez-Ruiz, Crelling 2008, and references therein).

In terms of their response to heating, all macerals are classified as reactive-, semi-reactive/semi-inert, or inert macerals. Reactive macerals (liptinite, vitrinite, micrinite, low-reflectance semifusinite, macrinite, funginite, inertodetrinite) are easily and completely destroyed by thermal processes; their original properties cannot be recognized in their solid residues. Inert macerals (especially pyrofusinite, pyrosemifusinite, secretinite, and highly-reflective macrinite and funginite) require much higher temperatures and/or longer time spans for complete thermal destruction; in practice, their original morphologies are easily recognizable in solid residues. The semi-reactive/semi-inert macerals behave in an intermediate manner (Taylor et al. 1998, and references therein; Suárez-Ruiz, Crelling 2008, and references therein).

Alterations of individual macerals due to heating also depend on the rank of the organic matter, the heating rate, the final temperature, the duration of heating, and the presence/absence of air (e.g. Taylor et al. 1998; Suárez-Ruiz, Crelling 2008). Knowledge of the behaviour of macerals during technological processes has proved very valuable to the understanding of maceral alterations in coal wastes exposed to self-heating (e.g. Taylor et al. 1998; Beamish et al. 2001; Sawicki 2004; Mastalerz et al. 2010; Misz-Kennan, Fabiańska 2010; Ribeiro et al. 2010; Misz-Kennan et al. 2011b). Of the three maceral groups, vitrinite responds to heating before other maceral groups do (Taylor et al. 1998). Liptinite, in contrast, undergoes vitrinitization and devolatilization at temperatures above 300°C (Mastalerz, Mastalerz 2000).

Heating rate appears to be one of the key factors that determine the morphology of altered macerals. However, the results are strongly rank dependent. Fast heating rates have less influence on the development of anisotropy in chars of low-rank vitrinites. With increasing heating rate, vitrinite macerals show a greater tendency to softening as indicated by rounded particle edges and/or by the fusion of individual particles into much larger irregular masses. The fluidity of vitrinite macerals also increases with heating rate, irrespective of rank. Vitrinites in anthracites do not show evidence of plasticity. Higher heating rates cause volatile release resulting in the formation of pores and thinner char walls. Middle-rank vitrinites develop mosaic structure that coarsens with increasing heating rate (Goodarzi, Murchison 1978; Murchison 2006).

At present, no commonly accepted classification of organic forms developed as a result of self-heating processes in coal wastes has been developed. However, in recent years, the author has been involved in several attempts to classify them (Misz et al. 2007; Misz-Kennan et al. 2009; Misz-Kennan, Fabiańska 2010; Misz-Kennan et al. 2011b). These attempts were based on numerous works describing the thermal alteration of organic matter in the vicinity of igneous intrusions (e.g. Goodarzi, Murchison 1978; Kwiecińska et al. 1995; Kwiecińska, Petersen 2004; Steward et al. 2005; Cooper et al. 2007; Singh et al. 2007b, 2008; Mastalerz et al. 2009; Rimmer et al. 2009) and coking and combustion processes (e.g. Taylor et al. 1998; Suárez-Ruiz, Crelling 2008).

A preliminary classification of organic matter in coal and coal wastes exposed to self-heating can be based on such criteria as the presence/absence of plasticity, changes in colour of individual macerals and their parts, the presence/absence of anisotropy, and the degree of preservation of original maceral properties. This classification includes the following forms: unaltered macerals, cracks and microfissures, oxidation rims (paler and darker in colour), plasticised particles (particles with porosity and particles with plasticised edges), bands, paler coloured particles, coke (massive, isotropic, anisotropic; porous), inertinite, pyrolytic carbon, natural chars, and unaltered particles (Misz-Kennan et al. 2009).

3.4. Chemical transformations of organic matter during heating

Thermal transformations of organic matter in coal differ considerably from those seen in coal wastes. In coal seams and in rocks associated with them, the changes are linked to the processes of coalification whereas, in coal waste dumps, they reflect weathering and self-heating. In this study, the terms thermal alteration and transformation will be used.

Organic matter present in coal wastes is mostly of kerogen III (coaly) type (e.g. Misz et al. 2007; Ribeiro et al. 2010; Misz-Kennan, Fabiańska 2010; Misz-Kennan et al. 2011b). Its chemical composition is strongly dependent on maceral composition and rank. Individual macerals display different chemical compositions related to their biological origin. Vitrinite and inertinite group macerals mostly derive from the lignin and cellulose of plant cell walls as well as tannins (Hatcher, Clifford 1997; Taylor et al. 1998). The compositions of liptinite macerals are much more complex with individual macerals comprising different chemical compounds reflecting their more varied biological origin; sporinite is composed of sporopollenin, cutinite of cutan, alginite of algaenan, and resinite of various waxes, resins, balsam, copal, latex, oils, and fats (Hatcher, Clifford 1997; Taylor et al. 1998; Killops, Killops 2005). Liptodetrinite comprises a mixture of these compounds. It merits emphasizing that the chemical compositions of coals change with rank, e.g. contents of polar groups generally decrease in line with changes in the elemental composition of the total coal, aromatic structures increase in size and aliphatic chains break-out and are introduced into the bitumen fraction (Hatcher, Clifford 1997; Killops, Killops 2005).

The general structural composition of coal includes fused benzene rings with associated functional groups joined together by ether linkages or sulphur bridges. With increasing maturity, the number of linkages or bridges decreases. At temperatures e.g. 300°C, weaker bridges such as $-CH_2-CH_2-$ and CH_2-O-CH_2- are broken first, followed by the loss of functional groups and the formation of non-condensable gases. The reactions encompass pyrolysis, bond cleavage, fission and production of tarry and volatile products. At temperatures < 300°C, organic compounds and their products are released during depolymerisations, water elimination, fragmentation, oxidation, char formation, and volatilisation/steam stripping of molecular traces (Oros, Simoneit 2000). All of the changes in organic matter are dependent on a number of factors such as maceral composition and rank (Huizinga et al. 1987) and heating history (Huizinga et al. 1987; Lu, Kaplan 1992; Raymond, Murchison 1992; Meyers, Simoneit 1999).

Biomarkers (biogenic markers, molecular fossils) have been applied in organic geochemistry for many reasons. For this role, they must have preserved the basic carbon skeleton of the parent compound and it must be possible to establish the chemical pathway of the alteration from parent compound to biomarker. Various groups of compounds are used as biomarkers, e.g. alkanes, acyclic isoprenoids, steranes, hopanes (Killops, Killops 2005, and references therein; Peters et al. 2005, and references therein). Polycyclic aromatic hydrocarbons are used for evaluation of maturity and thermal alteration (Radke 1987). Most of the maturity parameters are based on the relative abundances of two diastereoisomers (Tables 1, 2; Killops, Killops 2005; Peters et al. 2005) and involve a relative increase of the more thermally stable isomer in comparison to the original isomer of biological origin with biochemical stereochemistry (Farrimond et al. 1998).

Biomarkers have been used in many ways, including estimation of the degree of alteration of organic matter during maturation (e.g. Bray, Evans 1961; Allan, Douglas 1977; Radke et al. 1982, 1986; Radke 1987; Strachan et al. 1989a, b; Bishop, Abbot 1995; Dzou et al. 1995; Mayers, Simoneit 1999; Norgate 1999; Amijaya et al. 2006) and evaluation of the influence of temperature increases due to magmatic intrusion (e.g. Clayton, Bostick 1986; George 1992; Raymond, Murchison 1992; Bishop, Abbot 1993;

Farrimond et al. 1996; Amijaya et al. 2006). Recently, they have been used to identify organic matter in smoke from combustion and smouldering processes (Oros, Simoneit 2000; Simoneit 2002; Fabbri et al. 2009). Individual geochemical parameters of thermal maturation have different ranges of application depending on the reflectance of organic matter (Peters at al. 2005). In addition, the values of biomarker parameters may be influenced to various extents by processes such as interconversion (isomerisation), generation, and thermal destruction of organic compounds (Farrimond et al. 1998).

TABLE 1

Selected indicators of biological source and environment based on biomarkers

Short formula or parameter symbol	Total formula of parameter	Geochemical meaning and application	References
Σ (n-C_{12}-n-C_{22})/ Σ (n-C_{23}-n-C_{35})	Sum of C_{12}-C_{22} n-alkanes /sum of C_{23}-C_{35} n-alkanes	Higher content of long chain n-alkanes is indicative of vascular plants forming organic matter	Tissot, Welte 1984
n-C_{23}/n-C_{31}	Ratio of n-C_{23} and n-C_{31} alkane contents	High content of n-C_{21}, n-C_{23} and n-C_{25} compared to n-C_{29}, n-C_{31} and n-C_{33} is typical for organic matter originating from *Sphagnum*	Pancost et al. 2002
Pr/Ph	Pristane/pytane ratio	Pr/Ph > 1 – oxic environment of deposition	Didyk et al. 1978
		Pr/Ph < 1 – anoxic environment of deposition, (except kerogen III)	Jiamo et al. 1990
Pr/n-C_{17}	Pristane/ n-heptadecane ratio	Various interpretations; determination of degree of alteration of organic matter and water leaching	Leythaeuser, Schwartzkopf 1986
Ph/n-C_{18}	Phytane/ n-octadecane ratio	Various interpretations; determination of degree of maturation/alteration of organic matter and water leaching	Leythaeuser, Schwartzkopf 1986

Changes in biomarkers reflect configural isomerisation that occurs in acyclic isoprenoids, n-alkanes, steranes and triterpanes, a process that mostly involves hydrogen exchange. In steranes, the stereochemistry corresponds to the most stable thermodynamic configuration (e.g. C-8 and C-9). At C-10 and C-13, hydrogen exchange cannot alter the configuration as there is no hydrogen directly bonded to the stereogenic carbon atom to permit the process to occur. Thus, isomerisation is limited to C-14, C-17, and C-20 positions. Similar reactions are also involved in triterpane isomerisation. In C_{31}-C_{35} hopanes, the biologically conferred 22R configuration is preserved during the initial stages of diagenesis. Isomerisation results in a final equilibrium mixture of the same contents of 22R and 22S isomers. At the C-17 and C-21 positions, the configurations are initially mainly $17\beta,21\beta$. That isomer is the least thermally stable and is converted into the $17\beta,21\alpha$ or $17\alpha,21\beta$ isomers. With increasing temperature, the $17\beta,21\alpha$ isomer is converted almost

completely into the more stable $17\alpha,21\beta$ isomer. Hopanes with $17\beta,21\alpha$ configuration are named moretanes (Killops, Killops 2005).

TABLE 2

Selected indicators of degree of organic matter maturation based on biomarkers and aromatic hydrocarbons

Short formula or parameter symbol	Total formula of parameter	Geochemical meaning	References
CPI	CPI = 0.5{[(n-C$_{25}$+n-C$_{27}$+n-C$_{29}$+ n-C$_{31}$+n-C$_{33}$)/(n-C$_{24}$+n-C$_{26}$+n-C$_{28}$+ n-C$_{30}$+n-C$_{32}$)]+[(n-C$_{25}$+n-C$_{27}$+n-C$_{29}$+ n-C$_{31}$+n-C$_{33}$)/(n-C$_{26}$+n-C$_{28}$+n-C$_{30}$+ n-C$_{32}$+n-C$_{34}$)]}	Value decreases to about 1.0 with the increasing maturity	Bray, Evans 1961
C$_{31}$S/(S+R)	C$_{31}$S/(S+R) = 17α(H),21β(H)-29-homohopane 22S/(17α(H),21β(H)-29-homohopane 22S+17α(H),21β(H)-29-homohopane 22R)	Value increases with maturity from 0 to about 0.6; at R$_r$ = 0.7% parameter validity ends (equilibrium)	Ourisson et al. 1979; Seifert, Moldowan 1980
Ts/(Ts+Tm)	Ts/(Ts+Tm) = 18α(H)-22,29,30-trisnorneohopane/(18α(H)-22,29,30-trisnorneohopane+17α(H)-22,29,30-trisnorhopane)	Increase of Ts relative to Tm; ratio values increase from 0.0 to about 0.80-0.85	Seifert, Moldowan 1978
C$_{30}\beta\alpha/(\alpha\beta+\beta\alpha)$	C$_{30}\beta\alpha/(\alpha\beta+\beta\alpha)$ = 17β(H),21α(H)-29-hopane C$_{30}$/(17α(H),21β(H)-29-hopane C$_{30}$+17β(H),21α(H)-29-hopane C$_{30}$)	Decreases with maturity from about 0.8 to 0.0	Seifert, Moldowan 1980
C$_{30}\beta\beta/(\beta\beta+\alpha\beta+\beta\alpha)$	C$_{30}\beta\beta/(\beta\beta+\alpha\beta+\beta\alpha)$ = 17β(H),21β(H)-29-hopane /(17β(H),21β(H)-29-hopane +17β(H),21α(H)-29-hopane)	Decreases with maturity from about 0.8 to 0.0	Seifert, Moldowan 1980
MNR	MNR = 2-methylnaphthalene/ 1-methylnaphthalene	Increases with increasing degree of maturity; very sensitive to water leaching	Radke et al. 1994
DNR	DNR = (2,6-dimethylnaphthalene+ 2,7-dimethylnaphthalene)/ 1,5-dimethylnaphthalene	Increases with increasing degree of maturity	Radke et al. 1982
TNR-1	TNR-1 = 2,3,6-trimethylnaphthalene/ (1,3,6-trimethylnaphthalene+ 1,4,6-trimethylnaphthalene+ 1,3,5-trimethylnaphthalene)	Increases with increasing degree of maturity	Radke et al. 1986

TNR-2	TNR-2 = (1,3,7-trimethylnaphthalene+ 2,3,6-trimethylnaphthalene)/ (1,3,5 trimethylnaphthalene + 1,4,6-trimethylnaphthalene + 1,3,6 trimethylnaphthalene)	Increases with increasing degree of maturity	Radke et al., 1986
TNR-4	TNR-4 = 1,2,5- trimethylnaphthalene / (1,2,5-trimethylnaphthalene + 1,2,7-trimethylnaphthalene + 1,6,4-trimethylnaphthalene)	Increases with increasing degree of maturity	Peters et al., 2005
MPI-3	MPI-3 = (2-methylphenanthrene+ 3- methylphenanthrene)/ (1-methylphenathrene+ 9- methylphenanthrene)	Increases with increasing degree of maturity before decreasing	Radke, Welte, 1983
2-MP/2-MA	2-MP/2-MA = 2-methylphenanthrene/ 2-methylanthracene	Values depend on degree of influence of fire and self-heating	Fabiańska, 2007
MB/DBF	MB/DBF = (3-metylbiphenyl+ 4-methylbiphenyl)/dibenzofurane	Increases with increasing degree of alteration before decreasing	Radke, 1987

The mobility of methyl groups in lignin and other moieties during thermal degradation of kerogen and coal opens the possibility of methyl-group migration from less- to more thermodynamically stable sites in aromatic compounds. With advancing coalification, the thermodynamically more stable isomers became dominant in bitumens. Stability is determined by the degree of steric interaction between each methyl group and the substitutions on the immediately adjacent C atoms of the ring system (Radke 1987). More recent studies suggest that the distribution of methylated naphthalenes and phenanthrenes reflects the dilution of components in the bitumen inherited from diagenesis by components with different distributions generated from kerogen (Radke et al. 1990).

Various factors influence the transformation of biomarkers, e.g. the presence and composition of mineral matter and of water (Huizinga et al. 1987; Li, Kaplan 1992; Pan et al. 2009, 2010). Sterane diastereoisomerisation, for example, leading to formation of diasteranes in coals, is less responsive to heat than when this process occurs in shales (Raymond, Murchison 1992). Heating history (heating rate, end-heating temperature, and time) also plays a crucial role in the transformation of biomarkers. For a given rank, maturity indices are lower for rapidly heated organic matter than for the same matter heated slowly (Raymond, Murchison 1992). Coals are less sensitive to heat-driven losses of organic matter than are oil shales (Mayers, Simoneit 1999).

Water is known to retard pyrolysis (Huizinga 1987; Lewan 1997). The peak generation of bitumen is at *ca* 320°C and the major part of the bitumen decomposes to lighter hydrocarbons in the temperature range 360-400°C (Pan et al. 2009). It has been shown that the composition of minerals plays a role in the distribution of *n*-alkanes and

acyclic isoprenoids; the presence of calcite has no significant influence on the thermal evolution of these compounds whereas they are mostly destroyed in the presence of montmorillonite and minor alterations only occur in the presence of illite (Huizinga et al. 1987). Both of these clays significantly inhibit alkene formation during dry pyrolysis; their effect is substantially reduced when the proportion of clays to water is 2:1 (Huizinga et al. 1987). Polarity-difference bitumen fractionation occurs in the presence of clay minerals but is insignificant in the presence of calcite due to the fact that the small molecular diameter of *n*-alkanes allows them to enter clay mineral interlayers (Huizinga et al. 1987).

4. Thermal history of the coal waste dumps

4.1. Rymer Cones

The Rymer Cones dump was the dump of the Rymer Coal Mine, that is now closed (Fig. 1). At the beginning of the last century, the original dump was formed in the shape of three cones using what are now outdated techniques. The original waste material was essentially burnt out. In the period 1994-1999, the cones were redeveloped and enclosed with more recent coal wastes (Tabor 2002; Barosz 2003). During this redevelopment, two cones (No. 2 and No. 3) were dismantled; only cone No. 1 remained (Barosz 2003). Around the turn of the present century, the surface of this cone was covered by openwork concrete panels and fly ash as a block to the entry of air. Despite these efforts, self-heating restarted and intensified to the point that a decision to remove the panels and fly ash was taken. At present, the dump covers an area of 0.13 km^2, its height is +300 m above sea level and its capacity is $2.4 \cdot 10^6$ m^3. Currently, only the eastern slope and top of the dump are sealed and self-heating continues. The temperature fluctuations in the dump have been described in detail by Misz-Kennan and Tabor (2011) and Misz-Kennan et al. (2011a).

4.2. Starzykowiec

The Starzykowiec coal waste dump located within the area of the Chwałowice Coal Mine (Fig. 1) was probably started when the mine opened in 1903. In later years, coal mud collectors were constructed on top. In the early 1970s, the deposition of coal mud was stopped and mud from some of the collectors began to be exploited. Dismantling of the scarp took place up to 1990. The thermally-transformed wastes were used for rebuilding the nearby Niedobczyce railway station. In the early 1990s, the work stopped as the scarp was in danger of collapsing. When the scarp was being exploited from 1970-1990, the waste material was already completely altered and there was no active self-heating.

Up to 2005, mud exploitation continued and reclamation of the dump using wastes from the existing mining operation was undertaken. Since 2004, the west scarp has been surrounded by wastes from current production. In 2006, the scarp became thermally active (Miczajka 2008; Tabor 2002-2009; Misz-Kennan, Tabor 2011).
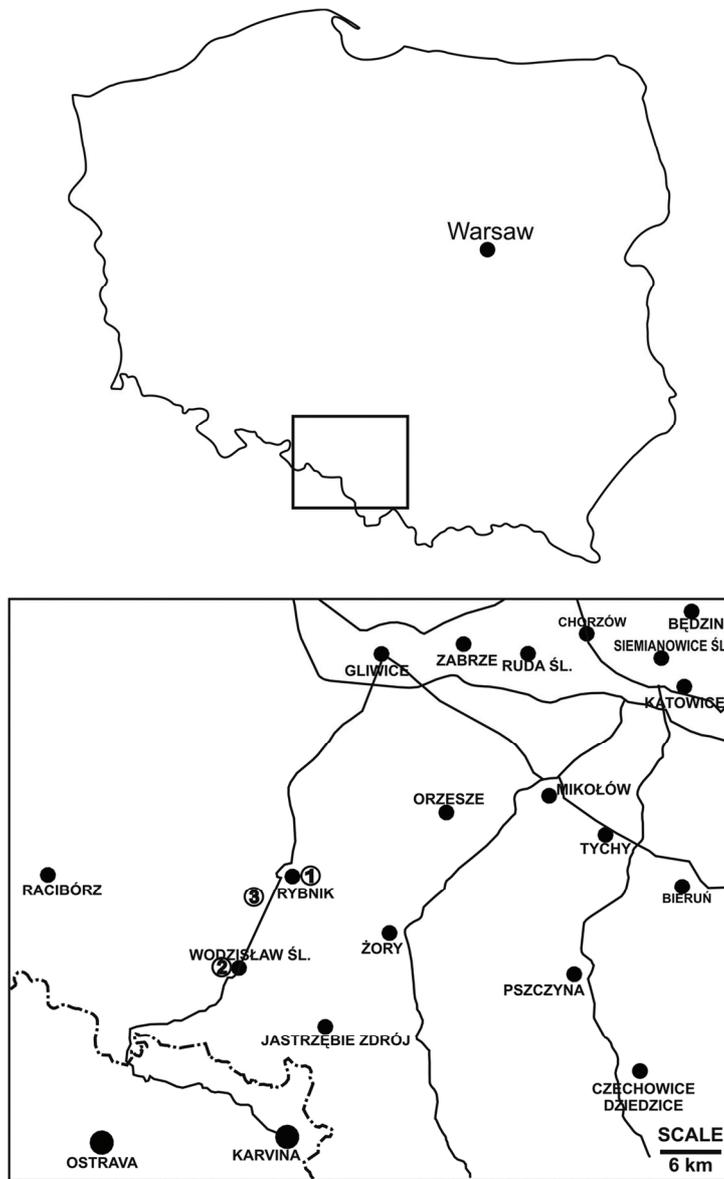
Fig. 1. Localities of the coal waste dumps. 1 – Starzykowiec, 2 – Marcel Coal Mine,
3 – Rymer Cones.

4.3. Marcel Coal Mine

The coal waste dump at the Marcel Coal Mine is an over-levelled dump that is an amalgamation of three old dumps formed at different times (Fig. 1). The history of the first part, Old Cones, started at the end of the 19th century and, eventually, two cones covered an area of 0.13 km^2 and their capacity has been estimated at $> 12 \cdot 10^6$ m^3. When dumping

stopped here in 1986, the height reached +353 m above sea level. Self-heating of varying intensity occurred throughout. In 1982, at the base of the old cones, a new dump was created on a flat surface covering an area of 0.33 km^2 at a height of +272 m above sea level and with a capacity of $3.7 \cdot 10^6$ m^3. This third dump, enclosing the two older dumps and covering an area of 0.56 km^2, has a capacity is $24.9 \cdot 10^6$ m^3. It rises +320 m above sea level (Barosz 2003; see Misz-Kennan, Tabor 2011 for a detailed history).

At the present time, the burnt-out waste material is used for road building. Material from current mining, deposited in place of the exploited wastes, is being compacted with vibrating rolls. However, self-heating is still taking place at several sites within the dump.

5. Methodology

5.1. Sample collection

Coal waste samples were collected at each of the three targeted coal waste dumps (Fig. 1). In total, 142 samples of coal wastes, three samples of fly ash, and four soil samples were collected. All were collected from places undergoing self-heating at the time of their collection. The weight of each sample was 1-2 kg.

5.1.1. The Rymer Cones dump

In the Rymer Cones dump, samples were collected once a month at locations where monthly monitoring of the dump takes place. This collection strategy provided additional information on the heating dynamics in the dump. The monthly monitoring included measurements of CO, CO_2, and O_2 contents, measurements of surface and interior temperatures, and visual observations. The interior temperature was measured at a depth of 0.8-1.0 m using a probe and thermometer (Tabor 2002; Barosz 2003). The methodology is described in detail in Misz-Kennan and Tabor (2011).

Samples were collected in October 2007 (R1, R3, R5, R7, R8, R18, R20), in April 2008 (RS24-RS34a), in May 2008 (RS40-RS53), and in June 2008 (RS54-RS62a). In total, 43 of the coal waste samples were collected 25-30 cm under the dump surface. Additionally, one sample (RRS0) of fly ash overlying heated coal wastes was collected in October 2007, and a further four samples of soil (RRSG1, RSG2, RSG4, and RSG6) and two samples of fly ash (RRS1 and RRS2) covering the dump in April 2008. Sample collection sites are indicated in Figure 2 and some examples of sampling sites in Figure 3a-d.

5.1.2. The Starzykowiec dump

For this research, a total of 48 samples were collected in the lower part of the dump at the Chwałowice Coal Mine. Currently, the dump is thermally active. The samples were again collected at sites where the monthly monitoring took place (Fig. 3e-f, 4a). Samples C1-C27 were collected during the period of October-December 2007 and samples CH1-CH22 during March-May 2008. All were collected 25-30 cm under the dump surface. At

the sampling sites, the temperature of the dump surface was measured and, in some instances, the temperature at a depth of *ca* 1 m also.
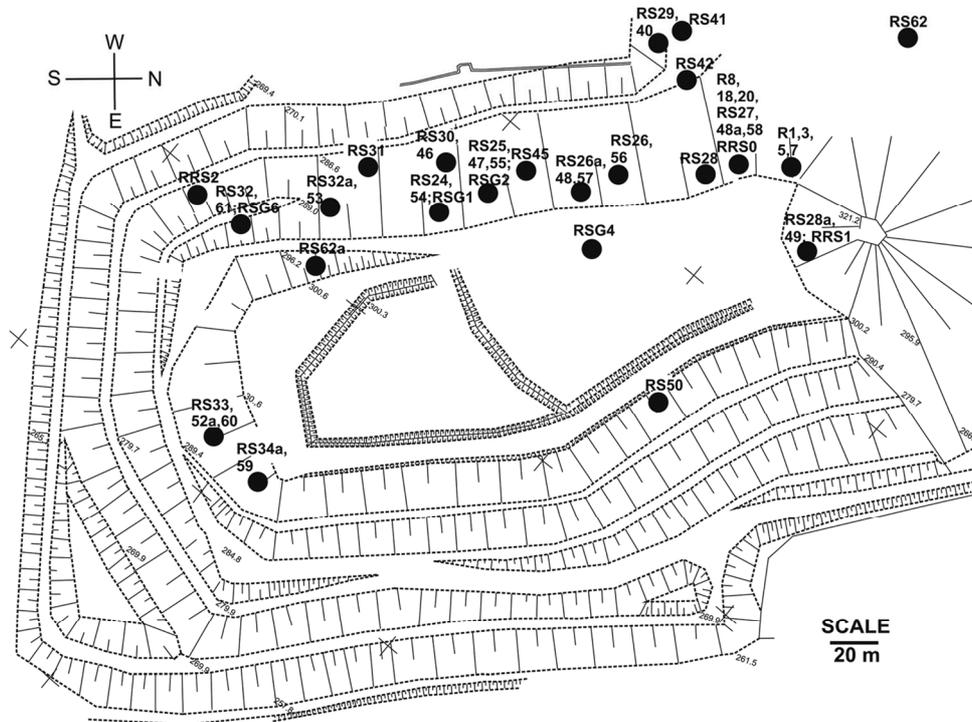
Fig. 2. Sample collection sites in the Rymer Cones coal waste dump.

5.1.3. The Marcel Coal Mine dump

In October 2007, 11 samples of coal wastes (samples M1 - M11) were collected on the northern slope of the dump over the coal mud collector in the Marcel Coal Mine dump (Fig. 4b). In May 2008, 23 samples of coal wastes (M12 – M23) were collected from a site in exploited burned-out wastes, one of several sites in the dump where self-heating was taking place (Fig. 4c). The place was redeveloped after the samples were collected. In February 2009, 14 samples (M30-M43) of coal wastes were collected at the south-west part of the top of the old burnt out dump that had been prepared for exploitation (Fig. 4d).

Some of the samples were collected on the surface of the dump (M12, M13, M14, M15, M16, M17, M18, M19, M20, M21, M22, and M23) and others about 30 cm below the surface (M12a, M13a, M14a, M15a, M16a, M17a, M18a, M19a, M20a, M21a, and M22a; Fig. 4c). Finally, two representative samples (M24 and M25) of coal wastes that were weathered but which showed no evidence of self-heating and one sample (M24a) of coal wastes from current production were also collected to provide a preliminary petrographic and geochemical comparison with weathered and self-heated wastes.
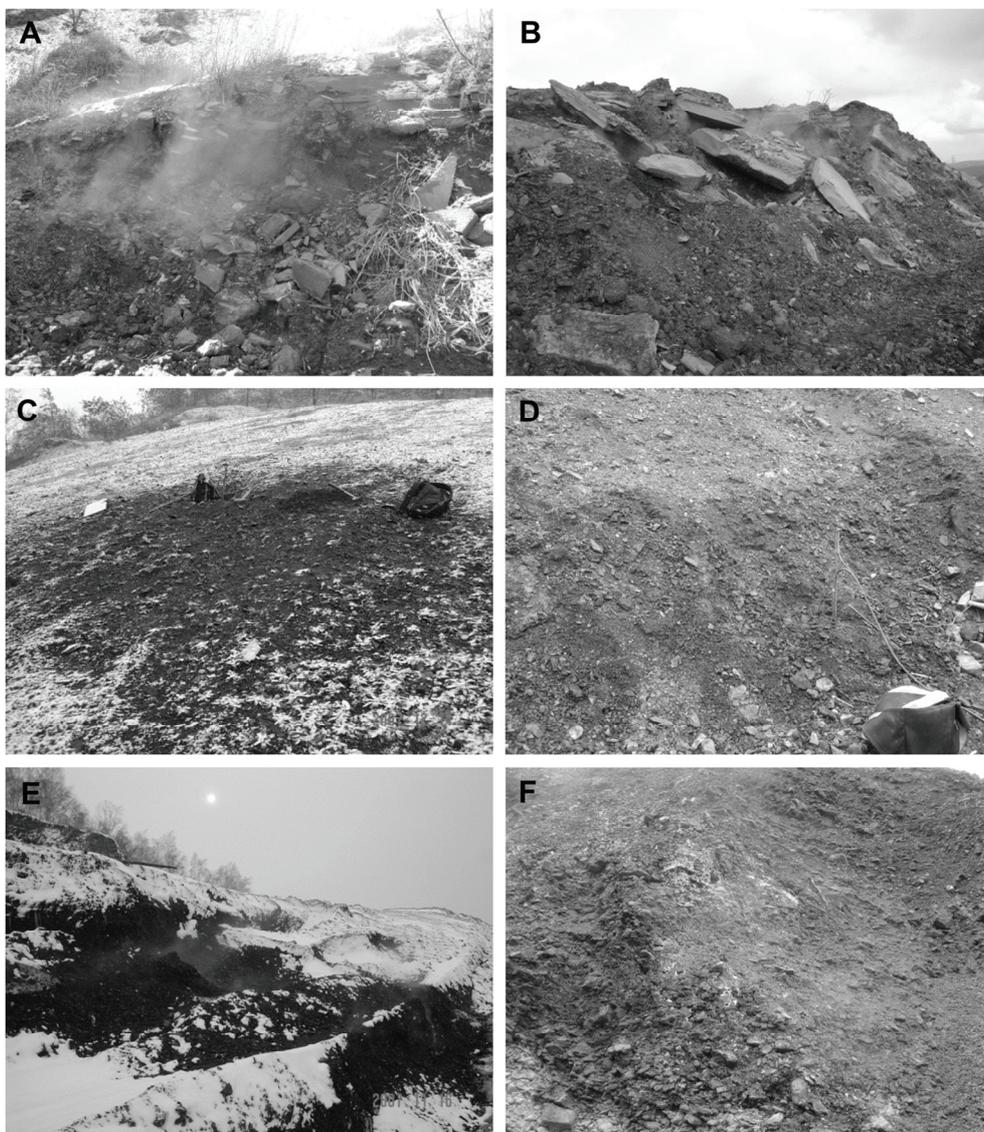
Fig. 3. Sampling sites. A, B – the Rymer Cones dump with grey blocks of the remnant fly ash cover; C – melted snow on the surface of the Rymer Cones dump; D – expulsions of hydrocarbons on the surface of the Rymer Cones dump (wastes with hydrocarbons are darker in colour); E, F – smoke coming from heated wastes in the Starzykowiec dump.
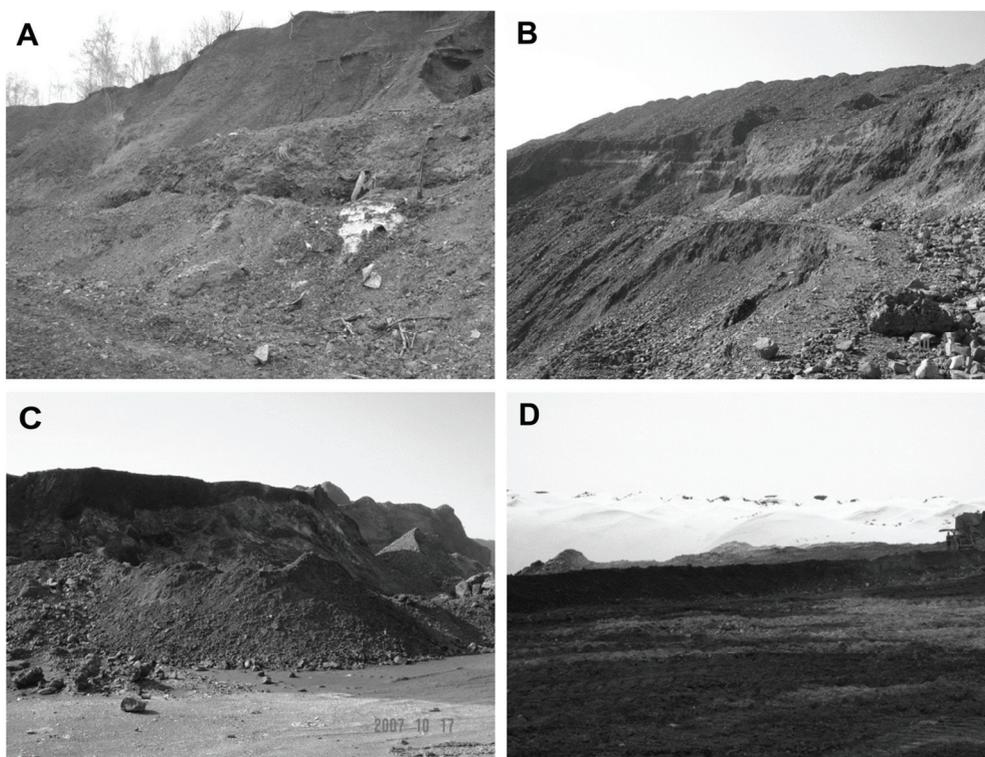
Fig. 4. Sampling sites. A – Starzykowiec dump; B – Marcel Coal Mine dump, sampling site for M1-M11; C – Marcel Coal Mine dump, sampling site for M12-M22a; D – Marcel Coal Mine dump, sampling site for M30-M43.

5.2. Analytical methods

Samples were dried at room temperature before being crushed in a metal mill to < 1 mm for petrographic analysis, to < 0.05 mm for proximate and ultimate analysis, and to < 0.02 mm for geochemical analysis. Samples for chemical analyses were stored in sealed plastic bags after each sample had been further wrapped in aluminium foil to avoid contamination by plasticiser chemicals in the bags.

Petrographic analyses were carried out on pellets of all samples prepared according to procedures described in PN-ISO 7404-2:2005. An optical Axioplan II microscope was used at magnification X500. Maceral compositions, including forms of maceral alteration and mineral contents, were determined for all samples at 500 points according to PN-ISO 7404-3:2001. Random reflectance (R_r) was measured on samples containing organic matter visible under the microscope. The measurements were taken according to PN-ISO 7404-5:2002 at 100-500 points depending on the level of alteration of the organic matter.

Geochemical analyses involved solvent extraction and gas chromatography-mass spectrometry (GC-MS). About 20 g of each sample was extracted with dichloromethane for about 20 min in an ultrasonic bath to obtain a solvent extract. For each, that procedure was

repeated 3-4 times. All extracts were collected, evaporated, and weighed. They were not separated into compound groups due to the low extractability of some samples.

An Agilent gas chromatograph 6890 with a DB-35 column (60 m × 0.25 mm i.d.), coated with a 0.25 μm stationary phase film and coupled with an Agilent Technology mass spectrometer 5973 was used. The experimental conditions were as follows: carrier gas - He; temperature - 50°C (isothermal for 2 min); heating rate - up to 175°C at 10°C/min, to 225°C at 6°C/min and, finally, to 300°C at 4°C/min. The final temperature (300°C) was held for 20 min. The mass spectrometer was operated in the electron impact ionisation mode at 70 eV and scanned from 50-650 Da. Data were acquired in a full scan mode and processed with the Hewlett Packard Chemstation software. All compounds were identified by using their mass spectra, comparison of peak retention times with those of standard compounds, interpretation of MS fragmentation patterns and literature data (Philp, 1985; the Wiley/NBS Registry of Mass Spectral 2000). Geochemical parameters were calculated using peak areas acquired in the manual integration mode.

Proximate and ultimate analyses were performed on 51 samples (29 from Rymer Cones, 26 from Starzykowiec, and 10 from Marcel Coal Mine) selected on the basis of their petrography and geochemistry, and that were representative of the variability they displayed. Proximate analyses involved the determination of moisture (M), ash (A), volatile matter contents (VM), and calorific value (Q_s). Ultimate analyses included determination of carbon (C), hydrogen (H), nitrogen (N), oxygen (O) by difference, and total sulphur (S_t) contents.

The petrographic and geochemical analyses were carried out in the Faculty of Earth Sciences, University of Silesia, Sosnowiec. The proximate and ultimate analyses were carried out according to standard procedures at the Main Research Laboratory Ltd. in Jastrzębie Zdrój (Poland).

6. The Rymer Cones dump – results

6.1. Temperature at a depth of 0.8-1.0 m

During the period of sample collection, temperatures at about 1 m below the dump surface were in the range 14.7-285°C. The lowest temperature was measured in May 2008 at the sample RS42 collection site, the highest during collection of RS60 and RS24 in June and April 2008 (Table 3; Fig. 2). However, in the southern part of the dump, the interior temperatures were somewhat lower (205 and 202°C, respectively) when RS33 and RS52a were collected in April and May 2008 – a month in which a sudden increase was noted. The reverse was seen in the western part of the dump; the temperature there decreased from 285°C in May 2008 when RS24 was collected to 227°C when RS54 was collected (Table 3). Fluctuations of about 30°C were measured in SE part of the dump (RS32 and RS61; Table 3).

Such temperature fluctuations are typical for dumps (Tabor 2002-2009; Misz-Kennan, Fabiańska 2010; Misz-Kennan, Tabor 2011). However, during the period of sample collection, fluctuations in the range of a few to several °C were more typical.

TABLE 3

The interior temperature (T_i) measured at a depth of 1m (Tabor 2002-2009), and petrographic composition and random reflectance values for samples from the Rymer Cones dump

Sample no.	T_i (°C)	Unaltered vitrinite (vol.%)	Vitrinite with cracks (vol.%)	Paler coloured vitrinite (vol.%)	Vitrinite with pores (vol.%)	Liptinite (vol.%)	Inertinite (vol.%)	Pyrolytic carbon (vol.%)	Coke (vol.%)	Mineral matter (vol.%)	R_r (%)	Standard deviation for R_r
R1	78.5	74.4	0.0	0.0	0.0	4.8	3.0	0.0	0.2	17.6	0.59	0.04
R3	78.5	23.8	0.0	0.0	0.0	0.2	1.4	0.0	0.0	74.6	0.69	0.04
R5	78.5	50.8	1.6	0.0	0.0	1.6	6.4	0.0	0.0	39.6	0.64	0.04
R7	78.5	5.4	0.0	0.0	0.0	10.8	13.0	0.0	0.0	70.8	0.80	0.07
R8	73.9	15.4	0.0	0.0	0.0	5.2	4.4	0.0	0.0	75.0	0.66	0.07
R18	73.9	0.0	3.0	33.0	0.0	3.6	12.8	0.0	0.4	47.2	0.77	0.05
R20	73.9	30.6	9.0	2.0	0.0	1.0	9.8	0.0	2.2	45.4	0.71	0.04
RS24	285.0	10.4	7.4	0.0	0.0	0.6	1.0	0.0	0.0	80.6	0.61	0.06
RS25	76.6	25.6	0.0	1.2	0.0	2.8	7.2	0.0	2.8	60.4	0.65	0.17
RS26	87.5	20.8	5.0	0.0	0.0	0.6	1.2	0.0	0.0	72.4	0.63	0.08
RS26a	67.5	0.0	0.0	0.0	0.0	0.0	0.0	0.0	0.0	100.0	-	-
RS27	67.2	26.8	0.0	0.0	0.0	2.6	3.4	0.0	0.0	67.2	0.53	0.04
RS28	68.7	8.8	0.4	0.0	0.0	1.0	1.4	0.0	0.0	88.4	0.56	0.06
RS28a	41.2	25.4	5.8	0.0	0.0	3.8	8.4	0.0	0.0	56.6	0.65	0.05
RS29	71.2	11.6	1.8	1.2	0.0	1.2	1.6	0.0	0.6	82.0	0.66	0.05
RS30	73.5	9.0	3.2	3.4	0.0	1.8	9.8	0.2	0.0	72.6	0.80	0.06
RS31	66.9	8.2	0.4	0.0	0.0	1.0	5.6	0.2	0.0	84.6	0.63	0.11
RS32	83.2	22.2	0.0	0.0	0.0	1.6	8.4	0.0	1.6	66.2	0.69	0.06
RS32a	78.4	7.4	0.0	0.2	0.0	0.8	0.4	0.0	0.0	91.2	0.67	0.07

RS33	205.0	14.0	1.0	3.6	0.0	0.2	1.2	0.0	1.4	78.6	0.81	0.06
RS34a	185.5	8.2	3.6	3.8	0.0	1.4	1.6	0.0	5.4	76.0	0.65	0.08
RS40	71.7	9.0	0.8	0.4	0.0	0.0	1.6	0.0	2.4	85.8	0.64	0.06
RS41	72.5	12.6	2.0	0.0	0.0	1.0	3.6	0.0	5.0	75.8	0.54	0.07
RS42	14.7	7.2	0.4	0.0	0.0	0.6	0.6	0.0	0.4	90.8	0.68	0.06
RS45	53.5	6.8	0.0	0.0	0.0	0.8	2.2	0.0	0.0	90.2	0.61	0.10
RS46	73.8	4.8	0.8	0.6	0.0	1.4	1.6	0.0	0.0	90.8	0.61	0.07
RS47	77.2	16.6	2.6	2.8	0.0	0.6	2.8	0.0	0.6	74.0	0.72	0.12
RS48	65.3	0.2	0.0	4.0	0.0	0.0	0.0	0.0	0.0	95.8	1.05	0.17
RS48a	66.6	14.2	0.2	0.0	0.0	0.8	5.0	0.0	0.0	79.8	0.63	0.04
RS49	47.3	23.4	0.6	0.0	0.0	3.6	6.2	0.0	0.6	65.6	0.64	0.05
RS50	82.7	4.8	0.0	0.2	0.0	0.0	0.0	0.0	4.8	90.2	0.63	0.13
RS52a	202.0	0.0	0.0	17.8	0.0	0.0	2.6	0.0	5.8	73.8	1.59	0.16
RS53	81.9	7.6	1.0	0.0	0.0	0.6	0.6	0.0	0.6	89.6	0.70	0.07
RS54	227.0	10.8	4.2	0.0	0.0	0.8	1.2	0.0	0.0	83.0	0.69	0.06
RS55	77.7	15.8	1.6	0.0	0.0	0.8	5.0	0.0	0.0	76.8	0.80	0.09
RS56	95.6	0.0	0.0	0.0	0.0	0.0	0.0	0.0	0.0	100.0	-	-
RS57	63.5	14.4	0.4	0.0	0.0	1.4	6.0	0.0	0.0	77.8	0.60	0.05
RS58	74.3	15.4	0.0	0.0	0.0	1.2	0.6	0.0	0.0	82.8	0.60	0.06
RS59	218.0	11.0	1.4	0.0	0.0	0.4	1.2	0.0	0.0	86.0	0.69	0.07
RS60	282.0	0.0	0.0	11.4	0.0	0.0	2.0	0.0	1.0	85.6	1.36	0.13
RS61	55.8	8.4	0.2	0.0	0.0	1.2	4.0	0.0	0.0	86.2	0.59	0.60
RS62	210.0	14.4	0.6	0.4	0.0	2.2	5.2	0.0	1.0	76.2	0.73	0.07
RS62a	163.5	6.2	1.2	5.6	0.0	0.0	0.4	0.0	0.2	86.4	1.19	0.10

In April and June 2008, in the upper SE part of the dump where samples RS34a and RS59 were collected (Fig. 2), the temperatures were 185.5 and 218°C, respectively. Until the end of 2007, the temperatures lay in the range 60-92°C and in the period January-September 2008, they were in the range 118-218°C. Later, and up to now, the temperature has ranged from 70-150°C. At another site, in the same part of the dump where samples RS33, RS52a, and RS60 were collected, temperatures had been high for several years. Until October 2007, the temperatures lay in the range 60-80°C before the self-heating processes intensified and temperatures reached as high as 306°C in March 2009. Subsequently, the temperatures dropped below 100°C (Tabor 2002-2009). In June 2008, when RS62 was collected at the base of what remained of cone No. 1, the temperature was 210°C. The temperature is still high there. The temperature in the upper part of the SW part of the dump (RS62a) was also very high (163.5°C) at the time of collection in June, 2008.

In the other parts of the dump, measured temperatures were lower, usually in the range 53.5-95.6°C. Temperatures of 41.2°C and 47.3°C were measured at the lower part of the remaining cone just above the surface of the top of the dump where RS28a and RS49 were collected.

6.2. Petrography

Mineral matter is usually the dominant component (60-95 vol.%) in the samples from the Rymer Cones dump (Table 3). Samples RS26a and RS56 are entirely composed of thermally transformed minerals, mainly represented by clay minerals altered to varying degrees. Pyrite commonly occurs as disseminated framboidal grains within vitrinite particles or clay minerals and as aggregates in the forms of balls or laminae. Carbonates occur in some samples, e.g. R3, R5, R18, R20, RS59, and RS61. Quartz occurs typically as large (several tens of μm) grains with rounded edges in most samples. In some instances, altered minerals occur together with unaltered macerals.

Organic matter comprises 23.5 vol.% of the wastes on average though individual sample contents are usually in the range 10-40 vol.% (Table 3). The following organic matter forms were recognized in the wastes from all three dumps at Rymer Cones: unaltered macerals of vitrinite (Fig. 5a-e), liptinite (Fig. 5b-e), and inertinite (Fig. 5b) groups; altered organic matter (vitrinite with cracks, pale-coloured vitrinites (Fig. 5f, 6a-b), porous particles, particles with oxidation rims (Fig. 6c-d), coke (Fig. 6e-f); newly formed pyrolytic carbon; and bitumen (Fig. 6g-h).

Unaltered macerals belonging to the vitrinite, liptinite, and inertinite groups, showing no signs of alteration, such as cracks, oxidation rims, pores, or elevated reflectance, are present in coal wastes that were exposed to relatively low temperature (Misz et al. 2007; Misz-Kennan, Fabiańska 2010; Misz-Kennan et al. 2011b). Thus, the vitrinite, liptinite, and inertinite classifications (ICCP 1998, 2001; Taylor et al. 1998; Sýkorová et al. 2005) can be applied to these forms.

Cracks are mainly seen in moderately altered particles. However, they can also occur in coked particles. The cracks are typically short and irregular when seen in vitrinite particles or they may lie perpendicular to the edges of particles, in some cases with oxidation rims (Misz-Kennan et al. 2009; Misz-Kennan, Fabiańska 2010).
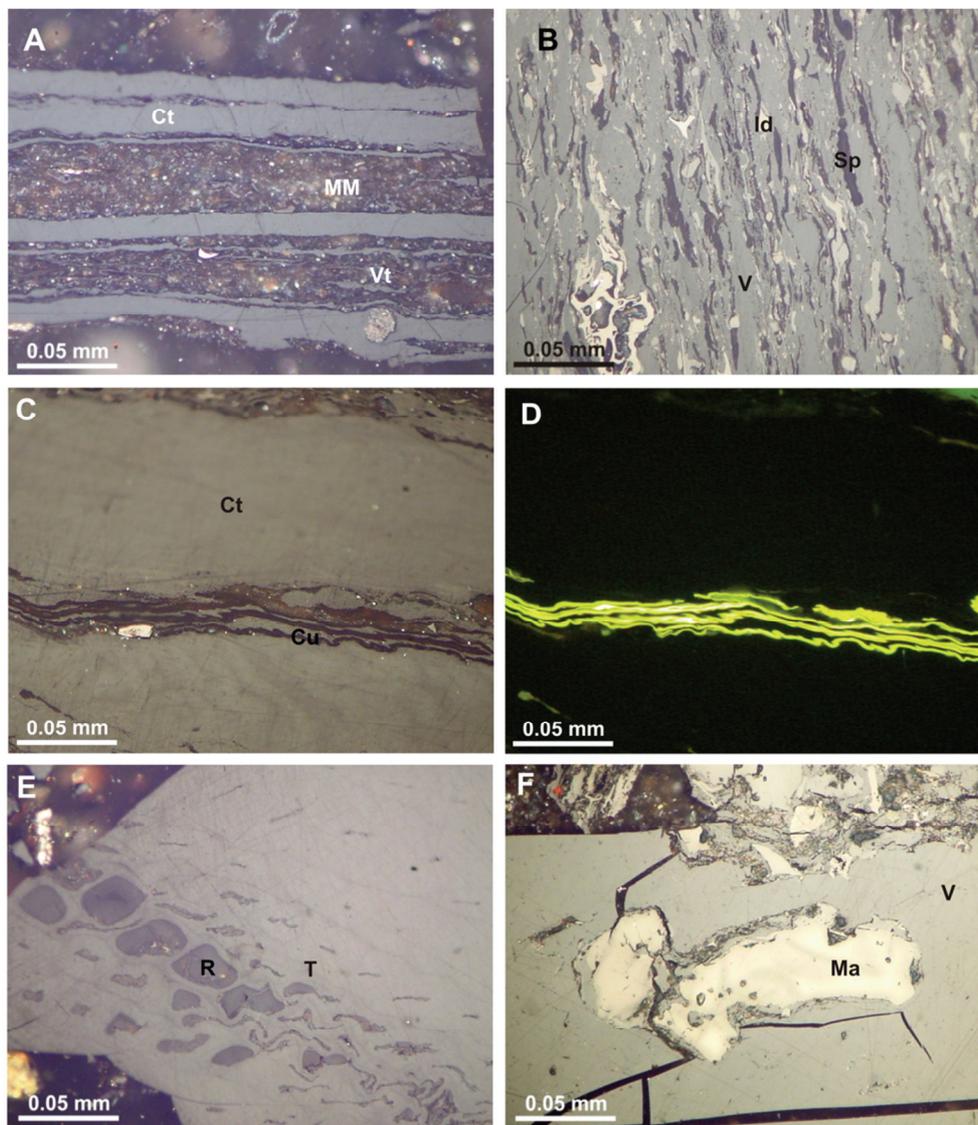
Fig. 5. Organic and mineral matter in coal wastes from the Rymer Cones dump (immersion oil).
A – collotelinite and mineral matter (sample RS30; white light); B – trimacerite particle (sample R18;
white light); C – cutinite, collotelinite, vitrodetrinite, and inertodetrinite associated with clay minerals
(sample RS48a; white light); D – cutinite, collotelinite, vitrodetrinite, and inertodetrinite associated
with clay minerals (sample RS48a; fluorescence); E – telinite with cells filled with resinite (sample
R5; white light); F – paler coloured vitrinite associated with macrinite and inertodetrinite (sample
RS60; white light). V – vitrinite; Ct – collotelinite; T – telinite; Vt – vitrodetrinite; Sp – sporinite;
Cu – cutinite; R – resinite; Ma – macrinite; Id – inertodetrinite; MM – mineral matter.
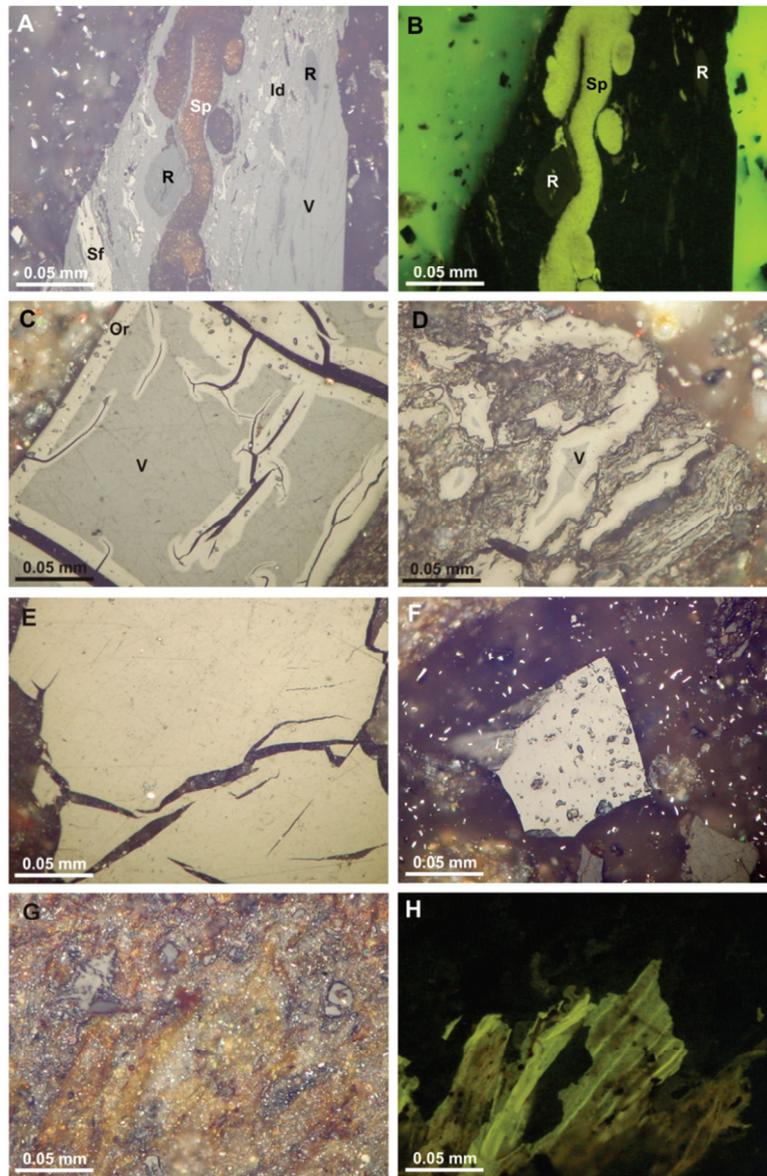
Fig. 6. Organic and mineral matter in coal wastes from the Rymer Cones dump (immersion oil).
A – trimacerite particle with megasporinite, and resinite (sample R18; white light); B – trimacerite
particle with megasporinite and resinite (sample R18; fluorescence); C – paler coloured oxidation
rims around the edge of vitrinite particle and along internal cracks (sample RS62a; white light);
D – paler-coloured oxidation rims around vitrinite particles associated with minerals (sample RS62a;
white light); E – massive isotropic coke (sample RS52a; white light); F – co-occurrence of coke and
unaltered vitrinite (sample RS33; white light); G – bitumens (sample RS48a; white light);
H – bitumens (sample RS48a; fluorescence).V – vitrinite; Sp – sporinite; R – resinite;
Sf – semifusinite; Id – inertodetrinite; Or – oxidation rims.

Paler-coloured particles, resulting from low heating rates (e.g. Goodarzi, Murchison 1978; Murchison 2006), contain small devolatilization pores of the type described elsewhere. Particles containing pores being a sign of their increased plasticity are formed during rapid increases in temperature (Taylor et al. 1998). They occur only in a few of the coal waste samples.

Oxidation rims mostly occur around the edge of vitrinite particles and along cracks within these particles. They may be paler in colour (Chandra 1962; Stach et al. 1982; Calemma et al. 1995; Ndaji, Thomas 1995; Misz et al. 2007) or darker (Ingram, Rimstidt 1984; Nelson 1989; Bend, Kosloski 1993). The paler-coloured rims display higher reflectance resulting from the higher aromaticity of oxidized coal and the combined effect of reaction temperature and chemical changes (Chandra 1962; Stach et al. 1982). These changes occur at temperatures of 200°C (Calemma et al. 1995; Ndaji, Thomas 1995). Darker oxidation rims characterised also by lower reflectance indicate that the parent (unaltered) particles formed during oxidation in the presence of moisture and are associated with the formation of humic acids (Bend, Kosloski 1993). Some instances of zoned oxidation rims may be interpreted as due to fluctuations of temperature within the dump (Misz et al. 2007).

White- or yellow-white coke occurs in strongly altered wastes in the dump. Massive, usually isotropic, coke likely reflects a low heating rate and a long heating time, probably under conditions of limited oxygen supply (Goodarzi, Murchison 1978; Murchison 2006). Porous, commonly isotropic, coke particles are probably indicative of a high heating rate and greater air access. Absent or weakly-marked anisotropy is typical of the wastes (Misz-Kennan et al. 2009; Misz-Kennan, Fabiańska 2010). In contrast, coals altered by igneous intrusions typically show strong mosaic anisotropy (Singh et al. 2007b; Mastalerz et al. 2009).

In cooler parts of the dump, pyrolytic carbon is a gaseous phase product associated with thermal cracking of volatiles. Under laboratory conditions, it is obtained at temperatures of 500°C (Taylor et al. 1998). It occurs as lamellar, dome shaped, highly anisotropic, worm-like or rope-like masses – the forms described by Singh et al. (2007b) from elsewhere.

Expulsions of bitumens result from the heating of organic matter present in the coal wastes. They occur as small droplets a few μm in diameter (Misz et al. 2007), fill pores between minerals (e.g. clay minerals), and in thread-like and irregular forms. They are probably adsorbed by vitrinite (Taylor et al. 1998).

The most commonly occurring vitrinite-group macerals found in the wastes of Rymer Cones are collotelinite (Fig. 5a, c-d), vitrodetrinite (Fig. 5a), and collodetrinite (Fig. 5b, 6a-b). In some of the wastes, corpogelinite and telinite with cell cavities filled with resinite (Fig. 5e) occur. Vitrinite macerals occur in both unaltered and altered forms. Altered vitrinite particles have irregular cracks and are paler in colour (Fig. 5f). Paler coloured oxidation rims occurring on particle edges and along cracks are rare (RS62a; Fig. 6c). In some cases, such rims also occur around vitrinite particles associated with minerals (Fig. 6d). Few signs of plasticity are evident.

The liptinite maceral group is represented mostly by sporinite, usually microsporinite (Fig. 5b), but also by megasporinite in some instances (Fig. 6a-b), cutinite (Fig. 5c-d), resinite (Fig. 5e, 6a-b), and liptodetrinite (Fig. 5b, 6a-b). Fusinite, semifusinite (Fig. 6a),

and inertodetrinite (Fig. 5b, 5d, 6a-b) are the most common inertinite macerals; funginite, macrinite (Fig. 5f), and micrinite are rare.

Coke (Fig. 6e), as the most intensely altered form of organic matter, is present as massive isotropic particles or as detritus occurring in association with transformed minerals. It occurs together with paler coloured vitrinite, vitrinite with cracks, and even unaltered vitrinite (Fig. 6f). The association of coke with vitrinite with a much lower degree of alteration indicates the formation of the coke in parts of the dump with much higher temperatures. The coke was probably introduced during the redevelopment of the dump.

Pyrolytic carbon is rarely encountered in the dumps. If present, it occurs as strongly anisotropic ribbons a few μm in width and several hundred μm in length.

In some samples (R5, R18, R20, RS41, RS48a, RS52, RS53, and RS62), irregular expulsions of bitumens are evident (Fig. 6g-h). They were not included in Tables 3, 4 because their abundance is too low to be revealed by petrographic observation (< 0.2 vol.%) in most samples.

Vitrinite macerals are the dominant component in most waste samples. Liptinite and inertinite macerals are less common or absent (Tables 3, 4). The exception is R7 in which liptinite and inertinite contents exceed that of vitrinite; their contents are the highest encountered in the Rymer Cones dump (10.8 and 13.0 vol.%, respectively; 37.0 and 44.5 vol.% mmf, respectively). In most instances, unaltered vitrinite is the dominant form and, in some samples, it is the only form of vitrinite (Tables 3, 4). Though paler coloured vitrinite is absent in many samples, it is the only form of vitrinite in RS52a and RS60 (17.8 and 11.4 vol.%, respectively; 67.9 and 79.2 vol.% mmf, respectively) and, in R18 and RS48, the dominant maceral form. The highest content of vitrinite with cracks occurs in R20 (9.0 vol.%; 16.5 vol.%, mmf).

Macerals of the liptinite group are absent from eight samples (Tables 3, 4). In the others, their content is < 5.2 vol.%. An exceptionally high liptinite content (10.8 vol.%) characterises R7. Inertinite is absent in four samples (Tables 3, 4). In the remainder, contents are < 13 vol.%.

Coke occurs in a number of samples, generally together with macerals altered to varying degrees (Tables 3, 4). When coke is present, contents range widely from 0.9-49.0 vol.%, mmf (Table 4).

Pyrolytic carbon is present only in RS30 and RS31, where its content is 0.2 vol.% (0.7 and 1.3 vol.%, mmf, respectively; Tables 3, 4). It is also occurs in samples RS45 and RS46 but below the detection limit (< 0.2 vol.%).

The random reflectance (R_r) values measured on vitrinite in the wastes are generally low, usually in the range 0.53-0.81% (Table 3). However, four samples contain vitrinite with R_r = 1.05-1.59%. The highest reflectance was measured in RS52a (Table 3). Most of the reflectograms are narrow, e.g. those for R1, R3, R5, R20, RS27, RS48a, RS49, and RS57 (Fig. 7a-b). Others are wider, e.g. those for R7, R8, RS26, R34a, RS46, RS47, RS53, RS59, and RS62 (Fig. 7c-d). Relatively wide reflectograms occur for RS25 with R_r = 0.72% (Fig. 7e) and all samples with higher reflectance (Fig. 7f-h).

TABLE 4

Petrography of coal waste samples from the Rymer Cones dump calculated on mineral matter free (mmf) basis

Sample no.	Unaltered vitrinite (vol.%)	Vitrinite with cracks (vol.%)	Paler coloured vitrinite (vol.%)	Vitrinite with pores (vol.%)	Liptinite (vol.%)	Inertinite (vol.%)	Pyrolytic carbon (vol.%)	Coke (vol.%)
R1	90.3	0.0	0.0	0.0	5.8	3.6	0.0	0.2
R3	93.7	0.0	0.0	0.0	0.8	5.5	0.0	0.0
R5	84.1	2.6	0.0	0.0	2.6	10.6	0.0	0.0
R7	18.5	0.0	0.0	0.0	37.0	44.5	0.0	0.0
R8	61.6	0.0	0.0	0.0	20.8	17.6	0.0	0.0
R18	0.0	5.7	62.5	0.0	6.8	24.2	0.0	0.8
R20	56.0	16.5	3.7	0.0	1.8	17.9	0.0	4.0
RS24	53.6	38.1	0.0	0.0	3.1	5.2	0.0	0.0
RS25	64.6	0.0	3.0	0.0	7.1	18.2	0.0	7.1
RS26	75.4	18.1	0.0	0.0	2.2	4.3	0.0	0.0
RS26a	0.0	0.0	0.0	0.0	0.0	0.0	0.0	0.0
RS27	81.7	0.0	0.0	0.0	7.9	10.4	0.0	0.0
RS28	75.9	3.4	0.0	0.0	8.6	12.1	0.0	0.0
RS28a	58.5	13.4	0.0	0.0	8.8	19.4	0.0	0.0
RS29	64.4	10.0	6.7	0.0	6.7	8.9	0.0	3.3
RS30	32.8	11.7	12.4	0.0	6.6	35.8	0.7	0.0
RS31	53.2	2.6	0.0	0.0	6.5	36.4	1.3	0.0
RS32	65.7	0.0	0.0	0.0	4.7	24.9	0.0	4.7
RS32a	84.1	0.0	2.3	0.0	9.1	4.5	0.0	0.0
RS33	65.4	4.7	16.8	0.0	0.9	5.6	0.0	6.5
RS34a	34.2	15.0	15.8	0.0	5.8	6.7	0.0	22.5
RS40	63.4	5.6	2.8	0.0	0.0	11.3	0.0	16.9
RS41	52.1	8.3	0.0	0.0	4.1	14.9	0.0	20.7
RS42	78.3	4.3	0.0	0.0	6.5	6.5	0.0	4.3
RS45	69.4	0.0	0.0	0.0	8.2	22.4	0.0	0.0
RS46	52.2	8.7	6.5	0.0	15.2	17.4	0.0	0.0
RS47	63.8	10.0	10.8	0.0	2.3	10.8	0.0	2.3
RS48	4.8	0.0	95.2	0.0	0.0	0.0	0.0	0.0
RS48a	70.3	1.0	0.0	0.0	4.0	24.8	0.0	0.0
RS49	68.0	1.7	0.0	0.0	10.5	18.0	0.0	1.7
RS50	49.0	0.0	2.0	0.0	0.0	0.0	0.0	49.0
RS52A	0.0	0.0	67.9	0.0	0.0	9.9	0.0	22.1
RS53	73.1	9.6	0.0	0.0	5.8	5.8	0.0	5.8
RS54	63.5	24.7	0.0	0.0	4.7	7.1	0.0	0.0
RS55	68.1	6.9	0.0	0.0	3.4	21.6	0.0	0.0
RS56	0.0	0.0	0.0	0.0	0.0	0.0	0.0	0.0
RS57	64.9	1.8	0.0	0.0	6.3	27.0	0.0	0.0
RS58	89.5	0.0	0.0	0.0	7.0	3.5	0.0	0.0
RS59	78.6	10.0	0.0	0.0	2.9	8.6	0.0	0.0
RS60	0.0	0.0	79.2	0.0	0.0	13.9	0.0	6.9
RS61	60.9	1.4	0.0	0.0	8.7	29.0	0.0	0.0
RS62	60.5	2.5	1.7	0.0	9.2	21.8	0.0	4.2
RS62a	45.6	8.8	41.2	0.0	0.0	2.9	0.0	1.5
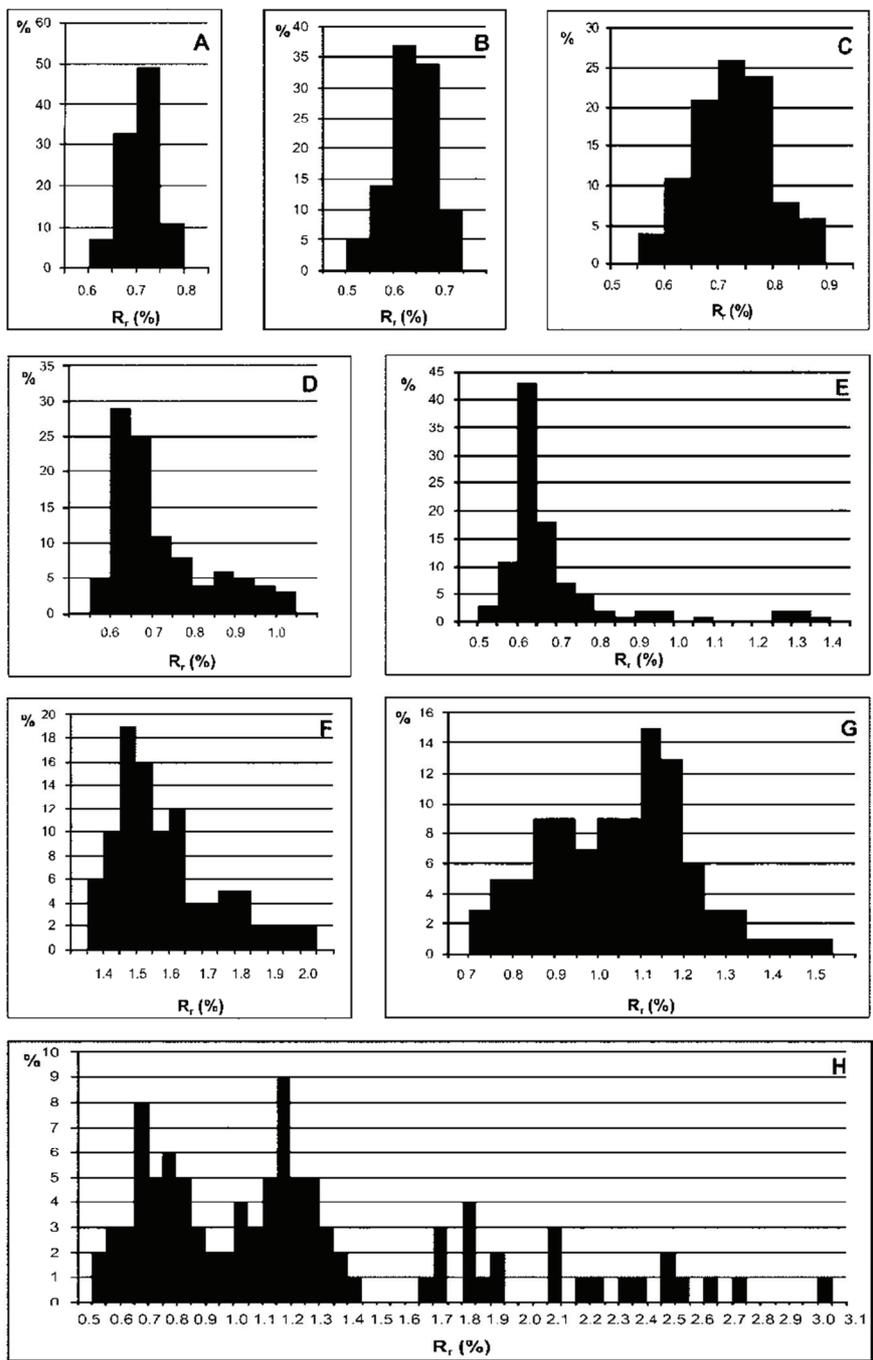
Fig. 7. Reflectograms for selected representative samples. A – sample R20, B – sample RS49,
C – sample RS62, D – sample RS47, E – sample RS25, F – sample RS48, G – sample RS52a,
H – sample RS62a.

6.3. Organic geochemistry

Solvent extract yields of most of the coal waste samples lie in the range 0.004-0.728 wt% (Table 5). The highest yields were obtained from RS34a and RS59 collected in the upper SE part of the dump and for RS30 and RS54 from the western slope. Samples RS30 and RS54 yielded considerably lower extract yields than RS46 and RS24 collected in the same places. The lowest extract yields (0.005 and 0.004 wt%, respectively) are for RS26a and RS56 which lack microscopically visible organic matter. Fly ash samples collected at the Rymer Cones gave, as might be expected, much lower extract yields (0.001-0.009 wt%). Yields for soils (0.007-0.117 wt%) compare with those of most coal samples.

Three main groups of chemical compounds characterise the wastes in the Rymer Cones dump, namely, n-alkanes, light aromatic hydrocarbons, and phenols and their derivatives. Geochemical indices of thermal maturation based on these compounds do not reveal any dependence on the site or time of sample collection.

n-Alkanes (m/z = 71), present in coal (e.g. Kotarba, Clayton 2003) and formed during pyrolysis (Huizinga et al. 1987; Leif, Simoneit 2000), were found in all of the wastes, however, their distribution differs in individual samples. The widest distribution of n-alkanes is from n-C_{11} to n-C_{35} (RS28a, RS49, and RS53; Fig. 8a), but, commonly the distribution is slightly narrower, in the range from n-C_{13} to n-C_{35}.

Most of the samples contain pyrolysates with a Gaussian n-alkane distribution. Some of the distributions are narrow (e.g. RS24, RS34a, RS59; Fig. 8b), others wide (e.g. RS26-RS27, RS48, RS50; Fig. 8c). Narrow chromatograms reflect the distribution of lighter n-alkanes with a maximum at n-C_{18} or n-C_{19} (R8, RS28, RS58, and RS59) or of heavier n-alkanes with a maximum at n-C_{21} (RS24, RS48a, and RS54). Some samples (R3, RS42, and RS62) contain slightly altered material with typical n-alkane distributions and high pristane contents. Several of the relatively unaltered samples (e.g. RS28a, RS49, RS53; Fig. 8a) contain lighter n-alkanes from n-C_{11} to n-C_{15}). Sample RS45 contains mostly light n-alkanes in the range from n-C_{13} to n-C_{18} (Fig. 8d).

Most samples show a slight predominance of odd-over-even carbon number n-alkanes, expressed as Carbon Preference Index (CPI), with values that range from 1.07 in RS33 to 1.71 in R3 (Table 5). Only in two samples (RS31 and RS48) are CPI values < 1. Long chain n-alkanes are dominant in most of the wastes. However, in R3, R5, RS26, RS33, RS47, and RS56, short chain n-alkanes predominate as is expressed by short-to-long chain n-alkane index values in the range 1.05-2.17.

The pristane to phytane ratio (Pr/Ph), used here for determining the oxicity of the organic matter deposition environment (Didyk et al. 1978; Kotarba, Clayton 2003), can also be used as an indicator of the transformation of organic matter (Misz et al. 2007; Misz-Kennan, Fabiańska 2010; Misz-Kennan et al. 2011b). In the wastes investigated here, values of Pr/Ph span a wide range (0.42-11.81). However, only in RS24, RS32, RS41, and RS62 are the Pr/Ph values < 1. Pristane to n-heptadecane (Pr/n-C_{17}) values also span a wide range, usually 0.05-4.60. Extremely high values of the later ratio characterize R3 (9.83) and R5 (12.19). Phytane to n-octadecane (Ph/n-C_{18}) values for most samples are < 1; only in five samples they are > 1.0 (Table 5).

TABLE 5

Extract yields and aliphatic biomarker parameters for samples of coal wastes, fly ash, and soils from the Rymer Cones dump

Sample no.	EY 1)	CPI 2)	$\Sigma1/\Sigma2$ 3)	$n\text{-}C_{23}/n\text{-}C_{31}$ 4)	Pr/Ph 5)	$\text{Pr}/n\text{-}C_{17}$ 6)	$\text{Ph}/n\text{-}C_{18}$ 7)	$C_{31}S/(S+R)$ 8)	Ts/(Ts+Tm) 9)	$C_{30}\beta\alpha(\alpha\beta+\beta\alpha)$ 10)	$C_{30}\beta\beta/(\beta\beta+\alpha\beta+\beta\alpha)$ 11)
						Coal wastes					
R1	0.640	-	-	-	-	-	-	0.56	0.93	0.38	0.01
R3	0.102	1.71	1.17	1.08	8.76	9.83	0.62	0.57	0.89	0.34	0.02
R5	0.526	1.70	1.60	1.30	8.60	12.19	0.81	0.55	0.89	0.38	-
R7	0.104	1.37	0.62	1.86	4.25	2.50	0.30	0.52	0.90	0.39	0.01
R8	0.050	1.49	0.13	2.67	3.24	1.70	0.30	0.53	0.86	0.36	0.01
R18	0.199	1.66	0.67	2.20	6.87	2.19	0.31	0.55	0.88	0.37	0.01
R20	0.702	1.48	0.68	0.92	9.15	4.60	0.67	0.58	0.85	0.38	0.01
RS24	0.022	-	0.03	-	0.64	0.64	0.14	-	-	-	-
RS25	0.036	1.09	0.27	5.80	2.55	1.33	0.27	0.47	0.78	0.35	0.01
RS26	0.101	1.10	2.05	4.45	3.02	1.30	0.24	0.56	0.74	0.37	0.01
RS26a	0.005	1.11	0.85	5.81	3.18	0.73	0.15	0.55	0.79	0.35	0.02
RS27	0.021	1.11	0.19	-	6.06	3.88	0.73	0.57	0.81	0.28	0.02
RS28	0.728	1.46	0.00	-	3.92	0.53	0.11	-	-	-	-
RS28a	0.283	1.47	0.41	3.13	9.45	3.59	0.41	-	-	-	-
RS29	0.050	1.41	0.70	2.44	6.91	2.32	0.26	0.58	0.80	0.34	0.02
RS30	2.251	1.32	0.01	-	2.03	0.27	0.04	-	-	-	-
RS31	0.012	0.79	0.69	6.67	6.67	1.45	0.20	0.55	0.87	0.37	0.01
RS32	0.050	1.38	0.92	2.00	0.42	0.05	0.55	0.55	0.90	0.32	0.02
RS32a	0.048	1.49	0.32	1.75	1.27	0.29	1.47	0.55	0.93	0.30	0.02
RS33	0.024	1.07	1.13	3.00	4.27	2.28	0.39	0.57	0.90	0.41	0.01
RS34a	6.355	-	-	-	2.83	0.39	0.12	-	-	-	-

RS40	0.041	1.34	0.44	12.29	1.21	1.37	5.67	0.56	0.85	0.33	0.02
RS41	0.027	1.39	0.71	3.58	0.98	0.40	3.42	0.56	0.89	0.34	0.02
RS42	0.020	1.33	0.78	2.91	8.91	2.88	0.29	0.57	0.89	0.03	0.13
RS45	0.197	1.27	0.07	-	10.04	1.30	0.14	0.55	0.90	0.33	0.02
RS46	0.043	-	0.07	-	7.01	0.70	0.07	0.57	0.86	0.33	0.02
RS47	0.187	1.22	1.05	65.33	4.88	0.67	0.09	0.55	0.83	0.43	0.01
RS48	0.007	0.91	0.37	12.75	5.01	0.83	0.12	0.57	0.87	0.37	0.01
RS48a	0.004	1.42	0.03	2.66	11.81	1.28	0.35	0.54	0.85	0.34	0.02
RS49	0.071	1.38	0.55	5.00	9.80	2.80	0.31	0.58	0.90	0.33	0.02
RS50	0.170	1.22	0.35	2.50	1.57	0.77	1.01	0.57	0.85	0.31	0.02
RS52a	0.012	1.28	0.57	6.09	2.35	0.61	0.22	-	-	-	-
RS53	0.030	1.43	0.33	2.88	4.33	0.54	0.24	0.55	0.81	0.34	0.02
RS54	7.780	1.18	0.16	-	1.33	0.36	0.06	-	-	-	-
RS55	0.202	1.20	0.30	35.50	3.71	0.42	0.07	0.59	0.81	0.41	0.01
RS56	0.004	-	2.17	1.76	1.39	1.39	0.27	0.54	0.87	0.33	0.02
RS57	0.007	1.11	0.61	10.50	3.28	1.01	0.22	-	-	-	-
RS58	0.086	1.51	0.07	1.50	3.40	0.71	0.10	0.55	0.87	0.33	0.02
RS59	1.083	1.48	0.02	-	2.01	0.15	0.05	0.58	0.82	0.31	0.02
RS60	0.015	1.29	0.67	2.62	2.02	2.21	0.47	-	-	-	-
RS61	0.026	1.32	0.68	4.75	8.53	2.68	0.36	0.57	0.90	0.33	0.02
RS62	0.025	1.43	0.92	2.79	0.94	0.32	2.83	0.60	0.89	0.33	0.02
RS62a	0.036	1.17	0.45	16.50	5.19	0.95	0.12	0.56	0.88	0.38	0.01
							Fly ash				
RRS0	0.009	1.66	0.36	-	5.30	1.01	0.16	-	-	-	-
RRS1	0.007	1.63	0.81	3.27	1.41	0.97	0.49	-	-	-	-
RRS2	0.001	0.83	0.71	6.18	2.61	0.16	0.07	-	-	-	-

	Soils										
	1	2	3	4	5	6	7	8	9	10	11
RSG1	0.007	2.70	0.52	0.69	4.28	1.19	0.22	-	0.90	0.01	0.00
RSG2	0.019	2.11	0.32	1.30	4.47	0.89	0.16	-	0.85	0.00	-
RSG4	0.117	5.06	0.76	0.42	0.87	1.01	1.01	0.00	0.56	0.01	-
RSG6	0.007	1.54	0.42	2.47	4.79	0.95	1.00	0.57	0.89	0.00	0.00

1) EY – Extract yield (wt%)

2) $CPI = 0.5\{[(n\text{-}C_{25}+n\text{-}C_{27}+n\text{-}C_{29}+n\text{-}C_{31}+n\text{-}C_{33})/(n\text{-}C_{24}+n\text{-}C_{26}+n\text{-}C_{28}+n\text{-}C_{30}+n\text{-}C_{32})] + [(n\text{-}C_{25}+n\text{-}C_{27}+n\text{-}C_{29}+n\text{-}C_{31}+n\text{-}C_{33})/(n\text{-}C_{26}+n\text{-}C_{28}+n\text{-}C_{30}+n\text{-}C_{32}+n\text{-}C_{34})]\}$; Carbon Preference Index; $m/z = 71$; thermal maturity parameter (Bray, Evans 1961).

3) $\Sigma1/\Sigma2 = [\Sigma$ (from $n\text{-}C_{13}$ to $n\text{-}C_{22}$)]/[Σ (from $n\text{-}C_{23}$ to $n\text{-}C_{35}$)]; $m/z = 71$, source indicator (Tissot, Welte 1984).

4) $n\text{-}C_{23}/n\text{-}C_{31}$; $m/z = 71$ (Pancost et al. 2002); source indicator.

5) Pr/Ph = pristane/phytane; parameter of environment oxicity (with exception of coals); $m/z = 71$ (Didyk et al. 1978).

6) $Pr/n\text{-}C_{17}$ = pristane/n-heptadecane; $m/z = 71$ (Leythaeuser, Schwartzkopf 1986).

7) $Ph/n\text{-}C_{18}$ = phytane/n-octadecane; $m/z = 71$ (Leythaeuser, Schwartzkopf 1986).

8) $C_{31}S/(S+R)$ = 17α(H),21β(H)-29-homohopane 22S/(17α(H),21β(H)-29-homohopane 22S+17α(H),21β(H)-29-homohopane 22R); $m/z = 191$; thermal maturity parameter (Peters et al., 2005).

9) Ts/(Ts+Tm) = 18α(H)-22,29,30-trisnorneohopane/(18α(H)-22,29,30-trisnorneohopane+17α(H)-22,29,30-trisnorhopane); $m/z = 191$; thermal maturity parameter (Peters et al. 2005).

10) $C_{30}\beta\alpha/(\alpha\beta+\beta\alpha)$ = 17β(H),21α(H)-29-hopane C_{30}/(17α(H),21β(H),21α(H)-29-hopane C_{30}+17β(H),21α(H)-29-hopane C_{30}); $m/z = 191$ (Seifert, Moldowan 1980).

11) $C_{30}\beta\beta/(\beta\beta+\alpha\beta+\beta\alpha)$ = 17β(H),21β(H)-29-hopane C_{30}/(17β(H),21β(H)-29-hopane C_{30}+17α(H),21β(H)-29-hopane C_{30}+17β(H),21α(H)-29-hopane C_{30}); $m/z = 191$ (Seifert, Moldowan 1980).

"–" compounds present, concentrations too low to calculate a parameter value.

Fig. 8. *n*-Alkane distribution in the Rymer coal waste extracts (m/z = 71). a – wide *n*-alkane distribution of a coal or kerogen III type; b – narrow *n*-alkane distribution in pyrolysate; c – wide *n*-alkane distribution in pyrolysate; d – narrow distribution of light *n*-alkanes. Sample numbers on plots.

Hopanes (m/z = 191), occur in most samples (Table 5). Values of $C_{31}S/(S+R)$ (explanation of the abbreviation given in Table 5) vary within a narrow range (0.47-0.60) showing the predominance of the geochemical diastereomer. Values of Ts/(Ts+Tm), (explanation of the abbreviation given in Table 5) also vary within a relatively narrow range from 0.74-0.93 (Table 5; Fig. 9).

Two ratios based on hopanes, $C_{30}\beta\alpha/(\alpha\beta+\beta\alpha)$ and $C_{30}\beta\beta/(\beta\beta+\alpha\beta+\beta\alpha)$, (explanations of the abbreviations given in Table 5) vary little in the wastes. The values of $C_{30}\beta\alpha/(\alpha\beta+\beta\alpha)$ generally lie in the range 0.28-0.43 and those of $C_{30}\beta\beta/(\beta\beta+\alpha\beta+\beta\alpha)$ in the range 0.01-0.02 (Table 5). Sample RS42 is the exception in having the lowest value (0.03) of $C_{30}\beta\alpha/(\alpha\beta+\beta\alpha)$ and highest value (0.13) of $C_{30}\beta\beta/(\beta\beta+\alpha\beta+\beta\alpha)$.

138
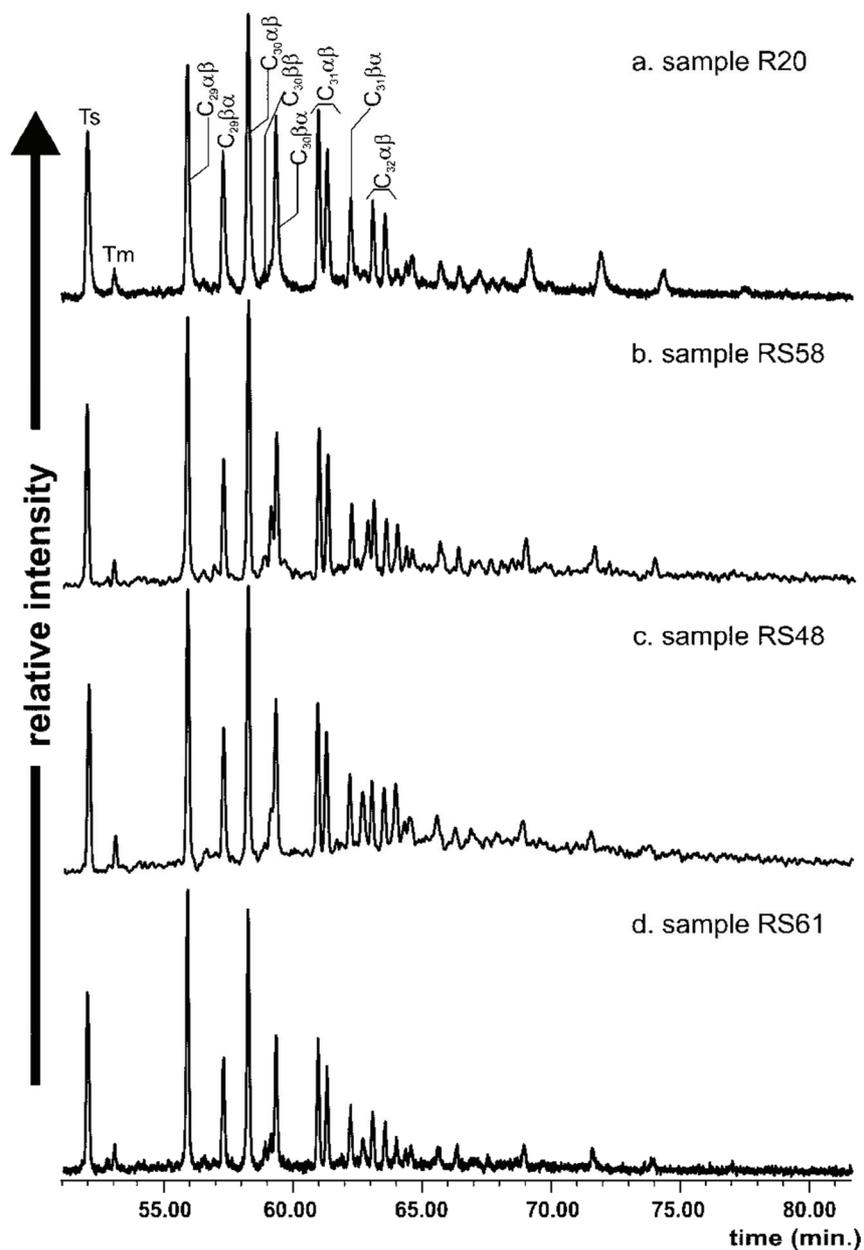
Fig. 9. Pentacyclic triterpane distribution in extracts from the Rymer Cones coal waste samples ($m/z = 191$). Ts – 18α(H)-22,29,30-trisnorneohopane, Tm – 17α(H)-22,29,30-trisnorhopane, $C_{29}\alpha\beta$ – $17\alpha,21\beta$(H)-30-norhopane, $C_{29}\beta\alpha$ – $18\alpha,21\beta$(H)-30-norneohopane, $C_{30}\alpha\beta$ – $17\alpha,21\beta$(H)-hopane, $C_{30}\beta\beta$ – $17\beta,21\beta$(H)-hopane, $C_{30}\beta\alpha$ – $17\beta,21\alpha$(H)-hopane, $C_{31}\alpha\beta$ – $17\alpha,21\beta$(H)-30-homohopane 22S and 22R, $C_{31}\beta\alpha$ – $18\alpha,21\beta$(H)-30-homohopane 22R, $C_{32}\alpha\beta$ – $17\alpha,21\beta$(H)-30-bishomohopane 22S and 22R.

139

In samples, C_{29}, C_{30}, and C_{31} hopanes are present in similar relative amounts (Fig. 10). $\alpha\beta$ hopanes strongly predominate over $\beta\alpha$ hopanes and, especially, over $\beta\beta$ hopanes (Fig. 11). The general overall trend is $\alpha\beta > \beta\alpha > \beta\beta$ hopanes. Sample RS45 contains the highest content of $\beta\beta$ hopanes and the lowest content of $\alpha\beta$ hopanes. Many samples (R1, R3, RS25-RS27, RS29, RS32-RS33, RS47, RS53, RS55, RS56, and RS59) lack $\beta\beta$ hopanes.

Alkylnaphthalene and alkylphenanthrene parameters of thermal maturation show no inter-site pattern or trend in values. Methylphenanthrene ratio values range from 0.29 in RS32a to 2.54 in RS49 (Table 6). Values of the Dimethylnaphthalene (DNR) and Trimethylnaphthalene ratios (TNR-1, TNR-2, TNR-4) fall in the ranges 0.63-10.19, 0.18-7.30, 0.38-1.36 and 0.37-0.81, respectively. The ranges of the Methylphenanthrene Index (MPI-3) and methylbiphenyl/dibenzofurane (MB/DBF) are 0.39-1.95 and 0.04-0.74, respectively (Table 6). Examples of alkylnaphthalene distributions are shown in Figure 12.
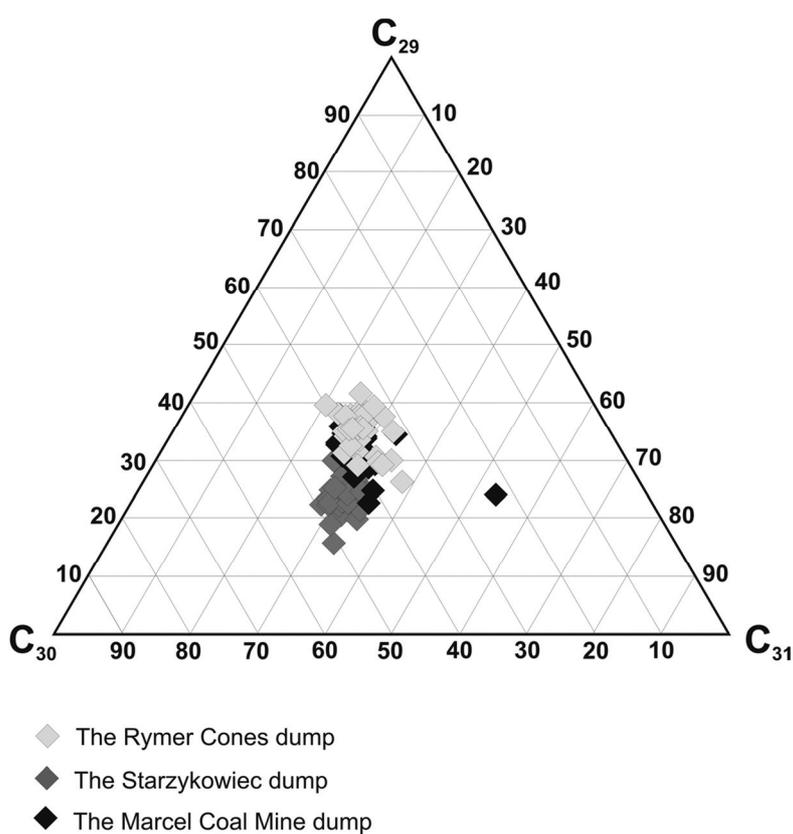
Fig. 10. Relative percentage contents of C_{29}, C_{30} and C_{31} hopanes calculated as a sum of 17α(H),21β(H)-, 17β(H),21α(H)- and 17β(H),21β(H)-hopane diastereomers in coal wastes from the dumps at Rymer Cones, Starzykowiec, and Marcel Coal Mine.

Unsubstituted polycyclic aromatic hydrocarbons (PAHs) are represented mostly by two-and three-ring PAHs (naphthalene m/z = 128, phenanthrene and anthracene, m/z = 178;

Fig. 13) and four-ring PAHs (fluoranthene and pyrene, *m/z* = 202, benzo[*ghi*]fluoranthene, benzo[*a*]anthracene and chrysene, *m/z* = 228). PAHs with five rings (benzo[*b+k*]fluoranthene, benzo[*a*]fluoranthene, benzo[*e*]pyrene, benzo[*a*]pyrene, and perylene, *m/z* = 252) are commonly present though their contents relative to other PAHs are usually < 15.38 rel.% (Table 7; Fig. 14). The highest contents of five-ring PAHs are in RS50 (38.77 rel.%) and RS33 (44.41 rel.%). Contents of individual compounds vary greatly in individual samples. Among two- and three-ring PAHs, phenanthrene is usually dominant. However, naphthalene dominates in R7, R18, R20, RS28, RS28a, RS32, RS45, RS48a, RS49, RS53, and RS61. Anthracene typically occurs in the lowest relative content except for RS29 which has the highest (41.83 rel.%) content.
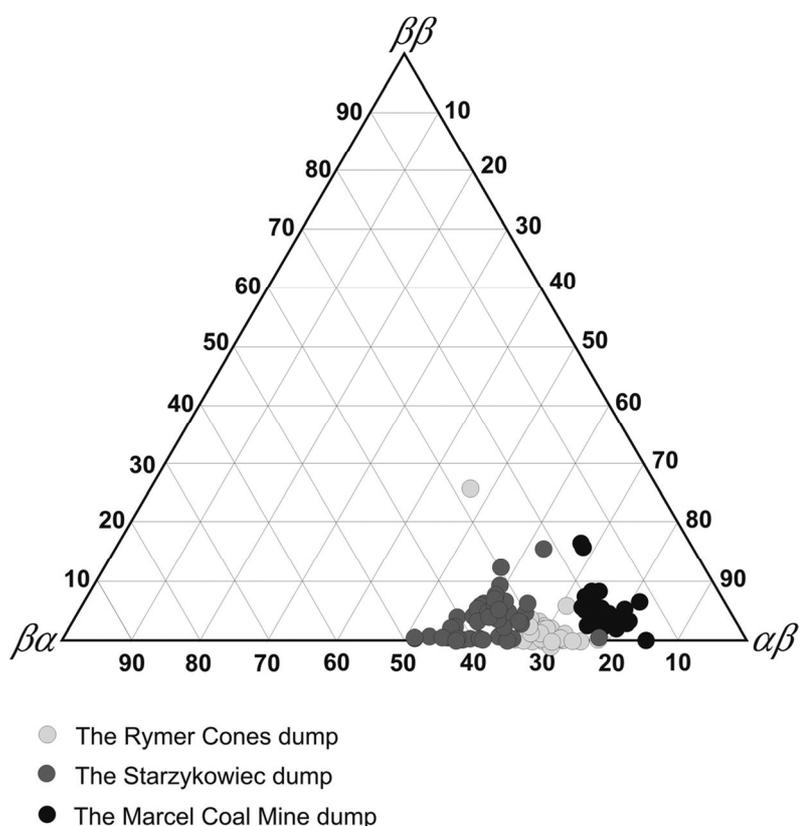
Fig. 11. Relative percentage contents of 17α(H),21β(H)-, 17β(H),21α(H)- and 17β(H),21β(H)-hopane diastereomers calculated for C_{29}, C_{30}, and C_{31} hopanes in coal wastes from the dumps at Rymer Cones, Starzykowiec, and Marcel Coal Mine.

PAHs with four rings are represented mostly by fluoranthene, pyrene, and chrysene. Benzo[*a*]anthracene occur in small relative contents and benzo[*ghi*]fluoranthene is lacking in all samples (Table 7). PAHs with five rings are usually present in a few rel. % though, in RS33 and RS50 which contain their highest contents, the relative contents of these individual compounds is also highest (Table 7).

TABLE 6

Aromatic hydrocarbon parameters for coal waste, fly ash, and soil samples from
the Rymer Cones dump

Sample no.	MNR	DNR	TNR-1	TNR-2	TNR-4	MPI-3	2-MP/ 2-MA	MB/DBF
	1)	2)	3)	4)	5)	6)	7)	8)
				Coal wastes				
R1	-	-	-	-	-	-	-	-
R3	0.55	0.81	-	-	-	-	-	0.12
R5	0.95	0.99	3.40	1.00	0.63	-	-	0.25
R7	0.95	1.08	-	-	-	-	-	0.10
R8	0.69	0.97	2.11	0.80	0.77	-	-	0.36
R18	1.52	1.53	1.60	0.98	0.51	0.39	-	0.66
R20	1.23	1.64	-	-	-	-	-	0.33
RS24	0.77	0.69	-	-	-	1.32	-	0.05
RS25	0.45	-	-	-	-	-	-	0.13
RS26	0.97	1.70	-	-	-	-	-	0.11
RS26a	0.92	1.98	2.24	1.18	0.59	1.49	-	0.15
RS27	0.53	0.76	-	-	-	-	-	-
RS28	1.27	1.17	7.30	1.17	0.37	-	-	0.13
RS28a	1.81	2.50	4.97	1.00	0.44	-	-	0.37
RS29	0.94	1.19	3.37	0.99	0.54	-	-	0.27
RS30	0.92	-	-	-	-	-	-	0.22
RS31	0.87	2.36	0.98	0.80	0.70	0.91	-	0.29
RS32	0.69	-	-	-	-	-	-	-
RS32a	0.29	-	-	-	-	-	-	0.27
RS33	0.90	0.63	2.26	0.97	0.58	-	-	0.20
RS34a	0.75	-	-	-	-	1.83	-	0.19
RS40	1.48	2.81	1.16	0.90	0.66	1.13	-	0.27
RS41	1.33	2.19	0.86	0.76	0.70	1.03	-	0.30
RS42	1.08	1.78	0.88	0.76	0.71	1.01	-	0.28
RS45	1.60	2.44	0.62	0.81	0.61	1.10	-	-
RS46	0.67	1.76	-	-	-	-	-	0.15
RS47	1.65	4.65	3.13	1.36	0.70	1.25	-	0.16
RS48	1.19	4.17	2.62	1.28	0.67	1.37	-	0.20
RS48a	0.72	-	-	-	-	1.33	-	-
RS49	2.54	4.12	0.67	-	-	0.68	-	0.46
RS50	0.66	5.26	-	-	-	-	-	-
RS52a	0.77	1.14	0.37	0.62	0.50	1.82	-	0.29
RS53	1.92	10.19	0.18	0.38	0.64	0.77	-	0.40
RS54	1.47	0.92	2.23	1.30	0.76	1.11	-	0.07
RS55	2.01	2.59	2.63	1.05	0.71	1.21	-	0.15

	MNR	DNR	TNR-1	TNR-2	TNR-4	MPI-3	2-MP/2-MA	MB/DBF
RS56	-	-	1.25	0.95	0.67	1.23	-	0.14
RS57	1.63	7.47	1.19	0.78	0.67	1.57	-	0.04
RS58	1.62	9.06	4.75	1.28	0.81	1.49	-	0.20
RS59	-	-	-	-	-	1.95	-	0.10
RS60	1.64	2.09	1.52	0.79	0.45	0.96	-	0.08
RS61	1.56	4.98	0.39	0.60	0.67	0.82	-	0.74
RS62	1.01	1.59	1.07	0.79	0.73	0.86	-	0.32
RS62a	1.60	3.10	1.39	0.97	0.59	1.31	-	0.23
Fly ash								
RRS0	0.70	-	1.20	1.63	0.39	-	-	-
RRS1	-	1.43	1.08	0.82	0.64	1.33	-	0.34
RRS2	-	-	-	-	-	-	-	0.19
Soils								
RSG1	0.85	1.66	1.24	0.88	0.64	1.43	-	-
RSG2	1.57	2.68	1.31	0.90	0.64	1.93	-	-
RSG4	0.33	3.41	0.74	0.48	0.80	0.82	-	-
RSG6	0.76	2.57	2.49	1.17	0.51	1.17	-	-

1) MNR = 2-methylnaphthalene/1-methylnaphthalene; m/z = 142; thermal maturity parameter (Radke et al. 1994).

2) DNR = (2,6-dimethylnaphthalene+2,7-dimethylnaphthalene)/1,5-dimethylnaphthalene; m/z = 156, thermal maturity parameter (Radke et al. 1982).

3) TNR-1 = 2,3,6-trimethylnaphthalene/(1,3,6-trimethylnaphthalene+1,4,6-trimethylnaphthalene +1,3,5-trimethylnaphthalene); m/z = 170, thermal maturity parameter (Radke et al. 1986).

4) TNR-2 = (1,3,7-trimethylnaphthalene+2,3,6-trimethylnaphthalene)/(1,3,5-trimethylnaphthalene +1,4,6-trimethylnaphthalene+1,3,6-trimethylnaphthalene); m/z = 170, thermal maturity parameter (Radke et al. 1986).

5) TNR-4 = 1,2,5-trimethylnaphthalene/(1,2,5-trimethylnaphthalene+1,2,7-trimethylnaphthalene +1,6,4-trimethylnaphthalene); m/z = 170, thermal maturity parameter.

6) MPI-3 = (2-methylphenanthrene+3-methylphenanthrene)/(1-methylphenanthrene+9-methyl-phenanthrene); m/z = 192; thermal maturity parameter (Radke,Welte 1983).

7) 2-MP/2-MA = 2-methylphenanthrene/2-methylanthracene; m/z = 192.

8) MB/DBF = (3-methylbiphenyl+4-methylbiphenyl)/dibenzofurane; m/z = 168; thermal maturity parameter (Radke 1987).

"–" compounds present but concentration too low to calculate a parameter value.

Phenol and its derivatives are widely present (Fig. 15). They originate through the thermal destruction of lignine units in vitrinite macerals (Horsfield 1989; Hatcher, Clifford 1997). In the investigated wastes, they are represented mainly by phenol, methylphenols (*o-, m-, p-* cresols), dimethylphenols (*m-, o-* ethylphenols), ethylmethylphenols, and ethylprophylphenols. Their absence is conspicuous in RS24, RS26a, RS28a, RS49, RS54, and RS57 collected at the top of the western slope of the dump. Sample RS48, from the same site as RS26a and RS57, does contain low relative amounts of phenols. Phenols are present mainly in the vicinity of the cone (R1, R3, R5, R7, R8, R18, R20, RS27, RS28, RS40, RS48a, and RS58), on the western slope of the dump (RS30, RS32a, RS45, RS46, RS53, and RS55), in the SW part of the dump (RS61 and RS62a), and in the southern part

of the dump (RS33, RS34a, RS52a, and RS59). Elsewhere, they are present in lower amounts.
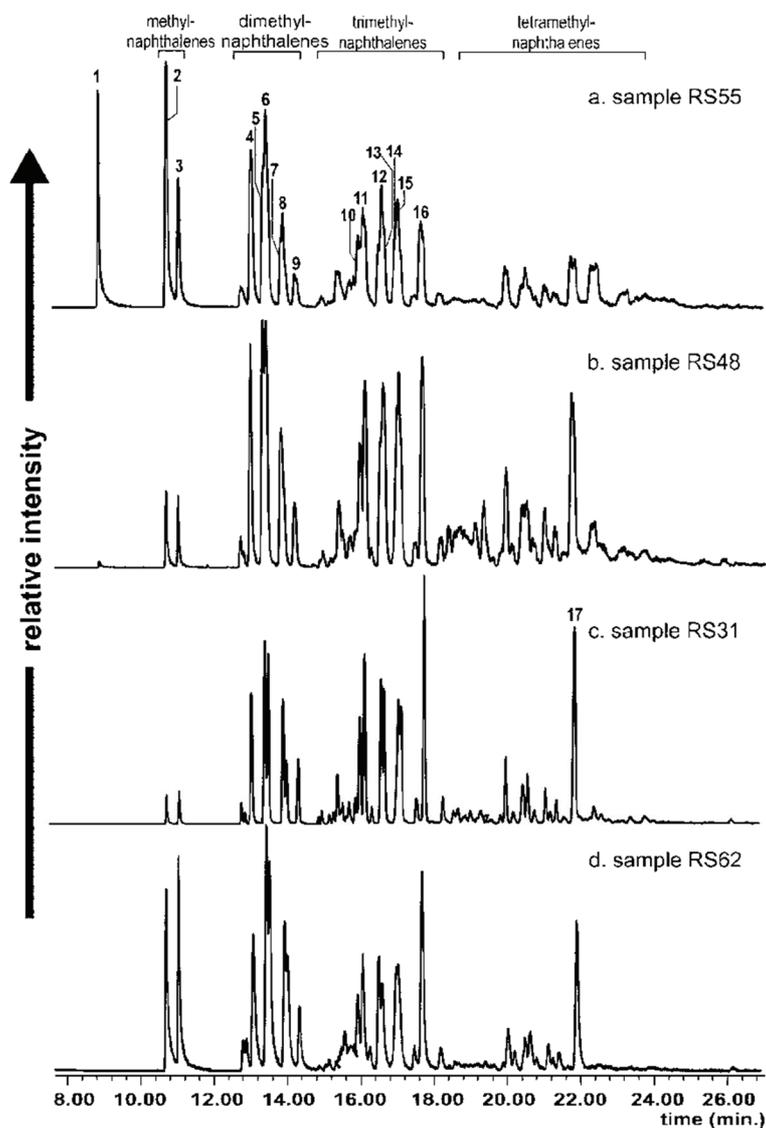
Fig. 12. Composed ion chromatogram showing distributions of naphthalene and alkylnaphthalenes in the Rymer Cones coal wastes extracts (m/z=128+142+156+170+184). 1: naphthalene, 2: 2-methylnaphthalene, 3: 1-methylnaphthalene, 4: 2,6+2,7-dimethylnaphthalene, 5: 1,3+1,7-dimethylnaphthalene, 6: 1,6-dimethylnaphthalene, 7: 1,4+2,3-dimethylnaphthalene, 8: 1,5-dimethylnaphthalene, 9: 1,2-dimethylnaphthalene,10: 1,3,7-trimethylnaphthalene, 11: 1,3,6-trimethylnaphthalene, 12: 1,4,6+1,3,5-trimethylnaphthalene, 13: 2,3,6-trimethylnaphthalene, 14: 1,2,7+1,6,7-trimethylnaphthalene, 15: 1,2,6-trimethylnaphthalene, 16: 1,2,5-trimethylnaphthalene, 17: 1,2,3,4-tetramethylnaphthalene.

144
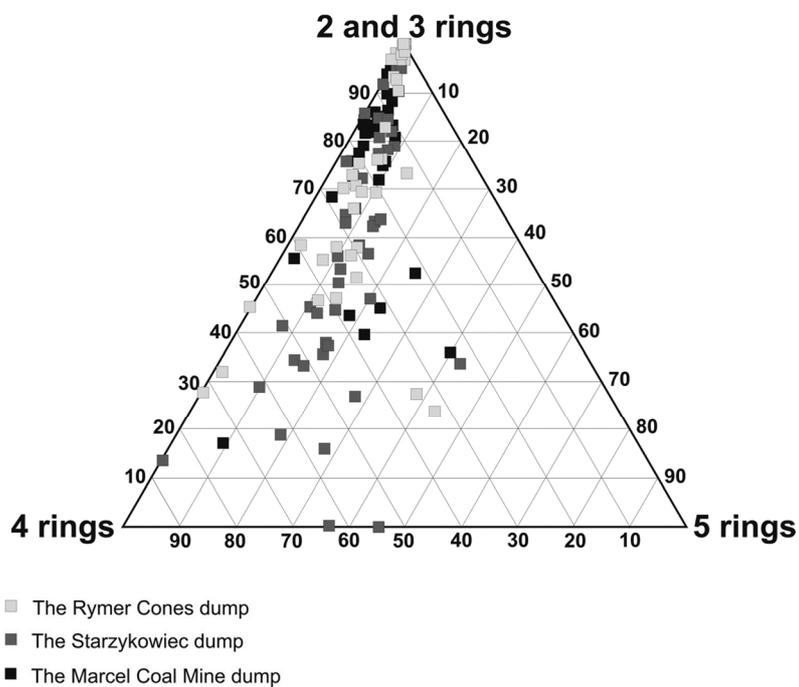
Fig. 13. Distribution of two-and three-, four-, five-ring polycyclic aromatic hydrocarbons in coal wastes from the dumps at Rymer Cones, Starzykowiec and Marcel Coal Mine, calculated as relative percentage concentrations.
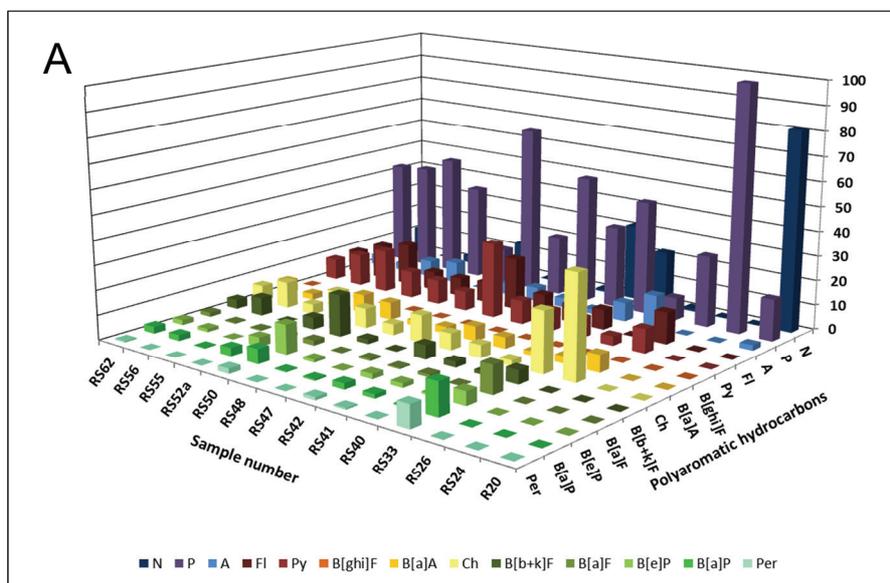
Fig. 14A. Distribution of PAHs in selected samples from the Rymer Cones coal wastes.
A – calculated as relative concentrations from ion chromatograms (m/z = 128, 178, 202, 228, and 252).
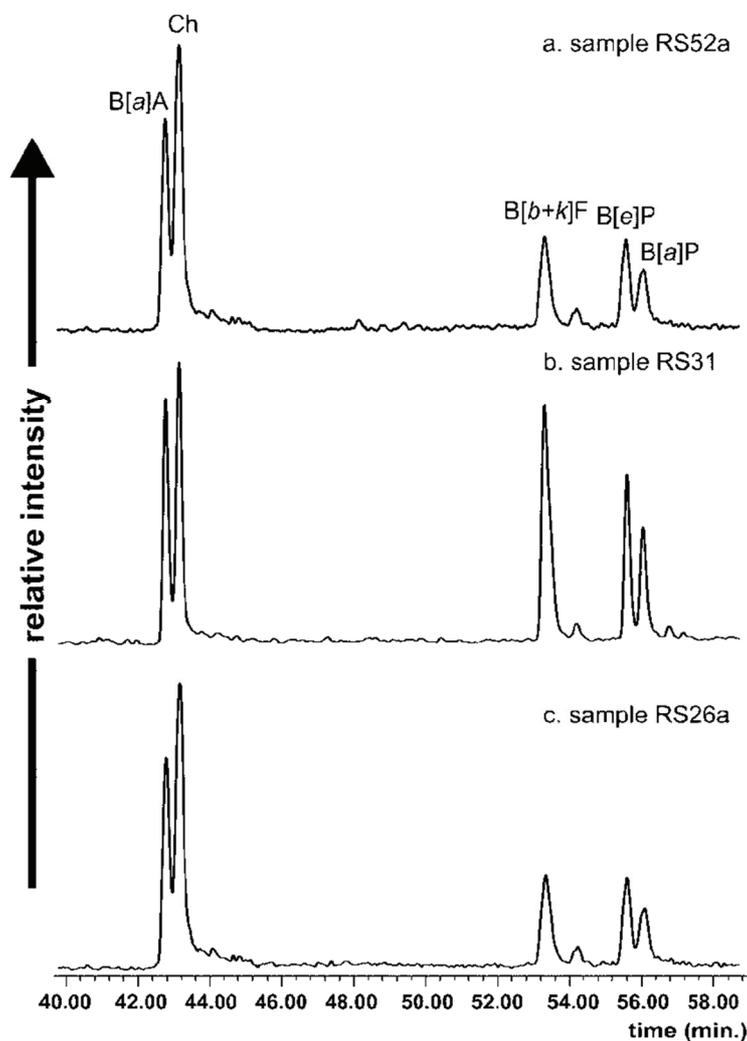
Fig. 14B. Distribution of PAHs in selected samples from the Rymer Cones coal wastes.
B – composed ion chromatograms of four- and five- ring PAHs (m/z = 228, 252). N – naphthalene,
P – phenanthrene, A – anthracene, Fl – fluoranthene,
Py – pyrene, B[ghi]F - benzo[g]fluoranthene+benzo[h]fluoranthene+benzo[i]fluoranthene,
B[a]A – benzo[a]anthracene, Ch – chrysene, B[$k+f$]F – benzo[k]fluoranthene+
benzo[f]fluoranthene, B[a]F – benzo[a]fluoranthene, B[e]P – benzo[e]pyrene,
B[a]P – benzo[a]pyrene, Per – perylene.
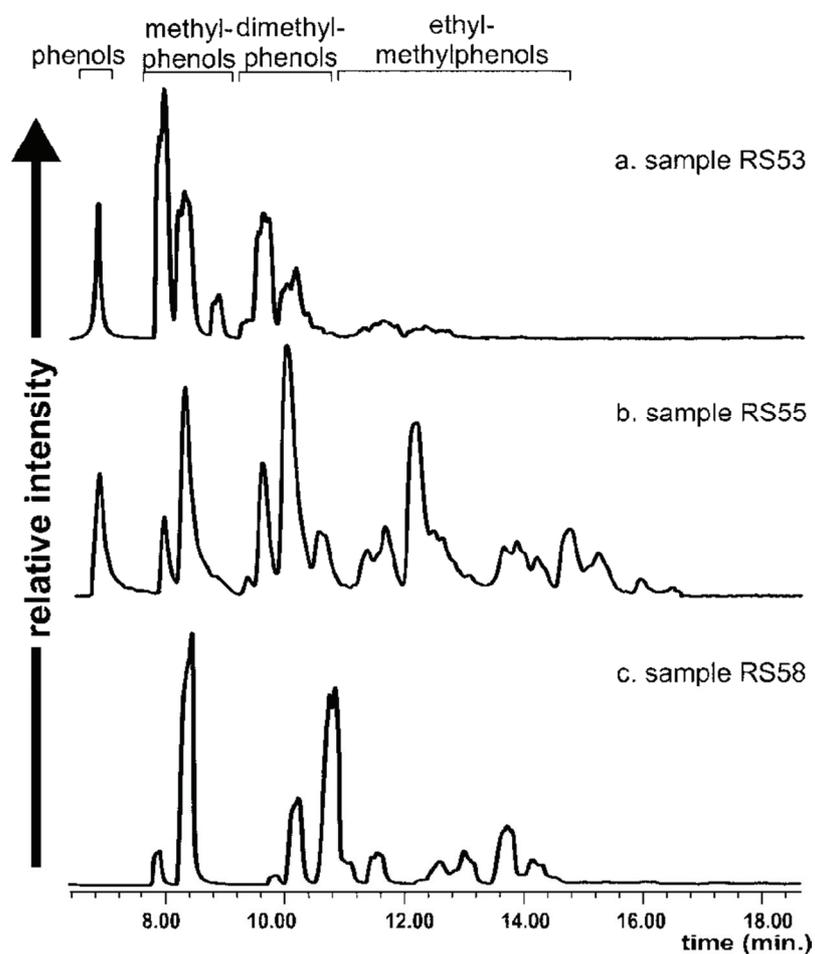
Fig. 15. Distribution of phenol and its derivatives in coal waste samples from the Rymer Cones dump (m/z = 94+108+122+136+150+164).

Chemical parameters of thermal maturation vary considerably in the fly ash and soil samples. Interestingly, hopanes and phenols are absent in fly ash samples (Table 5). In these, n-alkanes display the widest range (n-C_{13}-n-C_{22}) and their distribution is Gaussian with the maximum at n-C_{18} (RRS0 and RRS2; Fig. 16a). Except for RRS2, CPI values are higher than in the coal wastes. They also show a predominance of long-to-short chain n-alkanes that is reflected in $\Sigma1/\Sigma2$ values in the range 0.36-0.81. Pr/Ph shows the highest value (5.30) in RRS0 – a value probably due to generated hydrocarbons. Other fly ash Pr/Ph values are much lower. Pr/n-C_{17} and Ph/n-C_{18} values are also low (Table 5).
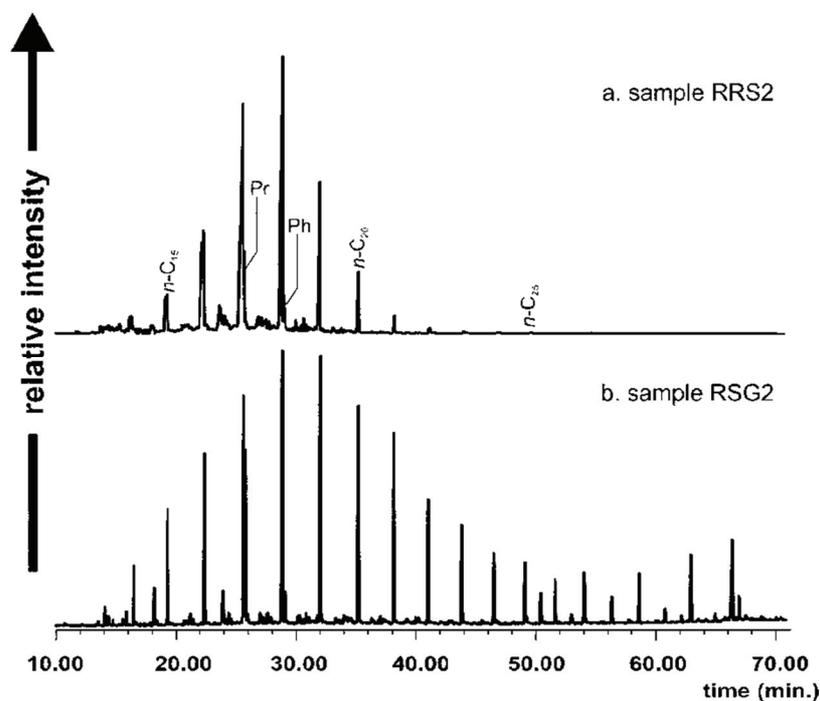
Fig. 16. *n*-Alkane distribution in (a) fly ash and (b) soil extracts (*m/z* = 71) from samples collected at the Rymer Cones dump.

Indices of thermal maturation based on substituted polycyclic aromatic hydrocarbons in the fly ash samples fall in the same range as for coal wastes (Table 6; Fig. 17a-b). Polycyclic aromatic hydrocarbons (PAHs) are absent in RRS0. In the other two samples, phenanthrene is the only representative of two- and three-ring PAHs. In general, four-ring PAHs are represented mostly by fluoranthene and pyrene. In RRS3, a small amount of chrysene was detected. All compounds of five-ring PAHs were found only in RRS2, none in RRS0 or RRS1 (Table 7).

The soil samples have a composition completely different from that of the fly ash. They all contain *n*-alkanes with the Gaussian distribution in the widest range from $n\text{-}C_{14}$ to $n\text{-}C_{35}$ (Fig. 16b). Sample RSG1 contains a mixture of pyrolysates generated at different temperatures. The CPI values for the soils are generally much higher than those for the coal wastes and long-chain *n*-alkanes predominate over their short-chain homologues; $\Sigma 1/\Sigma 2$ values are in the range 0.32-0.76. Except RSG4, all of the other samples have Pr/Ph values > 4. In RSG4, the value is < 1. $\text{Pr}/n\text{-}C_{17}$ and $\text{Ph}/n\text{-}C_{18}$ values are low (Table 5).

Hopanes in the soils are represented mainly by C_{29} and C_{30} hopanes. C_{31} hopanes are present only in RSG6 (25.78 rel.%). $\alpha\beta$ and $\beta\alpha$ hopanes are dominant in all soil samples while $\beta\beta$ hopanes are absent in RSG2 and RSG4 and, in RSG1 and RSG6, their contents are < 10 rel.%. Values of indices of thermal maturation based on hopanes are low or they were not calculated due to their absence or very low concentration (Table 5). However, Ts/(Ts+Tm) values in the range 0.56-0.90 compare to those in coal wastes (Fig. 18).

148
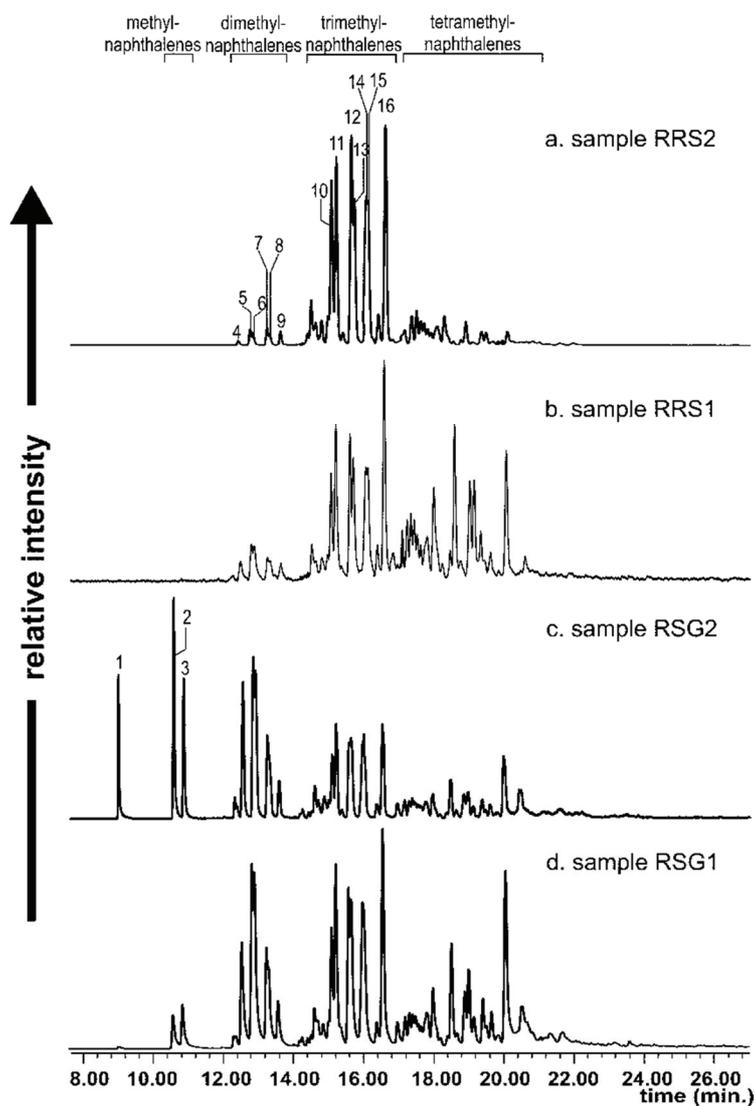
Fig. 17. Composed ion chromatogram showing distributions of naphthalene and alkylnaphthalenes in fly ash (a, b) and soil (c, d) extracts (m/z = 128+142+156+170+184) from samples collected at the Rymer Cones dump. 1: naphthalene, 2: 2-methlnaphthalene, 3: 1-methylnaphthalene, 4: 2,6+2,7-dimethylnaphthalene, 5: 1,3+1,7-dimethylnaphthalene, 6: 1,6-dimethylnaphthalene, 7: 1,4+2,3-dimethylnaphthalene, 8: 1,5-dimethylnaphthalene, 9: 1,2-dimethylnaphthalene, 10: 1,3,7-trimethylnaphthalene, 11: 1,3,6-trimethylnaphthalene, 12: 1,4,6+1,3,5-trimethylnaphthalene, 13: 2,3,6-trimethylnaphthalene, 14: 1,2,7+1,6,7-trimethylnaphthalene, 15: 1,2,6-trimethylnaphthalene, 16: 1,2,5-trimethylnaphthalene.

TABLE 7

Contents of PAHs in coal wastes, fly ash, and soils from the Rymer Cones dump (relative % calculated into total PAHs content)

| Sample no.	N	P	A	Fl	Py	B[ghi]F	B[a]A	Ch	B[b+k]F	B[a]F	B[e]P	B[a]P	Per
						Coal wastes							
R1	0.00	0.00	0.00	0.00	0.00	0.00	0.00	0.00	0.00	0.00	0.00	0.00	0.00
R3	17.25	82.75	0.00	0.00	0.00	0.00	0.00	0.00	0.00	0.00	0.00	0.00	0.00
R5	27.18	24.34	7.28	10.62	10.55	0.00	0.00	10.16	2.40	3.98	1.53	1.52	0.45
R7	46.25	23.71	0.00	6.58	4.34	0.00	0.00	8.41	1.67	3.54	1.53	2.90	1.06
R8	2.11	44.88	0.00	15.38	7.94	0.00	0.00	29.69	0.00	0.00	0.00	0.00	0.00
R18	81.71	5.45	6.23	1.56	1.56	0.00	1.17	1.17	0.39	0.00	0.39	0.39	0.00
R20	81.01	16.81	2.18	0.00	0.00	0.00	0.00	0.00	0.00	0.00	0.00	0.00	0.00
RS24	0.04	99.67	0.10	0.19	0.00	0.00	0.00	0.00	0.00	0.00	0.00	0.00	0.00
RS25	11.66	88.34	0.00	0.00	0.00	0.00	0.00	0.00	0.00	0.00	0.00	0.00	0.00
RS26	0.16	28.80	0.00	12.83	9.72	0.00	6.96	41.53	0.00	0.00	0.00	0.00	0.00
RS26a	0.02	55.55	1.42	8.82	8.05	0.00	5.10	12.19	3.76	0.27	2.50	0.88	0.21
RS27	0.00	100.00	0.00	0.00	0.00	0.00	0.00	0.00	0.00	0.00	0.00	0.00	0.00
RS28	96.16	3.84	0.00	0.00	0.00	0.00	0.00	0.00	0.00	0.00	0.00	0.00	0.00
RS28a	97.47	0.39	0.01	0.50	0.50	0.00	0.00	0.85	0.08	0.07	0.04	0.09	0.00
RS29	0.61	27.11	41.83	6.58	6.46	0.00	0.49	9.29	1.07	2.76	1.25	1.92	0.00
RS30	2.09	86.94	10.96	0.00	0.00	0.00	0.00	0.00	0.00	0.00	0.00	0.00	0.00
RS31	0.07	48.13	3.22	10.27	9.12	0.00	5.81	7.24	7.90	0.38	3.90	2.81	0.40
RS32	48.60	8.13	15.70	1.04	4.84	0.00	2.74	4.94	2.12	3.86	2.88	4.03	1.12
RS32a	45.36	54.64	0.00	0.00	0.00	0.00	0.00	0.00	0.00	0.00	0.00	0.00	0.00
RS33	1.20	9.00	13.34	0.00	3.81	0.00	2.92	24.47	5.53	11.37	5.46	13.07	8.98
RS34a	37.66	49.35	12.66	0.04	0.29	0.00	0.00	0.00	0.00	0.00	0.00	0.00	0.00

RS40	22.17	46.26	7.61	8.20	8.22	0.00	1.70	2.21	1.39	0.27	0.79	0.56	0.16
RS41	31.17	33.41	1.88	7.33	8.43	0.00	4.59	5.16	2.28	1.13	1.73	1.59	0.57
RS42	0.96	51.83	3.75	8.62	9.47	0.00	5.96	6.71	5.75	0.53	2.02	2.32	1.21
RS45	97.29	0.65	0.61	0.65	0.21	0.00	0.09	0.16	0.14	0.01	0.09	0.08	0.00
RS46	2.33	85.30	11.19	0.25	0.90	0.00	0.01	0.00	0.00	0.00	0.00	0.00	0.00
RS47	1.06	24.32	5.67	21.09	30.50	0.00	2.79	11.02	0.28	0.82	0.15	0.65	0.00
RS48	0.11	68.27	4.69	8.41	7.78	0.00	2.08	4.42	1.87	0.11	1.12	0.40	0.14
RS48a	88.84	8.02	1.45	0.52	0.66	0.00	0.26	0.17	0.00	0.00	0.00	0.00	0.00
RS49	85.13	7.28	0.42	1.74	1.77	0.00	0.83	1.08	0.83	0.05	0.45	0.21	0.07
RS50	13.61	14.11	0.00	7.56	9.84	0.00	7.05	7.97	16.85	2.00	11.92	5.94	2.06
RS52a	0.20	38.85	8.69	7.60	10.88	0.00	7.48	12.05	4.84	0.94	3.83	3.27	0.00
RS53	80.28	9.54	0.67	2.09	2.11	0.00	1.43	0.99	1.40	0.11	0.62	0.43	0.09
RS54	0.07	85.13	12.79	1.62	0.40	0.00	0.00	0.00	0.00	0.00	0.00	0.00	0.00
RS55	2.91	49.43	6.91	17.11	17.42	0.00	0.79	4.01	0.13	0.47	0.08	0.35	0.00
RS56	0.00	43.74	3.14	14.29	13.11	0.00	2.45	10.51	7.32	0.46	1.34	2.36	0.00
RS57	0.00	67.50	3.15	8.72	6.25	0.00	2.06	6.94	2.05	0.39	1.28	0.32	0.53
RS58	36.55	36.46	8.24	4.63	4.62	0.00	1.76	2.70	2.13	0.27	0.91	0.96	0.48
RS59	6.10	78.80	15.10	0.00	0.00	0.00	0.00	0.00	0.00	0.00	0.00	0.00	0.00
RS60	1.50	72.80	2.56	5.60	3.63	0.00	1.76	4.25	2.36	0.87	2.20	2.47	0.00
RS61	55.85	19.78	1.52	4.85	4.98	0.00	2.65	3.54	2.44	0.68	1.48	1.31	0.41
RS62	11.20	42.77	4.29	9.26	8.72	0.00	5.34	6.44	3.71	1.67	1.99	2.73	0.53
RS62a	1.19	62.37	6.90	9.64	8.18	0.00	1.78	6.22	0.79	0.79	1.13	0.30	0.17
Fly ash													
RRS0	0.00	0.00	0.00	0.00	0.00	0.00	0.00	0.00	0.00	0.00	0.00	0.00	0.00
RRS1	0.00	70.78	0.00	16.08	13.14	0.00	0.00	0.00	0.00	0.00	0.00	0.00	0.00
RRS2	0.00	47.09	0.00	13.49	11.46	0.00	0.00	1.20	4.12	9.47	7.07	3.24	2.85

				Soils									
RSG1	0.00	52.94	0.00	11.58	9.99	0.00	2.48	6.32	8.54	0.87	3.05	3.27	0.96
RSG2	3.87	38.08	26.18	12.13	7.59	0.94	2.51	8.71	0.00	0.00	0.00	0.00	0.00
RSG4	2.72	85.74	0.00	7.39	4.15	0.00	0.00	0.00	0.00	0.00	0.00	0.00	0.00
RSG6	0.00	52.99	0.00	9.77	11.23	0.00	11.60	0.00	7.87	0.00	4.90	1.63	0.00

N – naphthalene, P – phenanthrene, A – anthracene, Fl – fluoranthene, Py – pyrene, B(*ghi*)F – benzo(*g*)fluoranthene+benzo(*h*)fluoranthene+ benzo(*i*)fluoranthene, B(*a*)A – benzo(*a*)anthracene, Ch – chrysene, B(*k*+*j*)F – benzo(*k*)fluoranthene+benzo(*k*)fluoranthene, B(*a*)F – benzo(*a*)fluoranthene, B(*e*)P – benzo(*e*)pyrene, B(*a*)P – benzo(*a*)pyrene, Per – perylene.

Fig. 18. Pentacyclic triterpane distribution in the extracts from soil samples collected at the Rymer Cones dump (m/z = 191). Ts – 18α(H)-22,29,30-trisnorneohopane, Tm – 17α(H)-22,29,30-trisnorhopane, C$_{29}\alpha\beta$ – 17α,21β(H)-30-norhopane, C$_{29}\beta\alpha$ – 18α,21β(H)-30-norneohopane, C$_{30}\alpha\beta$ – 17α,21β(H)-hopane, C$_{30}\beta\beta$ – 17β,21β(H)-hopane, C$_{30}\beta\alpha$ – 17β,21α(H)-hopane, C$_{31}\alpha\beta$ – 17α,21β(H)-30-homohopane 22S and 22R, C$_{31}\beta\alpha$ – 18α,21β(H)-30-homohopane 22R, C$_{32}\alpha\beta$ – 17α,21β(H)-30-bishomohopane 22S and 22R, 1 – homohop-22(29)-en-3β-ol.

Values of indices based on polyaromatic hydrocarbons in the soils lie in the same range as for the coal wastes (Table 6; Fig. 17c-d).

PAHs with two- and three-rings dominate over four- and five-ring PAHs in all soil samples (Table 7). Phenanthrene is the main representative of these PAHs though anthracene is also present in considerable quantity in RSG2. Naphthalene is present only in RSG2 and RSG4 and at contents < 4 rel.%. Fluoranthene and pyrene are the dominating compounds of the four-ring PAHs. However, RSG1 and RSG2 also contain a marked amount of chrysene (6.32 and 8.71 rel.%, respectively). RSG6 contains the most benzo[a]anthracene (11.60 rel.%) and RSG1 (2.48 rel.%) and RSG2 (2.51 rel.%), similar amounts; there is none at all in RSG4. PAHs with five rings are absent in samples RSG2 and RSG4. Benzo[b+k]fluoranthene, benzo[a]pyrene, and benzo[e]pyrene are the most important in the remaining samples (Table 7).

Phenols are present in all soil samples but their distributions differ. They are present in relatively higher quantities in RSG2 and RSG6, much lower quantities in the remainder. Phenols except methylpropylphenols occur in RSG2 (Fig. 19a). Phenol is absent and ethylphenols are present in low relative amounts in RSG6 (Fig. 19b).
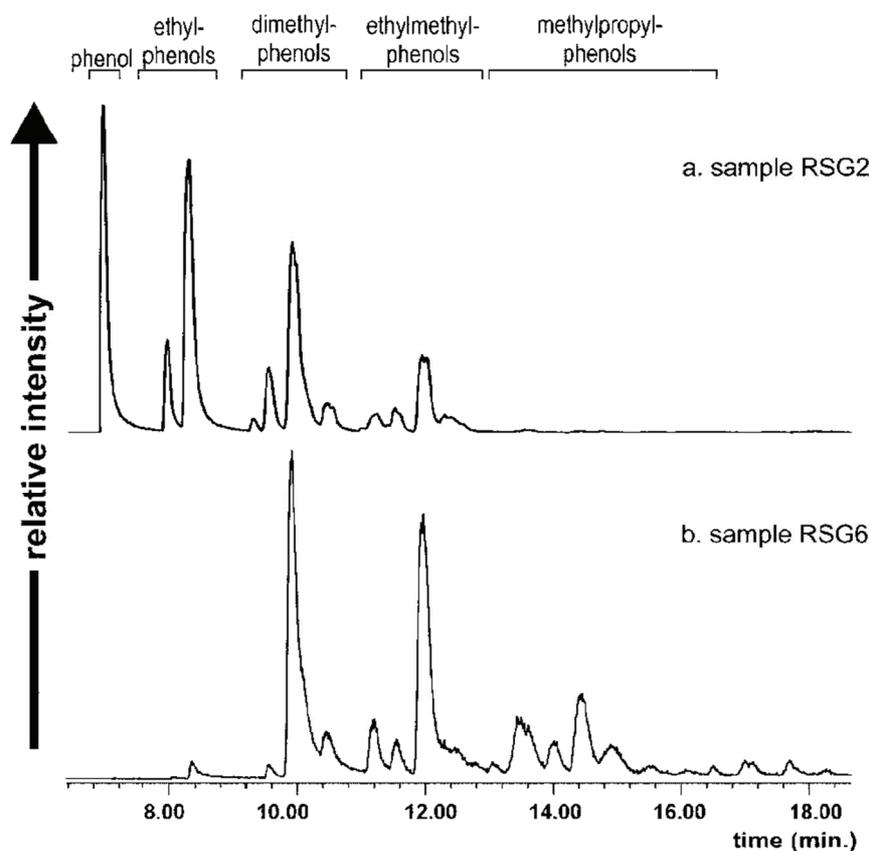
Fig. 19. Distribution of phenol and its derivatives in soils covering the Rymer Cones dump
(m/z = 94+108+122+136+150+164).

6.4. Proximate and ultimate analyses

The ash content (A^a) in waste samples collected in the Rymer Cones dump is on average 76.32 wt% (Table 8). Moisture contents (M^a) are low at < 3.30 wt%. Volatile matter content (VM^{daf}) is on average 76.32 wt%. Calorific values (Q_s^{daf}) range from 0.58-25.32 MJ·kg^{-1} and is lowest in RS26a. Carbon contents (C^{daf}) range widely with an average of 59.09 wt%. Hydrogen contents (H^{daf}) are < 6.88 wt% and nitrogen contents (N^{daf}) are < 3 wt%. Oxygen contents (O^{daf}) are on average 31.76 wt%. Total sulphur (S_t^a) is typically low - on average 0.56 wt%; RS34a is an exception (2.36 wt%; Table 8).

154

TABLE 8

Proximate and ultimate analyses of coal wastes from the Rymer Cones dump

Sample no.	M^a (wt%)	A^a (wt%)	VM^{daf} (wt%)	Q_s^{daf} (MJ·kg^{-1})	C^{daf} (wt%)	H^{daf} (wt%)	N^{daf} (wt%)	O^{daf} (wt%)	S_t^a (w.%)
RS24	1.96	62.22	63.18	25.32	68.68	5.14	1.23	22.17	1.00
RS25	2.65	75.49	51.05	17.70	59.47	4.25	2.20	33.07	0.22
RS26	3.13	72.66	53.20	17.83	59.48	4.34	2.31	31.23	0.64
RS26a	2.04	89.42	98.01	0.58	16.39	3.63	1.87	77.87	0.02
RS27	2.38	78.52	47.23	19.05	64.92	3.72	1.99	27.80	0.30
RS28	1.70	79.46	47.08	17.74	62.63	4.35	2.34	28.56	0.40
RS28a	3.30	59.44	44.34	24.16	68.71	4.64	1.61	22.87	0.81
RS29	1.52	82.00	49.88	17.52	60.07	4.19	1.94	32.71	0.18
RS30	0.93	79.04	63.85	18.80	57.91	5.34	2.00	32.10	0.53
RS31	1.87	84.62	57.66	12.24	45.89	4.96	1.63	47.00	0.07
RS32	2.37	81.60	64.88	12.39	47.41	4.93	1.50	45.04	0.18
RS32a	2.06	84.55	65.27	9.97	42.57	4.56	2.39	46.00	0.60
RS33	1.30	78.96	50.56	17.06	58.76	4.61	2.63	31.97	0.40
RS34a	1.81	70.46	56.33	25.32	71.76	4.76	2.24	12.73	2.36
RS40	1.99	79.95	62.90	20.65	66.45	4.87	1.66	35.11	0.13
RS41	1.38	73.90	54.85	19.95	64.72	6.07	1.25	26.42	0.38
RS42	1.30	78.56	59.68	17.71	59.58	5.91	1.49	32.13	0.18
RS44	1.66	59.64	53.95	22.36	65.37	5.09	1.47	25.71	0.91
RS45	0.98	79.66	54.55	17.71	57.33	6.56	2.38	29.44	0.83
RS46	0.72	81.40	63.98	17.77	58.72	6.88	1.85	29.64	0.52
RS47	1.84	71.56	51.95	20.62	64.29	6.05	2.03	26.50	0.30
RS48	1.90	83.15	70.10	9.63	49.50	5.48	1.61	42.74	0.10
RS48a	1.26	76.80	61.94	16.78	58.34	5.33	2.51	29.31	0.99
RS49	2.30	63.02	48.59	22.35	64.59	5.42	1.59	25.55	0.99
RS50	1.20	86.78	52.66	19.38	70.72	3.74	3.00	20.22	0.28
RS51	1.16	72.36	45.47	21.93	68.73	5.51	2.00	19.90	1.02
RS52	1.48	72.76	56.60	20.23	63.66	5.75	1.44	27.76	0.36
RS52a	1.30	73.79	48.45	20.05	65.44	4.86	2.57	24.41	0.68
RS53	1.84	81.50	76.23	13.64	51.62	6.60	2.04	35.17	0.76

M – moisture, A – ash, VM – volatile matter, Q_s – calorific value, C – carbon, H – hydrogen,
N – nitrogen, O – oxygen, S – sulphur, a – air dry basis, daf – dry ash free basis, t – total.

7. The Starzykowiec dump – results

7.1. Temperatures on the surface and within the dump

During the period of sample collection, surface temperatures ranged from 7-85°C. Temperatures at a depth of *ca* 1 m ranged from 24°C (sample CH12) to 448°C (sample CH3). Interior temperatures were, on average, several tens of °C higher than surface temperatures (Table 9).

TABLE 9

Surface temperatures (T_s) and interior temperatures (T_i) measured at a depth of 1m in the Starzykowiec dump (Tabor 2002-2009), and petrographic composition and random reflectance analyses for samples from the dump

Sample no.	T_s (°C)	T_i (°C)	Unaltered vitrinite (vol.%)	Vitrinite with cracks (vol.%)	Paler coloured vitrinite (vol.%)	Vitrinite with pores (vol.%)	Liptinite (vol.%)	Inertinite (vol.%)	Pyrolytic carbon (vol.%)	Coke (vol.%)	Mineral matter (vol.%)	R_r (%)	Standard deviation for R_r
C1	7	-	43.6	0.0	0.0	0.0	1.0	10.4	0.0	0.0	45.0	0.63	0.06
C2	31	-	5.2	2.0	0.0	0.0	0.0	0.2	0.0	0.2	92.4	0.62	0.05
C3	56	-	36.2	6.2	0.0	0.0	1.2	5.0	0.0	1.4	50.0	0.68	0.05
C4	15	-	20.0	1.4	0.0	0.0	2.0	5.0	0.0	1.4	70.2	0.60	0.06
C5	50	-	16.2	0.0	0.0	0.0	0.8	9.6	0.0	0.0	73.4	0.67	0.06
C6	19	-	7.8	0.0	0.6	0.0	1.0	0.8	0.0	0.0	89.8	0.68	0.06
C7	60	-	5.2	0.6	0.0	0.0	0.6	0.6	0.0	0.0	93.0	0.61	0.06
C8	43	-	13.6	0.0	0.2	0.0	2.2	7.6	0.0	0.2	76.2	0.62	0.06
C9	53	-	15.0	3.6	0.0	0.0	2.8	2.0	0.0	0.0	76.6	0.63	0.06
C11	-	140	0.2	0.6	0.6	0.0	0.0	0.0	0.0	0.0	98.6	0.79	0.12
C12	-	140	0.0	0.0	0.0	0.0	0.0	0.0	0.0	2.8	97.2	1.79	0.21
C13	-	140	9.4	0.0	1.0	0.0	3.4	3.8	0.0	0.0	82.4	0.68	0.06
C14	-	140	0.0	0.0	11.0	0.0	0.0	0.0	0.0	0.0	89.0	1.33	0.14
C15	40	-	8.2	0.6	0.0	0.0	1.0	2.0	0.0	0.0	88.2	0.67	0.06
C16	40	-	2.2	0.0	0.2	0.0	0.0	0.0	0.0	0.0	97.6	0.74	0.09
C17	40	-	0.0	0.0	5.2	0.0	0.0	0.0	0.0	0.2	94.6	1.53	0.50
C18	40	-	42.4	0.8	0.0	0.0	2.0	9.4	0.0	0.0	45.4	0.61	0.04
C19	60	-	61.4	0.2	0.0	0.0	5.2	12.0	0.0	0.0	21.2	0.62	0.03
C20	60	-	14.0	0.2	0.4	0.0	1.2	2.2	0.0	0.0	82.0	0.64	0.04
C21	-	130	22.4	0.0	0.0	0.0	1.4	3.2	0.0	0.6	72.4	0.69	0.09
C22	-	120	9.0	0.4	0.2	0.0	0.2	1.0	0.0	0.8	88.4	0.66	0.04
C23	-	125	4.4	0.0	5.6	0.0	0.4	0.8	0.0	0.0	88.8	0.78	0.08
C24	74	-	13.0	0.0	0.6	0.0	1.8	3.0	0.0	0.0	81.6	0.66	0.05
C25	-	130	25.0	0.6	0.0	0.0	1.2	3.0	0.0	0.0	70.2	0.62	0.05
C26	-	130	21.0	0.0	1.0	0.0	1.6	1.6	0.0	0.0	74.8	0.66	0.12

C27	-	130	12.2	1.0	1.2	0.0	0.6	0.4	0.0	0.2	84.4	0.70	0.05
CH1	-	32	19.8	0.2	0.4	0.0	1.6	1.4	0.0	0.0	76.6	0.62	0.04
CH2	-	315	12.0	0.6	0.8	0.0	0.8	5.6	0.0	0.0	80.2	0.68	0.08
CH3	-	448	11.2	1.4	2.8	0.4	0.4	4.0	0.0	0.4	79.4	0.88	0.16
CH4	39.5	-	13.0	0.6	0.2	0.0	0.6	2.4	0.0	0.0	83.2	0.82	0.32
CH5a	73	-	9.4	0.2	0.2	0.0	1.0	1.6	0.0	1.0	86.6	0.60	0.04
CH6	27	-	7.6	2.0	0.2	0.0	1.2	1.4	0.0	0.4	87.2	0.63	0.07
CH7	75	-	7.2	0.0	0.0	0.0	0.8	0.0	0.0	0.0	92.0	0.59	0.09
CH8	85	-	18.4	0.6	0.0	0.0	2.0	5.2	0.0	0.2	73.6	0.70	0.06
CH9	44.5	-	31.0	0.0	0.6	0.0	1.4	6.6	0.0	0.0	60.4	0.62	0.04
CH10	-	250	16.6	1.2	0.0	0.0	0.4	2.0	0.0	0.0	79.8	0.67	0.07
CH11	12	-	0.0	0.0	1.2	0.0	0.0	0.0	0.0	0.0	98.8	1.22	0.17
CH12	-	24	29.4	2.2	0.0	0.0	1.8	3.0	0.0	0.0	63.6	0.68	0.05
CH13	-	35.5	11.0	0.8	0.4	0.0	1.2	1.0	0.0	1.0	84.6	0.89	0.09
CH14	24	-	21.2	0.2	0.2	0.0	1.0	4.4	0.0	1.2	71.8	0.68	0.04
CH15	13	-	14.2	0.8	0.0	0.0	1.2	4.8	0.0	0.0	79.0	0.64	0.05
CH16	9	-	13.4	0.2	0.0	0.0	0.8	1.4	0.0	0.0	84.2	0.57	0.06
CH17	17	16.6	7.8	0.2	1.2	0.0	0.2	0.6	0.0	0.0	90.0	0.57	0.15
CH18	39	210	11.0	0.4	0.0	0.0	1.0	1.6	0.0	1.0	85.0	0.56	0.05
CH19	-	63.2	12.6	0.6	0.0	0.0	0.4	1.8	0.0	0.0	84.6	0.55	0.05
CH20	-	70.2	13.8	0.0	0.0	0.0	0.8	2.0	0.0	0.0	83.4	0.55	0.05
CH21	-	66	16.8	0.0	0.0	0.0	0.6	0.8	0.0	0.0	81.8	0.56	0.06
CH22	-	46.6	8.6	0.0	0.0	0.0	0.6	0.8	0.0	0.0	90.0	0.56	0.11

"-" measurement not taken

7.2. Petrography

The mineral matter content in the samples varies from 21.2-98.8 vol.%, usually 70-80 vol.% (Table 9). It mostly comprises clay minerals and framboidal pyrite and, in some cases, carbonates. In most samples, the clay minerals are partly altered due to heating.

Organic matter commonly occurs as lenses and laminae of various widths and lengths and as dispersed organic matter. It is represented mostly by vitrinite macerals in all samples except C12; this last is composed entirely of altered organic matter (coke) and minerals (Tables 9, 10). Vitrinite macerals occur as unaltered macerals (Fig. 20a), paler-coloured macerals (Fig. 20b-c), macerals with irregular cracks (Fig. 20b-c), and macerals with pores (Fig. 20d). Pale oxidation rims around the edges of some vitrinite particles and along cracks also occur in samples C17, CH2-CH4 (Fig. 20e-f). Vitrinite group macerals may occur alone (Fig. 20b, 20f) or with macerals of other groups and/or minerals, typically clay minerals and pyrite (Fig. 20a, 20c-e). The most common macerals of this group are collotelinite (Fig. 20a-c, 20f) and vitrodetrinite. Occasionally collodetrinite (Fig. 20a, 20c, 20e), corpogelinite, and telinite with cells filled with resinite, are present.

Most liptinite macerals except alginite are present in the wastes, e.g. sporinite (Fig. 20a, 20c, 20e). These macerals commonly occur with vitrinite, inertinite, and with minerals.

Fusinite, semifusinite (Fig. 20a, 20c), and inertodetrinite (Fig. 20a, 20c, 20e) are the most common macerals of the inertinite group. In some samples, macrinite (Fig. 20c), funginite, and micrinite occur.

Coke is present in several samples (Tables 9, 10; Fig. 21a-b) as an admixture deriving from other, much more strongly altered parts of the dump. The exception is C12 in which coke is the only form of organic matter microscopically visible.

Bitumens generated from macerals are seen in C4, C6-C9, C13, C15, C16, C18-27, CH1-CH3, CH5a-CH10, CH12-16, CH18, and CH21 (Fig. 21c-f). They occur as irregular- or thread-like forms in quantities < 0.2 vol.%.

Vitrinite maceral contents range from 1.2-61.6 vol.% (Table 9), 58.0-100.0 vol.%, mmf (Table 10). Several samples contain only unaltered vitrinite macerals (Tables 9, 10). Amounts range from 0.2 vol.% in sample C11 to 61.4 vol.% in sample C19, except for C12 and C14 which contain no unaltered vitrinite. Usually, unaltered vitrinite macerals occur together with macerals with cracks (e.g. C2-C4, CH18, and CH19) and with paler-coloured macerals (e.g. C6, C16, and CH9; Tables 9, 10). Unaltered vitrinite occurs with both forms of altered vitrinite in several samples (Tables 9, 10). Vitrinite with cracks dominates in C3 (6.2 vol.%). Paler-coloured vitrinite is the only form of organic matter in C14 and vitrinite with pores occurs only in sample CH3 (Tables 9, 10).

Liptinite is present in amounts up to 5.2 vol.% in sample C19 which also contains the highest content of unaltered vitrinite (Table 9). On a mmf basis, liptinite is most abundant in C13 (19.3 vol.%, mmf; Table 10).

Inertinite macerals occur in amounts up to 12.0 vol.% in sample C19 (Table 9). On a mmf basis, the highest content occurs in sample C5 (Table 10).

TABLE 10

Petrographic composition of coal waste samples from the Starzykowiec dump calculated on a mineral matter free (mmf) basis

Sample no.	Unaltered vitrinite (vol.%)	Vitrinite with cracks (vol.%)	Paler coloured vitrinite (vol.%)	Vitrinite with pores (vol.%)	Liptinite (vol.%)	Inertinite (vol.%)	Pyrolytic carbon (vol.%)	Coke (vol.%)
C1	79.3	0.0	0.0	0.0	1.8	18.9	0.0	0.0
C2	68.4	26.3	0.0	0.0	0.0	2.6	0.0	2.6
C3	72.4	12.4	0.0	0.0	2.4	10.0	0.0	2.8
C4	67.1	4.7	0.0	0.0	6.7	16.8	0.0	4.7
C5	60.9	0.0	0.0	0.0	3.0	36.1	0.0	0.0
C6	76.5	0.0	5.9	0.0	9.8	7.8	0.0	0.0
C7	74.3	8.6	0.0	0.0	8.6	8.6	0.0	0.0
C8	57.1	0.0	0.8	0.0	9.2	31.9	0.0	0.8
C9	64.1	15.4	0.0	0.0	12.0	8.5	0.0	0.0
C11	14.3	42.9	42.9	0.0	0.0	0.0	0.0	0.0
C12	0.0	0.0	0.0	0.0	0.0	0.0	0.0	100.0
C13	53.4	0.0	5.7	0.0	19.3	21.6	0.0	0.0
C14	0.0	0.0	100.0	0.0	0.0	0.0	0.0	0.0
C15	69.5	5.1	0.0	0.0	8.5	16.9	0.0	0.0
C16	91.7	0.0	8.3	0.0	0.0	0.0	0.0	0.0
C17	0.0	0.0	96.3	0.0	0.0	0.0	0.0	3.7
C18	77.7	1.5	0.0	0.0	3.7	17.2	0.0	0.0
C19	77.9	0.3	0.0	0.0	6.6	15.2	0.0	0.0
C20	77.8	1.1	2.2	0.0	6.7	12.2	0.0	0.0
C21	81.2	0.0	0.0	0.0	5.1	11.6	0.0	2.2
C22	77.6	3.4	1.7	0.0	1.7	8.6	0.0	6.9
C23	39.3	0.0	50.0	0.0	3.6	7.1	0.0	0.0
C24	70.7	0.0	3.3	0.0	9.8	16.3	0.0	0.0
C25	83.9	2.0	0.0	0.0	4.0	10.1	0.0	0.0
C26	83.3	0.0	4.0	0.0	6.3	6.3	0.0	0.0
C27	78.2	6.4	7.7	0.0	3.8	2.6	0.0	1.3
CH1	84.6	0.9	1.7	0.0	6.8	6.0	0.0	0.0
CH2	60.6	3.0	4.0	0.0	4.0	28.3	0.0	0.0
CH3	54.4	6.8	13.6	1.9	1.9	19.4	0.0	1.9
CH4	77.4	3.6	1.2	0.0	3.6	14.3	0.0	0.0
CH5a	70.1	1.5	1.5	0.0	7.5	11.9	0.0	7.5
CH6	59.4	15.6	1.6	0.0	9.4	10.9	0.0	3.1
CH7	90.0	0.0	0.0	0.0	10.0	0.0	0.0	0.0
CH8	69.7	2.3	0.0	0.0	7.6	19.7	0.0	0.8
CH9	78.3	0.0	1.5	0.0	3.5	16.7	0.0	0.0
CH10	82.2	5.9	0.0	0.0	2.0	9.9	0.0	0.0
CH11	0.00	0.0	100.0	0.0	0.0	0.0	0.0	0.0
CH12	80.8	6.0	0.0	0.0	4.9	8.2	0.0	0.0
CH13	71.4	5.2	2.6	0.0	7.8	6.5	0.0	6.5
CH14	75.2	0.7	0.7	0.0	3.5	15.6	0.0	4.3
CH15	67.6	3.8	0.0	0.0	5.7	22.9	0.0	0.0
CH16	84.8	1.3	0.0	0.0	5.1	8.9	0.0	0.0
CH17	78.0	2.0	12.0	0.0	2.0	6.0	0.0	0.0
CH18	73.3	2.7	0.0	0.0	6.7	10.7	0.0	6.7
CH19	81.8	3.9	0.0	0.0	2.6	11.7	0.0	0.0
CH20	83.1	0.0	0.0	0.0	4.8	12.0	0.0	0.0
CH21	92.3	0.0	0.0	0.0	3.3	4.4	0.0	0.0
CH22	86.0	0.0	0.0	0.0	6.0	8.0	0.0	0.0
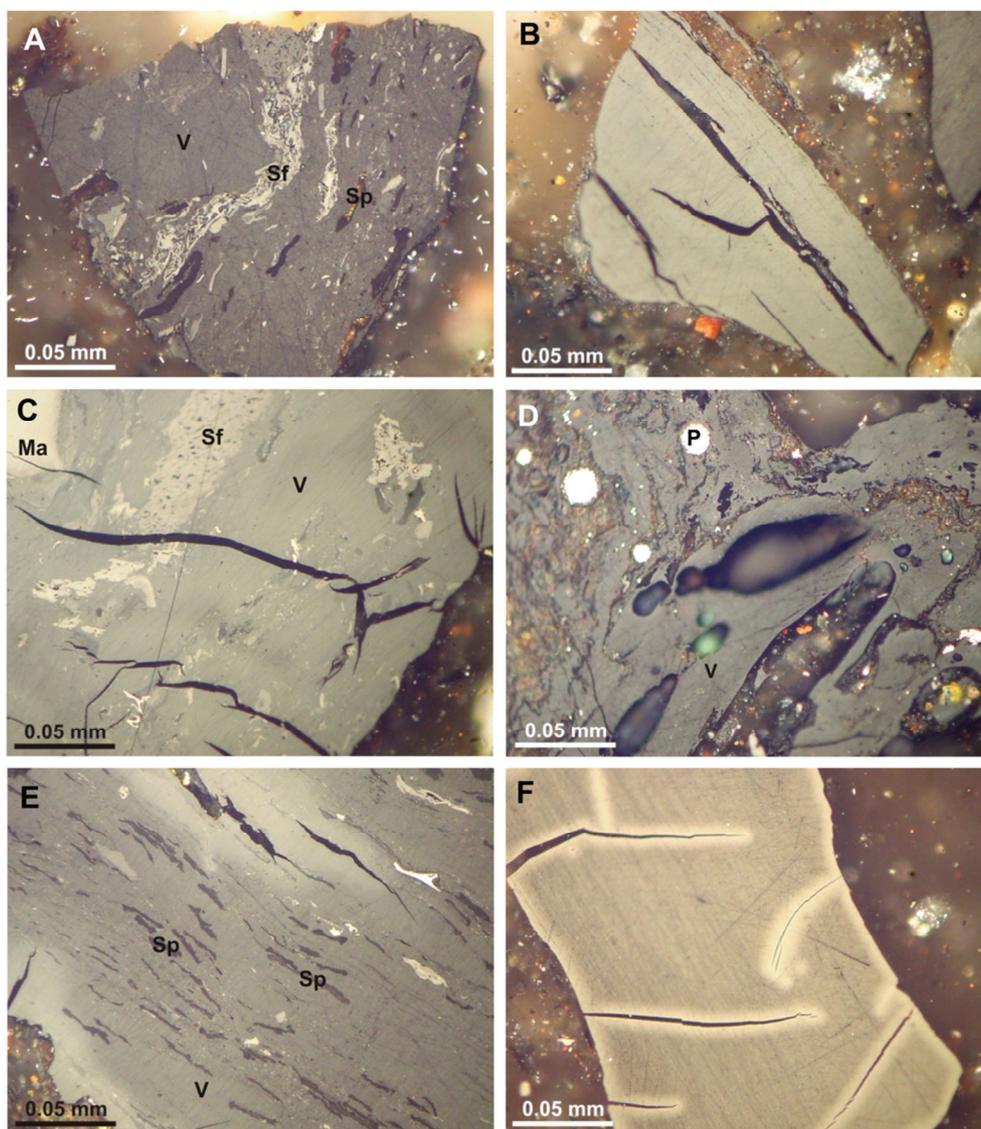
Fig. 20. Organic and mineral matter in coal wastes from the Starzykowiec dump (white light, immersion oil). A – trimacerite (sample CH21); B – paler coloured collotelinite (sample CH3); C – paler coloured trimacerite (sample CH3); D – vitrinite with pores, pyrite and clay minerals (sample CH3); E- paler coloured oxidation rims around the edge of trimacerite particle and along cracks within it (sample CH3); F – paler coloured oxidation rims around vitrinite particle (sample C17). V – vitrinite, Sp – sporinite, Sf – semifusinite, Ma – macrinite, P – pyrite.
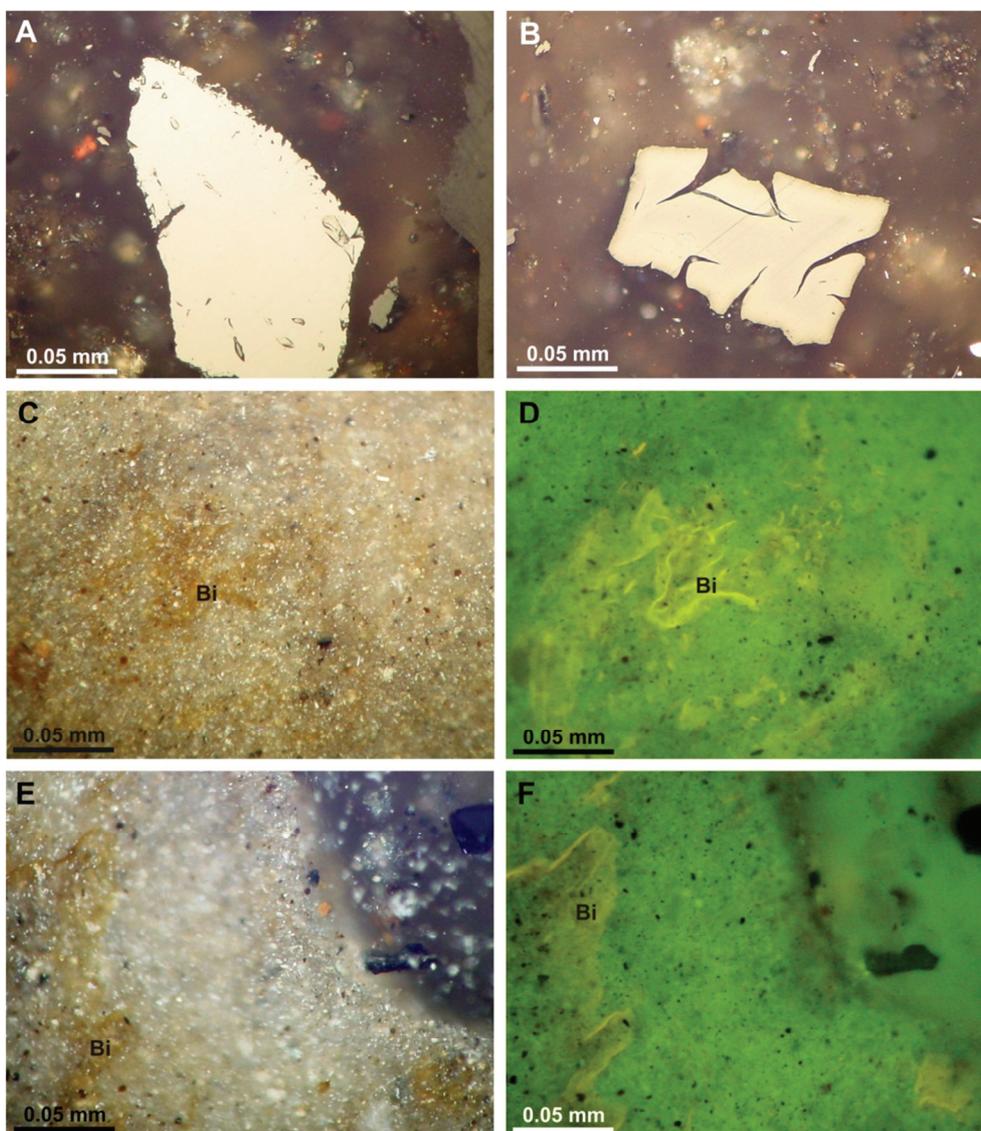
Fig. 21. Organic and mineral matter in coal wastes from the Starzykowiec dump (immersion oil).
A, B – massive coke (sample C17; white light); C, E – bitumines and clay minerals (sample CH16;
white light); D, F – bitumines and clay minerals (sample CH16; fluorescence). Bi – bitumen
expulsions.

Coke contents are usually < 1.4 vol.% (7.5 vol.%, mmf). The highest content of coke
occurs in sample C12 (2.8 vol.%, 100.0 vol.%, mmf; Tables 9, 10).

Random reflectance values (R_r) are typically low (0.55-0.89%). The low reflectance
can probably be explained as due to bitumens generated, during self-heating, from liptinite
migrating into the microcracks in vitrinite. Reflectograms are narrow (Fig. 22a). The

highest random reflectance (1.79%) was measured in C12 composed entirely of coke and relatively high reflectances values (1.22-1.54%) in C11, C14, and C17 (Table 9). The much wider reflectograms in these cases, and for CH3, reflect the varying degrees of alteration of individual particles (Fig. 22b-d).
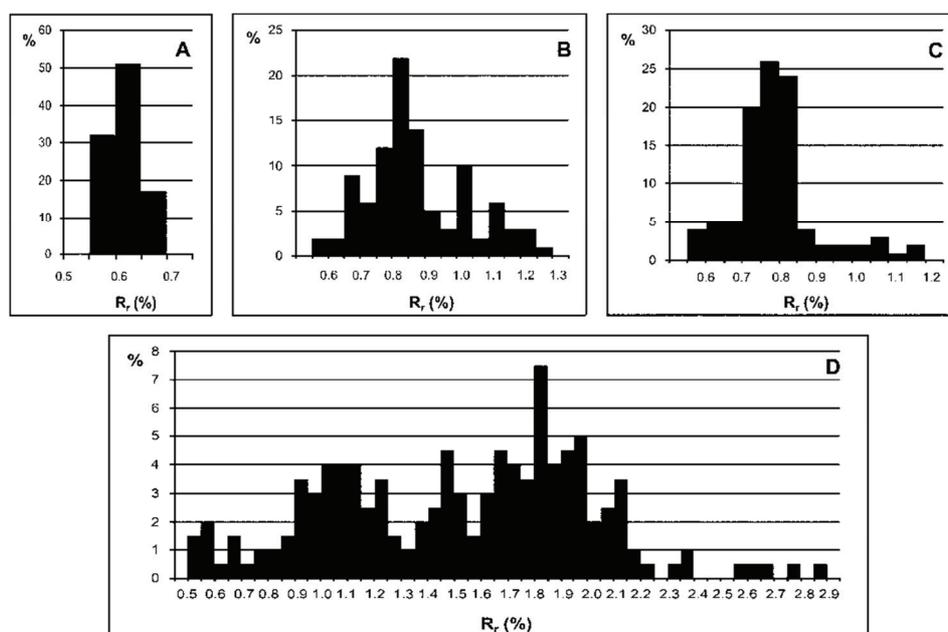
Fig. 22. Reflectograms of selected samples from the Starzykowiec coal waste dump. A – sample C19, B – sample CH3, C – sample C11, D - sample C17.

7.3. Organic geochemistry

Extract yields range from 0.002 wt% (CH7) to 0.164 wt% (C2) for the majority of samples collected at the Starzykowiec dump (Table 11). Only CH14 (0.256 wt%) and CH5a (0.704 wt%) have higher extract yields. The main groups of compounds in the samples are n-alkanes, acyclic isoprenoids (pristane and phytane), hopanes, polyaromatic hydrocarbons and their derivatives, and phenols.

n-Alkanes (m/z = 71) are the dominant group of compounds in most samples except for C17, C23, CH5a, CH10, and CH15. Their distribution contains compounds with variable ranges, usually from n-C_{13} to n-C_{35}. However, in C1-C3, C7-C9, C13, C19, C20, CH2-CH4, CH8, CH12, and CH18-CH21, lighter n-alkanes ranging from n-C_9 to n-C_{12} are also present (Fig. 23a).

Samples C1, C2, C5-C9, C13, C17-C22, C24, C27, CH1, CH4, CH6-CH9, CH12-CH15, and CH19-CH22 are unaltered or weakly altered with n-alkane distributions typical of coals or kerogen type III (Fig. 23a). In all such, there is a marked predominance of odd-over-even carbon number n-alkanes reflected in Carbon Preference Index (CPI) values in the range 1.48-2.07 (Table 11).

162
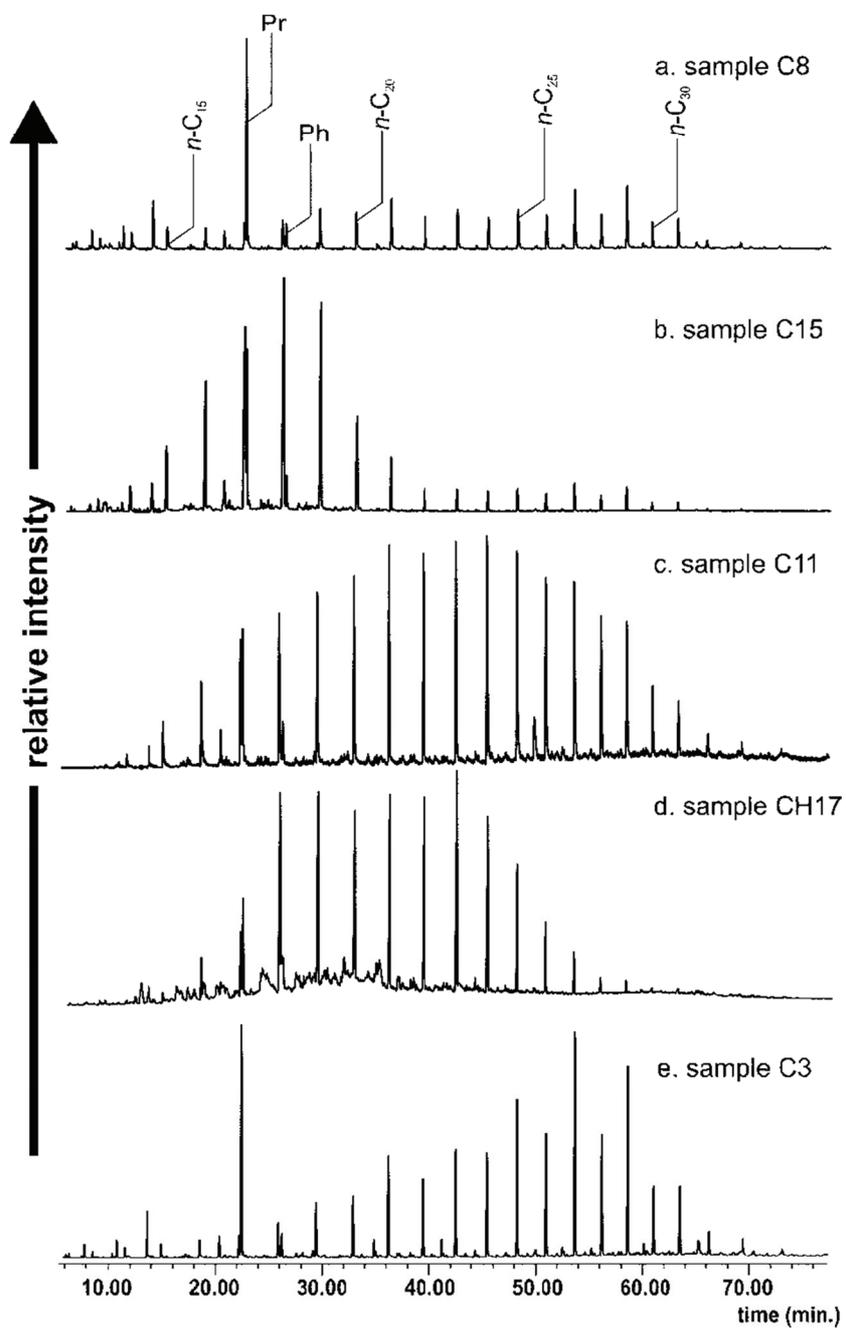
Fig. 23. *n*-Alkane distribution in selected Starzykowiec coal waste extracts (*m/z* = 71). a – wide
n-alkane distribution of a coal or kerogen III type; b – narrow *n*-alkane distribution in pyrolysate;
c – wide *n*-alkane distribution in pyrolysate; d – wide *n*-alkane distribution with two maxima,
e – mixture of unaltered sample and pyrolysate.

TABLE 11

Extract yields and aliphatic biomarker parameters for samples from the Starzykowiec coal waste dump

Sample no.	EY	CPI	$\Sigma1/\Sigma2$	$n\text{-}C_{23}/n\text{-}C_{31}$	Pr/Ph	$Pr/n\text{-}C_{17}$	$Ph/n\text{-}C_{18}$	$C_{31}S/(S+R)$	Ts/(Ts+Tm)	$C_{30}\beta\alpha/(\alpha\beta+\beta\alpha)$	$C_{30}\beta\beta/(\beta\beta+\alpha\beta+\beta\alpha)$
	1)	2)	3)	4)	5)	6)	7)	8)	9)	10)	11)
C1	0.077	2.07	0.67	1.80	11.76	11.76	0.72	0.50	0.72	0.51	0.03
C2	0.164	1.52	0.61	1.90	8.16	5.31	0.58	0.51	0.80	0.44	0.00
C3	0.036	1.66	0.82	1.28	9.77	10.88	0.67	0.46	0.74	0.46	0.05
C4	0.112	1.72	0.32	2.14	5.01	2.50	0.19	0.45	0.72	0.56	0.00
C5	0.106	1.81	0.58	1.26	7.29	6.55	0.76	0.40	0.70	0.54	0.00
C6	0.016	1.70	0.58	1.39	8.26	7.78	0.74	0.42	0.71	0.52	0.05
C7	0.023	1.65	0.54	1.60	6.35	6.22	0.73	0.44	0.71	0.47	0.00
C8	0.036	1.68	0.62	1.28	7.71	7.74	0.74	0.44	0.71	0.49	0.07
C9	0.059	1.71	0.60	1.76	7.79	7.59	0.69	0.46	0.73	0.52	0.00
C11	0.013	1.17	0.65	3.61	2.50	1.11	0.32	0.54	0.85	0.45	0.00
C12	0.111	1.35	0.59	3.50	1.19	0.82	0.28	0.49	0.78	0.53	0.00
C13	0.080	1.69	0.63	1.85	6.86	4.85	0.50	0.38	0.64	0.56	0.00
C14	0.018	1.37	0.46	1.04	0.93	1.41	1.87	-	-	-	-
C15	0.136	1.61	0.12	2.51	4.62	0.47	0.09	0.47	0.75	0.49	0.00
C16	0.051	1.48	0.37	3.99	5.78	1.30	0.16	0.43	0.67	-	0.00
C17	0.020	-	-	-	-	-	-	-	-	-	-
C18	0.123	1.99	0.71	1.38	9.28	11.03	0.69	0.46	0.67	0.53	0.07
C19	0.054	1.80	0.67	0.94	6.41	20.13	1.64	0.39	0.64	0.56	0.00
C20	0.063	1.77	0.51	1.42	8.89	11.80	0.76	0.46	0.72	0.45	0.04
C21	0.036	1.61	0.69	1.63	8.75	19.12	1.10	0.46	0.74	0.50	0.08
C22	0.016	2.05	0.73	0.86	11.02	30.58	2.85	0.38	0.71	0.53	0.00

C23	0.026	-	-	-	-	-	-	0.47	0.76	-	-
C24	0.077	1.68	0.69	1.56	9.77	15.05	0.87	0.46	0.76	0.50	0.00
C25	0.052	1.67	0.78	1.25	4.59	19.92	1.64	0.28	0.65	0.63	0.00
C26	0.149	1.79	0.75	1.29	6.06	14.25	1.40	0.35	0.73	0.57	0.00
C27	0.094	1.92	0.71	0.90	6.67	34.28	2.01	0.39	0.72	0.47	0.00
CH1	0.065	1.77	1.29	1.35	3.90	7.81	1.11	0.44	0.73	0.41	0.00
CH2	0.052	1.67	0.47	2.56	6.34	2.44	0.85	0.47	0.75	0.45	0.00
CH3	0.017	1.54	0.45	4.30	7.43	1.68	0.14	0.48	0.71	0.41	0.00
CH4	0.047	1.58	0.83	2.30	8.06	3.56	0.36	0.46	0.70	0.42	0.00
CH5a	0.704	-	-	-	-	-	-	0.34	0.65	-	-
CH6	0.103	1.64	2.08	1.14	6.17	11.29	0.98	0.43	0.76	0.40	0.00
CH7	0.002	1.57	1.83	1.08	6.59	-	-	0.40	0.78	0.47	0.00
CH8	0.037	1.74	1.18	1.57	8.24	-	-	0.52	0.76	0.34	0.00
CH9	0.021	1.78	1.33	2.27	7.50	-	-	0.47	0.73	0.43	0.00
CH10	0.070	-	-	-	-	-	-	0.37	0.71	0.47	0.00
CH11	0.009	1.10	0.67	3.26	1.84	-	-	0.48	0.73	0.34	0.00
CH12	0.013	1.61	0.95	2.14	7.48	-	-	0.44	0.69	0.37	0.00
CH13	0.059	1.73	1.65	1.32	6.47	-	-	0.44	0.71	0.39	0.00
CH14	0.256	1.75	2.59	1.20	6.07	9.93	0.87	0.37	0.66	0.48	0.00
CH15	0.079	-	-	-	-	-	-	0.48	0.73	0.37	0.00
CH16	0.077	1.60	2.36	1.55	5.97	10.49	0.96	0.45	0.72	0.35	0.00
CH17	0.056	1.48	0.54	86.64	3.67	1.52	0.16	0.44	0.65	0.49	0.00
CH18	0.013	1.57	0.18	2.20	7.02	0.53	0.11	0.46	0.74	0.42	0.00
CH19	0.075	1.53	1.09	2.15	6.38	3.18	0.45	0.44	0.63	0.38	0.00
CH20	0.066	1.56	0.84	2.09	7.06	3.11	0.40	0.44	0.69	0.37	0.00
CH21	0.010	1.57	0.70	2.06	6.05	2.29	0.32	0.50	0.73	0.38	0.00
CH22	0.018	1.48	1.14	2.32	6.23	3.55	0.53	0.49	0.73	0.36	0.00

1) EY – Extract yield (wt%)

2) CPI = $0.5\{[(n\text{-}C_{25}+n\text{-}C_{27}+n\text{-}C_{29}+n\text{-}C_{31}+n\text{-}C_{33})/(n\text{-}C_{24}+n\text{-}C_{26}+n\text{-}C_{28}+n\text{-}C_{30}+n\text{-}C_{32})] + [(n\text{-}C_{25}+n\text{-}C_{27}+n\text{-}C_{29}+n\text{-}C_{31}+n\text{-}C_{33})/(n\text{-}C_{26}+n\text{-}C_{28}+n\text{-}C_{30}+n\text{-}C_{32}+n\text{-}C_{34})]\}$; Carbon Preference Index; $m/z = 71$; thermal maturity parameter (Bray, Evans 1961).

3) $\Sigma 1/\Sigma 2 = [\Sigma$ (from $n\text{-}C_{13}$ to $n\text{-}C_{22})]/[\Sigma$ (from $n\text{-}C_{23}$ to $n\text{-}C_{35})$]; $m/z = 71$, source indicator (Tissot, Welte 1984).

4) $n\text{-}C_{23}/n\text{-}C_{31}$; $m/z = 71$ (Pancost et al. 2002); source indicator.

5) Pr/Ph = pristane/phytane; parameter of environment oxicity (with exception of coals); $m/z = 71$ (Didyk et al. 1978).

6) Pr/$n\text{-}C_{17}$ = pristane/n-heptadecane; $m/z = 71$ (Leythaeuser, Schwartzkopf 1986).

7) Ph/$n\text{-}C_{18}$ = phytane/n-octadecane; $m/z = 71$ (Leythaeuser, Schwartzkopf 1986).

8) C_{31}S/(S+R) = $17\alpha(\text{H}),21\beta(\text{H})$-29-homohopane 22S/($17\alpha(\text{H}),21\beta(\text{H})$-29-homohopane 22S+$17\alpha(\text{H}),21\beta(\text{H})$-29-homohopane 22R); $m/z = 191$; thermal maturity parameter (Peters et al. 2005).

9) Ts/(Ts+Tm) = $18\alpha(\text{H})$-22,29,30-trisnorneohopane/($18\alpha(\text{H})$-22,29,30-trisnorneohopane+$17\alpha(\text{H})$-22,29,30-trisnorhopane); $m/z = 191$; thermal maturity parameter (Peters et al. 2005).

10) $C_{30}\beta\alpha/(\alpha\beta+\beta\alpha) = 17\beta(\text{H}),21\alpha(\text{H})$-29-hopane $C_{30}/(17\alpha(\text{H}),21\beta(\text{H}),21\alpha(\text{H})$-29-hopane $C_{30})$; $m/z = 191$, (Seifert, Moldowan 1980).

11) $C_{30}\beta\beta/(\beta\beta+\alpha\beta+\beta\alpha) = 17\beta(\text{H}),21\beta(\text{H})$-29-hopane $C_{30}/(17\beta(\text{H}),21\beta(\text{H})$-29-hopane $C_{30}+17\alpha(\text{H}),21\beta(\text{H}),21\alpha(\text{H})$-29-hopane $C_{30})$; $m/z = 191$, (Seifert, Moldowan 1980).

"_" compounds present, concentrations too low to calculate a parameter value.

Samples containing pyrolysates (C4, C11-C12, C15, C16, CH2, CH17, and CH18) show a Gaussian distribution (Fig. 23b-d) and the predominance of odd-over-even carbon number n-alkanes is lower than in unaltered samples. CPI values are in the range 1.17-1.72 though the most altered sample (CH11) has the lowest CPI value of 1.10. The distribution of n-alkanes in pyrolysates is narrow – in the range from n-C_{12} to n-C_{22} with maxima at n-C_{16} in CH18, n-C_{18} in C15 and CH2, and n-C_{19} in C4 (Fig. 23b). In others, it is wide – in the range from n-C_{13} to n-C_{33} with maxima at n-C_{19} in C16 and n-C_{24} in C11 (Fig. 23c). C12 and CH17 display a bimodal distribution with maxima at n-C_{20} and n-C_{24}, and at n-C_{18} and n-C_{23}, respectively; this may indicate that they are mixtures of pyrolysates (Fig. 23d). A Gaussian n-alkane distribution is weakly marked in the most strongly altered sample (CH11).

Altered and unaltered material was found in C3, C14, C23, C25, C26, CH3, and CH16 (Fig. 23e). In these, there is also predominance of odd-over-even carbon number n-alkanes. CPI values in the range 1.37-1.79 are intermediate between those for weakly altered samples and those containing pyrolysates (Table 11).

The ratio of short-to-long chain n-alkanes expressed by $\Sigma(n$-C_{13} to n-$C_{22}) / \Sigma(n$-C_{23} to n-$C_{35})$, the $\Sigma1/\Sigma2$ index, also reflects the degree of sample alteration. Weakly-altered samples have generally higher values of this index in the range 0.51-2.59 compared to those for pyrolysates (0.12-0.65). Where both types of material are present together, the range is 0.46-2.36.

Similar data were obtained for acyclic isoprenoids, pristane and pytane and indices of thermal alteration based on them ($m/z = 71$). The ratio of pristane to phytane (Pr/Ph) is highest in the weakly-altered samples, lying in the range 3.90-11.76 (Table 11). It is generally lower (1.19-7.02) in waste samples containing pyrolysates. In material comprising a mixture of weakly- and more strongly-altered material, Pr/Ph values are intermediate (0.93-9.77). The pristane to n-heptadecane ratio (Pr/n-C_{17}), an indicator of degree of thermal alteration, reveals a similar pattern; values are highest (2.29-34.28) in weakly altered samples, lowest (0.47-2.50) in material with pyrolysates, and values are intermediate (1.41-19.92) where mixtures of weakly- and strongly-altered material are involved. The phytane to n-octadecane ratio (Ph/n-C_{18}) likewise follows a similar pattern; values tend to be the highests (0.32-2.85) for weakly-altered wastes, generally the lowest (0.09-0.32) for samples containing pyrolysates and usually intermediate for mixtures of variously-altered material (Table 11). An obvious exception to the pattern is the pyrolysate-bearing CH2 with a Ph/n-C_{18} value of 0.85.

Hopanes ($m/z = 191$) are present in all investigated samples except samples C14, C17, and C23 (Table 11). The level of sample alteration is expressed by values of the $C_{31}S/(S+R)$ in the range 0.28-0.54. The level of alteration is also expressed by values of Ts/(Ts+Tm) in the range 0.63-0.85 (Table 11). Sample C11 displays the highest values of both ratios and the highest relative contents of C_{29} and $\alpha\beta$ hopanes; $\beta\beta$ hopanes are absent. In contrast, sample C25 has the lowest value of $C_{31}S/(S+R)$, one of the lowest values of Ts/(Ts+Tm), and the lowest relative content of $\alpha\beta$. The values of $C_{30}\beta\beta/(\beta\beta+\alpha\beta+\beta\alpha)$ are very low (< 0.08) while the values of $C_{30}\beta\alpha/(\alpha\beta+\beta\alpha)$ are in the range 0.34-0.63 (Table 11). In general, C_{30} hopanes occur in the highest relative contents in samples from this dump (Fig. 10, 24). In all, $\alpha\beta$ hopanes dominate, occurring in 51.0-67.4 rel.%; $\beta\alpha$ and $\beta\beta$ hopane

contents are also lower. However, $\beta\alpha$ hopane relative contents are always higher than those of $\beta\beta$ (< 16 rel.%; Fig. 11). Hopanes with $\beta\beta$ configuration are absent in samples C2, C4, C5, C7, C9-C13, C19, C22, and C24-C27. Hopane distributions in selected samples are shown in Figure 24.


Fig. 24. Pentacyclic triterpane distribution in the extracts from selected Starzykowiec coal waste samples (m/z = 191). Ts – 18α(H)-22,29,30-trisnorneohopane, Tm – 17α(H)-22,29,30-trisnorhopane, C$_{29}\alpha\beta$ – 17α,21β(H)-30-norhopane, C$_{29}\beta\alpha$ – 18α,21β(H)-30-norneohopane, C$_{30}\alpha\beta$ – 17α,21β(H)-hopane, C$_{30}\beta\beta$ – 17β,21β(H)-hopane, C$_{30}\beta\alpha$ – 17β,21α(H)-hopane, C$_{31}\alpha\beta$ – 17α,21β(H)-30-homohopane 22S and 22R, C$_{31}\beta\alpha$ – 18α,21β(H)-30-homohopane 22R, C$_{32}\alpha\beta$ – 17α,21β(H)-30-bishomohopane 22S and 22R.

TABLE 12

Aromatic hydrocarbon parameters for samples from the Starzykowiec coal waste dump

Sample no.	MNR 1)	DNR 2)	TNR-1 3)	TNR-2 4)	TNR-4 5)	MPI-3 6)	2-MP/2-MA 7)	MB/DBF 8)
C1	0.89	1.45	0.21	0.38	0.62	0.49	-	-
C2	1.24	0.92	0.16	0.28	0.56	0.79	-	-
C3	0.88	0.91	0.25	0.41	0.77	0.68	-	-
C4	1.03	0.83	0.22	0.40	0.50	0.83	-	-
C5	0.78	0.53	1.75	0.99	0.57	0.79	-	-
C6	1.29	1.15	2.76	0.82	0.61	0.70	-	-
C7	0.71	0.78	2.01	0.77	0.55	0.38	-	-
C8	0.78	0.70	2.30	0.83	0.60	0.53	-	-
C9	0.92	0.92	2.35	0.75	0.59	0.46	-	-
C11	0.78	1.09	0.37	0.42	0.65	0.44	-	-
C12	0.90	1.11	0.29	0.30	0.63	0.66	-	-
C13	0.73	0.64	0.19	0.20	0.62	0.31	-	-
C14	0.57	1.11	0.26	0.23	0.54	-	-	-
C15	2.16	-	0.20	0.22	0.66	0.90	-	-
C16	1.09	1.30	0.19	0.23	0.71	0.29	-	-
C17	-	-	-	-	-	-	-	-
C18	0.71	0.42	0.38	0.29	0.50	0.23	-	-
C19	0.27	-	-	-	-	-	-	-
C20	0.52	0.76	0.23	0.20	0.73	0.31	-	-
C21	0.37	0.68	3.12	0.72	0.73	-	-	-
C22	-	-	-	-	-	-	-	-
C23	-	-	-	-	-	-	-	-
C24	0.55	0.81	2.91	0.78	0.71	0.51	-	-
C25	0.00	0.00	0.93	0.44	0.69	-	-	-
C26	0.00	-	-	-	-	-	-	-
C27	0.00	-	-	-	-	-	-	-
CH1	-	-	-	-	-	-	-	-
CH2	1.47	1.76	0.55	0.57	0.83	1.21	-	0.21
CH3	1.43	3.08	0.88	0.76	0.76	-	4.06	0.18
CH4	1.16	1.06	-	-	-	0.87	-	0.30
CH5a	-	-	-	-	-	-	-	-
CH6	0.38	-	-	-	-	-	-	-
CH7	0.28	-	-	-	-	-	-	-
CH8	1.14	2.09	0.60	0.59	0.67	0.87	1.97	0.32
CH9	0.82	0.96	-	-	-	-	-	0.34
CH10	-	-	-	-	-	-	-	-
CH11	1.14	1.94	1.42	0.97	0.66	1.45	-	0.39
CH12	1.41	1.80	0.32	0.51	0.61	0.81	7.52	0.36
CH13	0.79	1.03	-	-	-	-	-	0.30
CH14	0.41	-	-	-	-	-	-	-
CH15	-	-	-	-	-	-	-	-
CH16	0.41	-	-	-	-	-	-	-
CH17	1.15	0.98	0.45	0.36	0.64	1.72	-	0.34
CH18	1.70	1.61	2.35	1.17	0.81	1.22	-	0.17
CH19	0.86	0.97	0.31	0.47	0.63	0.84	8.82	0.31
CH20	1.72	1.26	2.68	1.12	0.83	1.01	-	0.35
CH21	1.24	1.17	-	-	-	1.00	-	0.24
CH22	0.97	1.68	0.53	0.57	0.66	0.76	3.82	0.33

1) MNR = 2-methylnaphthalene/1-methylnaphthalene; *m/z* = 142; thermal maturity parameter (Radke et al. 1994).
2) DNR = (2,6-dimethylnaphthalene+2,7-dimethylnaphthalene)/1,5-dimethylnaphthalene; *m/z* = 156, thermal maturity parameter (Radke et al. 1982).
3) TNR-1 = 2,3,6-trimethylnaphthalene/(1,3,6-trimethylnaphthalene+ 1,4,6-trimethylnaphthalene+1,3,5-trimethylnaphthalene); *m/z* = 170, thermal maturity parameter (Radke et al. 1986).
4) TNR-2 = (1,3,7-trimethylnaphthalene+2,3,6-trimethylnaphthalene)/ (1,3,5-trimethylnaphthalene+1,4,6-trimethylnaphthalene+1,3,6-trimethylnaphthalene); *m/z* = 170, thermal maturity parameter (Radke et al. 1986).
5) TNR-4 = 1,2,5-trimethylnaphthalene/(1,2,5-trimethylnaphthalene+ 1,2,7-trimethylnaphthalene+1,6,4-trimethylnaphthalene); *m/z* = 170, thermal maturity parameter.
6) MPI-3 = (2-methylphenanthrene+3-methylphenanthrene)/(1-methylphenanthrene+ 9-methylphenanthrene); *m/z* = 192; thermal maturity parameter (Radke, Welte 1983).
7) 2-MP/2-MA = 2-methylphenanthrene/2-methylanthracene; *m/z* = 192.
8) MB/DBF = (3-methylbiphenyl+4-methylbiphenyl)/dibenzofurane; *m/z* = 168; thermal maturity parameter (Radke 1987).
"–" compounds present but concentrations too low to calculate a parameter value.

Compared to other compounds, concentrations of methylnaphthalenes (*m/z* = 142), dimethylonaphthalenes (*m/z* = 156), and trimethylnaphthalenes (*m/z* = 170) are low. There are none in C17, C22, C23, C26, C27, CH1, CH5a, and CH15; Methylnaphthalene Ratio (MNR) values for the remainder range from 0.27-2.16 (Table 12). Dimethylnaphthalene Ratio (DNR) values fall in the range 0.42-3.08 and Trimethylnaphthalene Ratios (TNR-1, TNR-2, and TNR-4) in the ranges 0.16-3.12, 0.20-1.17, and 0.50-0.83, respectively. Values of the Methylphenanthrene Index (MPI-3; *m/z* = 192) range from 0.23-1.72 and values of methylbiphenyl/dibenzofuran (MB/DBF) from 0.17-0.39 (Table 12; Fig. 25).

Polyaromatic hydrocarbons (*m/z* = 128+178+202+228+252) are represented by two- to five-ring compounds. PAHs with more than five rings are absent (Fig. 13, 26). The amounts of individual compounds vary greatly (Table 13; Fig. 26). There are no PAHs in CH1, CH5a-CH7, CH10, and CH15. In the remainder, four-ring PAHs are represented by fluoranthene, pyrene, benzo[*ghi*]fluoranthene, benzo[*a*]anthracene, and chrysene. Among two- and three-ring PAHs (naphthalene, phenanthrene, anthracene), none occur in C14 and C25. Among five-ring PAHs (benzo[*b+k*]fluoranthene, benzo[*a*]fluoranthene, benzo[*e*]pyrene, benzo[*a*]pyrene, and perylene), none occur in CH11, CH14, and CH17. PAHs with two- and three- rings dominate in most samples. In C1, C3-C5, C14, C18, C19, C21, C25, C26, CH9, CH13, CH14, and CH16, PAHs with four rings dominate and, in C11, PAHs with five rings prevail over two-four ring PAHs (Table 13).

Phenols are also present in these coal wastes (Fig. 27). Present in varying quantities in all samples except C12, C14, CH7, CH9, CH12, and CH14, they are represented mainly by phenols, methylphenols (*m-, p-, o*-cresols), dimethylphenols (*m*-ethylphenols), tetramethylphenols and, in traces, aniline.
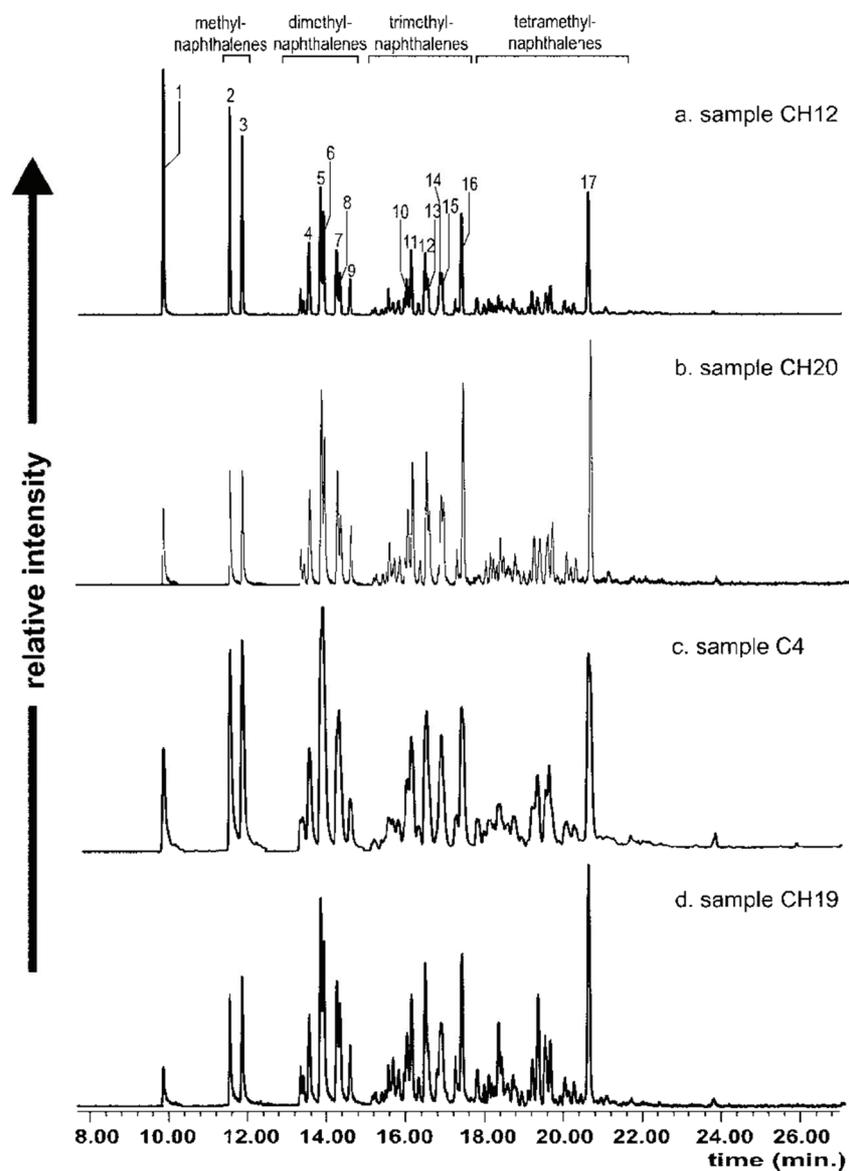
Fig. 25. Composed ion chromatogram showing distributions of naphthalene and alkylnaphthalenes in selected Starzykowiec coal waste extracts (m/z = 128+142+156+170+184). 1: naphthalene, 2: 2-methlnaphthalene, 3: 1-methylnaphthalene, 4: 2,6+2,7-dimethylnaphthalene, 5: 1,3+1,7-dimethylnaphthalene, 6: 1,6-dimethylnaphthalene, 7: 1,4+2,3-dimethylnaphthalene, 8: 1,5-dimethylnaphthalene, 9: 1,2-dimethylnaphthalene, 10: 1,3,7-trimethylnaphthalene, 11: 1,3,6-trimethylnaphthalene, 12: 1,4,6+1,3,5-trimethylnaphthalene, 13: 2,3,6-trimethylnaphthalene, 14: 1,2,7+1,6,7-trimethylnaphthalene, 15: 1,2,6-trimethylnaphthalene, 16: 1,2,5-trimethylnaphthalene.

TABLE 13

Contents of PAHs in coal wastes from the Starzykowiec dump (relative % calculated into total PAHs content)

Sample no.	N	P	A	Fl	Py	B[ghi]F	B[a]A	Ch	B[b+k]F	B[a]F	B[e]P	B[a]P	Per
C1	2.46	20.63	6.37	24.76	23.68	0.97	6.77	4.75	0.97	5.02	1.88	1.12	0.61
C2	29.44	15.24	17.04	10.38	10.56	1.22	3.12	4.41	1.95	1.95	3.18	1.50	0.00
C3	6.42	13.45	11.44	14.26	21.18	3.07	4.33	9.01	3.51	8.56	2.34	1.81	0.61
C4	9.53	15.82	12.54	17.76	17.85	1.06	4.55	4.55	3.35	7.37	3.98	1.65	0.00
C5	10.84	15.02	17.00	14.58	14.71	0.00	3.87	11.51	2.91	5.33	1.99	1.18	1.04
C6	27.35	13.03	17.92	10.17	11.92	0.00	3.01	3.36	2.61	4.98	2.59	2.47	0.58
C7	38.64	11.34	13.44	7.80	6.53	0.00	1.84	6.72	3.07	5.02	2.52	3.09	0.00
C8	75.92	4.27	4.09	5.08	2.22	0.00	0.69	2.19	1.30	2.73	0.27	1.24	0.00
C9	62.91	7.22	11.52	4.82	4.00	0.19	0.79	2.71	1.14	2.90	0.90	0.72	0.18
C11	0.00	13.17	18.32	3.44	10.69	2.72	4.31	4.31	8.52	14.48	8.15	11.90	0.00
C12	2.80	39.51	41.23	4.54	4.97	0.41	0.82	1.61	0.84	1.97	0.51	0.78	0.00
C13	61.20	6.74	10.82	3.62	5.52	0.48	0.76	2.96	1.91	3.32	1.01	1.10	0.57
C14	0.00	0.00	0.00	22.07	40.65	0.00	0.00	0.00	9.32	10.96	8.08	8.93	0.00
C15	5.59	33.20	56.24	1.08	1.89	0.05	0.38	0.30	0.31	0.48	0.14	0.30	0.04
C16	3.60	27.27	49.85	3.52	5.39	0.39	0.48	5.83	0.53	1.55	0.59	0.99	0.00
C17	4.03	8.81	59.42	1.93	11.84	0.42	0.82	6.19	3.60	2.94	0.00	0.00	0.00
C18	0.00	4.42	15.49	11.31	47.40	1.40	1.42	1.42	2.81	11.28	1.07	1.55	0.43
C19	40.58	0.00	0.00	25.74	12.24	0.00	10.15	3.63	3.28	1.10	1.56	1.31	0.40
C20	29.52	10.14	22.16	6.51	9.18	0.00	1.91	7.80	3.93	3.93	2.76	2.16	0.00
C21	21.97	3.81	12.47	18.29	14.78	0.96	1.18	10.05	1.97	8.18	2.45	3.90	0.00
C22	63.30	2.69	13.42	2.00	5.11	0.00	0.54	4.02	1.98	3.36	2.00	1.58	0.00
C23	3.39	6.79	53.55	2.82	11.96	0.00	0.69	13.75	2.49	1.37	1.97	1.23	0.00
C24	38.80	9.58	14.12	5.95	8.87	0.00	1.26	7.99	2.45	4.95	3.44	2.59	0.00

C25	0.00	0.00	0.00	6.74	22.36	0.00	3.72	21.89	12.91	17.03	8.83	6.51	0.00
C26	14.77	0.00	0.00	10.67	11.65	0.00	2.93	32.80	12.78	7.53	4.04	2.83	0.00
C27	47.22	0.00	0.00	3.98	4.44	0.00	1.90	22.32	4.90	5.80	4.88	4.56	0.00
CH1	-	-	-	-	-	-	-	-	-	-	-	-	-
CH2	32.26	22.58	23.28	8.55	5.65	0.00	0.64	2.70	1.65	0.90	0.41	1.14	0.23
CH3	7.46	59.58	9.34	10.67	6.96	0.36	1.49	2.33	0.25	0.76	0.21	0.38	0.21
CH4	35.95	11.41	17.85	10.52	8.76	0.00	0.83	6.46	1.07	2.84	1.22	2.63	0.47
CH5a	-	-	-	-	-	-	-	-	-	-	-	-	-
CH6	-	-	-	-	-	-	-	-	-	-	-	-	-
CH7	-	-	-	-	-	-	-	-	-	-	-	-	-
CH8	26.26	27.57	4.77	9.99	9.71	0.78	5.08	4.45	4.13	1.53	2.27	2.68	0.77
CH9	6.42	17.08	10.81	20.85	19.42	1.05	2.33	10.02	3.23	4.10	1.48	3.20	0.00
CH10	-	-	-	-	-	-	-	-	-	-	-	-	-
CH11	18.27	68.65	0.00	8.77	4.31	0.00	0.00	0.00	0.00	0.00	0.00	0.00	0.00
CH12	33.02	20.35	2.40	13.60	10.50	0.66	5.33	4.07	1.54	4.66	2.61	1.25	0.00
CH13	16.20	22.25	0.00	15.52	15.72	0.83	1.34	11.94	2.92	6.49	4.00	2.80	0.00
CH14	5.00	8.44	0.00	24.95	34.65	3.21	9.66	14.09	0.00	0.00	0.00	0.00	0.00
CH15	-	-	-	-	-	-	-	-	-	-	-	-	-
CH16	10.46	17.23	0.00	12.78	13.97	1.21	2.29	14.90	5.75	9.14	6.01	6.27	0.00
CH17	2.54	47.17	41.03	5.68	3.59	0.00	0.00	0.00	0.00	0.00	0.00	0.00	0.00
CH18	30.66	35.11	27.46	2.79	1.57	0.09	0.21	1.04	0.21	0.39	0.14	0.19	0.14
CH19	6.01	34.59	4.42	16.51	16.15	1.18	3.98	6.51	0.81	4.32	2.89	2.63	0.00
CH20	20.64	26.89	2.86	15.02	11.46	0.81	5.83	4.42	4.67	2.20	1.21	2.46	1.54
CH21	18.66	16.74	18.42	12.86	11.39	0.90	1.71	7.51	2.69	3.86	1.64	1.98	1.65
CH22	6.81	33.93	2.29	13.85	14.14	1.03	6.00	6.18	5.72	2.60	3.42	3.24	0.80

N – naphthalene, P – phenanthrene, A – anthracene, Fl – fluoranthene, Py – pyrene, B[a]A – benzo[a]anthracene, Ch – chrysene, B[ghi]F – benzo(g)fluoranthene+benzo(h)fluoranthene+benzo(i)fluoranthene, B[a]F – benzo[a]fluoranthene, B[e]P – benzo[e]pyrene, B[a]P – benzo[a]pyrene, Per – perylene.
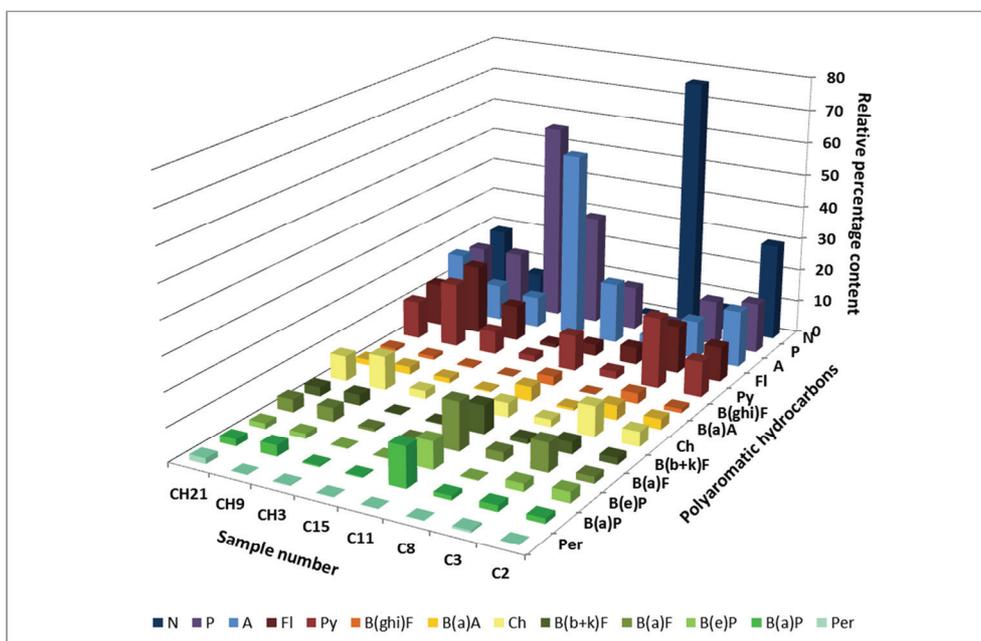
Fig. 26. Distribution of PAHs in selected samples from the Starzykowiec coal wastes calculated as
relative concentrations from ion chromatograms (*m/z* = 128, 178, 202, 228, and 252).
N – naphthalene, P – phenanthrene, A – anthracene, Fl – fluoranthene, Py – pyrene,
B(*ghi*)F – benzo(*g*)fluoranthene+benzo(*h*)fluoranthene+benzo(*i*)fluoranthene, B(*a*)A –
benzo(*a*)anthracene, Ch – chrysene, B(*k+f*)F –benzo(*k*)fluoranthene+benzo(*k*)fluoranthene,
B(*a*)F – benzo(*a*)fluoranthene, B(*e*)P – benzo(*e*)pyrene, B(*a*)P – benzo(*a*)pyrene, Per – perylene.

7.4. Proximate and ultimate analyses

Ash contents (A^a) in samples from the Starzykowiec dump are typically 70-85 wt%,
average 76.52 wt% (Table 14). Only in C18 and C19 is the ash content < 42.50 wt%.
Moisture contents (M^a) are low and usually < 3 wt% (average 2.01 wt%); an exception is
C19 with *ca* 4 wt%. Volatile matter contents (VM^{daf}) vary typically from 50-76 wt%
(average 59.11 wt%) with only C16 being exceptional with 92.84 wt%. Calorific values
(Q_s^{daf}) usually range from 7-25 MJ·kg^{-1}. C11 and C12 have the lowest calorific values (0.28
and 0.27 MJ·kg^{-1}, respectively) and, not surprisingly, the highest ash contents (Table 14).

Carbon contents (C^{daf}) typically range from 50-70 wt% (average 57.84 wt%), the
highest being 82.52 wt% in C19 that also has the highest calorific value (Table 14).
Hydrogen contents (H^{daf}) vary between 3.44-7.77 wt%. Nitrogen contents (N^{daf}) are low,
typically < 1.5 wt% but with CH3 an exception with 2.27 wt%. Oxygen contents (O^{daf}) are
usually 20-50 wt%; C19 is exceptionally low at 9.17 wt%. Total sulphur contents (S_t^a)
range up to 1.26 wt% (average 0.50 wt%).

174
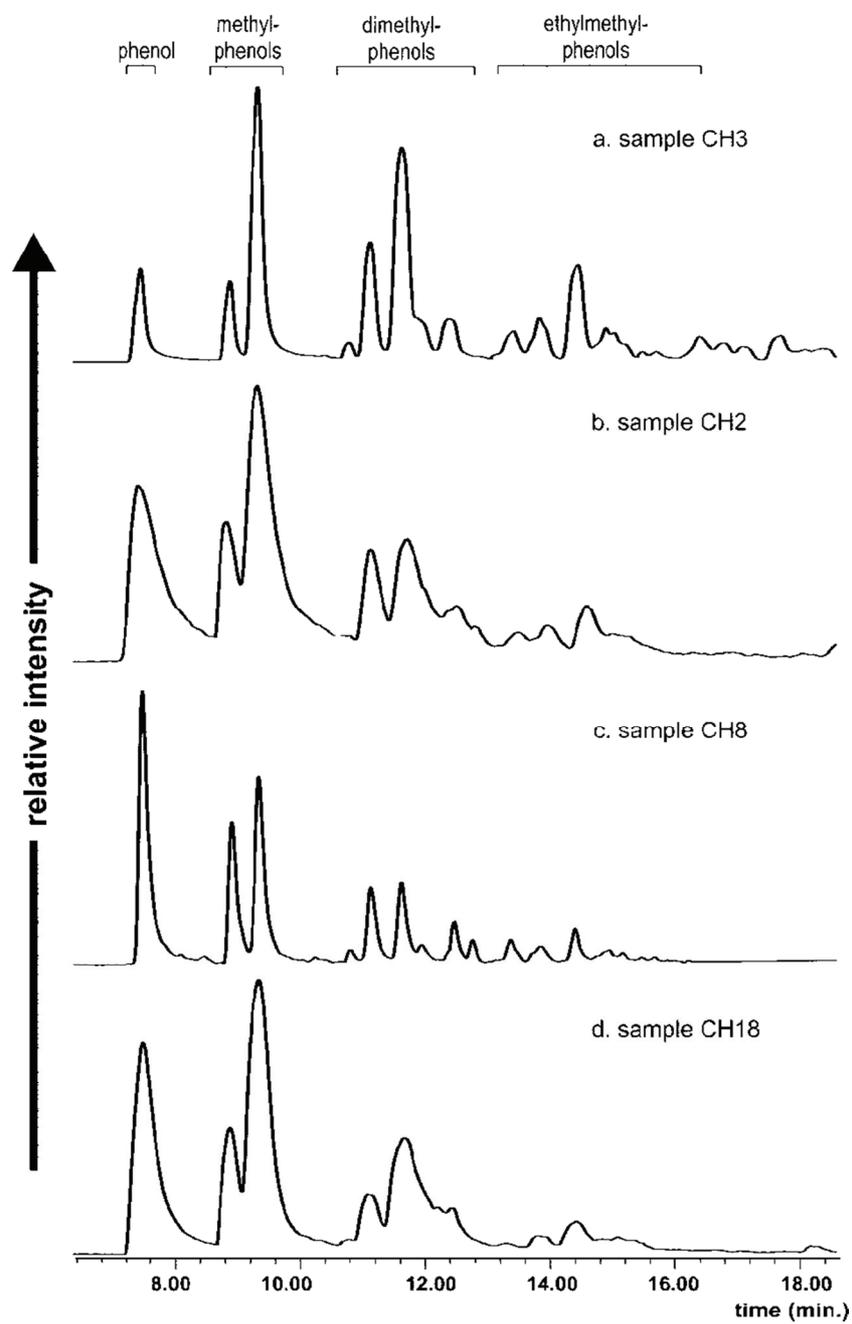
Fig. 27. Distribution of phenol and its derivatives in selected coal waste samples from the Starzykowiec dump (m/z = 94+108+122+136+150+164).

TABLE 14

Proximate and ultimate analyses of coal waste from the Starzykowiec dump

Sample no.	M^a (wt%)	A^a (wt%)	VM^{daf} (wt%)	Q_s^{daf} (MJ·kg^{-1})	C^{daf} (wt%)	H^{daf} (wt%)	N^{daf} (wt%)	O^{daf} (wt%)	S_t^a (wt%)
C11	1.06	89.78	76.20	0.28	34.93	7.75	0.76	54.91	0.15
C12	0.94	90.57	70.67	0.27	40.05	7.77	0.71	48.88	0.22
C13	1.92	78.60	56.26	16.86	57.49	6.31	1.08	32.80	0.45
C14	1.54	77.73	53.64	14.96	53.06	4.97	1.45	34.44	1.26
C15	1.41	84.36	60.65	12.85	49.89	6.96	1.12	39.35	0.38
C16	1.14	88.10	92.84	6.96	43.68	7.62	1.12	44.98	0.28
C17	1.66	77.91	45.62	15.20	57.27	5.14	1.47	30.35	1.18
C18	3.04	37.37	54.98	19.89	62.59	3.44	0.87	32.69	0.24
C19	3.94	42.50	44.62	31.09	82.52	5.79	1.31	9.17	0.65
C20	1.78	73.32	67.79	14.54	55.82	4.58	0.92	36.99	0.42
C21	2.61	71.80	57.13	18.87	61.74	5.43	1.41	29.31	0.54
C22	2.27	78.58	67.57	13.01	52.74	5.59	1.36	38.59	0.33
C23	1.85	76.19	54.74	16.78	59.65	5.28	1.50	31.28	0.50
C24	2.46	75.44	54.16	17.71	59.28	5.84	1.18	32.08	0.36
C25	2.88	68.11	49.43	21.53	64.12	6.38	1.41	26.75	0.39
C26	2.59	71.70	55.15	20.48	64.18	5.76	1.13	27.46	0.38
C27	2.54	70.18	65.58	17.60	60.12	5.06	1.17	32.48	0.32
CH1	2.54	72.25	52.32	19.51	63.86	5.71	1.39	25.35	0.93
CH2	2.54	61.52	61.30	20.36	65.11	4.62	1.14	26.99	0.77
CH3	2.19	77.52	59.44	13.57	52.74	5.08	2.27	36.77	0.64
CH4	1.40	79.12	58.68	16.91	59.55	5.60	1.23	31.67	0.38
CH5a	1.91	74.16	55.41	19.50	61.01	6.35	1.21	29.34	0.50
CH6	1.48	78.28	54.94	17.24	58.79	6.27	1.48	31.37	0.42
CH7	1.28	84.02	61.77	13.18	52.38	6.87	1.43	36.39	0.43
CH8	1.30	78.62	54.63	18.05	60.76	5.88	1.25	30.03	0.42
CH9	1.94	53.90	51.34	24.96	70.43	5.16	1.20	22.12	0.48

M – moisture, A – ash, VM– volatile matter, Q_s – calorific value, C – carbon, H – hydrogen, N – nitrogen, O – oxygen, S – sulphur, a – air dry basis, daf – dry ash free basis, t – total.

8. The Marcel Coal Mine dump - results

The properties of the waste samples collected at the Marcel Coal Mine dump show a strong dependence on the places where they were collected. These wastes contain varying amounts of organic matter.

8.1. Temperature on the surface and within the dump

The temperatures on the northern slope of the dump over the coal mud collector where samples M1-M11 were collected were about 500°C at a depth of *ca* 1m (Table 15). Where heating is taking place now and where the burned out wastes are being currently worked, and where samples M12-M23 were collected, the temperatures on the surface were much lower, in the range 50-70°C when the samples were collected. Much higher surface temperatures (> 200°C) were measured at the collection site of samples M30-M43. At this site, a mixture of gases, with a very strong asphyxiating smell, was venting to the atmosphere at the time.

8.2. Petrography

The petrographic analyses of the samples from the Marcel Coal Mine dump reflect, as noted above, their collection sites. In general, unaltered and paler-coloured vitrinite, and coke, are the dominant components.

Unaltered coal wastes (sample M24a) from current coal production contains 91.2 vol.% of minerals (Table 15), mostly clay minerals and carbonates. Unaltered macerals occur in these wastes. However, irregular cracks occur in a few vitrinite particles. Vitrinite is the dominant maceral group in this sample (Fig. 28a; Tables 15, 16). Inertinite is a minor component (0.4 vol.%; 4.5 vol.%, mmf) and liptinite does not occur. The random reflectance (R_r) measured on vitrinite is 0.72% and the reflectogram is narrow (Fig. 31a), confirming the absence of alteration.

Wastes exposed to weathering for a few years (M24 and M25) contain slightly lower amounts of mineral matter, 88.6 and 86.4 vol.%, respectively. The contents of all three maceral groups are similar in both samples (Tables 15, 16). The total vitrinite contents are 8.4 (M24) and 8.6 vol.% (M25). Liptinite and inertinite contents are slightly higher in sample M25 (2.6 and 2.4 vol.%) than in M24 (1.6 and 1.4 vol.%; Fig. 28b). Rare particles of vitrinite with irregular cracks are seen in M24. The vitrinite reflectances are the same as for unaltered wastes (0.72 and 0.74%, respectively) and the reflectograms are narrow (Fig. 31b).

Samples M1-M11 comprise organic matter altered to varying degrees. Though M8 contains relatively unaltered organic matter and the greatest amount of unaltered vitrinite (19.4 vol.%; 78.9 vol.%, mmf), it contains 4.4 vol.% (17.9 vol.%, mmf) of vitrinite with irregular cracks (Tables 15, 16). Unaltered vitrinite is also present in sample M10, a mixture of variously altered material that also contains vitrinite with cracks, paler-coloured vitrinite, and coke. Paler-coloured vitrinite (Fig. 28c-f) is the most common form of vitrinite in M1-M6 and M9; amounts range from 21.6-55.0 vol.% (Table 15), 46.1-79.1 vol.% mmf (Table 16). Vitrinite with pores (Fig. 28d-e), in M6 only 0.8 vol.% (1.2 vol.%, mmf), indicates a relatively higher heating rate. In M5, liptinite, represented mostly by sporinite (Fig. 28c), cutinite, and liptodetrinite (Fig. 28c) occurs in amounts up to 8.4 vol.% (10.4 vol.%, mmf). Inertinite, mainly represented by fusinite, semifusinite (Fig. 28c, 28e), inertodetrinite (Fig. 28c-e), and macrinite ranges up to 26.4 vol.% (46.8 vol.%, mmf) in M2. Rarely, funginite, secretinite (Fig. 28d), and micrinite are present, e.g. as fillings of cell lumens in telinite (Fig. 28f).

TABLE 15

Surface temperatures (T_s) and interior temperatures (T_i) measured at a depth of 1m in the Marcel coal waste dump (Tabor 2002-2009), and petrographic composition and random reflectance for samples from the dump

Sample no.	T_s (°C)	T_i (°C)	Unaltered vitrinite (vol.%)	Vitrinite with cracks (vol.%)	Paler coloured vitrinite (vol.%)	Vitrinite with pores (vol.%)	Liptinite (vol.%)	Inertinite (vol.%)	Pyrolytic carbon (vol.%)	Coke (vol.%)	Mineral matter (vol.%)	R_r (%)	Standard deviation for R_r
M1			0.0	0.0	55.0	0.0	6.6	23.6	0.0	0.0	14.8	1.01	0.06
M2			0.0	2.0	26.4	0.0	1.6	26.4	0.0	0.0	43.6	1.00	0.06
M3			0.0	3.6	21.6	0.0	1.2	8.4	0.0	0.0	65.2	1.03	0.05
M4			0.0	1.8	26.6	0.0	1.6	7.2	0.0	0.0	62.8	0.95	0.06
M5			0.0	0.8	46.6	0.0	8.4	25.0	0.0	0.0	19.2	0.99	0.05
M6	-	~500	0.2	0.8	50.8	0.8	0.0	11.6	0.0	0.0	35.8	1.31	0.09
M7			0.0	0.0	0.0	0.0	0.0	0.0	0.0	0.0	100.0	-	-
M8			19.4	4.4	0.0	0.0	0.8	0.0	0.0	0.0	75.4	0.76	0.05
M9			0.0	17.2	26.2	0.0	0.4	9.0	0.0	4.0	43.2	1.14	0.04
M10			9.2	0.4	13.8	0.0	0.4	5.6	0.2	14.4	56.0	1.23	0.28
M11			0.0	0.0	0.8	0.0	0.0	0.2	0.0	3.4	95.6	2.34	0.29
M12			3.6	0.0	0.6	0.0	0.6	2.2	0.0	4.0	89.0	2.69	2.09
M12a			4.8	0.2	1.4	0.0	0.4	1.0	0.0	4.4	87.8	2.32	1.79
M13			6.2	0.8	2.2	0.0	0.2	1.0	0.0	3.6	86.0	2.62	1.87
M13a			4.8	0.0	1.4	0.0	0.2	0.8	0.0	3.0	89.8	2.50	1.85
M14	50-70	-	4.6	1.0	2.4	0.0	1.0	1.4	0.2	6.8	82.6	2.56	1.87
M14a			3.8	0.6	3.2	0.0	0.4	1.2	0.0	5.0	85.8	1.68	0.97
M15			11.8	0.4	0.4	0.0	1.0	4.2	0.0	2.4	79.8	2.52	1.75
M15a			3.8	0.6	3.2	0.0	0.4	1.2	0.0	5.0	85.8	2.07	1.56
M16			5.4	0.2	1.8	0.0	0.0	1.2	0.0	10.0	81.4	2.57	1.84

M16a		0.4	0.4	2.4	0.0	0.0	0.4	0.0	6.4	90.0	2.53	1.32
M17		3.0	0.0	1.6	0.0	0.4	1.6	0.0	5.0	88.4	2.30	1.68
M17a		7.2	0.2	6.2	0.0	0.6	1.0	0.0	5.2	79.6	2.43	1.63
M18		2.8	0.0	2.2	0.0	0.0	0.6	0.0	2.0	92.4	1.71	1.18
M18a		3.8	0.2	0.2	0.0	0.0	2.6	0.0	8.4	84.8	2.07	1.30
M19		6.2	0.2	1.0	0.0	0.4	0.6	0.0	5.0	86.6	2.45	1.85
M19a		4.8	0.0	0.2	0.0	0.2	0.0	0.0	5.0	89.8	2.40	1.67
M20		6.0	0.0	0.4	0.0	0.2	1.2	0.0	2.6	89.6	2.37	1.73
M20a		11.6	0.0	2.4	0.0	0.2	2.8	2.8	0.0	80.2	2.14	1.50
M21		6.2	1.4	1.4	0.0	0.2	2.0	0.0	4.6	84.2	2.46	1.83
M21a		4.2	0.0	1.8	0.0	0.0	1.4	0.0	5.8	86.8	2.42	1.69
M22		2.6	0.0	1.0	0.0	0.2	0.4	0.0	3.8	92.0	2.31	1.54
M22a		5.2	0.6	0.6	0.0	0.0	1.2	0.0	6.4	86.0	1.98	1.31
M23		0.0	0.0	2.4	0.0	0.0	0.0	0.0	14.4	83.2	2.14	1.87
M24	-	8.4	0.0	0.0	0.0	1.6	1.4	0.0	0.0	88.6	0.72	0.05
M24a	-	7.6	0.8	0.0	0.0	0.0	0.4	0.0	0.0	91.2	0.72	0.05
M25	-	8.4	0.2	0.0	0.0	2.6	2.4	0.0	0.0	86.4	0.74	0.05
M30		0.0	0.0	0.0	0.0	0.0	0.0	0.0	0.0	100.0	-	-
M31		0.0	0.0	0.0	0.0	0.0	0.0	0.0	0.0	100.0	-	-
M32		0.0	0.0	0.0	0.0	0.0	0.0	0.0	3.0	97.0	4.64	0.45
M33		0.0	0.0	0.0	0.0	0.0	0.0	0.0	65.0	35.0	4.55	0.39
M34	>200	0.0	0.0	0.0	0.0	0.0	0.0	0.0	0.0	100.0	-	-
M35		0.0	0.0	0.0	0.0	0.0	0.0	0.0	3.2	96.8	4.86	0.58
M36		0.0	0.0	0.0	0.0	0.0	0.8	0.0	22.2	77.0	5.83	0.51
M37		0.0	0.0	0.0	0.0	0.0	0.0	0.0	0.0	100.0	-	-
M38		0.0	0.0	0.0	0.0	0.0	0.0	0.0	0.0	100.0	-	-
M39		0.0	0.0	0.0	0.0	0.0	0.0	0.0	0.0	100.0	-	-

M40	0.0	0.0	0.0	0.0	0.0	0.0	0.0	100.0	-	-
M41	0.0	0.0	0.0	0.0	0.0	0.0	1.2	98.8	5.16	0.95
M42	0.0	0.0	0.0	0.0	0.0	0.0	0.0	100.0	-	-
M43	0.0	0.0	0.0	0.0	0.0	0.0	0.0	100.0	-	-

"-" measurement not taken
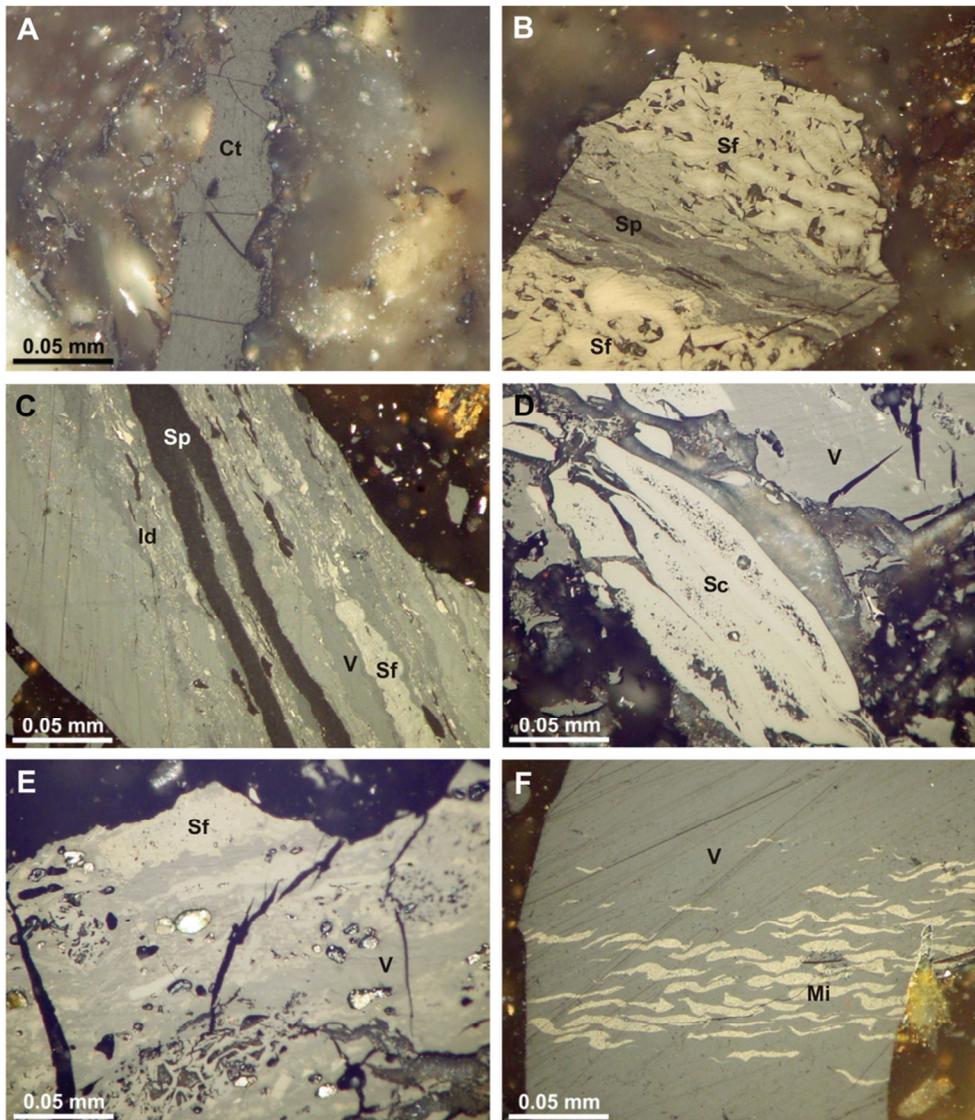
Fig. 28. Organic and mineral matter in coal wastes from the Marcel dump (white light, immersion oil). A – collotelinite (sample M24a), B – trimacerite (sample M25), C – trimacerite (sample M9), D – paler coloured vitrinite associated with secretinite and inertodetrinite (sample M6), E – paler coloured vitrinite associated with semifusinite and inertodetrinite (sample M6), F – paler coloured telinite with cell lumens filled with micrinite (sample M9). V – vitrinite, Ct – collotelinite, Sp – sporinite, Sf – semifusinite, Sc – secretinite, Mi – micrinite, Id – inertodetrinite.

TABLE 16

Petrographic composition of coal waste samples from the Marcel dump calculated
on a mineral matter free (mmf) basis

Sample no.	Unaltered vitrinite (vol.%)	Vitrinite with cracks (vol.%)	Paler coloured vitrinite (vol.%)	Vitrinite with pores (vol.%)	Liptinite (vol.%)	Inertinite (vol.%)	Pyrolytic carbon (vol.%)	Coke (vol.%)
M1	0.0	0.0	64.6	0.0	7.7	27.7	0.0	0.0
M2	0.0	3.5	46.8	0.0	2.8	46.8	0.0	0.0
M3	0.0	10.3	62.1	0.0	3.4	24.1	0.0	0.0
M4	0.0	4.8	71.5	0.0	4.3	19.4	0.0	0.0
M5	0.0	1.0	57.7	0.0	10.4	30.9	0.0	0.0
M6	0.3	1.2	79.1	1.2	0.0	18.1	0.0	0.0
M7	0.0	0.0	0.0	0.0	0.0	0.0	0.0	0.0
M8	78.9	17.9	0.0	0.0	3.3	0.0	0.0	0.0
M9	0.0	30.3	46.1	0.0	0.7	15.8	0.0	7.0
M10	20.9	0.9	31.4	0.0	0.9	12.7	0.5	32.7
M11	0.0	0.0	18.2	0.0	0.0	4.5	0.0	77.3
M12	32.7	0.0	5.5	0.0	5.5	20.0	0.0	36.4
M12a	39.3	1.6	11.5	0.0	3.3	8.2	0.0	36.1
M13	44.3	5.7	15.7	0.0	1.4	7.1	0.0	25.7
M13a	47.1	0.0	13.7	0.0	2.0	7.8	0.0	29.4
M14	26.4	5.7	13.8	0.0	5.7	8.0	1.1	39.1
M14a	26.8	4.2	22.5	0.0	2.8	8.5	0.0	35.2
M15	58.4	2.0	2.0	0.0	5.0	20.8	0.0	11.9
M15a	26.8	4.2	22.5	0.0	2.8	8.5	0.0	35.2
M16	29.0	1.1	9.7	0.0	0.0	6.5	0.0	53.8
M16a	4.0	4.0	24.0	0.0	0.0	4.0	0.0	64.0
M17	25.9	0.0	13.8	0.0	3.4	13.8	0.0	43.1
M17a	35.3	1.0	30.4	0.0	2.9	4.9	0.0	25.5
M18	36.8	0.0	28.9	0.0	0.0	7.9	0.0	26.3
M18a	25.0	1.3	1.3	0.0	0.0	17.1	0.0	55.3
M19	46.3	1.5	7.5	0.0	3.0	4.5	0.0	37.3
M19a	47.1	0.0	2.0	0.0	2.0	0.0	0.0	49.0
M20	57.7	0.0	3.8	0.0	1.9	11.5	0.0	25.0
M20a	58.6	0.0	12.1	0.0	1.0	14.1	14.1	0.0
M21	39.2	8.9	8.9	0.0	1.3	12.7	0.0	29.1
M21a	31.8	0.0	13.6	0.0	0.0	10.6	0.0	43.9
M22	32.5	0.0	12.5	0.0	2.5	5.0	0.0	47.5
M22a	37.1	4.3	4.3	0.0	0.0	8.6	0.0	45.7
M23	0.0	0.0	14.3	0.0	0.0	0.0	0.0	85.7
M24	73.7	0.0	0.0	0.0	14.0	12.3	0.0	0.0
M24a	86.4	9.1	0.0	0.0	0.0	4.5	0.0	0.0
M25	61.8	1.5	0.0	0.0	19.1	17.6	0.0	0.0

M30	0.0	0.0	0.0	0.0	0.0	0.0	0.0	100.0
M31	0.0	0.0	0.0	0.0	0.0	0.0	0.0	0.0
M32	0.0	0.0	0.0	0.0	0.0	0.0	0.0	100.0
M33	0.0	0.0	0.0	0.0	0.0	0.0	0.0	100.0
M34	0.0	0.0	0.0	0.0	0.0	0.0	0.0	0.0
M35	0.0	0.0	0.0	0.0	0.0	0.0	0.0	100.0
M36	0.0	0.0	0.0	0.0	0.0	3.5	0.0	96.5
M37	0.0	0.0	0.0	0.0	0.0	0.0	0.0	0.0
M38	0.0	0.0	0.0	0.0	0.0	0.0	0.0	100.0
M39	0.0	0.0	0.0	0.0	0.0	0.0	0.0	0.0
M40	0.0	0.0	0.0	0.0	0.0	0.0	0.0	0.0
M41	0.0	0.0	0.0	0.0	0.0	0.0	0.0	100.0
M42	0.0	0.0	0.0	0.0	0.0	0.0	0.0	100.0
M43	0.0	0.0	0.0	0.0	0.0	0.0	0.0	0.0

Coke, the most altered form of organic matter, occurs in M9-M11. It is the dominant form in M10 and M11 where it prevails over unaltered vitrinite, vitrinite with cracks, and paler-coloured vitrinite (Fig. 29a-b). The coke content (14.4 vol.%; 32.7 vol.%, mmf) is highest in M10 which also contains a significant amount of paler-coloured vitrinite (13.8 vol.%; 31.4 vol.%, mmf). However, M9 contains more vitrinite with cracks and paler-coloured vitrinite than coke (Tables 15, 16).

Pyrolytic carbon occurs in M10 (0.2 vol.%, 0.5 vol.% mmf) and M11(< 0.2 vol.%). Yellowish in colour, it has a ribbon-like morphology and displays a very strong anisotropy.

The mineral contents are significant in M1-M11. In these, they range from 14.8 vol.% in M1 to 100.0 vol.% in sample M7 (Table 15).

The reflectance of these wastes ranges from 0.76% in the least altered sample M8 to 2.34% in the most altered M11 (Table 15). The reflectograms of some samples are narrow and similar to the reflectograms of samples M24a and M24 (Fig 31a-b). Others show varying degrees of alteration with two maxima (Fig. 31c).

Samples M12-M22a came from a place that is self-heating at the moment. Their petrography reflects a mixture of strongly altered material containing coked organic matter and less altered material containing unaltered macerals (Tables 15, 16). Unaltered vitrinite is the dominant form of that maceral group in these wastes. Its content is from 0.4 vol.% (4.0 vol.%, mmf; M16a) to 11.8 vol.% (58.4 vol.%, mmf; M15). Contents of paler coloured vitrinite (Fig. 29c), present in all samples in the range from 0.2 vol.% (1.3 vol.%, mmf; M18a) to 6.2 vol.% (30.4 vol.%, mmf; M17a), are lower than those of unaltered vitrinite. Vitrinite with cracks occurs in most samples but contents are low; the maximum is 1.4 vol.% (8.9 vol.%, mmf) in M21. Rare vitrinites with paler-coloured oxidation rims are encountered (Fig. 29d). A few particles of vitrinite with pores occur in M17a and M22a in contents < 0.2 vol.%. Liptinite and inertinite contents in these wastes reach their maximum contents in M15 (1.0 and 4.2 vol. %, respectively; Tables 15, 16).
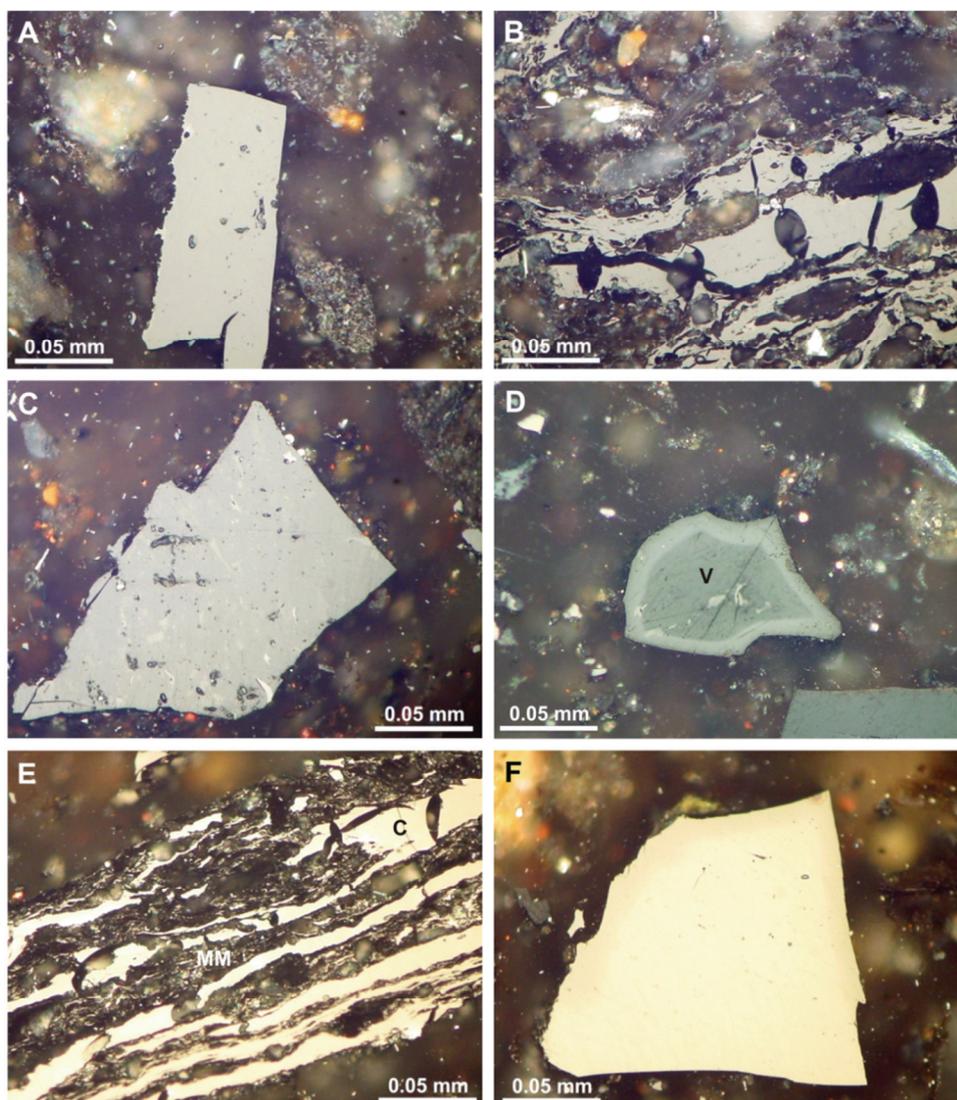
Fig. 29. Organic and mineral matter in coal wastes from the Marcel dump (white light, immersion oil).
A, B – coke (sample M11); C – paler coloured vitrinite and inertodetrinite (sample M12); D – paler
coloured oxidation rim around vitrinite particle (sample M21a); E – coke interlayered with mineral
matter (sample M14); F – massive coke (sample M14). V – vitrinite, C – coke, MM – mineral matter.

Coke (Fig. 29e-f) occurs in all samples, though its content is < 0.2 vol.% in M20a. In all other samples, coke contents are in the range 2.0-10.0 vol.% (11.9-77.3 vol.%, mmf). Pyrolytic carbon is present in samples M14 (0.2 vol.%; 1.1 vol.%, mmf) and M20a (2.8 vol.%; 14.1 vol.%, mmf). Irregular expulsions of bitumens with a marked yellow fluorescence occur in trace amounts in some samples (M12a, M13, M13a, M14, M14a, M15, M22, and M22a) and are always associated with clay minerals (Fig. 30).

184
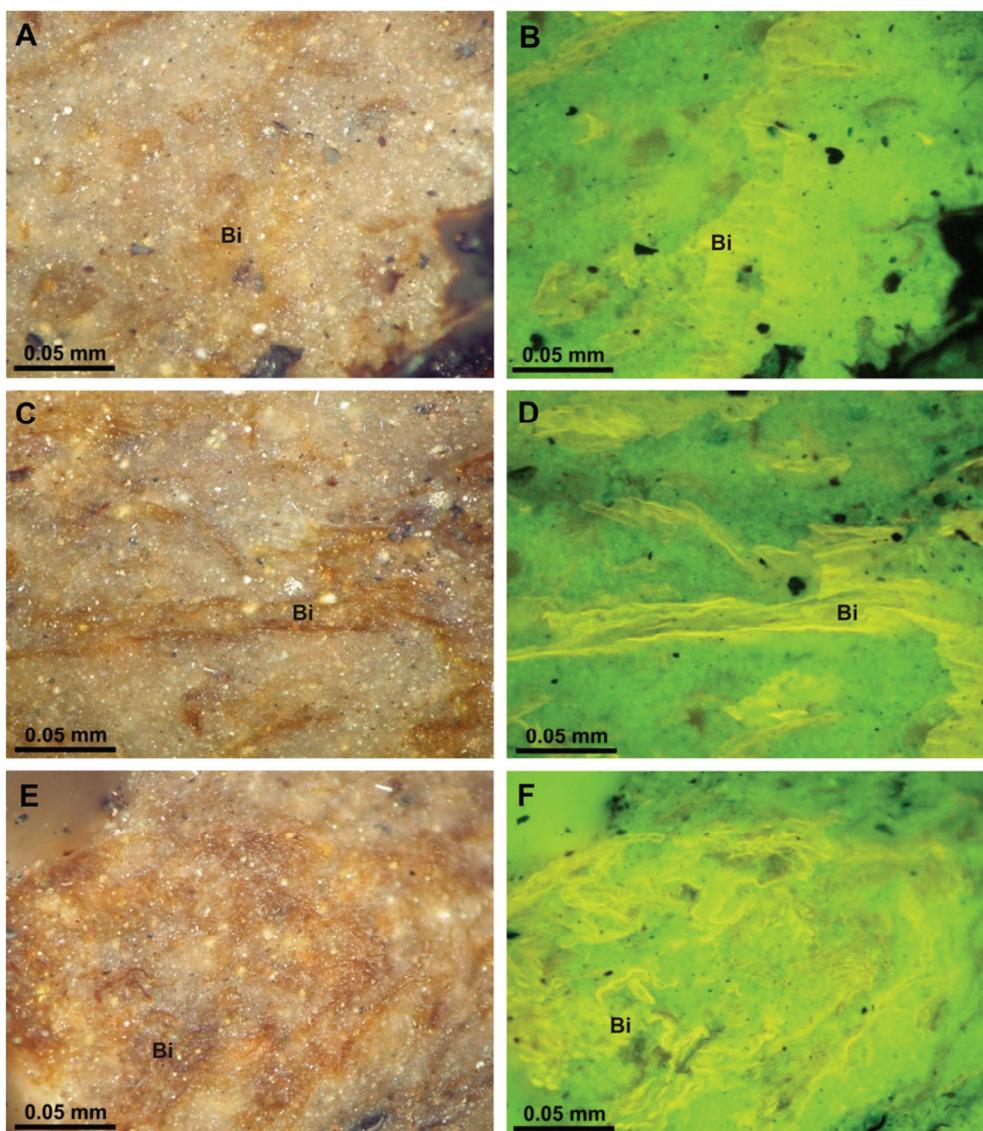
Fig. 30. Expulsions of bitumens in coal wastes from the Marcel dump (sample M15; immersion oil).
A, C, E – white light, B, D, F – fluorescence. Bi – bitumen expulsions.

Reflectance varies from 1.68% in M14a to 2.71% in M18; it is typically > 2.30%. All reflectograms are very wide, indicating that the samples comprise organic matter unaltered and altered to varying degrees (Fig. 31d).

Sample M23 contains 83.2 vol.% of mineral matter, coke (14.4 vol.%; 85.7 vol.%, mmf), and paler-coloured vitrinite (2.4 vol.%; 14.3 vol.%, mmf); there is no visible liptinite or inertinite present (Tables 15, 16). A reflectance of 2.14% indicates strong heating.
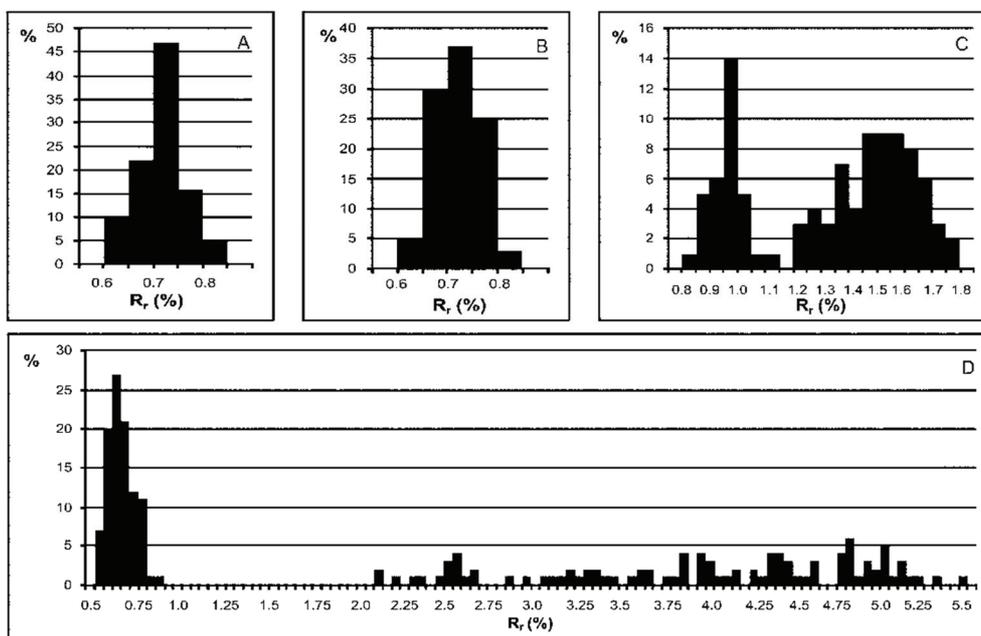
Fig. 31. Reflectograms of selected samples from the Marcel coal waste dump. A – sample M24a, B – sample M24, C – sample M10, D - sample M12a.

Mineral contents range from 35.0-100.0 vol.% in the most altered samples from the dump (M30-M43; Table 15). Microscopically visible organic matter is absent in M31, M34, M37-M39, and M43. The only forms of organic matter in the other samples are coke and inertinite. Coke contents range from 1.2-65.0 vol.% (96.5-100.0 vol.%, mmf). Inertinite is present only in sample M36 in 0.8 vol.% (3.5 vol.%, mmf; Tables 15, 16). The random reflectance, ranging from 4.55-5.83%, is the highest measured for the wastes collected.

8.3. Organic geochemistry

The wastes sampled at the Marcel Coal Mine dump vary considerably both in their extract yields and in the character of the compounds present. The differences reflect the collecting sites. The most commonly occurring chemical compounds are *n*-alkanes and their derivatives, acyclic isoprenoids, hopanes, and polyaromatic hydrocarbons. Most samples contain phenols.

Extract yields for all the wastes collected from the dump lie in the range from 0.002 wt% in M12 and M24a to 9.431 wt% in M18 (Table 17); for the majority, the yields are < 0.4 wt%. The highest extract yields were obtained from samples collected over the coal mud collector on the northern slope of the dump, and from M12-M23. The most altered samples contain no bitumen at all or, at most, very low quantities (0.003-0.006 wt%). Notably, the unaltered sample M24a provided the lowest extract yield of all, and the weathered samples M24 and M25, very low yields (0.017 and 0.026 wt%, respectively).

186

TABLE 17

Extract yields and aliphatic biomarker parameters for samples from the Marcel coal waste dump

Sample no.	EY	CPI	Σ1/Σ2	$n\text{-}C_{23}/n\text{-}C_{31}$	Pr/Ph	$Pr/n\text{-}C_{17}$	$Ph/n\text{-}C_{18}$	$C_{31}S/(S+R)$	$Ts/(Ts+Tm)$	$C_{30}\beta\alpha/(\alpha\beta+\beta\alpha)$	$C_{30}\beta\beta/(\beta\beta+\alpha\beta+\beta\alpha)$
	1)	2)	3)	4)	5)	6)	7)	8)	9)	10)	11)
M1	0.203	0.85	0.53	11.50	6.93	2.81	0.33	0.58	0.92	0.28	0.01
M2	0.150	1.26	0.59	8.17	8.00	2.42	0.30	0.61	0.95	0.28	0.02
M3	0.040	1.08	0.66	3.88	4.26	1.51	0.29	0.59	0.93	0.30	0.05
M4	2.502	1.09	0.65	5.25	4.41	1.26	0.26	0.60	0.91	0.27	0.04
M5	0.168	1.08	1.16	4.47	1.85	2.45	2.30	0.59	0.92	0.26	0.02
M6	0.969	1.11	-	4.52	1.78	2.31	2.00	0.59	0.92	0.25	0.03
M7	0.034	0.97	0.59	11.33	5.76	2.65	0.41	0.61	0.93	0.18	0.06
M8	0.076	0.91	0.41	10.67	2.69	0.33	0.31	0.58	0.92	0.27	0.15
M9	0.754	1.10	0.75	4.17	2.95	0.60	0.33	0.56	0.91	0.24	0.02
M10	0.116	1.27	0.66	6.10	7.43	3.59	0.37	0.57	0.92	0.27	0.04
M11	0.014	1.33	1.40	4.87	0.63	1.05	0.59	0.57	0.87	0.13	-
M12	0.002	0.96	0.38	24.50	1.41	2.37	3.40	0.59	0.91	0.27	0.04
M12a	0.085	1.23	0.28	17.50	4.14	0.91	0.15	0.58	0.89	0.25	0.10
M13	0.066	1.14	0.14	21.99	0.41	0.25	0.66	0.59	0.95	0.25	0.04
M13a	0.091	1.15	0.45	18.33	3.15	0.85	0.25	0.59	0.91	0.25	0.02
M14	0.022	1.59	0.73	52.48	0.23	0.57	1.93	0.60	0.86	0.21	-
M14a	0.048	1.19	0.71	12.38	6.12	2.04	0.19	0.59	0.92	0.28	0.03
M15	0.048	1.13	0.23	14.96	6.67	0.43	0.06	0.58	0.92	0.24	0.02
M15a	0.348	1.16	0.38	10.25	2.24	0.84	0.43	0.57	0.93	0.25	0.03
M16	0.682	1.08	0.09	22.02	8.13	0.65	0.11	0.58	0.90	0.26	0.04
M16a	0.107	1.21	0.17	20.03	6.13	0.47	0.09	0.57	0.90	0.24	0.04

M17	0.145	1.25	0.43	20.86	5.13	0.93	0.15	0.60	0.91	0.27	0.13
M17a	0.084	1.12	0.45	19.25	0.77	0.92	7.40	0.57	0.88	0.25	0.03
M18	9.431	1.18	0.14	-	0.89	2.07	10.88	0.57	0.99	0.24	0.02
M18a	0.270	1.05	0.17	38.00	1.75	0.60	0.32	0.58	0.86	0.26	0.04
M19	0.223	0.96	0.49	8.13	4.85	0.73	0.13	0.59	0.95	0.27	0.04
M19a	0.133	1.13	0.54	10.00	3.17	1.12	0.23	0.58	0.90	0.27	0.04
M20	0.192	1.22	0.26	19.48	1.35	3.09	8.32	0.57	0.80	0.30	0.06
M20a	2.183	1.18	0.23	14.68	1.55	2.57	6.80	0.57	0.81	0.29	0.06
M21	0.125	1.07	0.11	-	0.88	1.24	7.91	0.57	0.90	0.26	0.12
M21a	0.088	1.24	0.09	-	0.76	1.39	7.23	0.56	0.92	0.27	0.15
M22	0.225	0.97	0.12	-	1.85	0.60	0.33	0.59	0.86	0.28	0.18
M22a	0.052	1.13	0.32	16.33	2.62	0.77	0.29	0.60	0.87	0.29	0.14
M23	0.667	1.21	2.24	9.33	2.95	0.65	0.18	0.58	0.91	0.25	0.05
M24	0.017	0.90	0.35	11.04	7.03	1.54	0.22	0.59	0.94	0.25	0.04
M24a	0.002	1.03	0.80	3.33	4.32	4.32	1.00	0.58	0.93	0.24	0.01
M25	0.026	1.14	0.84	5.77	6.60	1.52	0.20	0.59	0.91	0.24	0.04
M30	-	-	-	-	-	-	-	-	-	-	-
M31	0.003	1.08	2.04	24.07	-	-	-	0.66	-	0.27	-
M32	-	-	-	-	-	-	-	-	-	-	-
M33	-	-	-	-	-	-	-	-	-	-	-
M34	-	-	-	-	-	-	-	-	-	-	-
M35	-	-	-	-	-	-	-	-	-	-	-
M36	-	-	-	-	-	-	-	-	-	-	-
M37	-	-	-	-	-	-	-	-	-	-	-
M38	0.006	0.88	4.22	6.36	-	-	-	0.55	0.92	0.27	0.06
M39	-	-	-	-	-	-	-	-	-	-	-

M40	0.003	0.96	3.52	5.47	-	-	-	-	-	-	-	-
M41	-	-	-	-	-	-	-	-	-	-	-	-
M42	-	-	-	-	-	-	-	-	-	-	-	-
M43	-	-	-	-	-	-	-	-	-	-	-	-

1) EY – Extract yield (wt%)

2) $CPI = 0.5\{[(n\text{-}C_{25}+n\text{-}C_{27}+n\text{-}C_{29}+n\text{-}C_{31}+n\text{-}C_{33})/(n\text{-}C_{24}+n\text{-}C_{26}+n\text{-}C_{28}+n\text{-}C_{30}+n\text{-}C_{32})] + [(n\text{-}C_{25}+n\text{-}C_{27}+n\text{-}C_{29}+n\text{-}C_{31}+n\text{-}C_{33})/(n\text{-}C_{26}+n\text{-}C_{28}+n\text{-}C_{30}+n\text{-}C_{32}+n\text{-}C_{34})]\}$; Carbon Preference Index; $m/z = 71$; thermal maturity parameter (Bray, Evans 1961).

3) $\Sigma 1/\Sigma 2 = [\Sigma \text{ (from } n\text{-}C_{13} \text{ to } n\text{-}C_{22})]/[\Sigma \text{ (from } n\text{-}C_{23} \text{ to } n\text{-}C_{35})]$; $m/z = 71$, source indicator (Tissot, Welte 1984).

4) $n\text{-}C_{23}/n\text{-}C_{31}$; $m/z = 71$ (Pancost et al. 2002); source indicator.

5) Pr/Ph = pristane/phytane; parameter of environment oxicity (with exception of coals); $m/z = 71$ (Didyk et al. 1978).

6) Pr/$n\text{-}C_{17}$ = pristane/n-heptadecane; $m/z = 71$ (Leythaeuser, Schwartzkopf 1986).

7) Ph/$n\text{-}C_{18}$ = phytane/n-octadecane; $m/z = 71$ (Leythaeuser, Schwartzkopf 1986).

8) C_{31} S/(S+R) = 17α(H),21β(H)-29-homohopane 22S/(17α(H),21β(H)-29-homohopane 22S+17α(H),21β(H)-29-homohopane 22R); $m/z = 191$; thermal maturity parameter (Peters et al. 2005).

9) Ts/(Ts+Tm) = 18α(H)-22,29,30-trisnorneohopane/(18α(H)-22,29,30-trisnorneohopane+17α(H)-22,29,30-trisnorhopane); $m/z = 191$; thermal maturity parameter (Peters et al. 2005).

10) $C_{30}\beta\alpha/(\alpha\beta+\beta\alpha)$ = 17β(H),21α(H)-29-hopane C_{30}/(17α(H),21β(H)-29-hopane C_{30}+17β(H),21α(H)-29-hopane C_{30}); $m/z = 191$, (Seifert, Moldowan 1980).

11) $C_{30}\beta\beta/(\beta\beta+\alpha\beta+\beta\alpha)$ = 17β(H),21β(H)-29-hopane C_{30}/(17β(H),21β(H)-29-hopane C_{30}+17α(H),21β(H)-29-hopane C_{30}+17β(H),21α(H)-29-hopane C_{30}); $m/z = 191$, (Seifert, Moldowan 1980).

"–" compounds present, concentrations too low to calculate a parameter value.

n-Alkanes (*m/z* = 71) are present in all unaltered and moderately altered samples, and also in some highly altered samples (Table 17). They occur in variable ranges, though typically from *n*-C_{13} to *n*-C_{35}. *n*-Nonane was found in M2, M14, M15, and M19. A wide *n*-alkane distribution is typical for most of the Marcel dump samples though a relatively narrow distribution characterises some, i.e. M7, M31, M38, and M40.

M24a has an *n*-alkane distribution typical of unaltered coal (Fig. 32a), with a slight predominance of odd-over-even carbon number *n*-alkanes as expressed by the CPI value of 1.03. A predominance of long-to-short chain *n*-alkanes is reflected in the $\Sigma1/\Sigma2$ value of 0.80. Sample M24, altered by weathering to a minor extent, has a high content of lighter *n*-alkanes (*n*-C_{10}-*n*-C_{16}; Fig. 32b). The *n*-alkanes in M25, likewise mildly alteration due to weathering, show a Gaussian distribution in the range *n*-C_{14}-*n*-C_{36} with a maximum at *n*-C_{21} (Fig. 32c). CPI values for both of the latter are *ca* 1.0 (Table 17). They are also characterised by a predominance of long-to-short chain *n*-alkanes as is reflected in low $\Sigma1/\Sigma2$ values; that of M24 (0.35) is particularly low.
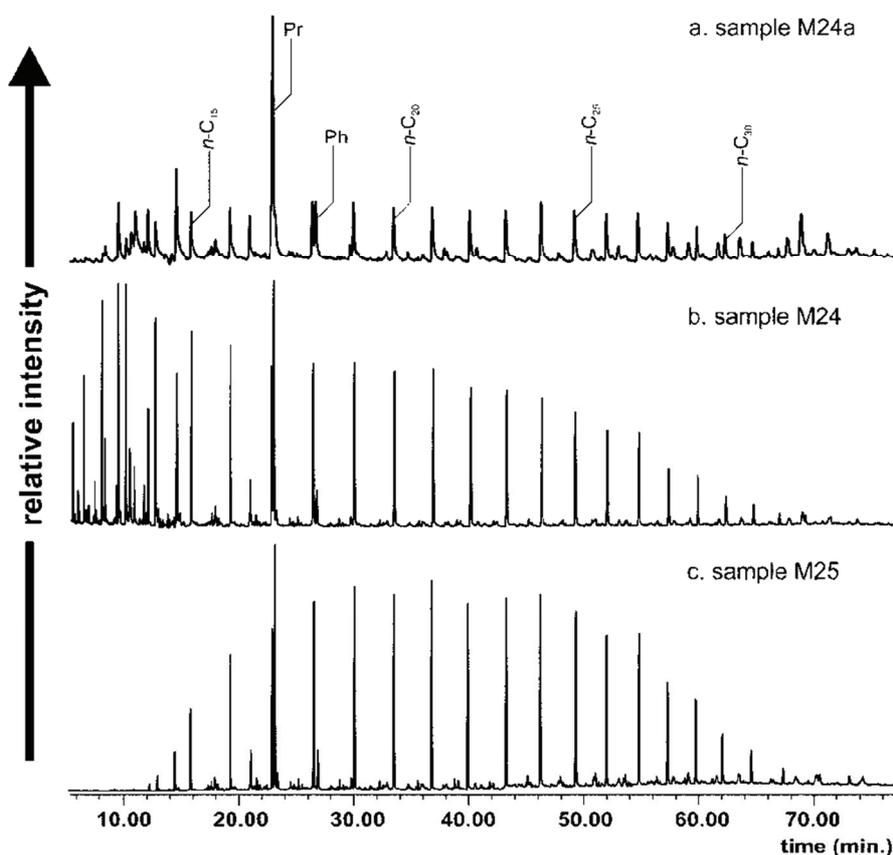

Fig. 32. *n*-Alkane distribution in selected Marcel coal waste extracts (*m/z* = 71). a – a wide *n*-alkane distribution of coal/kerogen III type; b – a wide *n*-alkane distribution of coal/kerogen III; c – a wide *n*-alkane distribution composed of bitumen from thermally unaltered organic matter and pyrolysate.

190

Wastes collected over the coal mud collector on the northern slope of the dump are weakly altered (M1, M2, and M7-M10; Fig. 33a) or moderately altered (M3-M6; Fig. 33b-c). M11 is the most strongly altered sample from there (Fig. 33d). The levels of alteration are reflected in a distribution of n-alkanes that is typically in the range n-C$_{13}$ to n-C$_{35}$. Weakly-altered samples have n-alkane distributions typical of unaltered coal. M3-M5, which contain pyrolysates, display a Gaussian n-alkane distribution (Fig. 33b-c). The most altered sample (M11) contains n-alkanes ranging from n-C$_{16}$ to n-C$_{32}$, and the highest
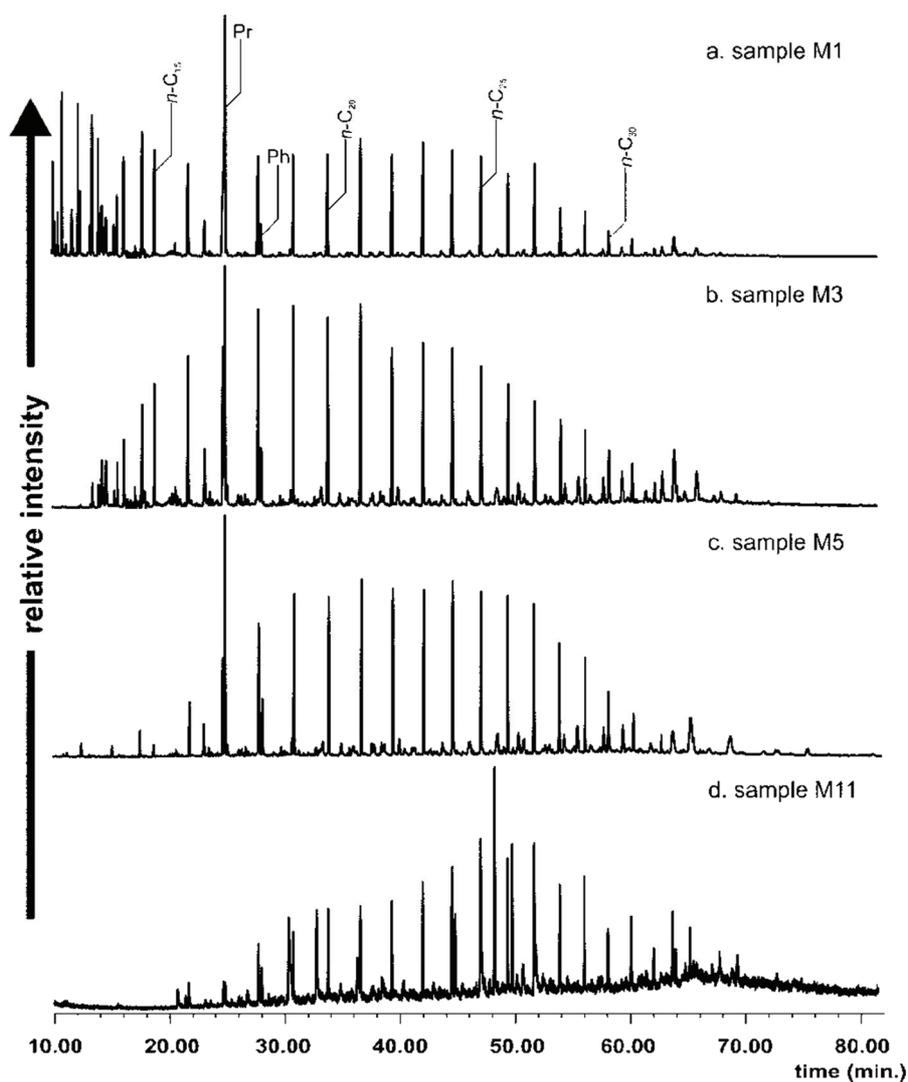
Fig. 33. n-Alkane distribution in selected Marcel coal waste extracts (m/z = 71). a – a wide n-alkane distribution of coal/kerogen III; b – a wide n-alkane distribution of a mixture of coal/kerogen III and pyrolysate; c – a wide n-alkane distribution of a mixture of coal /kerogen III and pyrolysate; d – a wide n-alkane distribution of pyrolytic type.

content of n-C$_{25}$ alkane (Fig. 33d). Long-to-short chain n-alkanes predominate in most samples in this set; values of $\Sigma 1/\Sigma 2$ range from 0.41-0.75. It is only in M5 and M11 that short chain n-alkanes predominate.

M12-M22a display a Gaussian n-alkane distribution typical of pyrolysates. Some of these wastes with a wide Gaussian distribution also contain light n-alkanes in the range n-C$_9$ to n-C$_{13}$ (M17 and M19; Fig. 34a). Many others have a wide Gaussian distribution containing n-alkanes in the range n-C$_{13}$ to n-C$_{35}$ (M12, M13a, M14a, M15a, M17a, M19a, M20, M20a, and M22a) or n-C$_{11}$ to n-C$_{31}$ (M12a, M13, M17, M18a, and M19). M14 and M13, also with wide n-alkane distributions in the range n-C$_9$-n-C$_{31}$ and n-C$_{11}$ to n-C$_{31}$, respectively (Fig. 34b-c), show two maxima indicative of different temperature ranges of origin. The maxima in M14 are at n-C$_{19}$ and n-C$_{23}$ and in M13 at n-C$_{18}$ and n-C$_{22}$.

A narrow n-alkane distribution is typical of M15, M16, M16a, M18, M21, M21a, and M22 (Fig. 34d-e). The distributions are in the ranges n-C$_{11}$ to n-C$_{20}$ for M16 with the highest contents of n-C$_{16}$ and n-C$_{17}$ alkanes (Fig. 34d), n-C$_{14}$ to n-C$_{21}$ (M15 and M16a), n-C$_{13}$ to n-C$_{24}$ (M18 and M22) and n-C$_{16}$ to n-C$_{24}$ (M21 and M21a); all have maxima that vary slightly from n-C$_{17}$ to n-C$_{21}$. Apart from the narrow n-alkane distribution, M16a also contains a high content of light n-alkanes in the range n-C$_{12}$ to n-C$_{14}$.

A slight predominance of odd-over-even carbon number n-alkanes is typical for M12a-M18a, M19a-M21a, and M22a) and in others (M12, M19, and M22) even number n-alkanes are present in slightly higher contents - as is expressed in CPI values in the ranges 1.05-1.59 and 0.96-0.97, respectively (Table 17). Sample M14 is characterized by the highest CPI value (1.59). A strong predominance of long-to-short chain n-alkanes is typical of all; values of $\Sigma 1/\Sigma 2$ range from 0.09-0.71.

M23 differs to some extent. n-Alkanes present in a wide range (n-C$_{11}$ to n-C$_{35}$), with the highest content of n-C$_{17}$, indicate a wide range of heating temperatures. The narrow Gaussian distribution is in the range n-C$_{23}$ to n-C$_{30}$. In this sample odd-over-even carbon number n-alkanes are slightly predominant and short-chain n-alkanes strongly dominate (Table 17).

The most strongly altered wastes (M30-M43) contain n-alkanes only in M31, M38, and M40. Only heavier n-alkanes ranging from n-C$_{18}$ to n-C$_{32}$ with narrow Gaussian distributions are present in these. CPI values are ca 1.0 (Table 17). A strong predominance of short-over-long chain n-alkanes with $\Sigma 1/\Sigma 2$ values of 2.04-4.22 is typical of these.

Acyclic isoprenoids (pristane and phytane; m/z = 71) occur in all but the most altered samples (M30-M43). Though the pristane to phytane (Pr/Ph) values are relatively high (4.32) in the unaltered sample M24a (Table 17), the weathered samples M24 and M25 show even higher values (7.03 and 6.60, respectively). In moderately altered material, Pr/Ph values are highly variable; the lowest value (0.63) was found in the highly altered M11. In others in this set, values range from 1.78 (M6) to 8.00 (M2). Even greater variation in Pr/Ph values are seen in more strongly altered samples M12-M22a; the values in these range from 0.23 (M14) to 8.13 (M16). On average, the ratio tends to be highest in the unaltered- and weathered material, and lowest in the highly altered samples.

A similar trend is seen in Pr/n-C$_{17}$ values (Table 17). The trend is reversed for Ph/n-C$_{18}$. Unaltered waste (M24a) has the highest value of Pr/n-C$_{17}$ (4.32), weathered material (M24 and M25) have much lower values (1.54 and 1.52, respectively), and moderately altered samples (M1-M11) have a range of values from 0.33 (M8) to 3.59

(M10). The most altered wastes (M12-M22a) have $Pr/n\text{-}C_{17}$ values that range from 0.25 (M13) to 3.09 (M20).
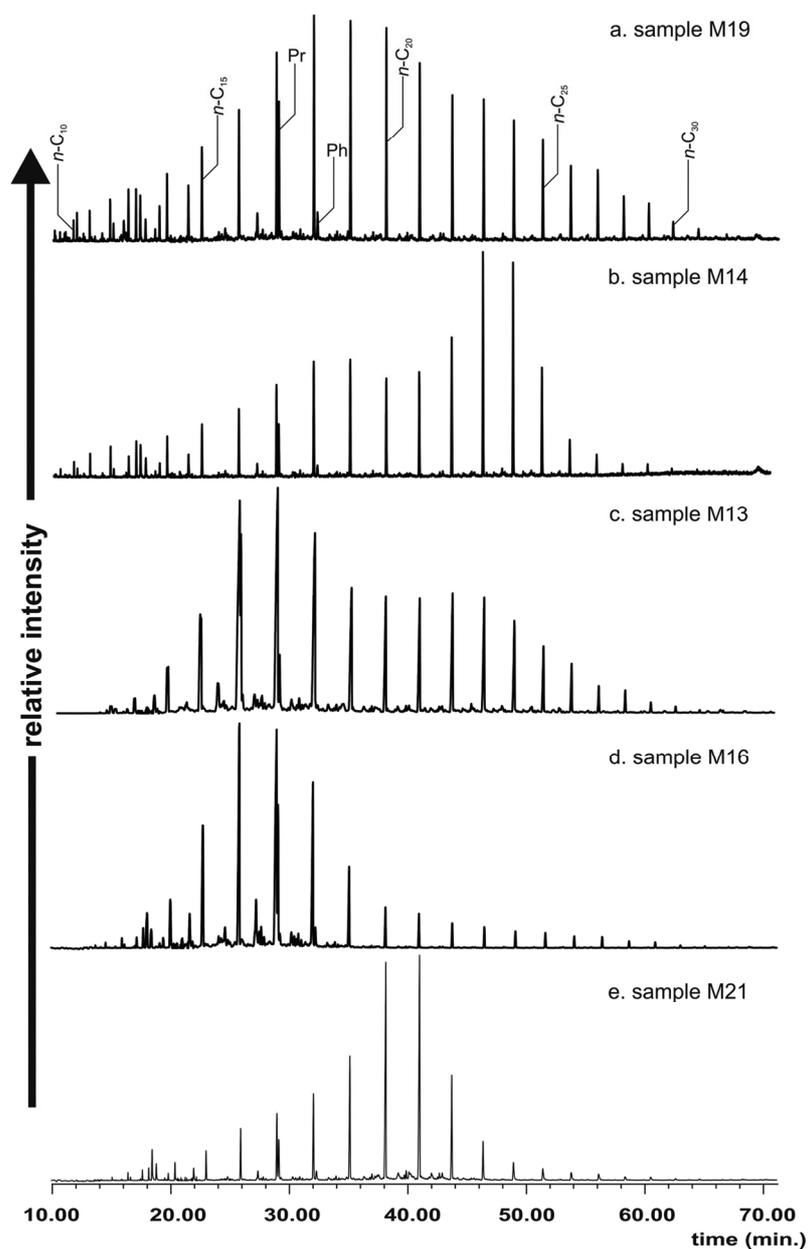
Fig. 34. *n*-Alkane distribution in selected Marcel coal waste extracts (*m/z* = 71). a – a wide *n*-alkane distribution in pyrolysate; b – a wide *n*-alkane distribution in pyrolysate; c – wide *n*-alkane distribution in pyrolysate; d – narrow distribution of lighter molecular-weight *n*-alkanes in pyrolysate; e – a narrow distribution of higher molecular-weight *n*-alkanes in pyrolysate.

Hopanoids ($m/z = 191$) are present in all wastes except the most altered ones (M30, M32-M37, M39, and M41-M43; Table 17). Excepting these, all samples show similar values of $C_{31}S/(S+R)$ in the range 0.55-0.66 (Table 17). Values of Ts/(Ts+Tm) are also similar in all (0.80-0.99). The moretanes to hopanes ratio, $C_{30}\beta\alpha/(\alpha\beta+\beta\alpha)$, ranges from 0.13 in M11 to 0.30 in M20. Low values of $C_{30}\beta\beta/(\beta\beta+\alpha\beta+\beta\alpha)$, ranging from 0.01 (M1 and M24a) to 0.18 (M22), are consistent with the high contents of $\alpha\beta$ hopanes (Fig. 10, 11, 35, 36).

Values of thermal indices based on aromatic hydrocarbons show strong correlations with collection sites (Table 18). The unaltered sample M24a shows the lowest value (0.52) of the Methylnaphthalene Ratio (MNR; $m/z = 142$) and the second lowest value (0.59) of the Methylphenanthrene Index (MPI-3; $m/z = 192$). The value of MB/DBF ($m/z = 168$) is 0.70 and is above the average (0.56) for all other samples. Other parameters based on aromatic hydrocarbons were not calculated for M24a due to low contents.

TABLE 18

Aromatic hydrocarbon parameters for samples from the Marcel coal waste dump

Sample no.	MNR	DNR	TNR-1	TNR-2	TNR-4	MPI-3	2-MP/2-MA	MB/DBF
	1)	2)	3)	4)	5)	6)	7)	8)
M1	1.18	2.07	1.97	1.36	0.52	0.83	32.50	0.51
M2	1.54	2.94	1.00	0.71	0.63	0.92	1.93	0.34
M3	1.00	1.43	1.25	0.96	0.42	0.84	21.33	0.37
M4	1.32	1.68	1.86	1.11	0.56	0.91	6.86	0.29
M5	0.61	0.87	1.73	1.13	0.60	0.81	15.40	0.87
M6	0.55	0.99	-	-	-	0.88	15.22	0.75
M7	0.68	0.92	0.99	0.81	0.50	0.85	13.50	1.04
M8	1.32	1.22	1.65	1.06	0.67	0.66	21.00	0.62
M9	0.99	2.08	1.94	1.10	0.42	1.10	32.67	0.64
M10	1.19	1.18	-	-	-	0.83	1.29	0.43
M11	-	-	1.48	1.01	0.64	-	-	-
M12	-	-	-	-	-	0.67	2.67	0.80
M12a	1.69	4.14	-	-	-	0.82	2.02	0.45
M13	1.74	1.43	-	-	-	1.28	15.17	0.90
M13a	1.69	1.22	-	-	-	0.41	2.93	0.57
M14	1.79	3.38	0.97	0.82	0.58	1.07	2.80	0.32
M14a	1.68	1.18	-	-	-	0.92	12.50	0.29
M15	1.94	3.59	0.89	0.78	0.57	1.12	4.22	0.47
M15a	1.73	1.15				1.05	3.64	0.72
M16	1.64	2.05				1.04	4.32	0.36
M16a	1.53	6.43	1.08	0.85	0.52	0.93	3.90	0.35
M17	1.50	1.62	3.73	1.49	0.54	0.90	6.67	0.38
M17a	1.36	1.62	2.74	1.30	0.66	0.70	4.67	0.33
M18	0.70	-	-	-	-	0.88	-	0.61
M18a	1.71	0.86	-	-	-	0.66	-	0.41

M19	2.04	3.36	0.61	0.68	0.53	1.22	3.58	0.41
M19a	1.37	3.27	-	-	-	1.16	14.20	0.63
M20	1.12	1.72	-	-	-	1.02	3.67	0.63
M20a	1.23	1.91	-	-	-	1.00	-	0.65
M21	1.90	3.99	-	-	-	0.79	-	0.58
M21a	2.04	4.23	1.29	0.91	0.69	0.68	3.64	0.50
M22	1.58	1.47	1.69	1.04	0.71	0.85	4.47	0.60
M22a	1.48	2.41	-	-	-	1.21	8.44	0.84
M23	1.68	2.62	1.20	0.86	0.52	1.15	2.50	0.37
M24	1.31	2.38	1.23	1.35	0.53	0.87	9.52	0.70
M24a	0.52	-	-	-	-	0.59	-	0.70
M25	0.56	1.92	-	-	-	0.97	-	0.62
M30	-	-	-	-	-	-	-	-
M31	-	-	-	-	-	-	-	-
M32	-	-	-	-	-	-	-	-
M33	-	-	-	-	-	-	-	-
M34	-	-	-	-	-	-	-	-
M35	-	-	-	-	-	-	-	-
M36	-	-	-	-	-	-	-	-
M37	-	-	-	-	-	-	-	-
M38	-	-	-	-	-	-	-	-
M39	-	-	-	-	-	-	-	-
M40	-	-	-	-	-	-	-	-
M41	-	-	-	-	-	-	-	-
M42	-	-	-	-	-	-	-	-
M43	-	-	-	-	-	-	-	-

1) MNR = 2-methylnaphthalene/1-methylnaphthalene; m/z = 142; thermal maturity parameter (Radke et al. 1994).

2) DNR = (2,6-dimethylnaphthalene+2,7-dimethylnaphthalene)/1,5-dimethylnaphthalene; m/z = 156, thermal maturity parameter (Radke et al. 1982).

3) TNR-1 = 2,3,6-trimethylnaphthalene/(1,3,6-trimethylnaphthalene+ 1,4,6-trimethylnaphthalene+1,3,5-trimethylnaphthalene); m/z = 170, thermal maturity parameter (Radke et al. 1986).

4) TNR-2 = (1,3,7-trimethylnaphthalene+2,3,6-trimethylnaphthalene)/ (1,3,5-trimethylnaphthalene+1,4,6-trimethylnaphthalene+1,3,6-trimethylnaphthalene); m/z = 170, thermal maturity parameter (Radke et al. 1986).

5) TNR-4 = 1,2,5-trimethylnaphthalene/(1,2,5-trimethylnaphthalene+ 1,2,7-trimethylnaphthalene+1,6,4-trimethylnaphthalene); m/z = 170, thermal maturity parameter.

6) MPI-3 = (2-methylphenanthrene+3-methylphenanthrene)/(1-methylphenanthrene+ 9-methylphenanthrene); m/z = 192; thermal maturity parameter (Radke, Welte 1983).

7) 2-MP/2-MA = 2-methylphenanthrene/2-methylanthracene; m/z = 192.

8) MB/DBF = (3-methylbiphenyl+4-methylbiphenyl)/dibenzofurane; m/z = 168; thermal maturity parameter (Radke 1987).

"–" compounds present but concentrations too low to calculate a parameter value.

Fig. 35. Pentacyclic triterpane distribution in extracts from selected Marcel coal waste samples that underwent weathering and moderate alteration (m/z = 191). Ts – 18α(H)-22,29,30-trisnorneohopane, Tm – 17α(H)-22,29,30-trisnorhopane, C$_{29}\alpha\beta$ – 17α,21β(H)-30-norhopane, C$_{29}\beta\alpha$ – 18α,21β(H)-30-norneohopane, C$_{30}\alpha\beta$ – 17α,21β(H)-hopane, C$_{30}\beta\beta$ – 17β,21β(H)-hopane, C$_{30}\beta\alpha$ – 17β,21α(H)-hopane, C$_{31}\alpha\beta$ – 17α,21β(H)-30-homohopane 22S and 22R, C$_{31}\beta\alpha$ – 18α,21β(H)-30-homohopane 22R, C$_{32}\alpha\beta$ – 17α,21β(H)-30-bishomohopane 22S and 22R.

Fig. 36. Pentacyclic triterpane distribution in extracts from more strongly altered Marcel coal waste samples ($m/z = 191$). Ts – 18α(H)-22,29,30-trisnorneohopane, Tm – 17α(H)-22,29,30-trisnorhopane, C$_{29}\alpha\beta$ – 17α,21β(H)-30-norhopane, C$_{29}\beta\alpha$ – 18α,21β(H)-30-norneohopane, C$_{30}\alpha\beta$ – 17α,21β(H)-hopane, C$_{30}\beta\beta$ – 17β,21β(H)-hopane, C$_{30}\beta\alpha$ – 17β,21α(H)-hopane, C$_{31}\alpha\beta$ – 17α,21β(H)-30-homohopane 22S and 22R, C$_{31}\beta\alpha$ – 18α,21β(H)-30-homohopane 22R, C$_{32}\alpha\beta$ – 17α,21β(H)-30-bishomohopane 22S and 22R.

The weathered samples (M24 and M25) also have low MNR values (1.31 and 0.56, respectively; Fig. 37a-b) in comparison to other samples from the Marcel dump. Their Dimethylnaphthalene Ratio (DNR) and Trimethylnaphthalene Ratios (TNR-1 and TNR-4; $m/z = 170$) are in the range of values for the wastes in this dump. The TNR-2 ratio for M24, is one of the highest for all samples collected in the dump. The MB/DBF values are relatively high in M24 and M25 in comparison to those of other samples (Table 18).

197
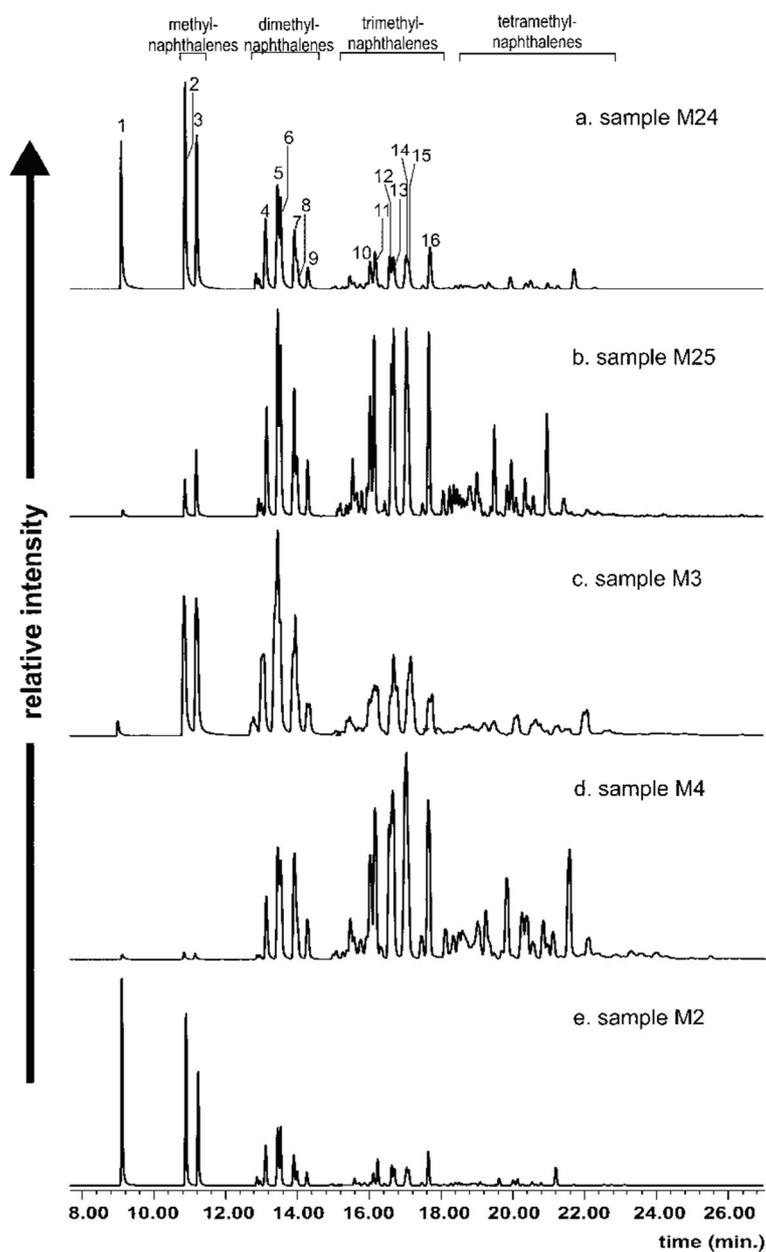
Fig. 37. Composed ion chromatogram showing distributions of naphthalene and alkylnaphthalenes in the Marcel coal waste extracts from unaltered, oxidized and moderately altered samples (m/z = 128+142+156+170+184). 1: naphthalene, 2: 2-methylnaphthalene, 3: 1-methylnaphthalene, 4: 2,6+2,7-dimethylnaphthalene, 5: 1,3+1,7-dimethylnaphthalene, 6: 1,6-dimethylnaphthalene, 7: 1,4+2,3-dimethylnaphthalene, 8: 1,5-dimethylnaphthalene, 9: 1,2-dimethylnaphthalene, 10: 1,3,7-trimethylnaphthalene, 11: 1,3,6-trimethylnaphthalene, 12: 1,4,6+1,3,5-trimethylnaphthalene, 13: 2,3,6-trimethylnaphthalene, 14: 1,2,7+1,6,7-trimethylnaphthalene, 15: 1,2,6-trimethylnaphthalene, 16: 1,2,5-trimethylnaphthalene, 17: 1,2,3,4-tetramethylnaphthalene.
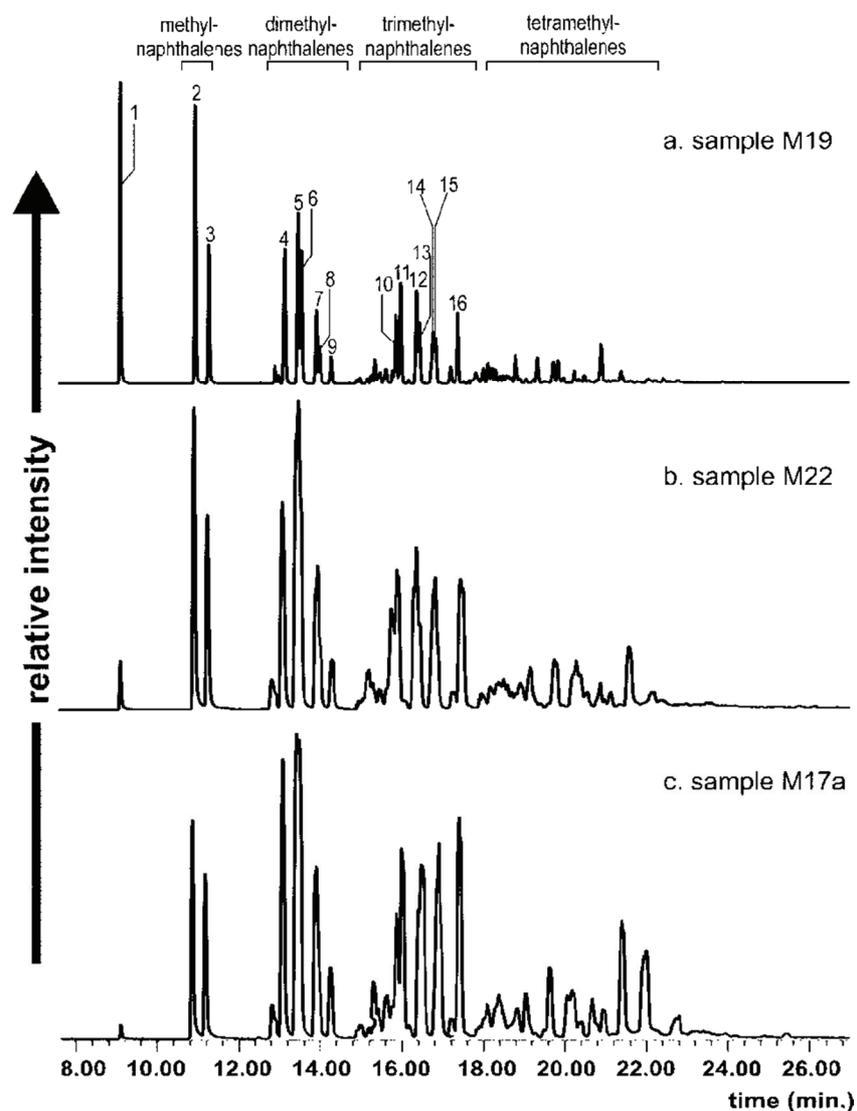
Fig. 38. Composed ion chromatogram showing distributions of naphthalene and alkylnaphthalenes in Marcel coal waste extracts from more strongly altered samples (m/z = 128+142+156+170+184).
1: naphthalene, 2: 2-methylnaphthalene, 3: 1-methylnaphthalene, 4: 2,6+2,7-dimethylnaphthalene,
5: 1,3+1,7-dimethylnaphthalene, 6: 1,6-dimethylnaphthalene, 7: 1,4+2,3-dimethylnaphthalene,
8: 1,5-dimethylnaphthalene, 9: 1,2-dimethylnaphthalene, 10: 1,3,7-trimethylnaphthalene,
11: 1,3,6-trimethylnaphthalene, 12: 1,4,6+1,3,5-trimethylnaphthalene, 13: 2,3,6-trimethylnaphthalene,
14: 1,2,7+1,6,7-trimethylnaphthalene, 15: 1,2,6-trimethylnaphthalene, 16: 1,2,5-trimethylnaphthalene,
17: 1,2,3,4-tetramethylnaphthalene.

Samples M1-M11 collected over the coal mud collector on the northern slope of the dump have relatively low values of MNR (0.55-1.54) and DNR (0.87-2.94; Fig. 37c-e) and also of TNR-1, TNR-2, and TNR-4 compared to the others. Values of the 2-methyl-

199

phenanthrene/2-methylanthracene (2-MP/2-MA; m/z = 192) ratio are distinctly higher in most of the material collected in that sampling site; most are in the range 13.50-32.67 (Table 18). Only M10, M2, and M4 have lower values. This ratio was not determined for M11 due to the very low contents of these compounds. MPI-3 and MB/DBF values are in the range characterizing other samples.

On average, the MNR and DNR values are higher in M12-M22a than in the other samples collected at the Marcel dump (Table 18). The MNR values range from 0.70 in M18 to 2.04 in M19, and DNR values from 0.86 in M18a to 6.43 in M16a (Table 18). TNR-1 and TNR-4 parameters based on trimethylnaphthalenes are higher on average, and TNR-2 ratios lower for these samples. 2-MP/2-MA values are usually in the range 2.02-8.44, significantly lower than for other samples; only M13, M14a, and M19a show higher values (Table 18). Values of MPI-3 and MB/DBF ratios are similar to those in other samples. The distribution of naphthalene and alkylnaphthalenes in M12-M22a is shown in Figure 38.

Two- and three-ring PAHs (m/z = 128+178+202+228+252) predominate in unaltered, weathered and moderately altered wastes (Fig. 13, 39; Table 19). Only in the most altered sample M38 do four-ring PAHs dominate over two- and three- and five-ring PAHs. The lowest relative contents of five-ring PAHs occur in samples M12-M22a. Samples M30-M37 and M39-M43 contain no aromatic hydrocarbons. In this case, they were probably destroyed by high temperatures.
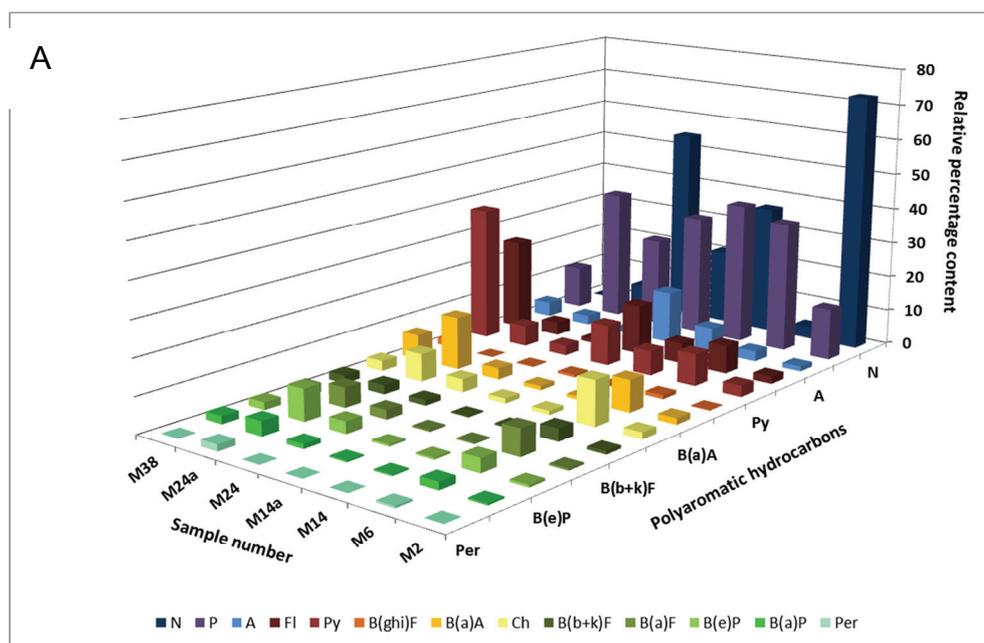
Fig. 39A. Distribution of PAHs in selected samples from the Rymer Cones coal wastes.
A – calculated as relative concentrations from ion chromatograms (m/z = 128, 178, 202, 228, and 252).

B
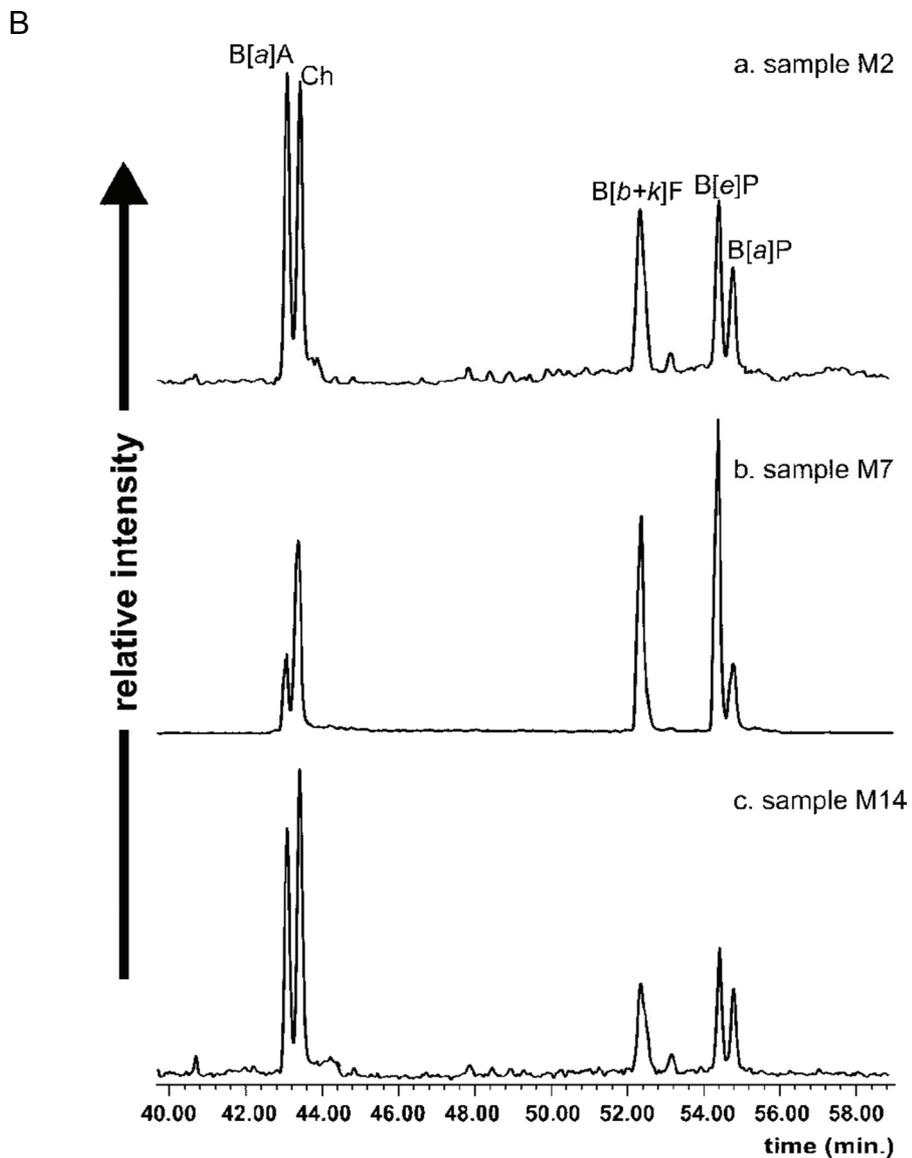
Fig. 39B. Distribution of PAHs in selected samples from the Rymer Cones coal wastes.
B – composed ion chromatograms of four and five rings PAHs (m/z = 228, 252). N – naphthalene,
P – phenanthrene, A – anthracene, Fl – fluoranthene, Py – pyrene,
B[ghi]F – benzo[g]fluoranthene+benzo[h]fluoranthene+benzo[i]fluoranthene,
B[a]A – benzo[a]anthracene, Ch – chrysene, B[$k+f$]F – benzo[k]fluoranthene+benzo[f]fluoranthene,
B[a]F – benzo[a]fluoranthene, B[e]P – benzo[e]pyrene, B[a]P – benzo[a]pyrene, Per – perylene.

TABLE 19

Contents of PAHs in coal wastes from the Marcel dump (relative % calculated into total PAHs content)

Sample no.	N	P	A	Fl	Py	B[ghi]F	B[a]A	Ch	B[b+k]F	B[a]F	B[e]P	B[a]P	Per
M1	48.59	15.73	21.75	2.31	3.01	0.23	2.78	1.85	0.69	1.16	0.93	0.83	0.14
M2	72.59	14.52	1.38	2.07	3.11	0.17	1.73	1.87	0.86	0.52	0.69	0.48	0.00
M3	3.64	29.86	38.24	3.64	5.10	0.73	4.73	4.55	2.55	2.40	2.18	1.64	0.73
M4	1.07	37.60	35.81	3.58	4.66	0.54	3.94	4.30	1.79	2.51	2.69	1.43	0.09
M5	2.40	35.25	1.37	8.56	9.58	1.44	8.56	10.61	5.13	7.19	6.16	3.08	0.68
M6	3.57	36.72	2.85	7.84	8.91	1.07	8.91	12.48	3.57	7.49	3.92	2.14	0.53
M7	0.00	18.51	17.79	4.27	5.52	0.71	4.09	9.96	8.01	11.03	16.19	3.56	0.36
M8	48.55	19.42	21.73	1.39	1.62	0.92	1.85	2.31	0.23	0.81	0.69	0.46	0.00
M9	0.35	72.49	1.38	4.14	4.49	0.69	2.07	5.52	2.83	2.07	2.76	1.04	0.17
M10	48.05	15.10	20.59	2.75	3.66	0.23	2.75	2.29	0.92	1.37	0.69	1.37	0.23
M11	0.00	19.54	31.60	7.49	6.51	0.00	2.28	5.86	3.58	7.49	4.89	10.75	0.00
M12	33.99	16.99	19.61	7.19	11.11	0.33	2.94	3.59	0.98	1.31	0.98	0.82	0.16
M12a	35.00	24.00	28.33	3.67	5.00	0.17	1.17	1.50	0.17	0.42	0.33	0.25	0.00
M13	53.37	12.98	16.83	7.21	3.85	0.24	1.44	2.16	0.48	0.63	0.34	0.36	0.12
M13a	0.00	0.00	0.00	0.00	0.00	0.00	0.00	0.00	0.00	0.00	0.00	0.00	0.00
M14	36.41	39.86	6.90	5.75	6.90	0.27	0.96	1.15	0.46	0.38	0.50	0.38	0.08
M14a	21.00	33.87	14.68	14.00	11.52	0.68	1.13	1.35	0.34	0.45	0.56	0.40	0.02
M15	76.06	19.56	2.17	0.00	0.87	0.94	0.00	0.14	0.18	0.07	0.00	0.00	0.00
M15a	8.54	33.82	35.18	6.15	7.86	0.51	2.39	2.73	0.68	1.02	0.63	0.44	0.03
M16	42.25	42.66	8.53	1.63	1.83	0.08	0.81	1.02	0.20	0.28	0.41	0.30	0.00
M16a	49.23	39.85	6.09	1.41	1.88	0.00	0.23	0.70	0.09	0.12	0.26	0.14	0.00
M17	48.08	34.34	2.29	4.12	4.58	0.32	1.83	2.29	0.46	0.69	0.78	0.23	0.00
M17a	0.66	68.58	11.21	7.25	7.91	0.16	0.99	1.32	0.00	0.66	0.79	0.46	0.00
M18	6.30	73.67	4.43	7.36	7.10	0.09	0.33	0.52	0.07	0.01	0.06	0.04	0.00
M18a	10.80	65.39	5.22	8.13	7.57	0.47	0.66	1.05	0.25	0.03	0.20	0.21	0.02
M19	42.41	37.96	4.44	4.44	4.85	0.20	1.41	2.02	0.61	0.40	0.69	0.48	0.08
M19a	37.65	24.42	27.82	3.05	3.14	0.20	0.85	1.36	0.37	0.51	0.34	0.25	0.03
M20	28.14	43.49	9.38	6.40	7.67	0.21	1.28	1.92	0.32	0.43	0.47	0.30	0.00

M20a	26.34	43.90	8.78	7.46	7.02	0.22	1.76	2.19	0.44	0.66	0.48	0.53	0.22
M21	69.62	20.89	3.16	1.90	2.53	0.00	1.27	0.63	0.00	0.00	0.00	0.00	0.00
M21a	70.71	20.20	2.69	2.02	2.36	0.00	1.35	0.67	0.00	0.00	0.00	0.00	0.00
M22	8.02	63.54	4.32	10.49	6.17	0.19	1.85	2.47	0.62	0.68	0.93	0.74	0.00
M22a	31.45	20.37	28.76	5.39	7.19	0.48	1.80	2.40	0.30	0.82	0.45	0.60	0.00
M23	30.51	21.67	3.42	11.69	24.81	1.00	2.00	2.28	0.57	0.71	0.78	0.50	0.06
M24	54.57	24.95	0.52	1.14	2.86	0.26	3.12	3.64	1.56	2.60	3.38	1.30	0.10
M24a	5.54	36.90	2.58	3.69	5.90	0.00	14.76	7.75	2.58	5.54	8.86	4.06	1.85
M25	0.00	0.00	0.00	0.00	0.00	0.00	0.00	0.00	0.00	0.00	0.00	0.00	0.00
M30	0.00	0.00	0.00	0.00	0.00	0.00	0.00	0.00	0.00	0.00	0.00	0.00	0.00
M31	0.00	0.00	0.00	0.00	0.00	0.00	0.00	0.00	0.00	0.00	0.00	0.00	0.00
M32	0.00	0.00	0.00	0.00	0.00	0.00	0.00	0.00	0.00	0.00	0.00	0.00	0.00
M33	0.00	0.00	0.00	0.00	0.00	0.00	0.00	0.00	0.00	0.00	0.00	0.00	0.00
M34	0.00	0.00	0.00	0.00	0.00	0.00	0.00	0.00	0.00	0.00	0.00	0.00	0.00
M35	0.00	0.00	0.00	0.00	0.00	0.00	0.00	0.00	0.00	0.00	0.00	0.00	0.00
M36	0.00	0.00	0.00	0.00	0.00	0.00	0.00	0.00	0.00	0.00	0.00	0.00	0.00
M37	0.00	0.00	0.00	0.00	0.00	0.00	0.00	0.00	0.00	0.00	0.00	0.00	0.00
M38	0.00	11.86	4.09	25.36	37.63	2.04	6.95	2.86	2.25	2.45	2.13	2.17	0.20
M39	0.00	0.00	0.00	0.00	0.00	0.00	0.00	0.00	0.00	0.00	0.00	0.00	0.00
M40	0.00	0.00	0.00	0.00	0.00	0.00	0.00	0.00	0.00	0.00	0.00	0.00	0.00
M41	0.00	0.00	0.00	0.00	0.00	0.00	0.00	0.00	0.00	0.00	0.00	0.00	0.00
M42	0.00	0.00	0.00	0.00	0.00	0.00	0.00	0.00	0.00	0.00	0.00	0.00	0.00
M43	0.00	0.00	0.00	0.00	0.00	0.00	0.00	0.00	0.00	0.00	0.00	0.00	0.00

N – naphthalene, P – phenanthrene, A – anthracene, Fl – fluoranthene, Py – pyrene, B(gh)F – benzo(g)fluoranthene+benzo(h)fluoranthene+ benzo(i)fluoranthene, B(a)A – benzo(a)anthracene, Ch – chrysene, B($k+f$)F – benzo(k)fluoranthene+ benzo(k)fluoranthene, B(a)F – benzo(a)fluoranthene, B(e)P – benzo(e)pyrene, B(a)P – benzo(a)pyrene, Per – perylene.

Phenols present in the waste samples from the Marcel dump (Fig. 40) are mostly represented by phenol, *o-, p-,* and *m*-cresols, *o-, m*-ethylphenols, di- and trimethylphenols, ethylmethylphenols, and, rarely, methylpropylphenols. They are mostly present in M5 and M12-M22a. Contents are low in M1, M8, M10, and M23 and they do not occur at all in M2-M4, M7, M9, M11, M24-M25, and M30-M43.
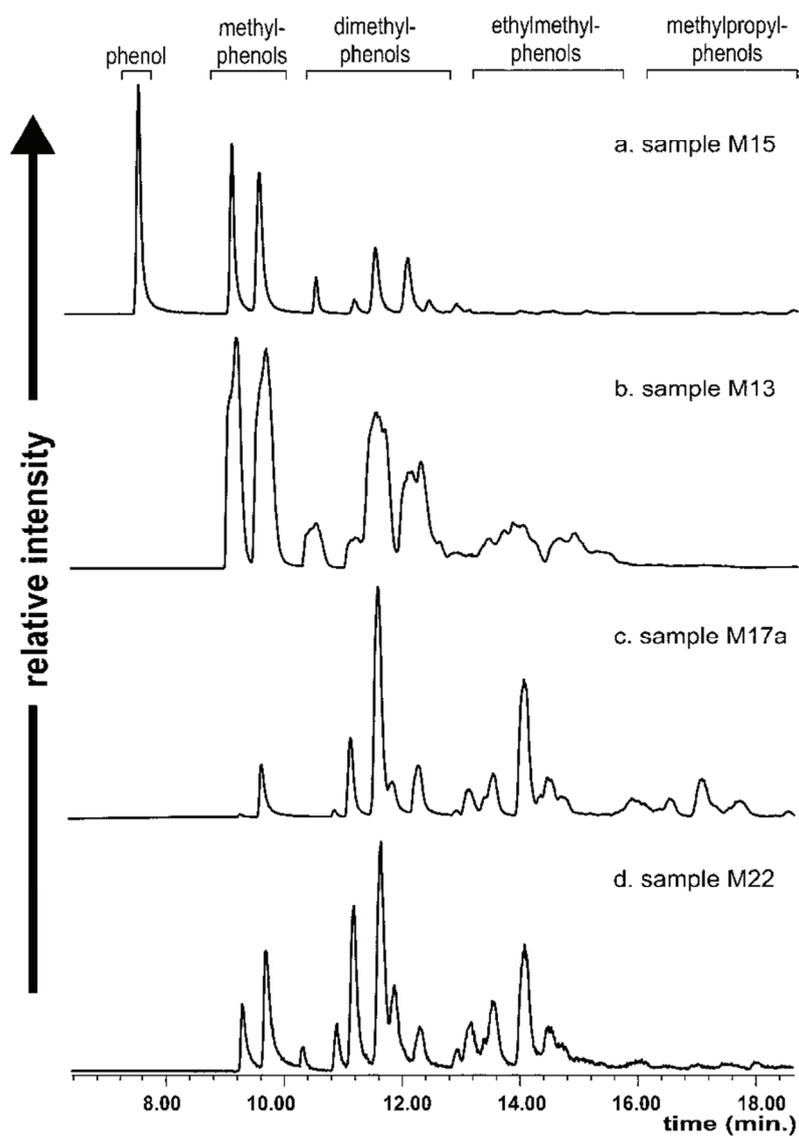
Fig. 40. Distribution of phenols in coal wastes from the Marcel Coal Mine dump
(m/z = 94+108+122+136+150+164).

8.4. Proximate and ultimate analyses

Ash contents (A^a) of the samples from the Marcel Coal Mine dump lie in the range 65.16-84.22 wt% (average 74.83 wt%; Table 20). Moisture contents (M^a) are low (0.99-3.19 wt%, average 2.20 wt%). Volatile matter contents range 43.83-65.17 wt% (average 51.30 wt%). The calorific value (Q_s^{daf}) is, on average, 18.93 MJ·kg^{-1}. Carbon contents (C^{daf}) range from 53.06-68.27 wt% (average 62.38 wt%), hydrogen from 4.56-6.69 wt% (average 5.39 wt%), nitrogen (N^{daf}) from 0.68-4.78 wt% (average 1.81 wt%), oxygen (O^{daf}) 15.74-39.12 wt% (average 22.46 wt%), and total sulphur contents (S_t^a) from 0.07-3.60 wt% (average 2.13 wt%), (Table 20).

TABLE 20

Proximate and ultimate analyses of coal waste from the Marcel Coal Mine dump

Sample no.	M^a (wt%)	A^a (wt%)	VM^{daf} (wt%)	Q_s^{daf} (MJ·kg^{-1})	C^{daf} (wt%)	H^{daf} (wt%)	N^{daf} (wt%)	O^{daf} (wt%)	S_t^a (wt%)
M12	3.01	72.22	44.73	20.20	65.00	4.56	1.45	19.46	2.36
M12A	2.12	74.86	43.83	21.73	67.77	4.91	1.39	16.72	2.12
M13	1.98	77.25	57.15	18.56	62.59	4.62	1.69	15.74	3.19
M13A	1.83	75.38	45.63	21.09	65.82	5.09	1.67	18.52	2.03
M15	3.19	65.16	47.42	21.29	63.82	5.21	1.77	17.82	3.60
M15A	2.02	76.01	52.07	21.41	68.27	6.01	1.55	21.62	2.10
M19	2.98	70.65	57.87	15.33	53.85	5.27	4.78	24.50	3.08
M19A	2.82	70.70	46.79	19.44	63.07	4.87	2.19	19.75	2.68
M24	1.08	84.22	65.17	12.55	53.06	6.67	0.68	39.12	0.07
M24A	0.99	81.82	52.36	17.71	60.50	6.69	0.93	31.30	0.10

M – moisture, A – ash, VM – volatile matter, Q_s – calorific value, C – carbon, H – hydrogen, N – nitrogen, O – oxygen, S – sulphur, a – air dry basis, daf – dry ash free basis, t – total.

9. Discussion

The processes taking place in the coal waste dumps undergoing weathering and self-heating began immediately after deposition of the wastes in the dumps. The complexity of the processes reflects the initial heterogeneity of the organic matter in the wastes, the quantity of the organic matter, the elemental and maceral composition, the coal rank, and the quantity and composition of the mineral fraction. All are, in turn, reflected by values obtained for a range of chemical parameters of thermal maturation (e.g. Strachan et al., 1989a; Raymond, Murchison, 1992; Peters et al., 2005; Pan et al., 2009, 2010).

External factors such as precipitation, melting snow, and wind direction and strength also play significant roles (e.g. Urbański 1983; Krishnaswamy et al. 1996b; Walker 1999; Moghtaderi et al. 2000; Tabor 2002; Tabor 2002-2009; Sawicki 2004; Pan et al. 2009, 2010; Misz-Kennan, Tabor 2011; Misz-Kennan et al. 2011a). Self-heating and self-

combustion are, in essence, almost random processes that change dynamically with time at any given place in a dump. Temperatures at individual spots show daily, seasonal, and longer- term fluctuations (Tabor 2002-2009; Misz-Kennan, Fabiańska 2010; Misz-Kennan, Tabor 2011). Commonly, in a given dump, heating and combustion occur over tens of years (e.g. Tabor 2002-2009). Dumps are by their very nature, randomized accumulations.

The term "self-heating" is precise in this situation. However, the term "self-combustion", traditionally used in describing high-temperature processes in the dumps, is less precise. Combustion processes involve a sequence of exothermic chemical reactions between a fuel and an oxidant that are accompanied by the production of heat and the conversion of chemical compounds such as CO, CO_2, SO_x, and NO_x. In coal waste dumps, the amount of oxidant (air) is usually limited and the processes are slow and usually flameless. Thus, the terms pyrolysis or smouldering may be more appropriate (Hadden, Rein 2009).

Water resulting from atmospheric precipitation and/or decomposition of organic compounds (e.g. Berkowitz 1985; Clemens et al. 1991; Wang et al. 2002a; Sokol 2005) participates in the reactions taking place. Thus, self-heating processes taking place in the presence of moisture may be termed hydropyrolysis. During hydropyrolysis, water acts as a solvent and reacts chemically, leading to the incorporation of water-derived hydrogen into organic matter (Lewan 1992; Leif, Simoneit 2000). During these processes, carbon dioxide is produced in increased amounts (Lewan 1992).

The presence of air in voids in the dump material seems to be essential for the initiation of self-heating which then continues under oxygen-depleted conditions. The chemical reactions are of the cracking and condensation type. Chemical compounds generated during self-heating can migrate within a dump (Misz-Kennan, Fabiańska 2010; Misz-Kennan et al. 2011b). Migration is multidirectional and driven by evaporation and leaching processes; the migration is generally from places of higher to lower temperature. Organic compounds in the range of 50-400 daltons have been found in completely burnt-out wastes with no microscopically visible organic matter (Misz-Kennan, Fabiańska 2010; Misz-Kennan at al. 2011b). On the other hand, organic compounds are commonly absent in wastes containing coked matter (Misz-Kennan et al. 2011b). In addition, organic compounds probably undergo fractionation as they move from place to place.

In the typical dump, migration paths are complex in direction and distance. In consequence some compounds may be adsorbed on nearby minerals, others may migrate to distant sites. Lighter compounds driven upwards by evaporation into cooler parts condense and those leached downwards by rain and melting snow take part in reactions with organic matter still present in the wastes. Radial migration of compounds away from heat sources is an additional complication. Wind influences the migration of compounds from the vents, however, it may also force migration of compounds back into deeper, higher-temperature environments where they would decompose again. Certainly, higher temperatures resulting from wind-induced additional oxygen input will influence decomposition of compounds and promote reactions with other organic and inorganic substances present in the coal wastes. Organic compounds of higher molecular weight are less mobile and are likely to be more predominant in the deeper parts of a dump. Migration paths are schematically summarized in Figure 41.
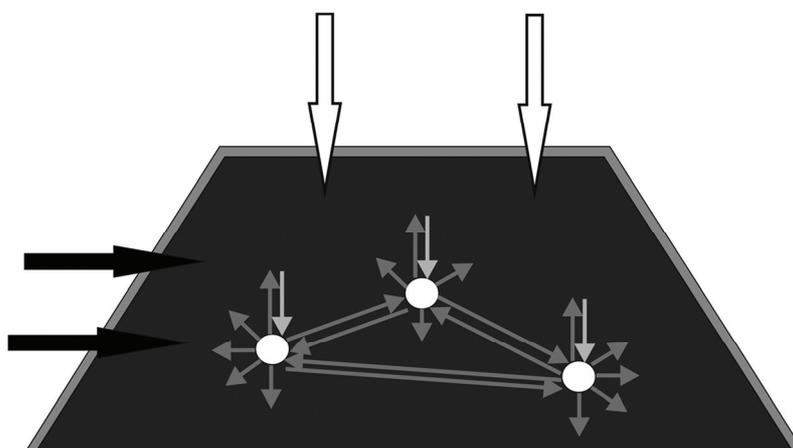
Fig. 41. A scheme of the processes taking place in a coal waste dump undergoing self-heating. White spots – heating places, black arrows – wind direction, white arrows – rain and snow falls, dark grey arrows – migration directions of thermally generated chemical compounds, pale grey arrows – direction of leaching and migration of compounds within the dump.

In terms of the organic matter present, all of the wastes examined in this work can be divided into four groups:
1. Wastes containing both microscopically-visible organic matter and extractable organic compounds, i.e. a bitumen fraction (R1, R3, R5, R7, R8, R18, R20, RS24-RS26, RS27-RS55, RS27-RS62a, M1-M25 and all samples from the Starzykowiec dump).
2. Wastes in which extractable organic compounds are absent even though petrographic organic constituents are present (RS26a, RS56, M32, M33, M35, M36, and M41).
3. Wastes in which microscopically-visible organic constituents are absent but extractable organic compounds are present (M31, M38, and M40).
4. Wastes lacking both microscopically-visible organic matter and extractable organic compounds (M30, M34, M37, M39, M42, and M43).

9.1. The Rymer Cones dump

The self-heating wastes in the Rymer Cones dump were covered with fly ash and clays to inhibit air access enhancing the self-heating processes in the dump interior. That undertaking failed and the whole dump is currently heating (Tabor 2002-2009; Misz-Kennan, Fabiańska 2010; Misz-Kennan, Tabor 2011).

Commonly, macerals in the wastes do not show alterations visible under a microscope (Fig. 5a-e) and their reflectance is low (0.50-0.70%). Their uniformly paler-grey colour and their lack of any signs of plasticity indicate that these altered macerals experienced a slow increase in temperature. Reflectance values in the range 0.70-1.59% are higher than in unaltered particles (e.g. R18, R30, RS33, RS34, RS47, RS52a, RS60, and RS62a; Fig. 5b, 6a; Tables 3, 4). As might be expected, the content of unaltered macerals decreases sharply with increasing reflectance and contents of paler-coloured vitrinite macerals increase. The coked organic matter in some wastes (RS25, RS25, RS34a, RS40, RS41, RS50, and RS52a;

Fig. 6e-f) is uniformly white or yellowish white and shows no anisotropy, also suggesting that heating rates in the dump were low. None of the wastes contain porous or anisotropic macerals that would indicate higher heating rates (Goodarzi, Murchison 1978; Murchison 2006). Oxidation rims of paler colour in RS62a (Fig. 6c-d) corresponds to a temperature of *ca* 200°C (Ndaji, Thomas 1995; Calemma et al. 1995) and increased aromatization (Chandra 1962; Stach et al. 1982).

Bitumens expelled from mostly liptinitic organic matter are evident in some wastes (RS30, RS34a, RS54, and RS59; Fig. 6g-h; Table 5). Their presence is not reflective of extract-yield values (Table 5); bitumens occur both in wastes of lowest extract yield (RS48a) and in others with yields as high as 0.702 wt% (R20; Table 5). Adsorption on clay minerals and vitrinite could explain their apparent absence in other samples (Huizinga et al. 1987; Pan et al. 2009, 2010). Adsorption in vitrinite probably decreases its reflectance.

Total sulphur contents in the wastes from Rymer Cones are generally low (< 1 wt%; Table 8) as is typical for non-marine sedimentary organic matter in which, if it is present at all, contents are low (Willey et al. 1981). Thus, organic sulphur does not have significant influence on the temperature of bitumen generation in the dump (Taylor et al. 1998), especially as sulphur compounds such as thiophene derivatives and thiophenols were found only in low contents in waste extracts or are absent.

Geochemical data gives further insight into the nature of the heated wastes. Wastes seeming to be unaltered under a microscope commonly show chemical features typical of thermally altered organic material. Most of the wastes contain compounds of pyrolytic origin. For example, samples R5, R7, R18, R20, RS28, RS33, RS40, RS45, RS49, RS52a, RS53, RS58, and RS61 contain phenols originating from the destruction of the lignine-originated structure-building macerals of vitrinite group. The abundance of phenol and cresols, both very soluble in water (Fakseness, Brandvik 2008), shows that these pyrolysates are of relatively recent origin and were not long exposed to weathering. Due to their relatively high solubility, these compounds are easily leached (Skręt et al. 2010) and, thus, potentially easily transported into the dump interior. It is relevant that phenols are absent in altered old dumps where heating ceased some years ago, e.g. the upper part of the Starzykowiec dump (Misz-Kennan et al. 2011b).

The Gaussian, monomodal *n*-alkane distribution (Fig. 8b-c) is typical of pyrolysates (e.g. Amijaya et al. 2006). *n*-Alkanes have two sources in coal wastes. In the primary organic matter of the wastes, they are the products of fatty-acid defunctionalisation and saturation of double bonds. Lighter *n*-alkanes can be the by-products of the decomposer organisms whose remains probably contribute to the formation of the humic substance or they can come from plant tissues. For example, common fatty acids such as palmitic and stearic acids produce *n*-hexadecane and *n*-octadecane, respectively. Long-chain *n*-alkanes can also originate from higher-plant waxes; they are dominated by n-C_{23} to n-C_{35} isomers that are typical of higher-plant leaf waxes (Killops, Killops 2005). As in rocks altered by heat from igneous intrusion, their small contents in the wastes also can be explained by heating (Bishop, Abbot 1995).

n-Alkanes are also formed during pyrolysis in cracking reactions linked to the breakdown of aliphatic kerogen (Allan, Douglas 1977; Huizinga et al. 1987; Leif, Simoneit 2000); in this case, their content increases with temperature (Huizinga et al. 1987; Stalker et al. 1998).

In pyrolysates, the *n*-alkane distribution probably reflects the major temperature range to which the wastes were exposed. Using the boiling temperatures of *n*-alkanes, it is possible to approximate the heating temperatures within the dump. Self-heating leads to the generation from organic matter of lighter *n*-alkanes in the range *n*-C_{11}-*n*-C_{14} (Fig. 8a, 8d) at temperatures of *ca* 150-300°C (Chemical Land21). RS45 contains only lighter *n*-alkanes (*n*-C_{13} to *n*-C_{18}; Fig. 8d), suggesting that they were generated in a temperature range of *ca* 200-330°C (Chemical Land21). These *n*-alkanes are liable to migrate away more easily from the heat source (Bishop, Abbot 1995). Several wastes contain a narrow range of *n*-alkanes, e.g. *n*-C_{13}-*n*-C_{21} (as in RS34a), probably reflectings narrow temperature ranges of *ca* 200-380°C (Chemical Land21). The presence of *n*-alkanes in the range *n*-C_{13}-*n*-C_{35} as in RS48 (Fig. 8c) indicates generation at *ca* 200-520°C. Wastes lacking visible organic matter (RS26a and RS56) contain *n*-alkanes in the wide range *n*-C_{16}-*n*-C_{35} and their chromatograms also have the Gaussian outline.

The absence of heavier *n*-alkanes (> *n*-C_{35}) in the surface wastes may reflect the lower mobilities of these higher molecular weight aliphatic compounds. They are probably present in the dump interior. That these pyrolysates were not affected by leaching may be indicated by the presence of lighter *n*-alkanes (and naphthalenes and phenols) easily soluble in water and prone to migrate. *n*-Alkanes are destroyed at temperatures > 450°C (Pan et al. 2009). Thus, their presence in the wastes without any microscopically visible organic matter was probably caused by their migration into sites of relatively low temperature where they precipitated.

The CPI index is one of the best indicators of thermal maturity in self-heated wastes. In coal seams and associated rocks in Upper Silesia, CPI values are similar and in the range 0.96-1.91 (Kotarba, Clayton 2003). The wastes from Rymer Cones have CPI values in the range 0.79-1.71 (Table 5) that seem to decrease with degree of alteration – a normal trend in organic-matter maturation (Allan, Douglas 1977). Up to a reflectance of 1.05%, the short-to-long chain *n*-alkane ratio does not show any correlation with degree of organic matter alteration. Above that reflectance value, the values of the *n*-alkane ratio increase in-line with an increasing input of lighter compounds, suggesting that condensation reactions occurred in these wastes (Fig. 42a; Allan, Douglas 1977). The predominance of shorter- to longer-chain *n*-alkanes (Table 5) is indicative of the generation of shorter chain *n*-alkanes homologues from wastes exposed to heating (Bishop, Abbot 1995).

A feature of interest in the wastes investigated here is the absence of unsaturated hydrocarbons (alkenes) that form as an intermediate stage during pyrolysis. Leif and Simoneit (2000) found that *n*-alkenes rapidly isomerise to internal alkenes via acid-catalyzed isomerisation under hydrothermal conditions. These *n*-alkenes simultaneously undergo reduction to *n*-alkanes, the major product, and oxidation to ketones via alcohols that are formed by hydration of the alkenes. Conditions of dry pyrolysis result in a deficiency of hydrogen and the formation of both alkenes and alkanes (Ishiwatari, Fukushima 1979).
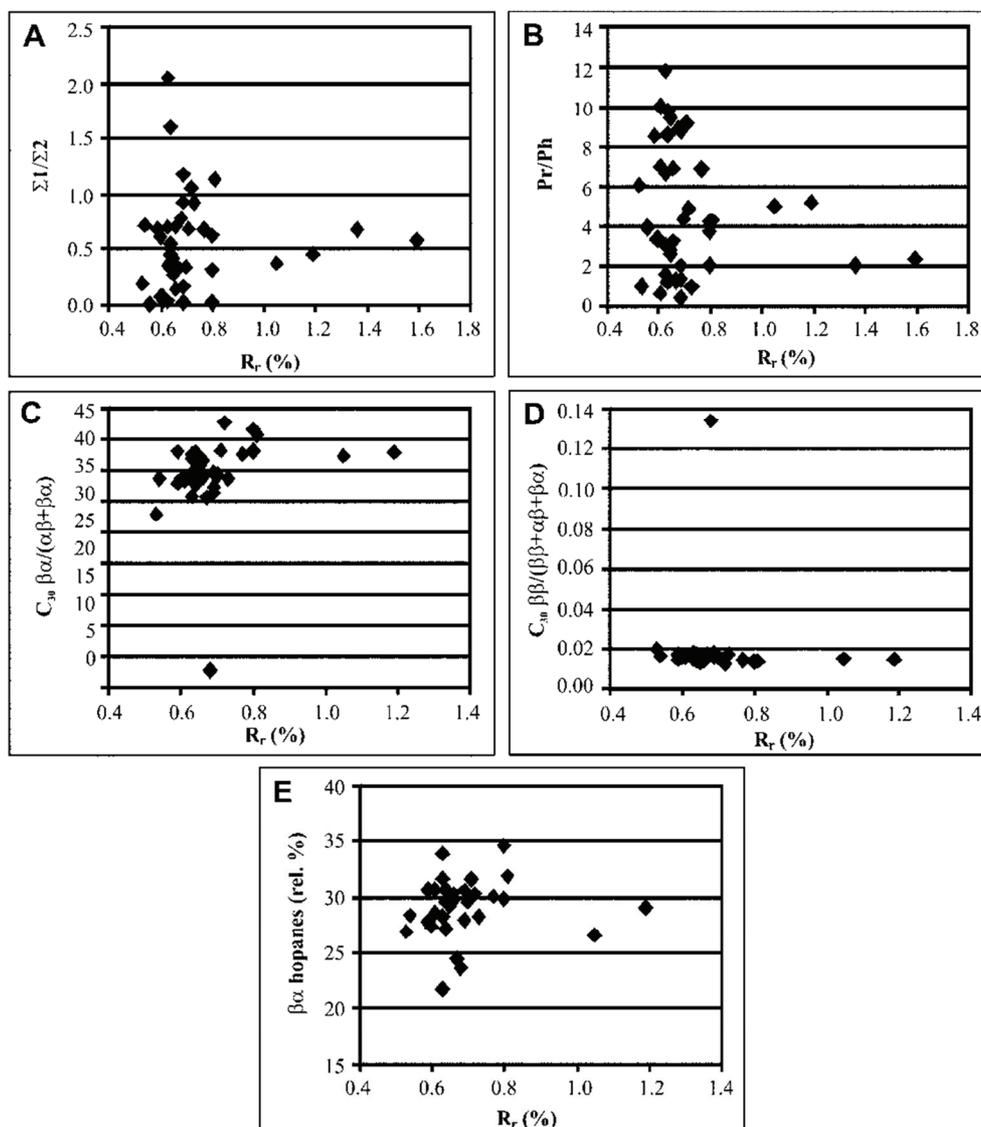
Fig. 42. Relationship between reflectance (R_r) and various geochemical parameters of thermal maturation based on A – *n*-alkanes, B – pristane and phytane and C-E – hopane-based geochemical parameters for the Rymer Cones dump. For parameter formulae, see Table 5.

The presence of pyrolysates is also marked by changes in the pristane to phytane ratio (Pr/Ph). This ratio is commonly used for determining the oxicity/anoxicity of the original depositional environment and the source of organic matter (Table 1; Didyk et al. 1978; Kotarba, Clayton 2003), and the level of maturity (Dzou et al. 1995; Amijaya et al. 2006). However, phytane can be generated from methanogenic- or halophyllic phytanyl lipids (Goosens at al. 1988a, b). It seems that the dominant source of pristane in the heated wastes was likely its generation from the kerogen macromolecule during catagenesis (Goosens at

al. 1988a, b) though generation during kerogen degradation has been postulated (Huizinga et al. 1987).

Most coals in the USCB show very high values of Pr/Ph. Values < 1.0 characterize coals with reflectance of *ca* 0.9% or higher. Floor and roof rocks associated with coal seams have notably lower Pr/Ph values than the coal itself (e.g. Pr/Ph for coal 5.98, for roof 1.08, for floor 0.83 where coal R_r is 0.59% and Pr/Ph for coal 5.82, for roof 0.88, for floor 0.62 where coal R_r is 0.90%; Kotarba, Clayton 2003). The Rymer Cones coal wastes display a wide of Pr/Ph values ranging from 0.42-11.81 (Table 5). They do not simply increase with the level of transformation in any simple way in the wastes with $R_r < 0.81\%$ as observed in other dumps (Misz et al. 2007; Misz-Kennan et al. 2011b). Above that reflectance, Pr/Ph decreases with increasing level of waste alteration (Fig. 42b), probably caused by aromatization processes and by heat-driven destruction of pristane (Dzou et al. 1995; Amijaya et al. 2006). The lack of any relationship between level of the waste transformation and Pr/Ph in the unaltered- and moderately-altered wastes with $R_r < 0.81\%$ probably reflects the generation of chemical compounds in deeper parts of the dump and their migration away from the source of heat. The same applies to most geochemical indices of thermal maturation calculated for the coal wastes; in all waste samples, reversals in the values of the various thermal indices occur at a reflectance of *ca* 1%. This pattern also suggests that the rate of heating was low. Otherwise, a significant shift into higher reflectances would be seen. Raymond and Murchison (1992) recorded such a shift in the reversal of the Methylphenanthrene Index (MPI) in the interval from *ca* $R_r = 1.35\%$ to *ca* $R_r = 2\%$ in rapidly heated coals.

The values of other acyclic isoprenoid ratios, i.e. pristane/*n*-heptadecane (Pr/*n*-C_{17}) with values in the range 0.05-12.19, and phytane/*n*-octadecane (Ph/*n*-C_{18}) with values in the range 0.04-5.67 (Table 5), also do not show any simple correlation with the level of waste alteration. Pr/*n*-C_{17} values decrease with increasing maturity and increase with increase in hydrogen expulsions (Leythaeuser, Schwarzkopf 1986). The Rymer Cones self-heated wastes do not show these trends; the dynamic conditions within the dump and migration of organic compounds within and outside the dump are possible reasons.

Membrane lipids of some bacteria are the source of hopanes (Ourisson et al. 1979). Ts and Tm are strongly dependent on the source and maturity (Peters et al. 2005). The Rymer Cones wastes have Ts/(Ts+Tm) values in the range 0.74-0.93 (Table 5) that show no correlation with the level of thermal alteration. A similar pattern holds for 22S and 22R homohopanes (*m/z* = 191). Both Ts/(Ts+Tm) and C_{31}S/(S+R) ratios are considered good indicators of maturity (e.g. Dzou et al. 1995). The fact that they have little obvious application at Rymer Cones may reflect the presence of water retarding alteration (Pan et al. 2010).

Values of $C_{30}\beta\alpha/(\alpha\beta+\beta\alpha)$ increase and values of $C_{30}\beta\beta/(\beta\beta+\alpha\beta+\beta\alpha)$ decrease with increasing alteration for wastes with $R_r < 0.81\%$ (Fig. 42c-d). This is linked to the fact that $\beta\beta$ hopanes have a biological configuration and are converted into $\beta\alpha$ and $\alpha\beta$ hopanes by diastereoisomerisation. It is believed that $\beta\beta$ hopanes represent the primary component, that $\beta\alpha$ hopanes are intermediate products and that $\alpha\beta$ hopanes are the final component (Seifert, Moldowan 1980; Ten Haven et al. 1992). Contents of $\alpha\beta$ hopanes resistant to conversion under pyrolysis conditions increase with progressive heating (Lu, Kaplan 1992); this occurs

before the conversion of $\beta\beta$ hopanes (Farrimond et al. 1998). That $\alpha\beta$ and $\beta\alpha$ hopane contents increase even when $\beta\beta$ hopanes are absent points to another source that is probably the hopane skeletons bound into kerogen (Farrimond et al. 1998). The conversion of $\beta\alpha$ moretanes into $\alpha\beta$ hopanes is probably a two-step free radical process that is thermodynamically controlled in kerogen (Seifert, Moldowan 1980). Regretably, the potential for applying these observations is limited in the dump (Misz et al. 2007; Misz-Kennan, Fabiańska 2010; Misz-Kennan et al. 2011b). Again, intra-dump migration is perhaps important here.

Sample RS42 from the lower part of the NW part of the dump (Fig. 2) shows a marked deviation from the general trend (Fig. 42c-d; Table 5). Values of $C_{30}\beta\alpha/(\alpha\beta+\beta\alpha)$ are appreciably lower in this sample, and $C_{30}\beta\beta/(\beta\beta+\alpha\beta+\beta\alpha)$ considerably higher, than in the other samples. Relative contents of C_{29}, C_{30}, and C_{31} hopanes (Fig. 10) and $\beta\beta$, $\beta\alpha$, and $\alpha\beta$ hopanes (Fig. 11) are similar in all samples. The fact that the relative content of $\beta\alpha$ hopanes, the intermediate stable diastereomers, tends to increase in the wastes with increasing degree of transformation (Fig. 42e) suggests that the wastes did not attain the degree of maturation at which the more stable $\alpha\beta$ hopanes would start to prevail over $\beta\alpha$ hopanes. This indicates that the wastes were relatively little altered, that they did not attain thermal stability and/or that migration took place. The absence of $\beta\beta$ hopanes in many samples (Fig. 9, 11) is partially related to the fact that they were likely converted into $\beta\alpha$ and $\alpha\beta$ hopanes during maturation and by thermal processes (Lu, Kaplan 1992; Farrimond et al. 1996). The exception is RS45 with the highest relative content of $\beta\beta$ hopanes (25.3 rel.%) compared to 0.34-5.80% in the remainder.

These hopane trends can be explained by the fact that the concentration of molecular species in the soluble state depends on the relative rates of formation and destruction (Dzou et al. 1995) – a continuous process in the coal waste dumps. Also bitumens released from kerogen that migrated may be an influence (Strachan et al. 1989a). The pattern might also be explained by the fact that hopane diastereoisomerisation requires more time to proceed to equilibrium (Grantham 1986) or it may reflect heating rate (Strachan et al. 1989a, b). In this context, the absence of unsaturated hopanoidal hydrocarbons (hopenes) may be significant. Leif and Simoneit (2000) found them to be the dominant triterpenoid released from kerogen during hydrous pyrolysis after one hour but to be absent after ten hours. Any hopenes in the wastes would likely have been destroyed.

Various thermal parameters based on aromatic hydrocarbons give an additional insight into the alteration of organic matter in the wastes. Methylnaphthalenes, dimethylnaphthalens and other aromatic compounds are generated during pyrolysis of vitrinite and sporinite (Horsfield 1989). Contents of aromatic compounds relative to *n*-alkanes increase with temperature and, at 400°C, aromatic components are dominant in pyrolysates (Pan et al. 2009). It has also been noted that the amount of aromatic hydrocarbons markedly increases with reflectance (Radke et al. 1986).
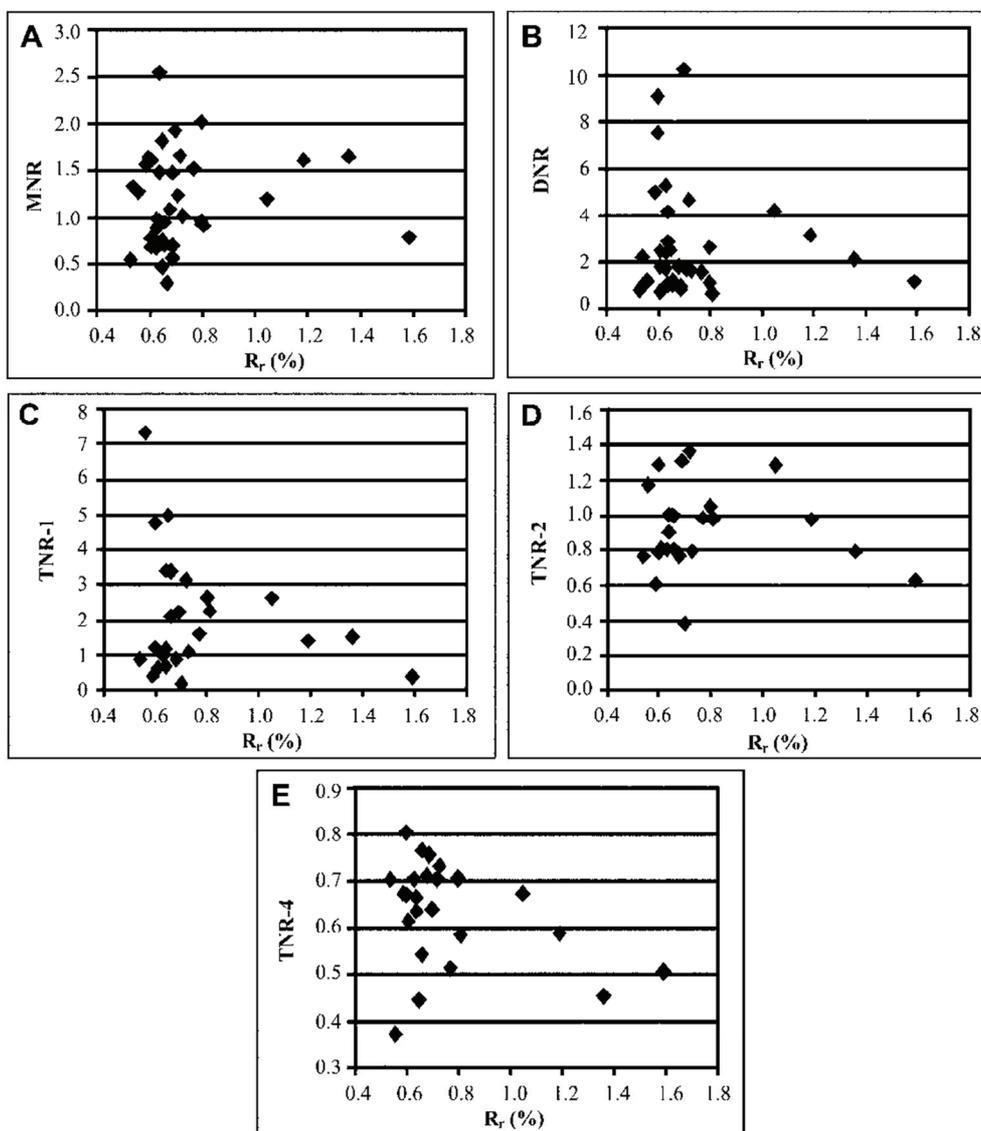
Fig. 43. The relationship between reflectance (R_r) and individual geochemical parameters of thermal maturation based on aromatic hydrocarbons for the Rymer Cones dump. For parameter formulae, see Table 6.

The Methylnaphthalene Ratio (MNR), generally considered as one of the most useful parameters (Radke et al. 1986; Raymond, Murchison 1992) shows a very poor correlation with thermal alteration in the dump (Fig. 43a); one reason is probably the fact that methylnaphthalenes are very soluble in water and are easily leached. The poor correlation may also indicate that water is involved in the pyrolysis reactions taking place in the dump interior. The Dimethylnaphthalene Ratio (DNR) is a much better indicator of the degree of alteration of organic matter. As with all these indices of thermal maturation, DNR shows no

213

correlation with $R_r < 0.81\%$ but, for more altered wastes, DNR values decrease with reflectance (r = 0.99; Fig. 43b). Similar patterns characterize all Trimethylnaphthalene Ratios (TNR-1, TNR-2, and TNR-4); values decrease with reflectance > 0.81% (Fig. 43c-e) in agreement with the fact that the contents of some trimethylnaphthalene isomers decrease with increasing reflectance (Willsch, Radke 1995). The corresponding correlation coefficients are -0.93, -0.97, and -0.80, respectively.

Individual unsubstituted PAHs have various sources, making any interpretation difficult. In general, the main sources are incomplete combustion of plant material in both natural, e.g. forest fires, and anthropogenic environments, e.g. combustion of fossil fuels and biomass (Radke et al. 1986). Combustion in settings with deficient oxygen leads to the cracking of organic matter into smaller molecules that recombine to form PAHs (Simoneit 1998). Some, e.g. perylene, probably have a biogenic origin linked to early diagenetic processes; their molecular structure is similar to that of polycyclic compounds of biogenic origin (Radke 1987; Jiang et al. 1998). Grice et al. (2009) believe that its presence might be connected with the activity of wood-degrading fungi. Steranes can also be converted into triaromatic hydrocarbons during aromatization (Radke 1987; Simoneit 1998). Other potential sources of PAHs are hopanoids in bacterial remnants and tetraterpenoids in green sulphur bacteria (Simoneit 1998). Naphthalenes can be generated from vitrinite macerals and from semifusinite of the inertinite group (Radke et al. 1986) which may partly explain their poor correlation with level of waste alteration. Pyrene is not present in pyrolystes generated at 240-320°C, but is present in considerable amounts at 400°C (Pan et al. 2009). The main source of anthracene and phenanthrene is believed to be subbituminous- and bituminous coal combustion (Simoneit 1998). Coals from the Upper Silesian Coal Basin contain three- to six-ring PAHs (Bojakowska, Sokołowska 2001). Oros and Simmoneit (2000) found that most PAHs in smoke from bituminous coal combustion and smouldering are two- to five-ring PAHs, with six-ring PAHs (anthranthrene) and seven-ring PAHs (coronene) constituting a minority and that PAHs with more than seven rings were absent.

The individual PAHs vary in their toxicity. It is generally accepted that for unsubstituted PAHs, a minimum four benzene rings is required for carcinogenic activity (Pickering et al. 1999). The most carcinogenic PAH is benzo[*a*]pyrene while benzo[*a*]anthracene has a weak carcinogenic effect (e.g. Pickering et al., 1999; Pickering 2000). Usually, the relative contents of four- and five-ring PAHs in the wastes from the Rymer Cones is much lower than the contents of PAHs with two and three rings (Table 7; Fig. 13, 14). However, in some samples (e.g. RS33), the relative contents of PAHs of higher molecular weight such as benzo[*a*]pyrene can be significant.

A lack of any correlation between vitrinite reflectance and relative contents of individual polyaromatic hydrocarbons is evident for Rymer Cones wastes with reflectance < 0.81%. In the highly altered wastes ($R_r > 1.05\%$), an increase in relative content with increasing alteration is best seen for five-ring PAHs (benzo[*b+k*]fluoranthene, benzo[*a*]fluoranthene, benzo[*e*]pyrene, benzo[*a*]pyrene; Fig. 44a-d; r = 0.85, 0.82, 0.96, and 0.94) and four-ring PAHs (chrysene; Fig 44e; r = 0.80); this feature is linked to thermal stress during combustion (Lu, Kaplan 1992; Jiang et al. 1998; Oros, Simoneit 2000). That the relative content of phenanthrene generally decreases with increasing reflectance > 0.81% (Fig. 44f) agrees with the findings of others (e.g. Willsch, Radke 1995). No direct relationship between the relative contents of two- and three-ring PAHs and four- and five-

214

ring PAHs is evident in wastes of reflectance < 0.81%. Above that value, the relative contents of two- and three-ring PAHs seems to decrease, and those of four- and five-ring PAHs increase with increasing reflectance – what is probably linked to increasing aromatisation (Willsch, Radke 1995).
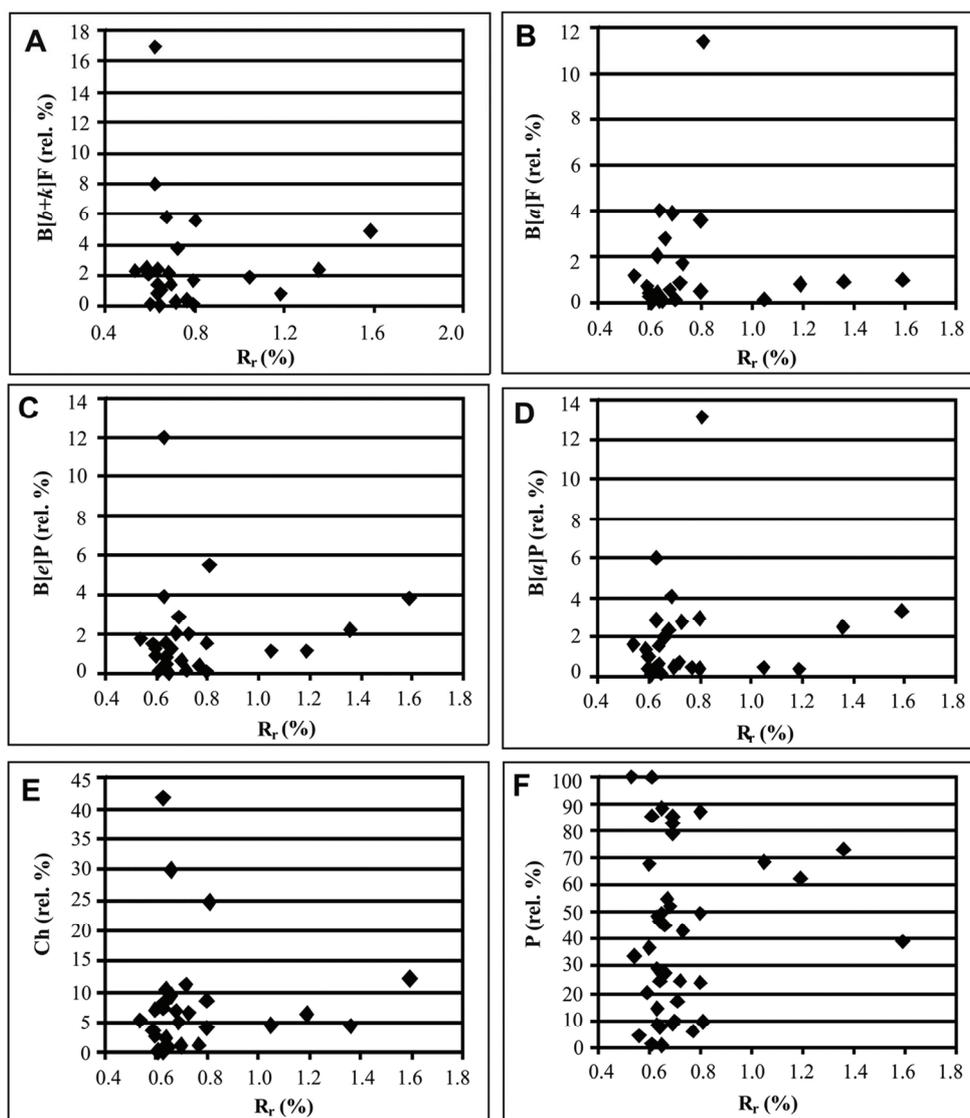
Fig. 44. The relationship between reflectance (R_r) and relative concentrations of polycyclic aromatic hydrocarbons for the Rymer Cones dump.

Though individual chemical parameters of thermal alteration show poor correlation with each other, some trends are evident. Values of $n\text{-}C_{23}/n\text{-}C_{31}$ tend to decrease with the increasing CPI (Fig. 45a). Pr/Ph values decrease with CPI values < 1.4; above, values seem

to be independent of further rise in CPI (Fig. 45b). Relative contents of C_{29} hopanes decrease and those of C_{31} hopanes increase with increasing CPI (r = -0.56 and 0.61; Fig. 45c-d). The Methylphenanthrene Index (MPI-3) also decreases with increasing CPI (Fig. 45e). Relative contents of fluoranthene, pyrene (Fig. 45f), benzo[*a*]anthracene, benzo[*b+k*]fluoranthene (Fig. 45g), chrysene, and benzo[*e*]pyrene (Fig. 45h) seem to decrease with increasing CPI. There appears to be a general trend of relative contents of two- and three-ring PAHs increasing with increasing CPI values, and the opposite for four- and five-ring PAHs.

The complexity of the thermal processes still taking place in the Rymer Cones dump, despite actions taken to inhibit self-heating, is probably the key influence for the lack of any dependence between geochemical and petrographical properties and sample location. Chemical migration within the dump is also important. It might be assumed that values of the chemical indices of thermal maturation for RS50 collected on the eastern slope of the dump where temperatures have remained low for many years would differ from those of samples collected from other parts of the dump. The fact that all fall in the same range suggests that migration has played and continues to play a crucial role. In addition, no seasonal changes in the various parameters were observed; the compounds generated during temperature fluctuations are mixing in the wastes.

Samples of fly ash and soils were collected in the Rymer Cones dump. It may be assumed that most compounds present in the fly ash cover of the dump originated from the destruction of organic matter during self-heating processes and are of pyrolytic origin as coal compounds were very likely completely destroyed during combustion. Differences in the occurrence of individual organic compounds and in the values of individual parameters of thermal alteration may be connected with differences in their adsorption and their volatility; the fly ash forms the top cover of the dump and is in direct contact with the atmosphere. The soils contain some compounds typical for very immature organic matter.

Extract yields from soil- and fly-ash samples fall in a low range compared to that of the values for the coal wastes and, as might be expected, are lower in fly ash than in soils (Table 5). However, the fact that these samples were collected in sites where expulsions of hydrocarbons were marked by darker patches on the dump surface may be relevant.

A typical feature of fly ash samples is the lack of phenols and hopanes (Table 5) and the Gaussian distribution of *n*-alkanes in the narrow range (*n*-C_{13}-*n*-C_{22}) and generated from the heated wastes probably at temperatures in the range *ca* 200-400°C (Chemical Land21). Values of CPI, ratios of short-to-long chain *n*-alkanes, Pr/Ph, and Ph/*n*-C_{18} are in the coal-waste ranges whereas those of *n*-C_{23}/*n*-C_{31} *n*-alkanes and Pr/*n*-C_{17} are in the lower ranges characterising the coal wastes. The absence of phenols can be attributed to their destruction during combustion, evaporation to the atmosphere or leaching to deeper parts of the dump. The absence of hopanes is probably connected with their destruction during the coal combustion that produced the fly ash, and to their absence in pyrolysates.

The chemical properties of the soils are influenced by their intrinsic chemistry and the pyrolysate composition. A Gaussian distribution of *n*-alkanes is seen in the soils covering the Rymer Cones dump but their range is much wider (from *n*-C_{14} to *n*-C_{35}) than that of the fly ash. This suggests that they were generated at temperatures of *ca* 230-520°C (Chemical Land21) or that a proportion of the *n*-alkanes originated with the soils. The soils may have acted as a trap for migrating *n*-alkanes generated elsewhere in the dump.

216
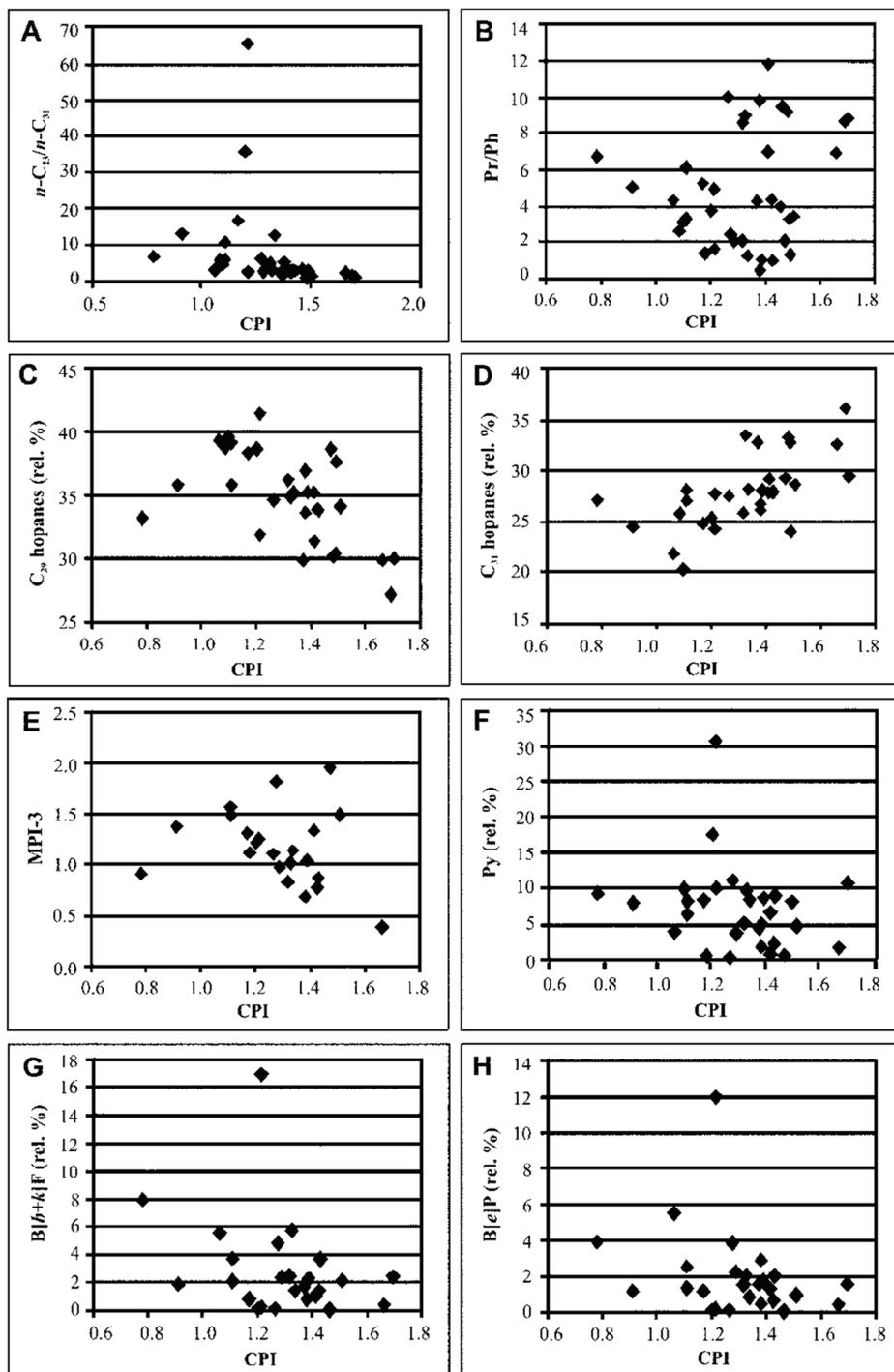
Fig. 45. Relationship between individual geochemical parameters of thermal maturation and relative concentrations of selected polyaromatic hydrocarbons for the Rymer Cones dump.

The soils also contain phenols, but with distributions differing considerably from sample to sample (Fig. 19). RSG2 contains phenol and ethylphenols in considerable amount whereas, in RSG6, dimethylphenols, ethylmethylphenols, and methylpropylphenols are dominant, phenol was absent and ethylphenols occur only in minor quantities. In the remaining two soil samples (RSG1 and RSG4), the various types of phenols are present in similar amounts. The presence of the unstable $\beta\beta$ hopanes of biological origin is most likely linked with the primary soil composition and the presence of recent fungi and bacteria (Killops, Killops 2005). Compared to the wastes, the soils also display high relative contents of intermediate $\beta\alpha$ hopanes.

9.2. The Starzykowiec dump

The Starzykowiec dump is one of the oldest in Upper Silesia and was built using outdated methods. Self-heating ceased a few tens of years ago in the upper part of the dump (Tabor 2002-2009; Misz-Kennan, Tabor 2011; Misz-Kennan et al. 2011b). The organic petrology, geochemistry, and mineralogy of that upper part of the dump have been discussed in detail elsewhere (Misz-Kennan et al. 2011b). Today, self-heating is still taking place in the lower part of the dump; it intensifies with increased precipitation in the spring and autumn (Tabor 2002-2009).

As in the Rymer Cones dump, temperature fluctuations, continuing degradation of organic matter and formation of new organic compounds, and their migration within and outside the dump (Fig. 41) also take place in the Starzykowiec dump. Both dumps are of similar age. The average mineral content is 79.6 vol.% (Table 9) and, in the Rymer Cones dump, 76.5 vol.% (Table 3). Four samples (C1, C3, C18, and C19) from the Starzykowiec dump have mineral contents $\leq$ 50 vol.%. The reflectance of original organic matter in the wastes is also similar to that in the Rymer Cones dump (Tables 3, 9). The lack of a fly ash cover is probably the cause of much reduced extract yields from the Starzykowiec samples (Tables 5, 11); the average extract yield for the Rymer Cones dump samples is 0.52 wt% and, for Starzykowiec samples, is 0.07wt%. Many Starzykowiec samples contain no bituminous fraction. Both dumps have been heating for the same span of time. Liptinite contents are similar in both. It may be that leaching moved the extractable bitumen fraction into the dump interior or to the outside.

The vitrinite reflectance of the organic matter in the coal wastes is usually in the range 0.50-0.89% (Table 9). Only samples C12, C14, C17, and CH11 show reflectance values above that range. The waste composition is dominated by unaltered vitrinite; contents can reach 61.4 vol.%. The content of paler-grey vitrinite increases with reflectance. These wastes also experienced slow heating as is evident in what are uniformly paler-coloured particles (Fig. 20b) and a general lack of porosity. Porosity suggesting higher heating rates is seen only in CH3 (Tables 9, 10; Fig. 20d) though oxidation rims on the edges of some particles, irregular cracks and paler coloured liptinite (Fig. 20e) suggest temperatures > 200°C. Massive isotropic coke in some samples (Fig. 21a-b) is the product of slow heating over a long time span (Goodarzi, Murchison 1978; Murchison 2006). Rare coke particles associated with unaltered vitrinite in some samples (e.g. C3, C4, C21, C22, C27, and CH5a) suggest that the coke may have formed in the upper part of the dump (Misz-Kennan et al. 2011b). Only in C12, with the highest reflectance, coke has formed in situ.

An interesting feature of the wastes in this dump is the presence of bitumen expelled mostly from liptinitic organic matter and co-occurring with clay minerals (Fig. 21c-f) in some samples. These expulsions have thread-like or irregular shapes and a strong yellow fluorescence. They were probably originally generated from organic matter at relatively high temperatures in deeper parts of the dump. The bitumen expulsions in the wastes are not related to high extract yields; they occur, e.g. in CH16 with an extract yield only slightly above the average for the dump (0.077 wt%; Table 11). In cases were bitumen expulsions and organic remnants are not seen under the microscope, and yet the samples provided high extract yields, it may be assumed that the bitumens were adsorbed on minerals. In those cases where bitumen expulsions are not microscopically visible in samples from the upper part of the dump, and where self-heating had ceased tens of years ago (Misz-Kennan et al. 2011b), water washing that continued for a few tens of years may explain the lack of bitumens.

The wastes also display varying levels of alteration. As with the Rymer Cones material, individual indices of thermal maturation based on aliphatic and aromatic hydrocarbons, and acyclic isoprenoids show poor correlations with the degree of alteration expressed by reflectance, especially for wastes of reflectance < 1% (Fig. 46). This suggests that other factors, possibly migration within and out of the dump, and temperature fluctuations, were responsible. With all of the indices, and with the relative contents of hopanes and individual polycyclic aromatic hydrocarbons, reverses in trends are seen at reflectances > 1%. In these cases, slow heating is indicated (Fig. 46). These reversals, at the same reflectance value, characterize the upper part of the Starzykowiec dump (Misz-Kennan et al. 2011b). For many indices, no consistent correlation with vitrinite reflectance is evident; the dynamic nature of the dump is probably responsible.

The presence of phenols (Fig. 27) in many waste samples suggests recent heating. However, the absence of phenol, and the presence of its methyl-, dimethyl-, and ethylmethyl homologues, indicate that any phenol was leached into other parts of the dump or was thermally destroyed (Skręt et al. 2010; Misz-Kennan et al. 2011b).

Some wastes are unaltered, with *n*-alkane distributions typical for unaltered coal (Fig. 23a). However, in most samples, the input of pyrolysates results in a Gaussian *n*-alkane distribution (Fig. 23b-e). The *n*-alkanes originated by cracking of organic compounds of higher molecular weight. The presence of lighter *n*-alkanes in the range of *n*-C_{12}-*n*-C_{22} indicates that the bitumen fraction was not affected by water washing. In the Starzykowiec material, the *n*-alkanes show both monomodal (Fig. 23b-c, 23e) and bimodal distributions (Fig. 23d). Some wastes (C4, C15, CH2, and CH18) contain *n*-alkanes generated over a narrow temperature range, reflected in a narrow distribution (Fig. 23b) that suggests generation at *ca* 210-380°C (Chemical Land21). The wide *n*-alkane distributions of other wastes samples (e.g. C11 and C16; Fig. 23c) suggest generation over a much wider temperature range of *ca* 210-520°C (Chemical Land21). There are also wastes with a mixture of pyrolysates formed in different temperature ranges characterised by two maxima (Fig. 23d) and some that contain a mixture of unaltered organic matter and pyrolysate (Fig. 23e). As in the Rymer Cones wastes, alkenes are absent. The alkenes likely isomerised into *n*-alkanes under the long-term influence of heat and hydrothermal activity (Leif, Simoneit 2000).
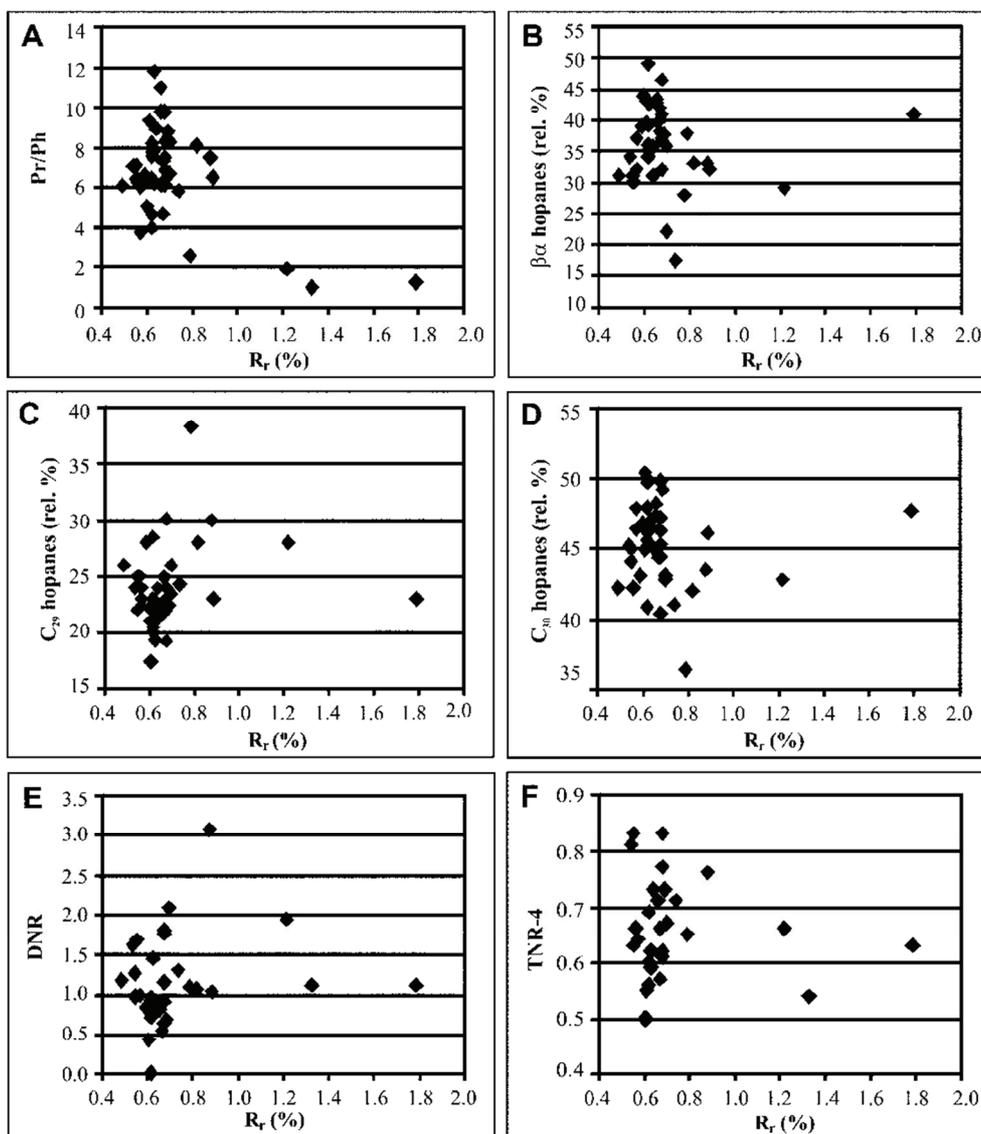
Fig. 46. The relationships between reflectance (R_r) and various parameters of thermal maturation for the Starzykowiec coal waste dump. For parameter formulae, see Tables 11 and 12.

Some geochemical indicators of thermal maturation (Tables 11, 12) show that the Starzykowiec wastes are relatively weakly altered. CPI values are always > 1.1 and decrease in wastes of reflectance < 1%. Pr/Ph values in most wastes are > 1.0 except in C14. Samples C17, C23, CH5a, CH10, and CH15 lack pristane and phytane. The values of Pr/Ph seem to decrease with increasing vitrinite reflectance > 1% (Fig. 46a). Values of pristane/n-heptadecane reaching 34.28 in C27 also suggest a low level of thermal alteration.

Values of phytane/*n*-octadecane are much lower, reaching, for example, only 2.85 in C22 (Table 11).

A low level of thermal alteration is also reflected by relatively high contents of $\beta\beta$ hopanes and lower contents of geochemical diastereomers, i.e., $\beta\alpha$ and $\alpha\beta$ hopanes (Fig. 11). The relative contents of $\beta\alpha$ hopanes tends to decrease up to $R_r = 0.89\%$ and, above that, their contents increase (Fig. 46b); this is the opposite to the pattern in the Rymer Cones dump (Fig. 42e). No such relationship is seen for initial $\beta\beta$ and final $\alpha\beta$ diastereomers. At the thermal stage reached in this dump, the intermediate $\beta\alpha$ hopanes reflect an intermediate stage of its equilibrium. This is also reflected in the opposed trends of the changes in the relative contents of C_{29} and C_{30} hopanes in more altered wastes; C_{29} hopanes decrease (Fig. 46c) and C_{30} hopanes increase (Fig. 46d) with increasing reflectance. As in Rymer Cones, the relative contents of C_{31} hopanes remain unchanged in more altered wastes.

Correlations between the degree of thermal alteration expressed by vitrinite reflectance values and parameters based on aromatic hydrocarbons are also much poorer than they are for the Rymer Cones dump. Only thermal parameters based on naphthalenes and their derivatives (DNR, TNR-4; Fig. 46e-f) show a tendency to decrease with increasing alteration in wastes of $R_r > 1\%$ in Starzykowiec.

Relative contents of individual PAHs show no relationship with degree of waste thermal alteration. However, there is some tendency for contents of four- and five-ring PAHs to increase, and those of two- and three-ring PAHs to decrease with increasing vitrinite reflectance.

In most samples, two- and three-ring PAHs dominate over four- and five-ring PAHs, however, in some samples four ring, and in C11 five-ring PAHs dominate (Table 13; Fig. 13, 26). The content of benzo[*a*]pyrene, the most carcinogenic PAH, is low (usually < 4 rel.%). Only in sample C11 is the content high, which may reflect secondary oxidation and biodegradation processes (Hadibarata 2009; Kyin et al. 2009).

Though they display poor correlations with reflectance, individual parameters of thermal maturation show somewhat better correlations with CPI (Fig. 47). Values of indices based on acyclic isoprenoids (Pr/Ph, Pr/*n*-C_{17}, and Ph/*n*-C_{18}) increase with increasing CPI (r = 0.70, 0.66, and 0.49, respectively; Fig. 47a-c), i.e. they decrease with decreasing degrees of thermal alteration. Relative contents of C_{29} hopanes decrease with increasing CPI (r = -0.64; Fig. 47d) and those of C_{30} hopanes increase (r = 0.54; Fig. 47e). Individual polyaromatic hydrocarbons correlate poorly with CPI with the exception of phenanthrene; its relative contents decrease with increasing CPI (r = -0.58; Fig. 47f). Correlations involving the relative contents of two- and three-ring PAHs that decrease with increasing CPI, and those of four- and five-ring PAHs that show the reverse, are relatively much stronger.
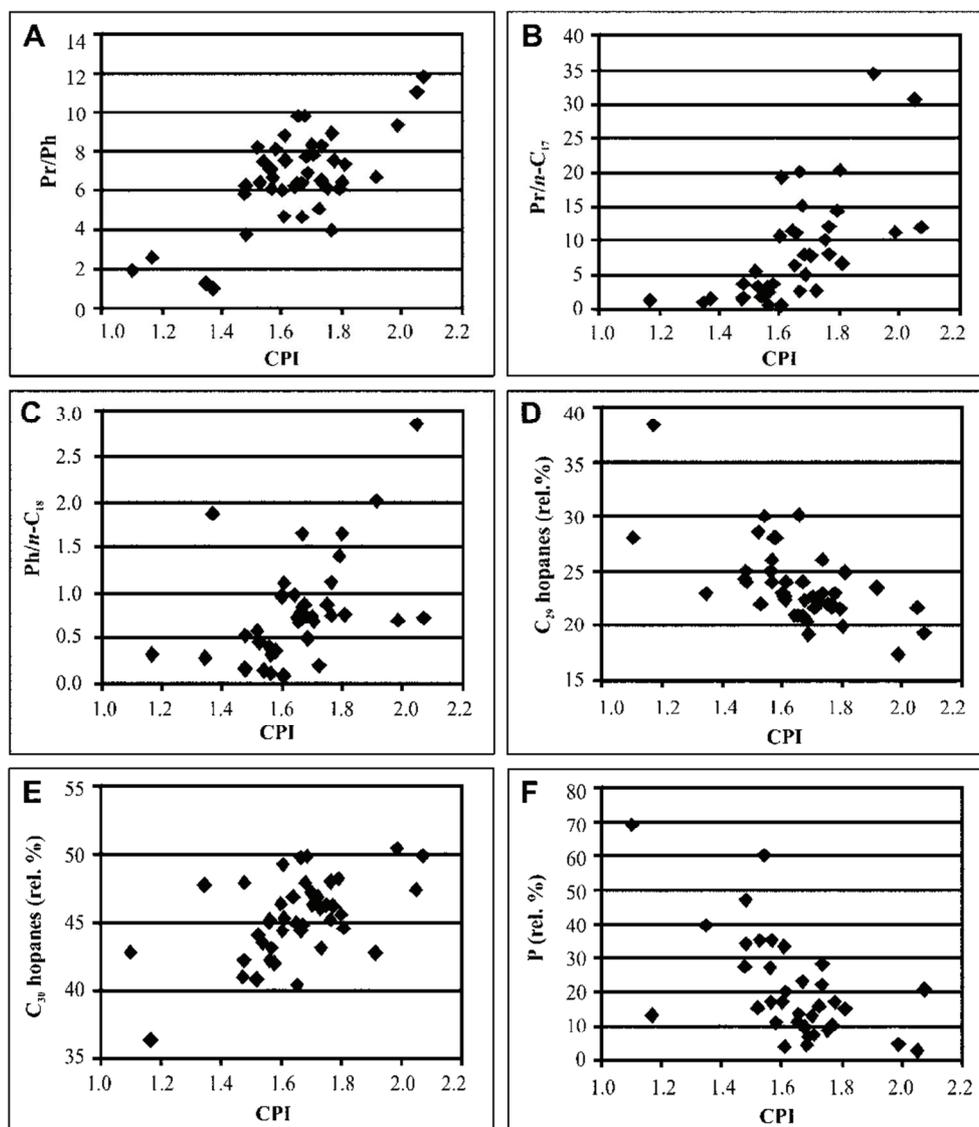
Fig. 47. The relationship between Carbon Preference Index (CPI) and various indices of thermal maturation for the Starzykowiec coal waste dump. For parameter formulae, see Table 11. For relative concentration of phenanthrene, see Table 13.

9.3. The Marcel Coal Mine dump

The Marcel Coal Mine dump is the largest of the dumps investigated. Self-heating has occurred there for tens of years and occurs now in several places located hundreds of meters from each other. The dump contains wastes that are altered by self-heating and self-combustion to varying degrees. Most waste samples contain organic matter visible under the microscope with the exception of M7, M30, M31, M34, M37-M41, and M43 (Tables

222

15, 16). Organic compounds were detected in M7, M31, M38, and M40. Organic matter, either microscopically visible or extractable, is absent in M30, M34, M37, M39, M42, and M43 (Tables 17-19).

The mineral content in the wastes averages 82 vol.% (Table 15), similar to the contents in the other coal waste dumps (Tables 3, 9). There is a marked difference in total sulphur content between the wastes in the Marcel dump (2.13 wt%, Table 20) and those in Rymer Cones and Starzykowiec dumps (0.56 and 0.50 wt%, respectively; Tables 8, 14).

Extract yields from the Marcel samples, on average 0.51 wt%, are similar to those from Rymer Cones and higher than those from Starzykowiec. The differences may be related to the duration of water leaching.

The original organic matter in the Marcel wastes is the most coalified and provides the highest vitrinite reflectance values compared to the other two waste dumps (Tables 3, 9, 15). The reflectance of organic matter in the wastes deriving from current coal production is 0.72% (M24a; Fig. 31a). The normal *n*-alkane distribution (Fig. 32a), the CPI value of *ca* 1.0 and the high Pr/Ph (4.32; Table 17) also reflect the lack of alteration.

Values of vitrinite reflectance determined for weathered wastes (M24 and M25; 0.72 and 0.74%, respectively; Table 15; Fig. 31b) are similar to those of unaltered wastes. Values for weathered wastes in the other dumps may be as low as 0.50% (Tables 3, 9). The remaining waste samples (M1-M23 and M30-M43) from the Marcel dump give vitrinite reflectance values > 0.76% (Table 15; Fig. 31c-d). Samples M12-M22a are particularly heterogeneous, containing strongly altered wastes comprising coked organic matter and much less altered wastes that have undergone thermal transformation in the dump at the place of their collection. This, of course, makes any interpretation particularly difficult as, due to the migration of bitumen within the dump, chemical compounds of variable origin may be included in the sample extracts.

The lack of any signs of plasticity in most wastes indicates that the temperature rose slowly. Pores within some vitrinite particles are only seen in samples M6, M17a, and M22a (Fig. 28d-e; Tables 15, 16). These particles were probably locally exposed to higher temperatures and may have contained liptinite macerals. All of the remaining macerals are uniformly paler in colour and display higher reflectance (Fig. 29c). Rarely, as in M21a, paler- coloured oxidation rims (Fig. 29d) are indicative of temperatures > 200°C.

Paler-coloured vitrinite is the dominant component in all wastes. M8, characterized by a slightly elevated vitrinite reflectance value (0.76%) and the highest unaltered vitrinite content is an exception, as is M7, the most intensely altered sample. They reflect a slow temperature rise (Goodarzi, Murchison 1978; Murchison 2006).

Coke is present as the only component in some wastes (M32, M33, M35, M36, and M41) and is associated with unaltered and other variously altered macerals in other samples (M9-M11, M12-M20, and M21-M23; Tables 15, 16; Fig. 29a-b, 29e-f). The coke is always isotropic and present in massive forms or as laminae and detritus, suggesting that it was formed by low-rate heating. Probably the unaltered wastes known for their tendency to self heat were mixed with altered wastes containing coked organic matter in an attempt to avoid that process.

Microscopically visible bitumens are present in some of the wastes (e.g. M15; Fig. 30) appear to be a typical feature of self-heated wastes where the temperature was rising slowly – even samples in which the liptinite content from which bitumens were mostly

generated is only a few per cent. They are present in wastes for which the extract yields (0.022-0.225 wt%) are lower than the average (0.51 wt%) for all waste samples from the Marcel dump (Table 17). On the other hand, waste samples with the highest extract yields (M4, M18, and M20a) have no microscopically-visible bitumens. The visible bitumens were adsorbed on minerals.

The presence of pyrolytic carbon in some samples (M10, M14, and M22a; Tables 15, 16) suggests they formed by condensation of volatiles at low temperature. These volatiles were likely generated during decomposition of organic matter at high temperatures elsewhere in the dump.

All of the wastes investigated have very complex chemical compositions. The absence of solvent-extractable organic compounds in samples M30, M32-M37, M39, and M41-M43 suggests that the compounds were thermally destroyed. As noted above, the extract yields (Table 17) in the coal wastes from the Marcel dump are similar, on average, to those from wastes in the Rymer Cones dump, and much higher than those from the Starzykowiec dump. All the indicators of thermal maturation (Tables 17-19) confirm that the wastes in the Marcel dump are the most altered of all those examined in this study.

Organic matter in the wastes in the interior of the dump was heated to higher temperatures than that in wastes located close to the dump surface. Organic compounds with various molecular weights, generated during slow heating, likely underwent fractionation during any migration within the dump. At the same time, atmospheric precipitation would tend to drive some compounds downwards into deeper parts of the dump where they would be reheated. Many migrating organic compounds probably reacted with other organic and inorganic compounds that they encountered. Minerals in the wastes would have played a significant role in these very complicated processes (Huizinga et al. 1987; Pan et al. 2009, 2010); for example, many of the migrating compounds would have been adsorbed on them.

In comparison with the Rymer Cones and Starzykowiec dumps, individual parameters of thermal alteration, and relative contents of hopanes and polyaromatic hydrocarbons calculated for the Marcel dump, show the weakest correlations with vitrinite reflectance. The individual indices of thermal alteration also display poor correlations with each other. This is probably a reflection of the complicated thermal history of individual sites, and also of fluctuations in temperature in the dump. The fact that samples M12-M22a contain a mixture of strongly altered, relatively unaltered- and weakly-altered material by self-heating is an additional complexity. However, even the exclusion of those samples does not significantly improve many of the correlations. Reverses in trends with increase in reflectance were observed in many cases, but at relatively high reflectance values of *ca* 1.5% R_r. Many geochemical indicators of thermal maturation display tendencies and patterns in the Marcel dump that differ from those seen in the other dumps. This may be a reflection of some or all the factors noted above and the degree of transformation of the original organic matter.

n-Alkanes are one of the most important groups of organic compounds present in these wastes. As elsewhere, the absence of their unsaturated homologues, alkenes, is an indication of long heating times and hydrous pyrolysis (Leif, Simoneit 2000). In most Marcel dump wastes, *n*-alkanes show Gaussian distributions typical for pyrolysates (Fig.

32c, 33b-c, 34a-e). Many samples (Fig. 32b, 33a) contain lighter n-alkanes that were likely generated during thermal cracking of organic matter.

Coal waste sample M25, exposed to weathering for some years, is characterized by a wide, typically pyrolytic, n-alkane distribution with a maximum at n-C_{21}, and also by a high Pr/Ph (Fig. 32c; Table 17). Sample M24, also weathered, is characterized by a considerable amount of lighter n-alkanes, and a high Pr/Ph (Fig. 32b). The difference between these two waste samples suggests limited water washing.

More intensely altered wastes contain n-alkanes generated during various stages of heating and over various temperature ranges. Some of these may have been returned to the dump interior due to atmospheric precipitation and as a result, been heated to high temperatures and perhaps adsorbed on minerals. Some of the n-alkanes may have originated through the cracking of compounds earlier generated from organic waste matter.

n-Alkane boiling temperatures give some insight into the temperatures of their generation in the dump. A wide distribution of n-alkanes in the range n-C_{13}-n-C_{33} with a maximum at n-C_{21}, as in sample M3 (Fig. 33b), suggests their formation at temperatures of ca 210-520°C. Narrow distributions, as in M16 and M21 (Fig. 34d-e), suggest temperature ranges of ca 170-370°C for M16 and ca 260-420°C for M21 (Chemical Land21). The irregular n-alkane distributions of samples M14 and M13 (Fig. 34b-c) indicate that the n-alkanes were generated over a wide temperature range with maxima at n-C_{23} and n-C_{17}, respectively. In the case of M14, they formed at temperatures in the range ca 135-500°C with a peak at ca 360-410°C. The n-alkanes in M13 were generated at temperatures between ca 170-500°C; in this case, however, the likely peak temperatures were much lower at ca 260-325°C; Chemical Land21).

Values of CPI ca 1.0 suggest relatively high levels of maturation of the original organic matter in the wastes at the time of dumping. In all waste samples, the CPI values fall in the range 0.96-1.59 (Table 17). CPI values decrease with increasing reflectance in the Rymer Cones and Starzykowiec dumps but, in the Marcel dump, they increase up to R_r = 1.5%, then decrease (Fig. 48a).

All waste samples from this dump, except M5, M11, M23, M31, M38, and M40, show a marked predominance of long-over-short chain n-alkanes. Short chain n-alkanes dominate mostly in the most intensely altered wastes. Values of Pr/Ph higher than in unaltered wastes indicate that considerable amounts of pristane were formed from kerogen during catagenesis (Goosens at al. 1988a, b). Values of other parameters based on acyclic isoprenoids (pristane/n-heptadecane and phytane/n-octadecane) are very variable (Table 17), again reflecting the complex heating regime in the wastes.

The wastes from the Marcel dump contain the highest relative contents of final $\alpha\beta$ hopanes and relatively low contents of intermediate $\beta\alpha$ hopanes compared to the wastes in the other two dumps (Fig. 11). Surprisingly, initial $\beta\beta$ hopanes are relatively common and are present even in M38, one of the most altered samples. They are absent only in M14 and M31. Waste samples M21a and M22 contain two of the highest contents of $\beta\beta$ hopanes at 15 rel.% and 16 rel.%, respectively, in comparison not only with the wastes from the Marcel dump, but also with the wastes of the other two dumps. There is, as yet, no explanation for this. In the Marcel wastes, all of the parameters of thermal alteration based

on hopanes have similar values and, thus have limited potential application in unravelling the thermal history.

Parameters based on aromatic hydrocarbons show almost no pattern of correlation with vitrinite reflectance. The exception is MPI-3 in which values increase up to 1.5% and above which the trend is reversed (Fig. 48b).
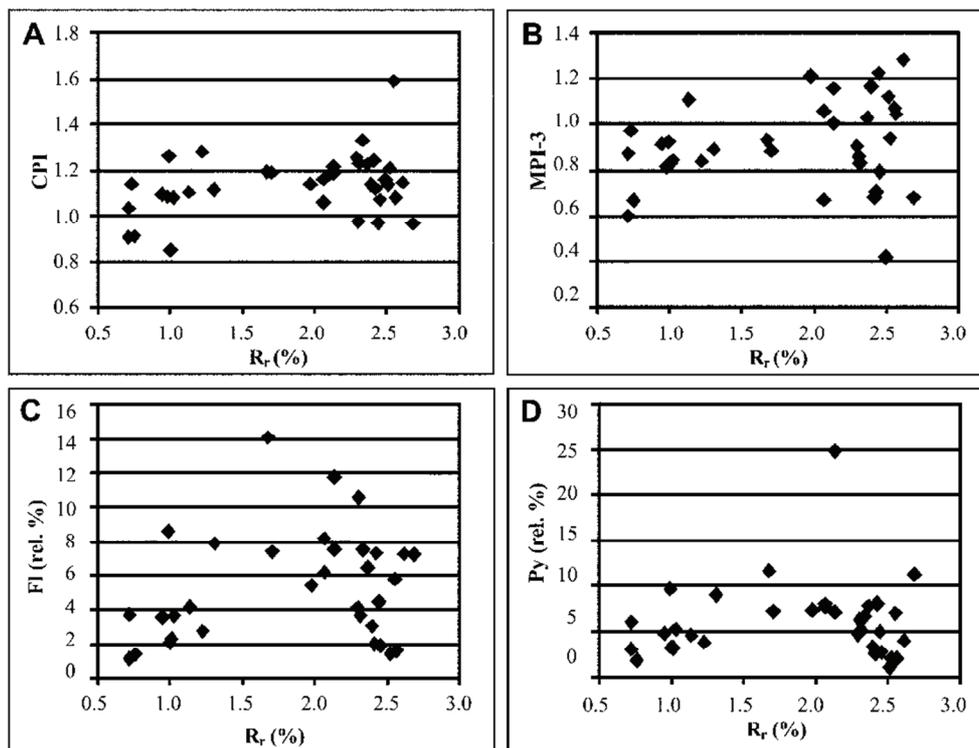
Fig. 48. The relationships between reflectance (R_r) and A – CPI, B – MPI-3, C – fluoranthene (Fl), and D – pyrene (Py) for the Marcel Coal Mine dump. For parameter formulae, see Tables 17 and 18. For relative concentrations of fluoranthene and pyrene, see Table 19.

A characteristic feature of the wastes from the Marcel dump is their relatively high contents of two- and three-ring PAHs and relatively low contents of five-ring PAHs compared to wastes from the other dumps (Table 19; Fig. 13, 39). This is especially marked in M12-M22a. Individual PAHs show a weak correlation with reflectance. Only four-ring PAHs, notably fluoranthene (Fig. 48c) and pyrene (Fig. 48d), give relative-content values that increase with reflectance up to 1.5% and then decrease. The limited contents of most PAHs probably reflect the thermal destruction of these compounds.

10. Conclusions

Oxidation leading to self-heating began immediately after the deposition of the wastes in the dumps at Rymer Cones, Starzykowiec, and Marcel Coal Mine. Self-heating, self-

combustion, and smouldering/hydropyrolysis occurred in a setting with limited access for air and in the presence of water. The processes took place very slowly over periods of many years.

All three maceral groups are present in the wastes. Vitrinite macerals are those most affected by the self-heating. They are present in the wastes mainly as unaltered macerals and macerals of paler-grey colour. Some vitrinite particles are characterized by irregular cracks and paler-coloured oxidation rims. The common lack of evidence for plasticity in the macerals, and their uniform paler colour, is indicative of slow heating. The presence of isotropic massive coke and dispersed coked organic matter associated with minerals also indicates that heating was slow over a long time in all three dumps.

The temperature and duration of heating was not enough to result in the complete transformation of the organic compounds constituting the original macerals. Microscopically, visible organic matter is lacking only in the most altered wastes. Only rare particles with plasticised edges or pores formed during devolatilisation are indicative of sudden heating.

A characteristic feature of some of the wastes is the presence of bitumen expulsions generated during self-heating. They commonly occur in association with minerals. The occurrence of these bitumens is independent of extract yields. Their absence in wastes characterized by high extract yields indicates that bitumens were absorbed on minerals in these. The presence of extractable bitumens in samples without any microscopically visible organic matter suggests their migration from sites of higher temperature elsewhere and their precipitation on minerals. Bitumens are absent in dumps where heating ceased some years ago; in these cases, they were probably washed away by rain.

The major chemical compounds present or generated in the wastes include n-alkanes, acyclic isoprenoids, hopanes and moretanes, PAHs and their derivatives, and phenols. Some of these, e.g. PAHs and phenols, are significant environmental toxicants.

The presence of n-alkanes, PAHs, and phenols is partly linked to the thermal decomposition of vitrinite and partly to the chemical composition of the primary organic matter in the wastes. Under conditions similar to hydropyrolysis that continued for many years and perhaps aided by mineral properties, it is likely that any n-alkenes and hopenes, once present but now absent, underwent isomerisation into n-alkanes and hopanes, respectively.

Dumps or parts of dumps where heating ceased some years ago are depleted in all of these compounds. Phenol and its derivatives are found only in wastes recently heated. All were probably rain-leached into deeper parts of the dumps, or outside the dumps.

Many factors influence the distribution of individual chemical compounds in the dumps and the conclusions that can be drawn from geochemical parameters of thermal maturation is based on sample analyses. The nature of the organic matter, the quantities of minerals and their properties, dynamic temperature fluctuations and the migration of chemical compounds within and to the outside of the dumps due to water washing and evaporation are the most important factors.

It is also highly probable that compounds generated at different temperatures and in different places mixed during any migration. Petrographic and chemical analyses show that, in some wastes, unaltered organic matter and material of pyrolytic origin are in close association. Mixing is a further factor disturbing correlations between vitrinite reflectance

227

and values of individual chemical parameters of thermal maturation. Despite all of these potentially interfering influences, all calculated geochemical parameters of thermal maturation tend to change trend at vitrinite reflectance values of *ca* 1%.

The organic compounds in the waste dumps have the characters of compounds affected by heat but little disturbed by water washing as indicated by the presence of phenol and its homologues. The presence of light *n*-alkanes is clearly indicative of limited leaching; the absence of light *n*-alkanes, and phenol with its homologues, is typical of dumps in which self-heating processes ceased some years ago.

The presence of *n*-alkanes in different ranges and of different distribution types suggests generation in discrete heating spots at different temperatures. Some wastes contain *n*-alkanes generated within relatively narrow temperature ranges, others over much wider ranges. In some wastes, *n*-alkanes were probably generated at different/fluctuating temperatures or they originated from both unaltered organic matter and pyrolysates; bimodal distributions suggest so.

The level of thermal transformation of the wastes is reflected in the distribution of hopane diastereomers. Their absence in many wastes is due to thermal destruction. The final $\alpha\beta$ hopanes predominate in the wastes and the initial $\beta\beta$ hopanes are absent in many. Notably, in the wastes of the Marcel Coal Mine dump in which the original organic matter is the most coalified, $\beta\beta$ hopane contents reach the highest levels seen in any of the three dumps.

A characteristic feature of all the wastes is the presence of the two- to five-ring PAHs that are typical products of the thermal alteration of hard coals. PAHs with more than five rings are not present. The spatial distribution of the PAHs is probably mainly influenced by temperature fluctuations as they do not show any pattern related to dump geometry.

Any investigation of alterations in coal wastes resulting from self-heating and self-combustion in waste dumps is a challenge. The vary nature of the dumps means that they are heterogeneous from the day they were first formed. Many factors influence the thermal transformations of organic matter in the wastes, namely, maceral composition, coal rank, and heating conditions including heating rate, the final heating temperature, and the duration of heating. The presence and properties of any minerals present are also important. In addition, the processes involved are made even more complicated by temperature fluctuations within the dump, atmospheric precipitation, and potential migration of compounds through the intrinsically permeable waste material. Water-washing that takes place during heating and after the thermal processes cease is also a significant process.

The tools of organic petrography and gas chromatography-mass spectrometry, used together, provide complementary data crucial to any attempt at defining the processes that happen within waste dumps. Each dump has to be examined as a separate entity as all are different with regard to waste properties and self-heating history. If the internal processes that occurred in the dumps can be established, any environmental impact they might have, or may have had, will be open to more definitive evaluation.

11. Glossary of terms

Biomarkers – complex organic compounds occurring in rocks and showing little or no change in structure from their parent organic molecules in living organisms.

Carbominerites – association of macerals and minerals (20-60% clay minerals, carbonates and silica, and 5-20% sulphides)

Coal wastes – wastes generated during coal mining and coal separation processes, composed mostly of minerals and various amount of coaly matter

Combustion – thermal process taking place in the presence of air

Durite – microlithotype composed of macerals of liptinite and inertinite groups

Macerals – microscopically recognizable organic constituents of coal distinguished on the basis of colour, fluorescence, reflectance, morphology, and size. They also differ in origin and behaviour during technological processes. Three maceral groups are distinguished: huminite/vitrinite, liptinite, and inertinite

Microlithotypes – associations of one, two or three groups of macerals

Pyrolysis – thermal process taking place in the absence of oxygen and leading to destruction of organic compounds

Self-heating – processes associated with a slow rise in temperature, e.g. coal, coal wastes and preceded by oxidation of organic matter

Vitrite – microlithotype composed of vitrinite-group macerals

12. References

Allan, J., & Douglas, A.G. (1977). Variations in the content and distribution of n-alkanes in a series of carboniferous vitrinites and sporinites of bituminous rank. *Geochimica et Comochimica Acta*, 41(9), 1223-1230. DOI: 10.1016/0016-7037(77)90068-0.

Alonso, M.I., Valdés, A.F., Martínez-Tarazona, R.M., & Garcia, A.B. (2002). Coal recovery from fines cleaning wastes by agglomeration with colza oil: a contribution to the environment and energy preservation. *Fuel Processing Technology,* 75(2), 85-95. DOI: 10.1016/S0378-3820(01)00233-8.

Amijaya, H., Schwarzbauer, J., & Littke, R. (2006). Organic geochemistry of the Lower Suban coal seam, South Sumatra Basin, Indonesia: Paleoecological and thermal metamorphism implications. *Organic Geochemistry,* 37(3), 261-279. DOI: 10.1016/j.orggeochem.2005.10.012

Barosz, S. (2002). Monitoring of the dismantling and reclamation of the coal waste dumps. Proceedings - VII Conference "Long term proecological undertakings in the Rybnik Coal Area", October 2002 (pp. 149-156). Rybnik, (in Polish).

Barosz, S. (2003). *Technical, economical and environmental conditions of management of coal waste dumps using the mines from the Rybnik Coal District as examples.* Unpublished doctoral dissertation, Academy of Mining and Metallurgy, Cracow, Poland (in Polish).

Beamish, B.B., Barakat, M.A., & George, J.D.St. (2001). Spontaneous-combustion propensity of New Zealand coals under adiabatic conditions. *International Journal of Coal Geology*, 45(2-3), 217-224. DOI: 10.1016/S0166-5162(00)00034-3.

Beamish, B.B. (2005). Comparison of the R_{70} self-heating rate of New Zealand and Australian coals to Suggate rank parameter. *International Journal of Coal Geology,* 64(1-2), 139-144. DOI: 10.1016/j.coal.2005.03.012.

Bend, S.L., & Kosloski, D.M. (1993). A petrographic examination of coal oxidation. *International Journal of Coal Geology,* 24(1-4), 233-243. DOI: 10.1016/0166-5162(93)90012-Y.

Berkowitz, N. (1985). *The chemistry of coal.* Amsterdam-Oxford-New York-Tokyo: Elsevier.

Bishop, A.N., & Abbott, G.D. (1993). The interrelationship of biological maker maturity parameters and molecular yields during contact metamorphism. *Geochimica et Cosmochimica Acta,* 57(15), 3661-3668. DOI: 10.1016/0016-7037(93)90147-O.

Bishop, A.N., & Abbott, G.D. (1995). Vitrinite reflectance and molecular geochemistry of Jurassic sediments: the influence of heating by Tertiary dykes (northwest Scotland). *Organic Geochemistry,* 22(1), 165-177. DOI: 10.1016/0146-6380(95)90015-2.

Bojakowska, I., & Sokołowska, G. (2001). Polycyclic aromatic hydrocarbons in hard coals from Poland. *Geological Quarterly*, 45(1), 87-92.

Bray, E.E., & Evans, E.D. (1961). Distribution of *n*-parafins as a clue to recognition of source beds. *Geochimica et Cosmochimica Acta,* 22(1), 2-15. DOI: 10.1016/0016-7037(61)90069-2.

Brooks, K., Svanas, N., & Glasser, D. (1988). Evaluating the risk of spontaneous combustion in coal stockpiles. *Fuel,* 67(5), 651-656. DOI: 10.1016/0016-2361(88)90293-1.

Calemma, V., Del Piero, G., Rausa, R., & Girardi, E. (1995). Changes in optical properties of coals during air oxidation at moderate temperature. *Fuel,* 74(3), 383–388. DOI: 10.1016/0016-2361(95)93471-O.

Carras, J.N., Day, S.J., Saghafi, A., & Williams, D.J. (2009). Greenhouse gases emissions from low-temperature oxidation and spontaneous combustion at open-cut coal mines in Australia. *International Journal of Coal Geology,* 78(2), 161-168. DOI: 10.1016/j.coal.2008.12.001.

Chandra, D. (1962). Reflectivity and microstructure of weathered coals. *Fuel,* 41, 185-193.

Chemical Land 21. *n-Alkanes.* Retrieved May 10, 2011, from http://chemicalland21.com/industrialchem/organic/n-OCTADECANE.htm

Clayton, J.L., & Bostick, N.H. (1986). Temperature effects on kerogen and on molecular and isotropic composition of organic matter in Pierre Shale near an igneous dyke. *Organic Geochemistry,* 10(1-3), 135-143. DOI: 10.1016/0146-6380(86)90017-3.

Clemens, A.H., & Matheson, T.W. (1996). The role of moisture in the self – heating of low – rank coals. *Fuel,* 75(7), 891-895. DOI: 10.1016/0016-2361(96)00010-5.

Clemens, A.H., Matheson, T.W., & Rogers, D.E. (1991). Low temperature oxidation studies of dried New Zealand coals. *Fuel,* 70(2), 215-221. DOI: 10.1016/0016-2361(91)90155-4.

Cooper, J.R., Crelling, J.C., Rimmer, S.M., & Whittington, A.G. (2007). Coal metamorphism by igneous intrusion in the Raton Basin, CO and NM: Implications for generation of volatiles. *International Journal of Coal Geology,* 71(1), 15-27. DOI: 10.1016/j.coal.2006.05.007.

Cygankiewicz, J. (1996). Estimation of the development of self-ignition centers on the basis of the precise analysis of coal mine air samples. *Scientific Papers of Central Mining Institute*, Katowice, 14, 505-530 (in Polish).

Ćmiel, S., & Misz, M. (2005). Petrographic changes in coal caused by coal wastes fires. Proceedings - LXXVI Meeting of Polish Geological Society, 14-16 September, 2005 (pp. 43-50). Rudy near Rybnik. Polish Geological Institute, Polish Geological Society (Warsaw), (in Polish).

Didyk, B.M., Simoneit, B.R.T., Brassel, S.C., & Eglinton, G. (1978). Organic geochemical indicators of paleoenvironment conditions of sedimentation. *Nature,* 272, 216–222. DOI: 10.1038/272216a0.

Dzou, L.I.P., Noble, R.A., & Senftle, J.T. (1995). Maturation effects on absolute biomarker concentration in a suite of coals and associated vitrinite concentrates. *Organic Geochemistry,* 23(7), 681-697. DOI: 10.1016/0146-6380(95)00035-D.

Evans, K.A., Gandy, C.J., & Banwart, S.A. (2003). Mineralogical, numerical and analytical studies of the coupled oxidation of pyrite and coal. *Mineralogical Magazine,* 67(2), 381-398. DOI: 10.1180/0026461036720107

Fabiańska, M. (2007). Organic geochemistry of brown coals from the selected Polish basins. Katowice: Publisher of University of Silesia (in Polish).

Fabbri, D., Torri, C., Simoneit, B.R.T., Marynowski, L., Rushdi, A.I. , Fabiańska, M.J. (2009). Levoglucosan and other cellulose and lignin markers in emissions from burning of Miocene lignites. *Atmospheric Environment*, 43(14), 2286-2295. DOI: 10.1016/j.atmosenv.2009.01.030.

Faksenss, L.G., & Brandvik, P.J. (2008). Distribution of water soluble components from Arctic marine oil spills – A combined laboratory and field study. *Cold Regions Science and Technology*, 54(2), 97–105. DOI: 10.1016/j.coldregions.2008.03.005.

Farrimond, P., Bevan, J.C., & Bishop, A.N. (1996). Hopanoid hydrocarbon maturation by an igneous intrusion. *Organic Geochemistry,* 25(3-4), 149-164. DOI: 10.1016/S0146-6380(96)00128-3.

Farrimond, P., Taylor, A., & Telenæs, N. (1998). Biomarker maturity parameters: the role of generation and thermal degradation. *Organic Geochemistry,* 29(5-7), 1181-1197. DOI: 10.1016/S0146-6380(98)00079-5.

Finkelman, R.B. (2004). Potential health impacts of burning coal beds and waste banks. *International Journal of Coal Geology,* 59(1-2), 19-24. DOI: 10.1016/j.coal.2003.11.002.

George, S.C. (1992). Effect of igneous intrusion on the organic geochemistry of a siltstone and an oil shale horizon in the Midland Valley of Scotland. *Organic Geochemistry,* 18(5), 705-723. DOI: 10.1016/0146-6380(92)90097-H.

Goodarzi, F. & Murchison, D.G. (1978). Influence of heating-rate on the anisotropy of carbonized vitrinites. *Fuel,* 57(5), 273-284. DOI: 10.1016/0016-2361(78)90004-2.

Goossens, H., Due, A., de Leeuw, J.W., van de Graaf, B., & Schenck, P.A. (1988a). The Pristane Formation Index, a new molecular maturity parameter. A simple method to assess maturity by pyrolysis/evaporation-gas chromatography of unextracted samples. *Geochimica et Cosmochimica Acta*, 52(5), 1189-1193. DOI: 10.1016/0016-7037(88)90272-4.

Goossens, H., de Lange, F., de Leeuw, J.W., & Schenck, P.A. (1988b). The Pristane Formation Index, a molecular maturity parameter. Confirmation in samples from the Paris Basin. *Geochimica et Cosmochimica Acta*, 52(10), 2439-2444. DOI: 10.1016/0016-7037(88)90301-8.

Grantham, P.J. (1986). Sterane isomerisation and moretane/hopane ratios in crude oils derived from Tertiary source rocks. *Organic Geochemistry,* 9(6), 293-304. DOI: 10.1016/0146-6380(86)90110-5.

Grice, K., Lu, H., Atahan, P., Asif, M., Hallmann, C., Greenwood, P., Maslen, E., Tulipani, S., Williford, K., & Dodson, J. (2009). New insights into the origin of perylene in geological samples. *Geochimica et Cosmochimica Acta,* 73(21), 6531-6543. DOI: 10.1016/j.gca.2009.07.029.

Grossman, S.L., Davidi, S., & Cohen, H. (1994). Emission of toxic and fire hazardous gases from open air coal stockpiles. *Fuel,* 73(7), 1184-1188. DOI: 10.1016/0016-2361(94)90257-7.

Hadden, R., & Rein, G. (2009). Ignition and suppression of smouldering coal fires in small-scale experiments. 6[th] Mediterranean Combustion Symposium, June 7-11, 2009. Ajaccio, Corsica, France. Retrieved May 10, 2011 (http://www.see.ed.ac.uk/~grein/rein_papers/Hadden_SuppresingCoalfires_2009.pdf).

Hadibarata, T. (2009). Oxidative degradation of benzo[a]pyrene by the ligninolytic fungi. In Y. Obayashi, T. Isobe, A. Subramanian, S. Suzuki, & S. Tanabe, (Eds.) *Interdisciplinary Studies on Environmental Chemistry vol.2 - Environmental Research in Asia for establishing a scientist's network* (pp. 309-316). Tokyo: TERRAPUB.

Hanak, B., & Nowak, G. (2008). Thermally altered coals in self-combusted mine dump from Upper Silesia coal basin. Proceedings from International Conference on Coal and Organic Petrology ICCP-TSOP Joint Meeting, September 21-27, 2008 (p. 105). Oviedo, Spain.

Hatcher, P.G., & Clifford, D.J. (1997). The organic geochemistry of coal: from plant materials to coal. *Organic Geochemistry,* 27(5-6), 251-274. DOI: 10.1016/S0146-6380(97)00051-X .

Horsfield, B. (1989). Practical criteria for classifying kerogens: Some observations from pyrolysis-gas chromatography. *Geochimica et Cosmochimica Acta,* 53(4), 891-901. DOI: 10.1016/0016-7037(89)90033-1.

Hower, J.C., Henke, K., O'Keefe, J.M.K., Engle, M.A., Blake, D.R., & Stracher, G.B. (2009). The Tiptop coal-mine fire, Kentucky: Preliminary investigation of the measurement of mercury and other hazardous gases from coal-fire gas vents. *International Journal of Coal Geology,* 80(1), 63-67. DOI: 10.1016/j.coal.2009.08.005.

Huizinga, B.J., Tannenbaum, E., & Kaplan, I.R. (1987). The role of minerals in the thermal alteration of organic matter. IV. Generation of *n*-alkanes, acyclic isoprenoids, and alkenes in laboratory experiments. *Geochimica et Cosmochimica Acta,* 51(5), 1083-1097. DOI: 10.1016/0016-7037(87)90202-X.

Ingram, G.R., & Rimstidt, J.D. (1984). Natural weathering of coal. *Fuel,* 63(3), 292-296. DOI: 10.1016/0016-2361(84)90002-4.

International Committee for Coal and Organic Petrology (2001). New inertinite classification (ICCP system 1994). *Fuel,* 80(4), 459-471. DOI: 10.1016/S0016-2361(00)00102-2.

International Committee for Coal and Organic Petrology (1998). New vitrinite classification (ICCP system 1994). *Fuel,* 77(5), 349-358. DOI: 10.1016/S0016-2361(98)80024-0.

Ishiwatari, R., & Fukushima, K. (1979). Generation of unsaturated and aromatic hydrocarbons by thermal alteration of of young kerogen. *Geochimica et Cosmochimica Acta,* 43(8), 1343-1349. DOI: 10.1016/0016-7037(79)90124-8.

Itay, M., Hill, C.R. & Glasser, D. (1989). A study of the low temperature oxidation of coal. *Fuel Processing Technology,* 21(2), 81-97. DOI: 10.1016/0378-3820(89)90063-5.

Jiamo, F., Guoing, S., Jiayou, X., Eglington, G., Gowar, A.P., Ronfeng, J., Shanfa, F., & Pingan, P. (1990). Application of biological markers in the assessment of paleoenvironments of Chinese non-marine sediments. *Organic Geochemistry,* 16(4-6), 769-779. DOI: 10.1016/0146-6380(90)90116-H.

Jiang, C., Alexander, R., Kagi, R. I. & Murray, A.P. (1998). Polycyclic aromatic hydrocarbons in ancient sediments and their relationship to paleoclimate. *Organic Geochemistry,* 29(5-7), 1721-1735. DOI: 10.1016/S0146-6380(98)00083-7.

Jones, J.C. (2000). On the role of times to ignition in the thermal safety of transportation of bituminous coals. *Fuel,* 79(12), 1561-1562. DOI: 10.1016/S0016-2361(00)00003-X.

Kaymakçi, E., & Didari, V. (2002). Relations between coal properties and spontaneous combustion parameters. *Turkish Journal of Engineering and Environmental Sciences,* 26(1), 59-64.

Killops, S., & Killops, V. (2005). *Introduction to organic geochemistry* (2 ed.). Oxford: Blackwell Publishing.

Kotarba, M.J., & Clayton, J.L. (2003): A stable carbon isotope and biological marker study of Polish bituminous coals and carbonaceous shales. *International Journal of Coal Geology*, 55(2-4), 73-94. DOI: 10.1016/S0166-5162(03)00082-X.

Van Krevelen, D.W. (1993). *Coal Typology – Chemistry – Physics – Constitution*. Amsterdam: Elsevier.

Krishnaswamy S., Bhat S., Gunn R.D., & Agarwal P.K. (1996a). Low – temperature oxidation of coal. 1. Single – particle reaction – diffusion model. *Fuel,* 75(3), 333-343. DOI: 10.1016/0016-2361(95)00180-8.

Krishnaswamy, S., Agarwal, P.K., & Gunn, R.D. (1996b). Low – temperature oxidation of coal. 3. Modelling spontaneous combustion in coal stockpiles. *Fuel,* 75(3), 353-362. DOI: 10.1016/0016-2361(95)00249-9.

Kuenzer, C., Zhang, J., Tetzlaff, A., van Dijk, P., Voigt, S., Mehl, H., & Wagner, W. (2007). Uncontrolled coal fires and their environmental impact: Investigating two arid mining regions in north-central China. *Applied Geography,* 27(1), 42-62. DOI: 10.1016/j.apgeog.2006.09.007.

Kwiecińska, B., & Petersen, H.I. (2004). Graphite, semi-graphite, natural coke, and natural char classification – ICCP System. *International Journal of Coal Geology*, 57(2), 99-116. DOI: 10.1016/j.coal.2003.09.003.

Kwiecińska, B., Muszyński, M., Vleeskens, J., & Hamburg, G. (1995). Natural coke from the La Rasa Mine, Tineo, Spain. *Mineralogia Polonica,* 26(2), 3-14.

Kyin, B., Maung, A.T., Begum, B., Haque, M., Hemalika, S., & Sudrajat, T. (2009). Remediation of Polycyclic Aromatic Hydrocarbons polluted soils using Fenton's reagent. *Journal of Applied Sciences in Environmental Sanitation,* V(N), 63-68.

Liu, Ch., Li, S., Qiao, Q., Wang, J., & Pan, Z. (1998). Management of spontaneous combustion in coal mine waste tips in China. *Water, Air, and Soil Pollution,* 103(1-4), 441-444. DOI: 10.1023/A:1004922620264.

Liu, L., & Zhou, F. (2010). A comprehensive hazard evaluation system for spontaneous combustion of coal in underground mining. *International Journal of Coal Geology*, 82(1-2), 27-36. DOI: 10.1016/j.coal.2010.01.014.

Leif, R.N., & Simoneit, B.R.T. (2000). The role of alkenes produced during hydrous pyrolysis of a shale. *Organic Geochemistry,* 31(11), 1189-1208. DOI: 10.1016/S0146-6380(00)00113-3.

Lewan, M.D. (1992). Water as a source of hydrogen and oxygen in petroleum formation by hydrous pyrolysis. American Chemical Society, Division of Fuel Chemistry Preprints 37(4), 1643-1649.

Lewan, M.D. (1997). Experiments on the role of water in petroleum formation. *Geochimica et Cosmochimica Acta,* 61(17), 3691-3723. DOI: 10.1016/S0016-7037(97)00176-2.

Leythaeuser, D., & Schwarzkopf, Th. (1986). The pristane/*n*-heptadecane ratio as an indicator for recognition of hydrocarbon migration effects. *Organic Geochemistry,* 10(1-3), 191-197. DOI: 10.1016/0146-6380(86)90022-7.

Lu, P., Liao, G.X., Sun, J.H., & Li, P.D. (2004). Experimental research on index gas of the coal spontaneous at low-temperature stage. *Journal of Loss Prevention in the Process Industries,* 17(3), 243-247. DOI: 10.1016/j.jlp.2004.03.002.

Lu, S.-T., & Kaplan, I.R. (1992). Diterpanes, triterpanes, steranes, and aromatic hydrocarbons in natural bitumens and pyrolysates from different humic coals. *Geochimica et Cosmochimica Acta*, 56(7), 2761-2788. DOI: 10.1016/0016-7037(92)90358-P.

Machnikowska, H., Łuczak, A., & Kubacki, A. (2003). Effect of oxidation method on properties and structure of coals and lithotypes. *Karbo 3*, 157–164 (in Polish).

Mastalerz M., & Mastalerz K. (2000). Volcanic and post-volcanic hydrothermal activity in the Intrasudetic Basin, SW Poland: implications for mineralization. In: M. Glickson & M. Mastalerz (eds.), *Organic Matter and Mineralization: Thermal Alteration, Hydrocarbon Generation and Role in Metallogenesis* (pp. 185-203). Dordrecht: Kluwer Academic Publishers.

Mastalerz, M., Drobniak, A., & Schimmelmann, A. (2009). Changes in optical properties, chemistry and micropore and mesophase characteristics of bituminous coal at the contact with dikes in the Illinois Basin. *International Journal of Coal Geology*, 77(3-4), 310-319. DOI: 10.1016/j.coal.2008.05.014.

Mastalerz, M., Drobniak, A., Hower, J.C., & O'Keefe, J.M.K., (2010). Spontaneous combustion and coal petrology. In: G.B. Stracher, E.V. Sokol, & A. Prakash (Eds), *Coal and Peat Fires: A Global Perspective: Volume 1: Coal - Geology and Combustion* (pp. 47-62). Amsterdam: Elsevier.

Meyers, P.A., & Simoneit, B.R.T. (1999). Effects of extreme heating on the elemental and isotopic compositions of an upper cretaceous coal. *Organic Geochemistry*, 30(5), 299-305. DOI: 10.1016/S0146-6380(99)00015-7.

Miczajka, M. (2008). Information from the Chwałowice Coal Mine staff. Unpublished.

Misra, B.K., & Singh, B.D. (1994). Susceptibility to spontaneous combustion of Indian coals and lignites: an organic petrography authopsy. *International Journal of Coal Geology,* 25(3-4), 265-286. DOI: 10.1016/0166-5162(94)90019-1.

Misz, M., Fabiańska, M., & Ćmiel, S. (2007). Organic components in thermally altered coal waste: Preliminary petrographic and geochemical investigations. *International Journal of Coal Geology*, 71(4), 405-424. DOI: 10.1016/j.coal.2006.08.009.

Misz-Kennan, M., Kus, J., Flores, D., Avila, C., Christanis, K., Hower, J., Kalaitzidis, S., O'Keefe, J., Marques, M., Pusz, S., Ribeiro, J., Suárez-Ruiz, I., Sýkorová, I., Wagner, N., & Životić, D. (2009). Report of the 2009 Round Robin Exercise of the Self-heating of Coal and Coal Wastes Working Group. *ICCP News Letter,* 48, 58-60.

Misz-Kennan, M., & Fabiańska, M. (2010). Thermal transformation of organic matter in coal waste from Rymer Cones (Upper Silesian Coal Basin, Poland). *International Journal of Coal Geology,* 81(4), 343-358. DOI: 10.1016/j.coal.2009.08.009.

Misz-Kennan, M., & Tabor, A. (2011). The thermal history of selected coal waste dumps in the Upper Silesian Coal Basin (Poland). In G.B. Stracher, E.V. Sokol & A. Prakash (Eds.), *Coal and Peat Fires: A Global Perspective, Volume 3 - Case Studies*. Amsterdam: Elsevier, Scheduled for publication in 2011 (or early 2012).

Misz-Kennan, M., Gardocki, M., & Tabor, A. (2011a). Fire Prevention in Coal Waste Dumps as Exemplified by the Rymer Cones Dump (Upper Silesian Coal Basin, Poland). In G.B. Stracher, E.V. Sokol & A. Prakash (Eds.), *Coal and Peat Fires: A Global Perspective, Volume 3 - Case Studies*. Amsterdam: Elsevier, Scheduled for publication in 2011 (or early 2012).

Misz-Kennan, M., Fabiańska, M., & Ciesielczuk, J. (2011b). Thermal transformations of the waste rocks at the Starzykowiec coal waste dump, Poland. In G.B. Stracher, E.V. Sokol & A. Prakash (Eds.), *Coal and Peat Fires: A Global Perspective, Volume 3 - Case Studies*. Amsterdam: Elsevier, Scheduled for publication in 2011 (or early 2012).

Moghtaderi, B., Dlugogorski, B.Z., & Kennedy, E.M. (2000). Effect of wind flow on the self-heating characteristics of coal stockpiles. *Process Safety and Environmental Protection*, 78(6), 445-453. DOI: 10.1205/095758200530998.

Murchison, D. (2006). The influence of heating rates on organic matter in laboratory and natural environments. *International Journal of Coal Geology,* 67(3), *145-157*. DOI: 10.1016/j.coal.2005.11.005

Ndaji, F.E., & Thomas, K.M. (1995). The effect of oxidation on the macromolecular structure of coals. *Fuel,* 74(6), 932-937. DOI: 10.1016/0016-2361(95)00019-2.

Nelson, C.R. (1989). *Chemistry of coal weathering. Coal Science and Technology 14,* Amsterdam, Oxford, New York, Tokyo: Elsevier.

Norgate C.M., Boreham C.J., & Wilkins A.J. (1999): Changes in hydrocarbon maturity indices with coal rank and type, Biller Coalfield, New Zealand. *Organic Geochemistry*, 30(8), 985-1010. DOI: 10.1016/S0146-6380(99)00082-0.

O'Keefe, J.M.K., Hanke, K.H., Hower, J.C., Engle, M.A., Stracher, G.B., Stucker, J.D., Drew, J.W., Staggs, W.D., Murray, T.M., Hammond III, M.L., Adkin, K.D., Mullins, B.J., & Lemley, E.W. (2010). CO_2, CO, and Hg emissions from the Truman Shepherd and Ruth Mullins coal fires, eastern Kentucky, USA. *Science of the Total Environment,* 408(7), 1628-1633. DOI: 10.1016/j.scitotenv.2009.12.005.

Oros, D.R. & Simoneit, B.R.T. (2000). Identification and emission rates of molecular tracers in coal smoke particulate matter. *Fuel*, 79(5), 515-536. DOI: 10.1016/S0016-2361(99)00153-2.

Ourisson, G., Albrecht, P., & Rohmer, M. (1979). The hopanoids. Paleochemistry of a group of natural products. *Pure and Applied Chemistry*, 51(4), 709-729.

Pan, C., Geng, A., Zhong, N., Liu, J., & Yu, L. (2009). Kerogen pyrolysis in the presence and absence of water and minerals: Amounts and compositions of bitumen and liquid hydrocarbons. *Fuel*, 88(5), 909-919. DOI: 10.1016/j.fuel.2008.11.024.

Pan, C., Geng, A., Zhong, N., & Liu, J. (2010). Kerogen pyrolysis in the presence and absence of water and minerals: Steranes and triterpenoids. *Fuel,* 89(2), 336-345. DOI: 10.1016/j.fuel.2009.06.032.

Pancost, R.D., Baas, M., van Geel, B., & Sinninghe Damste, J.S. (2002). Biomarkers proxies for plant inputs to peats: an example from a sub-boreal ombrotrophic bog. *Organic Geochemistry,* 33(7), 675–690. DOI: 10.1016/S0146-6380(02)00048-7.

Parafiniuk, J.,& Kruszewski, Ł. (2009). Ammonium minerals from burning coal-dumps of the Upper Silesian Coal Basin (Poland). *Geological Quarterly*, 53(3), 341-356.

Peters, K.E., Walters, C.C., & Moldowan, J.M. (2005). *The Biomarker Guide. vol.2. Biomarkers and Isotopes in Petroleum Exploration and History*. (2 ed.). Cambridge, New York, Melbourne: Cambridge University Press.

Pickering, R.W. (1999). A toxicological review of Polyaromatic Hydrocarbons. *Journal of Toxicology: Cutaneous and Ocular Toxicology,* 18(2), 101-135. DOI: 10.3109/15569529909037562.

Pickering, R.W. (2000). Toxicity of Polyaromatic Hydrocarbons other than benzo(a)pyrene: a review. *Journal of Toxicology: Cutaneous and Ocular Toxicology,* 19(1), 55-67. DOI: 10.3109/15569520009051478.

Pone, J.D.N., Hein, K.A.A., Stracher, G.B., Annegarn, H.J., Finkelman, R.B., Blake, D.R., McCormack, J.K., & Schroeder, P. (2007). The spontaneous combustion of coal and its by-products in the Witbank and Sasolburg coalfields of South Africa. *International Journal of Coal Geology,* 72(2), 124-140. DOI: 10.1016/j.coal.2007.01.001.

Radke, M. (1987). Organic geochemistry of aromatic hydrocarbons. In J. Brooks, D. Welte, (Eds.), *Advances in Petroleum Geochemistry, vol. 2* (pp 141-205). London, Academic Press.

Radke, M., & Welte, D.H. (1983). The methylphenanthrene index (MPI): a maturity parameter based on aromatic hydrocarbons. In: M. Bjoroy, P. Albrecht, C. Cornford, K. de Groot, G. Eglinton, E. Galimov, D. Leythaeuser, R. Pelet & G. Speers (Eds), *Advances in Organic Geochemistry 1981* (pp. 504–512). Chichester: John Wiley and Sons, Inc.

Radke, M., Willsch, H., Leythaeuser, D., & Teichmüller, M. (1982). Aromatic components of coal: relation of distribution pattern to rank. *Geochimica et Cosmochimica Acta,* 46(10), 1831-1848. DOI: 10.1016/0016-7037(82)90122-3.

Radke, M., Welte, D.H., & Willsch, H. (1986). Maturity parameters based on aromatic hydrocarbons: influence of organic matter type. *Organic Geochemistry,* 10(1-3), 51-63. DOI: 10.1016/0146-6380(86)90008-2.

Radke, M., Willsch, H., & Teichmüller, M. (1990). Generation and distribution of aromatic hydrocarbons in coals of low rank. *Organic Geochemistry,* 15(6), 539-563.

Radke, M., Rullkötter, J., & Vriend, S.P. (1994). Distribution of naphthalenes in crude oils from the Java Sea: Source and maturation effects. *Geochimica et Cosmochimica Acta,* 58(17), 3675-3689. DOI: 10.1016/0016-7037(94)90158-9.

Raymond, A.C., & Murchison, D.G. (1992). Effects of igneous activity on molecular-maturation indices in different types of organic matter. *Organic Geochemistry,* 18(5), 725-735. DOI: 10.1016/0146-6380(92)90098-I.

Ribeiro, J., Ferreira da Silva, E., & Flores, D. (2010). Burning of coal waste piles from Douro Coalfield (Portugal): Petrological, geochemical and mineralogical characterization. *International Journal of Coal Geology,* 81(4), 359-372. DOI: 10.1016/j.coal.2009.10.005.

Rimmer, S.M., Yoksoulian, L.E., & Hower, J.C. (2009). Anatomy of an intruded coal, I: Effect of contact metamorphism on whole-coal geochemistry, Springfield (No. 5) (Pennsylvanian) coal, Illinois Basin. *International Journal of Coal Geology,* 79(3), 74-82. DOI: 10.1016/j.coal.2009.06.002.

Rosiek, F., & Urbański, J. (1990). Influence of some physical properties of coal on their self-ignition. Wrocław: Scientific Publications of Mining Institute of Wrocław Technical University, 59, 27-32 (in Polish).

Querol, X., Izquierdo, M., Monfort, E., Alvarez, E., Font, O., Moreno, T., Alastuey, A., Zhuang, X., Lu, W., & Wang, Y. (2008). Environment characterization of burnt coal gangue banks at Yangquan, Shanxi Province, China. *International Journal of Coal Geology,* 75(2), 93-104. DOI: 10.1016/j.coal.2008.04.003.

Quintero, J.A., Candela, S.A., Rios, C.A., Montes, C., & Uribe, C. (2009). Spontaneous combustion of the Upper Paleocene Cerrejón Formation coal and generation of clinker in La Guajira Peninsula (Carribean Region of Colombia). *International Journal of Coal Geology,* 80(3-4), 196-210. DOI: 10.1016/j.coal.2009.09.004.

Sahu, H.B., Mahapatra, S.S., & Panigrahi, D.C. (2009). An empirical approach for classification of coal seams with respect to the spontaneous heating susceptibility of Indian coals. *International Journal of Coal Geology, 80*(3-4), 175-180. DOI: 10.1016/j.coal.2009.10.001.

Sawicki, T. (2004). Spontaneous combustion in stock piles as the cause of fire. *Karbo*, 1, 56–59 (in Polish).

Seifert, W.K., & Moldowan, J.M. (1978). Application of steranes, terpanes and monoaromatics to the maturation, migration and source of crude oils. *Geochimica et Cosmochimica Acta, 42*(1), 77-95. DOI: 10.1016/0016-7037(78)90219-3.

Seifert, W.K., & Moldowan, J.M. (1980). The effect of thermal stress on source-rock quality as measured by hopane stereochemistry. *Physicas and Chemistry of Earth, 12*, 229-237. DOI: 10.1016/0079-1946(79)90107-1.

Sensogut, C., & Cinar, I. (2000). A research on the tendency of Ermenek District coals to spontaneous combustion. *Mineral Resources Engineering*, 9(4), 421-427. DOI: 10.1142/S0950609800000342.

Shi, T., Wang, X., Deng, J., & Wen, Z. (2005). The mechanism at the initial stage of room-temperature oxidation of coal. *Combustion and Flame, 140*(4), 332-345. DOI: 10.1016/j.combustflame.2004.10.012.

Simoneit, B.R.T. (1998). Biomarker PAHs in the environment. In A.H. Neilson (Ed.). *PAHs and related compounds. The handbook of environmental chemistry. vol. 3 Part 1* (pp.176-221). Berlin Heidelberg: Springer-Verlag.

Simoneit, B.R.T. (2002). Biomass burning — a review of organic tracers for smoke from incomplete combustion. *Applied Geochemistry, 17*(3), 129-162. DOI: 10.1016/S0883-2927(01)00061-0.

Singh A.K., Singh R.V.K., Singh M., Chandra H., & Shukla, N.K. (2007a). Mine fire gas indices and their application to Indian underground coal mine fires. *International Journal of Coal Geology, 69*(3), 192-204. DOI: 10.1016/j.coal.2006.04.004.

Singh, A.K., Singh, M.P., Sharma, M., & Srivastava, S.K. (2007b). Microstructures and mictrotextures of natural cokes: A case study of heat-affected coking coals from the Jharia coalfield, India. *International Journal of Coal Geology, 71*(2-3), 153-175. DOI: 10.1016/j.coal.2006.08.006.

Singh, A.K., Sharma, M., & Singh, M.P. (2008). Genesis of natural cokes: Some Indian examples. *International Journal of Coal Geology, 75*(1), 40-48. DOI: 10.1016/j.coal.2008.01.002.

Skarżyńska, K.M. (1995a): Reuse of coal mining wastes in civil engineering. Part 1: Properties of minestone. *Waste Management, 15*(1), 3-42. DOI: 10.1016/0956-053X(95)00004-J.

Skarżyńska, K.M. (1995b). Reuse of coal mining wastes in civil engineering. Part 2: Utilization of minestone. *Waste Management, 15*(2), 83-126. DOI: 10.1016/0956-053X(95)00008-N.

Skręt, U., Fabiańska, M.J., & Misz-Kennan, M. (2010). Simulated water-washing of organic compounds from self-heated coal wastes of the Rymer Cones Dump (Upper Silesia Coal Region, Poland). *Organic Geochemistry* 41(9), 1009-1012. DOI: 10.1016/j.orggeochem.2010.04.010.

Smith, M.A., & Glasser, D. (2005). Spontaneous combustion of carbonaceous stockpiles. Part II. Factors affecting the rate of the low-temperature oxidation reaction. *Fuel*, 84(9), 1161-1170. DOI: 10.1016/j.fuel.2004.12.005.

Sokol, E.V. (2005). High-temperature processes of organic fuel decomposition as a thermal source for pyrometamorphic transformations. In G.G. Lepezin (Ed.), *Combustion metamorphism* (pp. 22-31). Novosybirsk: Publishing House of the Siberian Branch of Russian Academy of Sciences (in Russian).

Stach, E., Mackowsky, M.-Th., Teichmüller, M., Taylor, G.H., Chandra, D., & Teichmüller, R. (1982). *Stach's Textbook of Coal Petrology*. Berlin: Gebrüder Borntraeger.

Stalker, L., Larter, S.R., & Farrimond, P. (1998). Biomarker binding into kerogens: evidence from hydrous pyrolysis using heavy water (D$_2$O). *Organic Geochemistry, 28*(3-4), 239-253. DOI: 10.1016/S0146-6380(97)00103-4.

Steward, A.K., Massey, M., Padgett, P.L., Rimmer, S.M., & Hower, J.C. (2005). Influence of a basic intrusion on the vitrinite reflectance and chemistry of the Springfield (No. 5) coal, Harrisburg, Illinois. *International Journal of Coal Geology, 63*(1-2), 58-67. DOI: 10.1016/j.coal.2005.02.005.

Strachan, M.G., Alexander, R., van Bronswijk, W., & Kagi, R.I. (1989a). Source and heating rate effects upon maturity parameters based on ratios of 24-ethylcholestane diastereomers. *Journal of Geochemical Exploration, 31*(3), 285-294. DOI: 10.1016/0375-6742(89)90106-4.

Strachan, M.G., Alexander, R., Subroto, E.A., & Kagi, R.I. (1989b). Constraints upon the use of 24-ethylcholestane diastereomer ratios as indicators of the maturity of petroleum. *Organic Geochemistry, 14*(4), 423-432. DOI: 10.1016/0146-6380(89)90007-7.

Stracher, G.B. (ed.) (2007). *Geology of coal fires: case studies from around the world. Reviews in Engineering Geology* (pp. 283). XVIII, Colorado: The Geological Society of America, ISBN: 978-0-8137-4118-5.

Stracher, G.B., & Taylor, T.P (2004). Coal fires burning out of control around the world: thermodynamic recipe for environmental catastrophe. *International Journal of Coal Geology,* 59(1-2), 7-17. DOI: 10.1016/j.coal.2003.03.002.

Strumiński, A., & Rosiek, F. (1990). The evaluation of the endogenic fire-hazards in the Lower Silesian Coal Basin in the light of the tendency for the coal to self-ignite. Wrocław: Scientific Publications of Mining Institute of Wrocław Technical University, 59, 33-43 (in Polish).

Stukalova, I.E., & Rusinova, O.V. (2007). Thermal alteration of coal in the Khasyn coalfield, Magadan region, Russia. *International Journal of Coal Geology,* 71(4), 462-470. DOI: 10.1016/j.coal.2006.11.005.

Suárez-Ruiz I., & Crelling J. (2008). *Applied Coal Petrology. The Role of Petrology in Coal Utilization.* Amsterdam: Elsevier.

Sýkorová, I., Pickel, W., Christanis, K., Wolf, M., Taylor, G.H., & Flores, D. (2005). Classification of huminite— ICCP System 1994. *International Journal of Coal Geology,* 62(1-2), 85-106. DOI: 10.1016/j.coal.2004.06.006.

Szafer, M., Urbański, H., & Tabor, A. (1994). Rules for the re-cultivation of coal waste dumps using modern techniques. Katowice: Central Mining Institute (in Polish).

Tabor, A. (2002). Monitoring of coal waste dumps, re-cultivated dumps and other collection sites of Carboniferous waste rocks in the light of many years experience. Proceedings - VII Conference "Long term proecological undertakings in the Rybnik Coal Area", October 2002 (pp. 131-141). Rybnik, (in Polish).

Tabor, A. (1999). Technical – ecological problems in coal waste collection [in Polish]. Proceedings - IV Conference "Conditions in the local plans for land development in towns and communes of the Rybnik Coal Area", October 1999 (pp. 195-202). Rybnik, (in Polish).

Tabor, A. (2002-2009). Reports from the monitoring of coal waste dumps. Unpublished materials (in Polish).

Taylor G.H., Teichmüller M., Davis A., Diessel C.F.K., Littke R., & Robert R. (1998). *Organic Petrology. A New Handbook incorporating some revised parts of Stach's Textbook of Coal Petrology.* Berlin: Gebrüder Borntraeger.

Ten Haven, H.L., Littke, R., & Rullkötter, J. (1992). Hydrocarbon biological markers in Carboniferous coals of different rank. In J.M. Moldowan, P. Albrecht & R.P. Philp (Eds.). *Biological markers in sediments and petroleum* (pp. 142-154). New Jersey : Prentice Hall.

The Wiley/NBS Registry of Mass Spectral Data. Wiley, New York.

Tissot, B.P., & Welte, D.H. (1984). *Petroleum Formation and Occurrence.* Berlin: Springer Verlag.

Urbański J. (1983). Technical re-cultivation of mine waste dumps with particular reference to fire protection. Training Materials, Katowice: The Association of Mining Engineers and Technics (in Polish).

Wachowicz, J. (2008). Analysis of underground fires in Polish hard coal mines. *Journal of China University of Mining and Technology,* 18(3), 332-336. DOI: 10.1016/S1006-1266(08)60070-X.

Wagner M. (1980). Thermal alterations of bituminous coal in fire zones of mining dumps. *Scientific Papers of Academy of Mining and Metallurgy,* 6(2), 5-14.

Walker, S. (1999). *Uncontrolled fires in coal and coal wastes.* London: IEA Coal Research. (CCC/16). ISBN 92-9029-3247-1.

Wang, H., Dlugogorski, B.Z., & Kennedy, E.M. (1999). Experimental study on low-temperature oxidation of an Australian coal. *Energy and Fuels,* 13(6), 1173-1179. DOI: 10.1021/ef990040s.

Wang, H., Dlugogorski, B.Z., & Kennedy, E.M. (2002a). Examination of CO_2, CO, and H_2O formation during low-temperature oxidation of a bituminous coal. *Energy and Fuels,* 16(3), 586-592. DOI: 10.1021/ef010152v.

Wang H., Dlugogorski B.Z., & Kennedy E.M. (2002b). Thermal decomposition of solid oxygenated complexes formed by coal oxidation at low temperatures. *Fuel,* 81(15), 1913-1923. DOI: 10.1016/S0016-2361(02)00122-9.

Wang, H., Dlugogorski, B.Z., & Kennedy, E.M. (2003). Pathways for production of CO_2 and CO in low – temperature oxidation of coal. *Energy and Fuels,* 17(1), 150-158. DOI: 10.1021/ef020095l.

Willey, C., Iwao, M., Castle, R.N., & Lee, M.L. (1981). Determination of sulfur heterocycles in coal liquids and shale oils. *Analytical Chemistry,* 53(3), 400-407. DOI: 10.1021/ac00226a006.

Willsch, H., & Radke, M. (1995). Distribution of polycyclic aromatic compounds in coals of high rank. *Polycyclic Aromatic Compounds*, 7(4), 231-251. DOI: 10.1080/10406639508009627.

Zhao, Y., Zhang, J., Chou, C.-L., Li, Y., Wang, Z., Ge, Y., & Zheng C. (2008). Trace element emission from spontaneous combustion of gob piles in coal mines, Shanxi, China. *International Journal of Coal Geology,* 73(1), 52-62. DOI: 10.1016/j.coal.2007.07.007.

List of reviewers

The editors are grateful to the following who gave their time and expertise to act as referees for papers submitted to publication in 2010:

Marek Awdankiewicz

Olaf Borkiewicz

Ömer Bozkaya

Evgeny Galuskin

Callum J. Hetherington

James Hower

Anna Sophia Knox

Rune B. Larsen

Raymond Macdonald

Maciej Manecki

Leszek Marynowski

Jan Michalik

Milan Novak

Maria Sass-Gustkiewicz

Zbigniew Sawłowicz

Maja Stanisławska

Eligiusz Szełęg

Jan Środoń

COMEF

Brand	Description
ALCATEL ADIXEN	pompy próżniowe: bezolejowe, olejowe, Rootsa, turbomolekularne oraz helowe wykrywacze nieszczelności, mierniki próżni i szeroki asortyment podzespołów
AMBIOS	mikroskopy sił atomowych (AFM), STM
ANTON PAAR	mikrofalowe systemy do przygotowania próbek (mineralizatory mikrofalowe) oraz do syntezy związków organicznych, SAXSess
CAMECA	mikrosondy jonowe SIMS magnetyczne i kwadrupulowe, mikrosondy elektronowe
CLIMATS SAPRATIN	komory: klimatyczne, solne, temperaturowe, szoku termicznego
CRESSINGTON	napylarki do napylania węglem oraz metalami
DANSENSOR	przemysłowe mierniki O_2 i CO_2, analizatory gazów on-line, miksery gazów, wykrywacze nieszczelności w opakowaniach, analizatory przepuszczalności gazów, analizatory atmosfery modyfikowanej w pakowaniu żywności
GORATEC	aparatura do pomiaru i analizy promieniowania podczerwonego, bezkontaktowy pomiar temperatury, kamery termowizyjne
HITACHI	mikroskopy elektronowe: skaningowe, transmisyjne, STEM, FIB
HORIBA	analizatory węgla i siarki, analizatory azotu, tlenu i wodoru, granulometry, analizatory oleju w wodzie, analizatory XRF, analizatory siarki w paliwach
JOBIN YVON	siatki dyfrakcyjne, monochromatory, elipsometry, spektrofluorometry spektrometry: ICP, GDS, ISKROWE, RAMANOWSKIE
NEWPORT	elementy optyczne, optyka światłowodowa, siatki dyfrakcyjne, filtry, stoły optyczne, układy mikromechaniczne, układy optomechaniczne oraz akcesoria
ORIEL	monochromatory, źródła światła, lampy kalibracyjne, oświetlacze, symulatory światła słonecznego, spektrometry FT-IR
PARK SYSTEMS	mikroskopy sił atomowych (AFM)
RIBER	systemy MBE
SECOMAM	spektrofotometry, analizatory wody i ścieków, analizatory biochemiczne
SETARAM	kalorymetry (CALVET, DSC), dylatometry wysokotemperaturowe, analizatory termiczne (TG,TG-DTA, TG-DSC, TGA-MS, TG-FTIR)
SKYSCAN	urządzenia do rentgenowskiej wysokorozdzielczej tomografii komputerowej
THERMO ELECTRON	spektrometry dyspersji energii EDS oraz WDS do mikroskopów elektronowych spektrometry AUGER, XPS (ESCA) - urządzenia VG SCIENTIFIC
SPECTRA PHYSICS	lasery: gazowe, na ciele stałym (YAG), pikosekundowe, femtosekundowe, wzmacniacze optyczne
WALTER-BAI	uniwersalne maszyny wytrzymałościowe, pełzarki

Stowarzyszenie Naukowe im. Stanisława Staszica

adres: 31-124 Kraków, ul. Dolnych Młynów 7/1

tel./fax (12) 632-76-93, e-mail: geo-staszic@wp.pl

Stowarzyszenie Naukowe im. Stanisława Staszica istnieje od 1998 roku. Zrzesza m.in. pracowników naukowych krakowskich wyższych uczelni, głównie Akademii Górniczo-Hutniczej.

Główne cele Stowarzyszenia

1. Promocja nauki, techniki, kultury i sztuki, szczególnie propagowanie i upowszechnianie myśli technicznej.
2. Wykonywanie prac naukowych, badawczych i innych, prowadzonych samodzielnie lub we współpracy z wyższymi uczelniami i innymi jednostkami badawczymi oraz podmiotami gospodarczymi.
3. Reprezentowanie interesów ludzi nauki, techniki, kultury i sztuki przed władzami państwowymi i innymi.
4. Podejmowanie wszelkich inicjatyw, mających na względzie dobro ludzi nauki, techniki, kultury i sztuki. Pomoc i wsparcie dla twórców będących w trudnej sytuacji życiowej oraz dla dzieci i młodzieży o szczególnych uzdolnieniach lub z rodzin zagrożonych.
5. Dotowanie prac naukowych i popularno-naukowych (książki, skrypty, podręczniki, albumy itp.).
6. Inicjowanie, popieranie i prowadzenie międzynarodowej wymiany technicznej.
7. Wspieranie wszelkich akcji dobroczynnych i charytatywnych zaproponowanych przez członków Stowarzyszenia.

Zakres prac (m.in.)

- Badania własności geomechanicznych skał i węgla.
- Prace badawcze i ekspertyzy w zakresie doboru obudowy wyrobisk korytarzowych.
- Oceny stateczności oraz prognozowania przemieszczeń górotworu pod wpływem eksploatacji.
- Analizy chemiczne szkieł przemysłowych i specjalnych wraz z analizą pierwiastków akcesorycznych i lądowych.
- Badanie właściwości fizykochemicznych szkieł.
- Opinie w zakresie szkła budowlanego, technicznego, gospodarczego, opakowaniowego i innych asortymentów.
- Projektowanie syntez szkieł o żądanych właściwościach.
- Pomiary deformacji powierzchni terenu w rejonach eksploatacji górniczej wraz z analizą wpływów eksploatacji na obiekty budowlane i inżynierskie.
- Prognozowanie deformacji górotworu i powierzchni w rejonach eksploatacji głębinowej złóż rud miedzi, węgla kamiennego, soli, gazu ziemnego i ropy naftowej.
- Analizy wpływu eksploatacji na wyrobiska kopalniane (przekopy, szyby) i ocena zagrożenia tych obiektów.

o Ocena zagrożenia obiektów na terenach podlegających wpływom eksploatacji górniczej.
o Oprogramowanie komputerowe dla celów prognoz deformacji na terenach górniczych, analiz wyników pomiarów deformacji i oceny zagrożeń
o Opracowanie i budowa systemów informacji o terenie górniczym (GIS).
o Analiza zagrożeń w rejonach likwidowanych obiektów górniczych oraz na terenach dawnej eksploatacji górniczej.
o Wycena podmiotów gospodarczych, nieruchomości, znaków firmowych – pełny pakiet usług.
o Organizowanie warsztatów szkoleniowych dla rzeczoznawców.
o Organizacja seminariów, konferencji itp.
o Wydawanie czasopisma – „Geoturystyka".

Kontrahenci Stowarzyszenia (m.in.)

✧ KGHM „Polska Miedź" S.A.
✧ KWB „Bełchatów" S.A.
✧ Polskie Górnictwo Naftowe i Gazownictwo S.A.
✧ Elektrownia „Turów" S.A.
✧ Kompania Węglowa S.A.
✧ Jastrzębska Spółka Węglowa S.A.
✧ Państwowy Instytut Geologiczny S.A.
✧ Polska Akademia Nauk
✧ Akademia Górniczo-Hutnicza
✧ Uniwersytet Jagielloński
✧ Politechnika Krakowska
✧ Politechnika Szczecińska
✧ Centrum Badawczo-Projektowe Miedzi „CUPRUM" Sp. z o.o.
✧ Pilkington Automotive Poland S.A.
✧ Guardian Industries Poland Sp. z o.o.
✧ Koksownia "Przyjaźń" Sp. z o.o.

Wiarygodność naszych usług, zadowolenie naszych Zleceniodawców i ciągłe doskonalenie naszych działań są naszym celem nadrzędnym, co potwierdza uzyskany prze Stowarzyszenie w styczniu 2005 roku certyfikat jakości zgodny z normą ISO 9001: 2000

Zapraszamy do współpracy i korzystania z naszych usług

Laboratory of Scanning Microscopy of Biological
and Geological Sciences
Faculty of Biology and Earth Sciences
Jagiellonian University

Division of Field Emission Scanning Electron Microscopy
and Microanalysis at the Institute of Geological Sciences
30-063 Kraków, ul. Oleandry 2a; Poland
www.uj.edu.pl/LabFESEM

Division of Field Emission Scanning Electron Microscopy and Microanalysis at the Institute of Geological Sciences is equipped with modern cold field emission scanning electron microscope (FESEM) HITACHI S-4700 and energy dispersive spectrometer (EDS) NORAN Vantage.

Analytical possibilities:
- Magnification up to 500 000x,
- High resolution imaging (1.5 nm at 15 kV or 2.1 nm at 1 kV and 12 mm working distance),
- two SE (secondary electrons) detectors (upper and lower) with energy filter, possibility of mixing of SE and BSE (backscattered electrons) signals,
- Backscattered electrons detector (YAG BSE; TV mode),
- Cathodoluminescence detector,
- EDS system for spot chemical analysis, line scan, and mapping of elements distribution,
- 45° specimen tilt,
- Digital image acquisition (as JPEG, TIFF and BMP files)

FESEM – EDS system can be applied for high magnification observation of various objects and chemical analysis with high spatial resolution, e.g.:
- Morphology and chemical composition of components of rocks, soils, industrial products and wastes, biological materials,
- Observation of structure of rocks, soils and sediments,
- Analysis of morphology and chemical composition of atmospheric dust and aerosols,
- Analysis of chemical composition of archaeological artefacts,
- Analysis of composition of pigments, glasses, tissues, paper, metals in conservation of objects of cultural heritage.

FESEM – EDS system is very efficient; software is user-friendly. Preparation of analytical documentation is very easy. Facilities for samples preparation are also available in the Laboratory.

FESEM – EDS laboratory offers two scholarships for Ph.D. or M.Sc. Students in the field of Earth sciences (10 hours of free access to FESEM-EDS + samples preparation + technical assistance).

For more information, contact please:
Marek Michalik   (Institute of Geological Sciences, Jagiellonian University)
          +48 12 6334603 or +48 604 147828 or e-mail: marekmichalik@uj.edu.pl
Anna Łatkiewicz (Institute of Geological Sciences, Jagiellonian University)
          +48 12 6334603 or +48 693 318544 or e-mail: alatk@geos.ing.uj.edu.pl

Universitas Jagellonica
Cracoviensis

INSTRUCTIONS FOR THE AUTHORS

The scope of the journal:
Mineralogia Polonica publishes original papers in the scope of widely understood mineralogical sciences (i.e. mineralogy, petrology, geochemistry, environmental sciences, applied mineralogy, etc.). All papers are reviewed and the author is obliged to make corrections suggested by a referee, or give, in a written form, reasons for not doing so.

Original research papers up to 30 pages (1800 characters per page), review papers, short notes (e.g. new interesting occurrences of minerals), book reviews and letters to the editors with comments on papers published could be submitted. Authors of larger manuscripts should contact the Editor before submission.

Text submission:
The papers should be submitted to the address: mineralogia@mineralogia.pl

Conditions of acceptance:
In a letter which should accompany the manuscript, the submitting author must state that all authors involved have accepted the final version of the manuscript. The letter must also state that the manuscript has not previously been published elsewhere, either in full or in part, and that while under review for *Mineralogia*, will not be submitted to any other publication for consideration.

Preparation of scripts:

The title of your paper

Elizabeth M. GREY[1]*, Krzysztof B. GRANICKI[2], Ibrahim ÇELIN[1,2]

[1] *Oxford University, School of Geosciences, Oxford O2B 0D0, UK; e-mail: greye@ox.ac.uk*
[2] *Institute of Geosciences, Jagiellonian University, ul. Oleandry 2a, 30-063 Kraków, Poland; e-mail: nowak@bo.ac.com, ibcelin@md.com*
* Corresponding author

Abstract. Here write your concise abstract. Give as much hard data as possible. Avoid vague general statements. State what results were obtained, not what was being done. Avoid quoting references in the abstract. The abstract should be limited to 100-150 words.

Key-words: mineral, rock type, process, Antarctica, up to five entries from most to least important

1. Introduction
Please, treat this document as a template for the paper you intend to submit to *Mineralogia*. The headings used are only examples. Use Oxford English style and spelling. Use -ize not -ise, but remember about common exceptions: advise, analyse, catalyse, devise, emphasise, exercise, synthesise.

2. Samples
This is how to use abbreviations: 15 s (not sec), 5 min (not min.), 1980s, 1999/2000 (e.g. for an academic year), 1998-1999 (not 1998-99), Mts (Mountains), *ca* (circa). With "e.g." and "i.e.", there is a comma before, but not after the abbreviations. For valid mineral names and their spelling, check the

current International Mineralogical Association (IMA) list at http://pubsites.uws.edu.au/ima-cnmnc. An example of formatting geographical coordinates is given in the parentheses (19° 12'-19° 14' N 83° 12'-83° 14' E).

3. Methods

When using acronyms (especially those not commonly used), spell out name in full and follow with the acronym in parentheses when used for the first time, e.g. Sensitive High Resolution Ion Microprobe (SHRIMP), X-ray absorption spectroscopy (XAS). Use the acronym later on in the text, e.g. XAS.

4. Results

4.1. Units and numbers

Use only SI units. There is always space between a number and a unit: *10 mg*, *2.76 mm*. Degrees and percentages are exceptions: *10°C, 25.67%, 2.57wt%*. Numbers from one to ten in the text are in the written form, e.g. *five samples*, then quoted in digits: 11, 12, etc. Therefore: *twofold*, but *20-fold*. Contributions: *5 l per hour* or *5l h^{-1}*. Note the use of a decimal point, not a comma: *2.76 mm*. A comma separates off thousands in numbers larger than 9999, so *6000* but *12,000*.

4.2. Figures

Keep the number of figures as low as possible. Name illustrations and photographs as figures and number them consecutively. In the text refer to, e.g. Figure 1. In parentheses use the short form (Fig. 1). Each figure requires a caption and, if necessary, explanations.

Acceptable formats are jpg, tiff. Please, export your vector diagrams as tiff or jpg. Figures should not be wider than 13 cm. The resolution must be at least 600 dpi for black-and-white images and at least 300 dpi for greyscale and colour illustrations. If no colour figures will be printed, submit only their greyscale versions.

An extra charge will be levied if the authors wish to have colour figures printed. For further information, please contact the Editors.

4.3. Tables

Submit tables in your text. Please avoid long listings and select appropriate data to visualize your research but not to make a full documentation. Check your summations. In the text refer to Table 1 or to (Table 1) when in parentheses. When writing "below detection" (b.d.) in your tables, remember to quote specific detection limits in the methods section.

5. Discussion

Keep your discussion separate from the results. Use the following citation scheme: Nowak (2008), Nowak and Smith (2008), Nowak et al. (2008) in the text, while (Nowak 2008) or (Nowak, Smith 2008) or (Nowak et al. 2008) in parentheses. In the text use "et al." when there are three or more authors. Note semi-colon in parentheses: (Nowak 2008; Werner 2005). Use 2007a, b when there is more than one paper of the same author(s) in one year (Nowak 2007a, b).

Please use our references scheme, as shown in the paper document *New referencing style.pdf*. Some examples are also shown in chapter *7. References* in this template. Write journal titles in full in italics, e.g. *Earth Science Reviews*. Only papers cited in the text can be included in the reference list. Sort the reference list alphabetically and then chronologically, if necessary.

Text originally published in language other than English, should have their titles translated in brackets. Transliterate the titles to Latin alphabet should they require conversion from another lettering system.

6. Conclusions

Submit your text converted to a **pdf format**, including all of the figures and tables in one file. The original figures may be required once your text has been accepted.

Please, comply with all the requirements to save paper and avoid additional work, delays and extra costs of technical editing. Should you have any specific enquires, please, contact the editors.

7. References

Pyle, J. M., Spear, F. S., Rudnick, R. L., & McDonough, W. F. (2001). Monazite-Xenotime-Garnet Equilibrium in Metapelites and a New Monazite-Garnet Thermometer. *Journal of Petrology, 42*(11), 2083-2107. DOI: 10.1093/petrology/42.11.2083.

Pettijohn, F.J. (1957). *Sedimentary Rocks* (2 ed.)*.* New York: Harper & Brothers.